MINECO - Proyecto INSIGHT (CGL2011-30005-C02-02)

Ocean Facilities Exchange Group (OFEG)

ImagiNg large SeismogenIc and tsunamiGenic structures of the Gulf of Cadiz with ultra-High resolution Technologies (INSIGHT-Leg1)

Caracterización de grandes estructuras sismogénicas y tsunamogénicas del Golfo de Cádiz con tecnologías de muy alta resolución

Cruise Report
INSIGHT-Leg 1

R/V Sarmiento de Gamboa (SDG-68)
29th April – 18th May 2018

Chief Scientist
Dr. Eulàlia Gràcia i Mont

Principal Investigators (PIs)
Dr. Roger Urgeles & Dr. Eulàlia Gràcia

Institut de Ciències del Mar – CSIC (Barcelona)

Authors

This report has been written and compiled by Eulàlia Gràcia, Roger Urgeles, Marcel Rothenbeck, Emanuel Wenzlaff, Anja Steinführer, Torge Kurbjuhn, Rafael Bartolomé, Claudio Lo Iacono and Miquel Camafort with the contributions of the scientific and technical cruise members on board the R/V Sarmiento de Gamboa, hereafter referred as INSIGHT cruise party (See section 2: Participants).

Acknowledgements

We acknowledge the Captain, Jose Manuel Pérez Erias, the officers (Arnau Rovira and Lidia Pérez-Marcelino), and all the crew of the R/V Sarmiento de Gamboa for their professional work during cruise operations, which made possible the success of the INSIGHT-Leg 1 cruise.

We thank the UTM-CSIC technical team (Rober, Ezequiel, Juan, Hector, Camilo, Mario, Pirri y Antonio) for their guidance, effort, and exquisite assistance throughout the data collection. The GEOMAR AUV team (Marcel, Anja, Manu and Torge) are deeply acknowledged for their professionalism, collaboration, and expertise in using their vehicle "Abyss" that helped us to obtain a very high-quality dataset. We also thank the UTM-CSIC ship manager Javier Prades for collaboration with the cruise logistics and planning, and the UTM-CSIC director Jordi Sorribas for their support.

Grateful thanks to Jordi Sorribas and Miguel Angel Ojeda for their negotiations through the Ocean Facilities Exchange Group (OFEG) with GEOMAR AUV-manager Peter Linke. All of them made possible to use the GEOMAR AUVs during the INSIGHT-Leg 1 cruise.

We gratefully acknowledge financial support from *Ministerio Economia y Competividad* through national project ***INSIGHT "ImagiNg large SeismogenIc and tsunamiGenic structures of the Gulf of Cadiz with ultra-High resolution Technologies (INSIGHT-Leg1)"*** (CGL2011-30005-C02-02, PIs: Roger Urgeles and Eulàlia Gràcia) and **Ocean Facilities Exchange Group** (OFEG) for allowing us to use the AUVs "Abyss" from GEOMAR (Germany).

Table of Contents

Abstract

Large earthquakes, submarine landslides and the tsunami they might originate are geohazards of great societal concern because they may impact world economies and struck coastal populations. Examples of these events are the 2004 northern Sumatra and 2011 Tohoku earthquakes and respective tsunamis. However, earthquakes of magnitude $M_w > 8.0$ in areas of relatively slow tectonic deformation and with long recurrence intervals, such as the external part of the Gulf of Cadiz, might also have a significant impact. The most relevant is the 1755 Lisbon earthquake, related submarine landslides and destructive tsunami. The occurrence of faults and landslides able to trigger a catastrophic tsunami reveals that the Gulf of Cadiz is one of the highest geohazard areas in Europe. Migration of sub-seafloor fluids has also been widely documented in the Gulf of Cadiz and such fluids are strongly related to the earthquake cycle and to the occurrence of submarine landslides. Understanding of these active processes can only be developed by using ultra-high-resolution tools able to map with unprecedented detail faults, submarine landslides and fluid escape structures. State-of-the-art techniques are used during INSIGHT-Leg 1, such as microbathymetry obtained from an autonomous underwater vehicle (AUV), sub-bottom profiles, HR multi-channel seismic data (MCS), and groundtruthing using sediment cores.

Key words: *Active faults, fluid flow, submarine landslides, earthquakes, tsunamis, ultra-high resolution technologies*

1. Introduction

Geological hazards, such as earthquakes and submarine landslides, are a major societal concern. They are capable of generating tsunami that threaten coastal communities, infrastructure, and global economies at distances of many thousands of kilometers (Morgan et al., 2009). Examples of such earthquakes and associated slope failures are found in the southwestern margin of the Iberian Peninsula, such as the 1755 Lisbon earthquake and tsunami and the 1969 Horseshoe earthquake (Fukao 1973, Buforn et al. 1995, 2004, Baptista et al. 1998, Gràcia et al., 2003, Martínez-Solares and López-Arroyo 2004, Vizcaino et al., 2006, Terrinha et al., 2009). The Gulf of Cadiz represents one of the most hazardous areas in Europe (Papadopoulos et al. 2014), despite the long recurrence period for large earthquakes and tsunamis generated offshore (Gràcia et al. 2010).

The INSIGHT Leg 1 cruise has been programmed in the frame of the INSIGHT project (ImagiNg large SeismogenIc and 6ery6fically structures of the Gulf of Cadiz with ultra-High resolution Technologies) granted in 2016 and which lasts until 2020. INSIGHT is a national project that belongs to the Spanish National Plan of Research, Development and Innovation (R+D+I), and lead by the Marine Science Institute (ICM-CSIC) in Barcelona. The general objective of the INSIGHT-Leg 1 cruise is to image and characterize, with the highest possible resolution, selected active seismogenic faults, large slope failures and investigate their relation with fluid seepage in the Gulf of Cadiz. The large-scale features of most of these elements, such as fault systems and slope failures have been previously mapped and characterized (i.e. geometry, dynamics and kinematics) during recent projects. These structures may also represent a seismic and tsunamigenic hazard for the surrounding coasts of South Iberia and North Africa.

Figure 1.1. *The 1st November 1755 Lisbon earthquake and tsunami.*

1.1. Objectives

The main scientific objectives of the INSIGHT project are:

a) To characterize in detail, the 4D architecture of major elements at the origin of geohazards (faults and submarine landslides) and their relation with fluid seepage.
b) To evaluate the role of large faults and associated submarine landslides as potential tsunami generators.

To properly understand the physical phenomena and obtain a precise definition of the fault seismic parameters and dynamics of the submarine landslides we need higher resolution data than previously acquired. Thus, the aims of the cruise are twofold:

a) To characterize at the highest resolution **selected active seismogenic faults** located in the Gulf of Cadiz, such as the Marques de Pombal Thrust-fault, the Lineament South in two different locations (i.e. deep basin and shelf area), characterized by the presence of fluid seepage to the seafloor (i.e. active mud volcanoes).

b) To image with unprecedented resolution the seismic structure of **mass movements often associated to active faults and presence of active fluid seepage**, such as the Marques de Pombal slide-complex, the Ginsburg mud volcano and the Lolita salt diapir

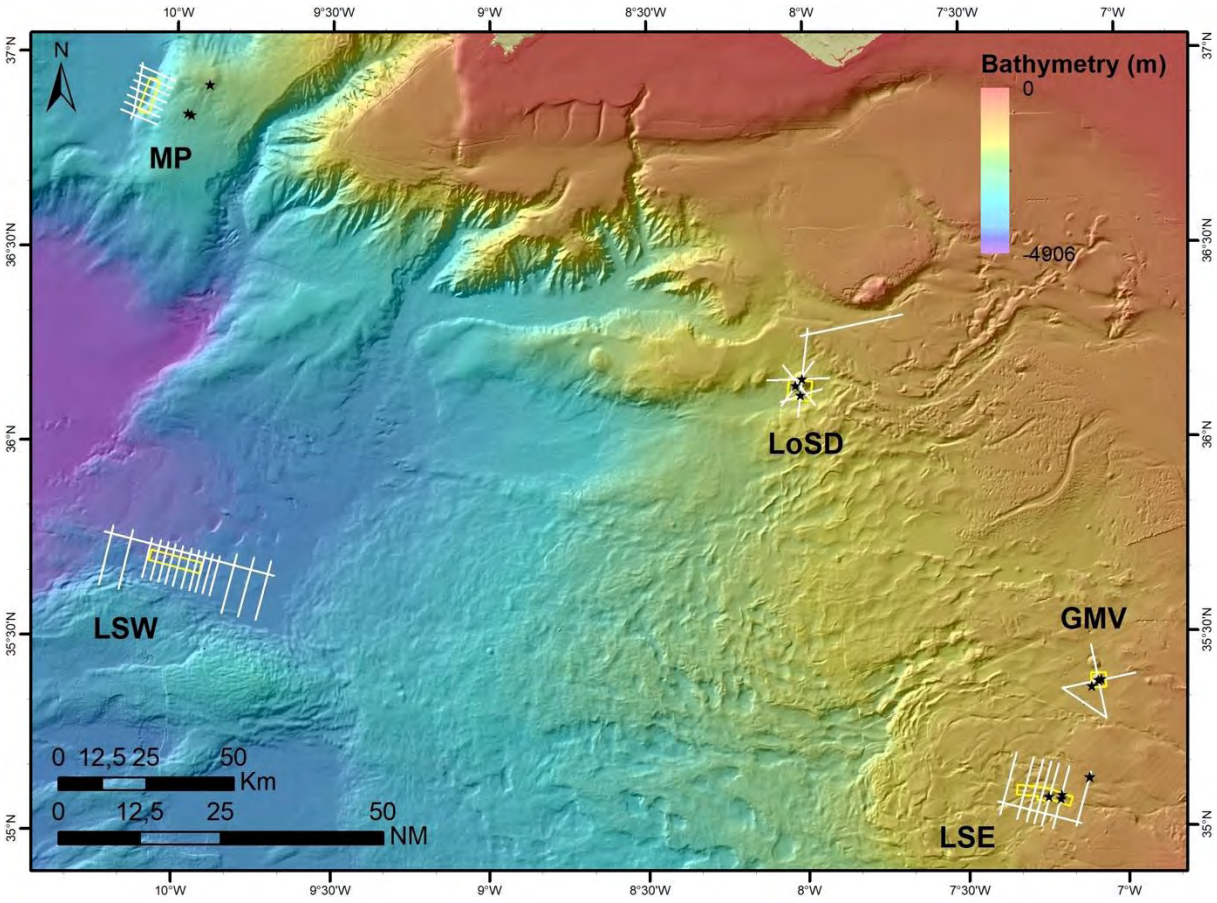

Figure 1.2. *Map of the five study areas of the INSIGHT-Leg 1 cruise.*

The INSIGHT project builds up on more than 15-year experience gained during successive national and European projects and successive cruises to carry out geological and geophysical studies on the South Iberian Margin fault systems and determine their seismic potential. The INSIGHT team is composed by researchers specialized on geomorphology, active tectonics, submarine landslides, marine seismics, geotechnical measurements, and mapping. Members of the team have experience using HOVs, AUVs and ROVs. The INSIGHT cruise represents

a step further in understanding the hazard associated to active faults and submarine landslides in the Gulf of Cadiz.

1.2. The INSIGHT Leg-1 cruise

In the frame of the national project INSIGHT we have been allocated a total of 17 days of shiptime in April-May 2018 onboard the Spanish RV "Sarmiento de Gamboa" to carry out a first ultra-high-resolution study of active faults and slope failures in the Gulf of Cadiz. This cruise has been devoted to acoustic seafloor investigation of selected fault systems and slope failures using the **Autonomous Underwater Vehicle "Abyss"** from GEOMAR-Kiel (Germany) and a **2D-high-resolution seismic system**. The HR-2D seismic system is composed of a 450 m long streamer and an airgun array seismic source system. During the cruise, in addition to the AUV and HR-2D seismic surveys, we will be using other marine geophysical methods, such as swath-bathymetry, parametric sub-bottom profiler and sediment sampling (coring). The INSIGHT-Leg1 cruise has been carried out in the Gulf of Cadiz in the frame of national and international initiatives such as Ocean Facilities Exchange Group (OFEG), COST Action "FLOWS", and ETN "Marie Curie" SLATE.

The INSIGHT-Leg 1 cruise consisted in a 15-day in situ investigation using state-of-the-art underwater vehicles (AUV) to survey the active seismogenic faults and large submarine landslides of the Gulf of Cadiz (Marquês de Pombal Fault and slides, Lineament South-West, Portimao Bank Fault and slides, and Lineament South-East) located in the Portuguese and Moroccan margins. These fault systems have been well characterized (i.e. geometry and kinematics, seismostratigraphy, seismic potential) during previous national and European projects. In the frame of the ongoing Spanish project INSIGHT we were allocated shiptime onboard the Spanish RV "Sarmiento de Gamboa" (SdG) to carry out a *in situ* marine investigation of active faults and associated landslides. The cruise (29 April-18 May 2018) has been devoted to acoustic and high-resolution seismic investigation (i.e. AUV micro-bathymetry, sub-bottom profiler, HR-MCS and gravity coring) to search for surface ruptures, seafloor deformation, submarine slide characterization and fluid flow mud-volcano structures.

The INSIGHT project is directly related to large national and international initiatives related to active faulting, submarine landslides, fluid flow, and seismic hazard, such as: COST Action FLOWS, EMODNET-HRSM, Action MARGES (France), Geo-PRISMS (USA), Integrated-Ocean Drilling Program (I-ODP), MSCA "SLATE" and Fault2SHA.

Figure 1.2. *The AUV Abyss before entering into the container to recover the data.*

Figure 1.3. *Hector Sánchez (UTM-CSIC) doing a training course explaning how to use the bathymetric and parametric echosounders.*

2. Participants

2.1. Scientific personnel

Laia Gràcia i Mont	Chief Scientist ICM-CSIC (Barcelona)	hperea@icm.csic.es
Roger Urgeles Esclasans	Parasound & MCS (Kingdom Suite) ICM-CSIC (Barcelona)	urgeles@icm.csic.es
Rafael Bartolomé de la Peña	MCS processing & QC ICM-CSIC (Barcelona)	rafael@icm.csic.es
Claudio Lo Iacono	Bathymetry processing & QC NOC-Southampton (UK)	cllo@noc.ac.uk
Miquel Camafort Blanco	AUV & MCS planning ICM-CSIC (Barcelona)	camafort@icm.csic.es
Sara Martínez Loriente	Bathymetry & Parasound acquisition ICRAG centre Dublin (Ireland)	sara.martinez@icrag-centre.org
Davide Mencaroni	Bathymetry & Parasound acquisition ICM-CSIC (Barcelona)	mencaroni@icm.csic.es
Cristina S. Serra	Bathymetry & Parasound acquisition ICM-CSIC (Barcelona)	csserra@icm.csic.es
Pedro G. Terrinha	MCS acquisition IPMA-Lisboa (Portugal)	pedro.terrinha@ipma.pt
Morgan Peix	MCS acquisition ENSTA-Bretagne (France)	morgan.peix@ensta-bretagne.org

William Meservy	MCS acquisition ICM-CSIC (Barcelona)	11ery11fi.meservy@icm.csic.es
Eduard Rubio Culebras	MCS processing & dron pilot GEOMEDIA (Barcelona)	eduardrubio@gmail.com
Ennio Piazza	MCS processing UB (Barcelona)	gnegnop@gmail.com
Jonathan Ford	MCS processing OGS-Trieste (Italy)	jford@inogs.it
Zoraida Roselló Espuny	Video and photo aZorafilms (Barcelona)	azorafilms@gmail.com
Marcel Rothenbeck	AUV "Abyss" chief GEOMAR (Germany)	mrothenbeck@geomar.de
Anja Steinführer	AUV "Abyss" processing GEOMAR (Germany)	asteinfuehrer@geomar.de
Emanuel Wenzlaff	AUV "Abyss" Technician GEOMAR (Germany)	ewenzlaff@geomar.de
Torge Kurbjuhn	AUV "Abyss" Technician GEOMAR (Germany)	tkurbjuhn@geomar.de
Zoraida Roselló Espuny	Video and photo aZorafilms (Barcelona)	azorafilms@gmail.com

Figure 2.1. *Scientific, technical and crew parties of INSIGHT-Leg1 in the port of Vigo.*

Figure 2.2. *Scientific, technical and crew parties in the evacuation drill exercise.*

2.2. Technical personnel

Roberto González Álvarez	Chief of UTM Team & mechanics UTM (Barcelona)	rbgonzalez@utm.csic.es

Ezequiel González Bernárdez	MCS acquisition responsible UTM (Vigo)	egonzalez@utm.csic.es
Juan José Martínez Roman	MCS acquisition UTM (Vigo)	jmartínez@utm.csic.es
Héctor Sánchez Martínez	Acoustics acquisition UTM (Vigo)	hsanchez@utm.csic.es
Camilo J. Gómez López	Mechanics (airguns/gravity corer) UTM (Vigo)	cjgomez@utm.csic.es
Mario Sánchez Mosquera	Mechanics (airguns/gravity corer) UTM (Vigo)	msanchez@utm.csic.es
Peregrino Cambeiro Beiro	Mechanics (airguns/gravity corer) UTM (Vigo)	pirri@utm.csic.es
Antonio Sandoval Díaz	Computer technician UTM (Vigo)	sandoval@utm.csic.es

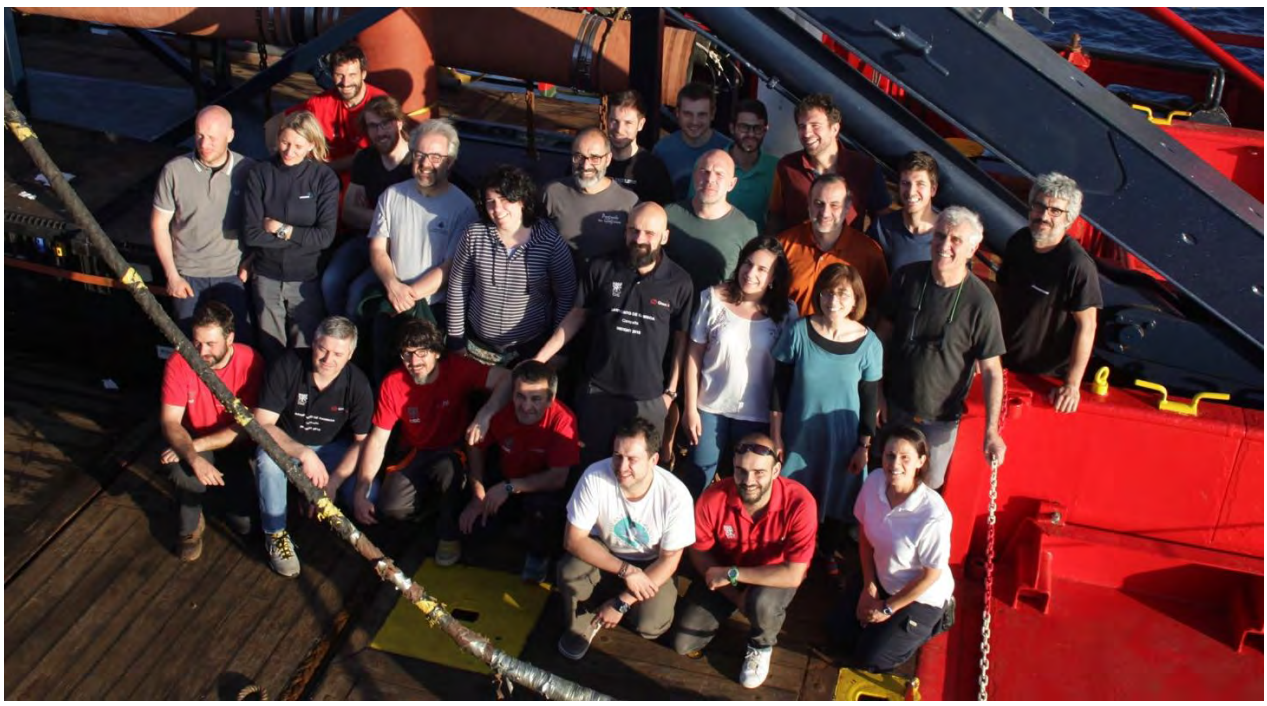

Figure 2.4. *Scientific, technical and crew team at the end of the cruise transiting to Cádiz.*

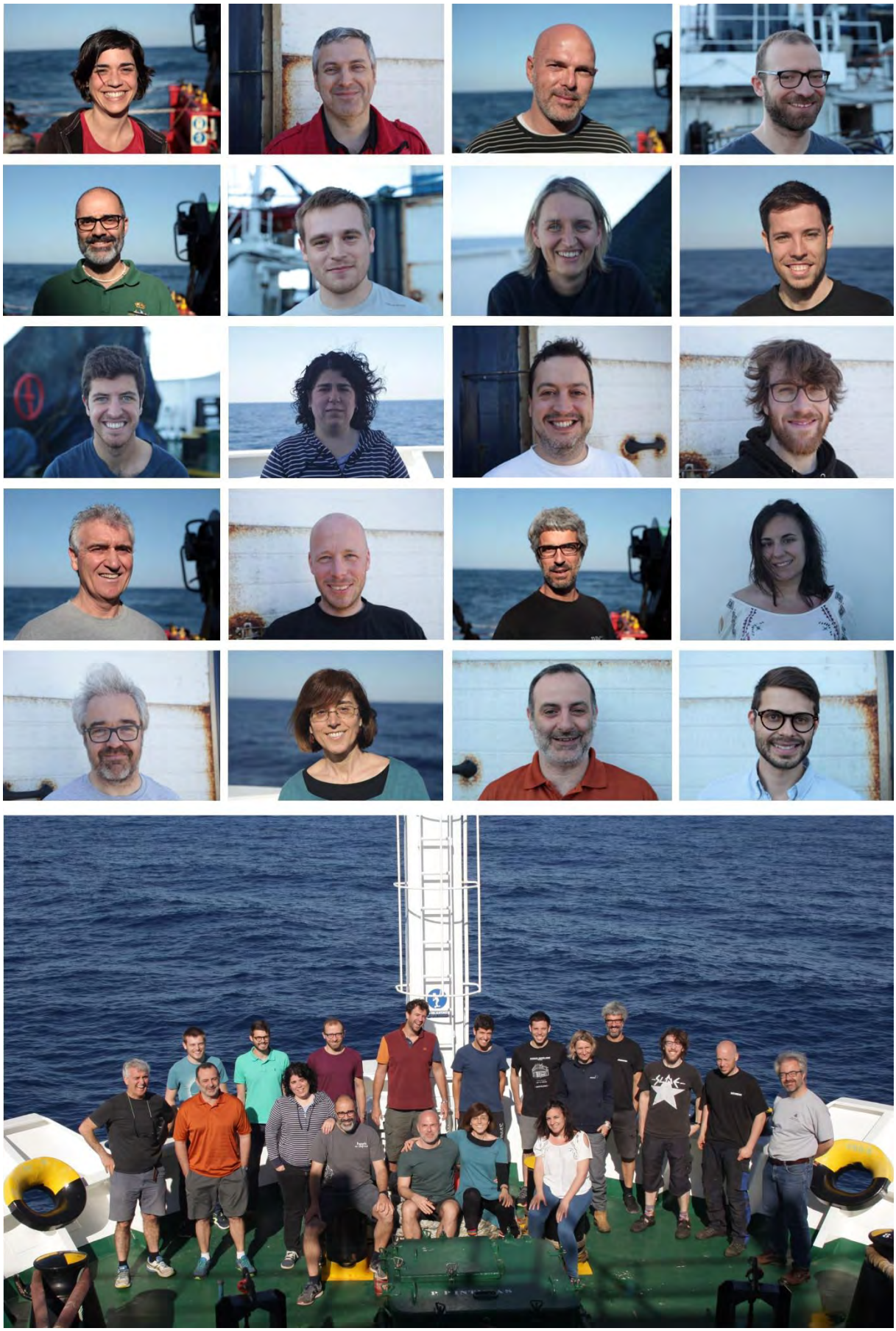

Figure 2.5. *Faces of scientific and technical team, and group photo at the end of the cruise.*

2.3. Crew personnel

José Manuel Pérez Erias	Captain
Arnau Rovira Gols	1st Official
Lidia Yurena Pérez Marcelino	2nd Official
Benjamin Lecuona Fernández	Chief Engineer
Paulino Suarez Seijas	1st Engineer
José Ramón Martinez Bacelar	Bossom
Antonio Fernández Pérez	Marine
Luis Camarés Fortes	Marine
Jose Francisco Trasbach Vidal	Marine
José Carlos Riál Vila	Marine
Jaime Costa Boubeta	Greaser
Juan Carlos Riobo Fernández	Greaser
José Rafael Mesura García	Greaser

Sergio Romero Lema	1st Cook
José Manuel Cousillas Varela	2nd Cook
Miguel Rodríguez Souto	Student
Lidia González Martínez	Student
Debora Baña Méndez	Student

2.4. Acronyms and addresses

1. ICM-CSIC (Barcelona)
Institut de Ciències del Mar – CSIC, CMIMA (Barcelona)
Passeig Marítim de la Barceloneta, 37-49
10 elona
Ph. +34 93 230 95 00 / FAX +34 93 230 95 55

10. **UTM-CSIC (Vigo)**
Unidad de Tecnologia Marina – CSIC, Sede Vigo
Av. Da Beiramar, 29
36202 Vigo (Pontevedra)
Ph. +34 986 21 10 41

10. **NOC (United Kingdom)**
National Oceanography Centre
European Way,
Southampton SO14 3ZH
Ph. +44 23 8059 6666

4. I-CRAG (Ireland)
Irish Centre for Research in Applied Geosciences
University College Dublin
Belfield, Dublin 4
Ph. +353 1 716 2939

5. IPMA (Portugal)
Instituto Português do Mar e da Atmosfera
Av. De Brasília 6
1449-006 Lisboa
Ph: (+351) 213 027 039

6. ENSTA-Bretagne (France)
École nationale supérieure de techniques avancées Bretagne
2 Rue François Verny
29200 Brest
Tel. +33 2 98 34 88 00

7. Hellenic Centre for Marine Research (Greece)
P.O. Box 2214
71003 Iraklion, Crete
Tel +30 2810 337752 / FAX +30 2810 337822

8. Universitat de Barcelona (Spain)
Facultat de Geologia, Campus de Pedralbes
08028 Barcelona
Tel. +34 93 402 13 72 / FAX +34 93 402 13 40

9. Università Di Roma – La Sapienza (Italy)
Piazzale Aldo Moro, 5
00185 Roma
Tel. +39 06 4991 2841 / FAX +39 06 4991 2812

10. International Centre for Theoretical Physics (Italy)
Strada Costiera, 11
34151 Trieste
Tel. +39 040 2240 111

11. Geo Marine Survey Systems (The Netherlands)
Sheffieldstraat 8
3047 AP Rotterdam
Tel. +31 10 4155755 / FAX +31 10 4155351

11. Azorafilms (Spain)
azorafilms@gmail.com
Tel. +34 617 49 32 05

3. The vessel B/O Sarmiento de Gamboa

The oceanographic vessel B/O "Sarmiento de Gamboa" (Figure 3.1) belongs to the Consejo Superior de Investigaciones Científicas (CSIC) and is based in the port of Vigo (Spain), where it was built and launched on January 30th, 2006. The research carried out on this vessel is directed and funded mainly by the R+D+I National Plan and the European Framework Program.

The *Unidad de Tecnologia Marina* (UTM-CSIC) is accountable for the maintenance of the scientific equipment of the vessel and provides the necessary supporting technical staff for the marine expeditions. Since it is a Large Facility, the Ministry of Economy and Competitiveness (MINECO), through the Committee for Coordination of Oceanographic Vessels' Activities (COCSABO), undertake the responsibility for the scientific management of the vessel.

Table 3.1. *Characteristics of the B/O Sarmiento de Gamboa*

Length	70.5 m
Arm	15.5 m
Draw	4.9 m
Maximum speed	15 knots
Autonomy	40 days
Crew	16
Scientists	26
Navigation	2 x radars ARPA ECDIS
	Dynamic positioning DYNAPOS B.V.
Positioning	2 x DGPS
Communication	GMDSS
Satellite communication	INMARSAT F Fleet 77

Table 3.2. *Equipment onboard the B/O Sarmiento de Gamboa*

Acoustics	ATLAS HYDROSWEEP DS (Deep water multibeam echosounder)
	ATLAS Parasound P.35 (Sub-bottom sediment profiler)
Coring	Gravity corer 3 m and 5 m
	Multicorer KC Denmark 6 × ø100 × 600 mm
Water column	Lockheed Martin Sea-Air SystemsSippican MK21
	CTD profiler Sea Bird 911 plus to continuous acquisition with rosette of 24 Niskin bottles and LADCP option

Figure 3.1. *The B/O Sarmiento de Gamboa sailing in the Gulf of Cadiz (dron photo).*

4. Geological setting: The Gulf of Cadiz

The SW Iberian Margin, located at the eastern end of the Azores-Gibraltar zone, is characterized by a significant seismic activity, consequence of the transpressive plate boundary between the Eurasian and African Plates (e.g. Grimison and Chen, 1986). In this area the NW-SE plate convergence (4.5-5.6 mm/year; Nocquet et al., 2004) is accommodated through a widespread tectonically active deformation zone (e.g. Hayward et al., 1999; Zitellini et al., 2009), source of the largest earthquakes and tsunamis that affected Western Europe since historical times.

In the SW Iberian Margin seismicity is characterized by shallow to deep earthquakes of low to moderate magnitude (M_w < 5.5) (Buforn et al. 1995, 2004; Stich et al. 2003, 2006, 2010). However, this region is also the source of the largest and most destructive earthquakes that have affected Western Europe (AD 1531, 1722, 1755 and 1969) (Fukao, 1973) (Fig. 4.1). The 1755 Lisbon Earthquake (estimated M_w > 8.5) destroyed Lisbon (intensity X-XI MSK) and was accompanied by tsunamis that devastated the SW Iberian and NW African coasts (Baptista et al., 1998; Baptista and Miranda, 2009).

On the basis of geological evidence, geophysical data and tsunami modeling (e.g., Gutscher et al., 2002; Gràcia et al., 2003a,b; Zitellini et al., 2004, 2009), different geodynamic models and mechanisms have been proposed for the source of the Lisbon Earthquake (Gutscher et al., 2002; Gràcia et al., 2003a; Zitellini et al., 2004, 2009; Stich et al., 2007; Terrinha et al., 2003). However, none of these models satisfactorily accounts for the estimated magnitude of the earthquake and tsunami arrival times at the different localities onshore.

The deployment of 24 OBS (Ocean Bottom Seismographs) during a year at the external part of the Gulf of Cadiz in the frame of the EU NEAREST project, shows that earthquakes in the Horseshoe Abyssal Plain are generated in the upper mantle at depths between 40 and 60 km (Stich et al., 2010; Geissler et al., 2010). Along the same line the source of deep earthquakes, the Horseshoe Abyssal Thrust (HAT) has been identified on wide-angle seismics modelling (Martínez-Loriente et al., 2014). The HAT suggests onset of subduction at the external part of the Gulf of Cadiz (Martínez-Loriente et al., 2014; Silva et al., 2017). Furthermore, the AD1755 and AD1969 earthquakes (M_w>8.0) occurred around the Horseshoe Plain area.

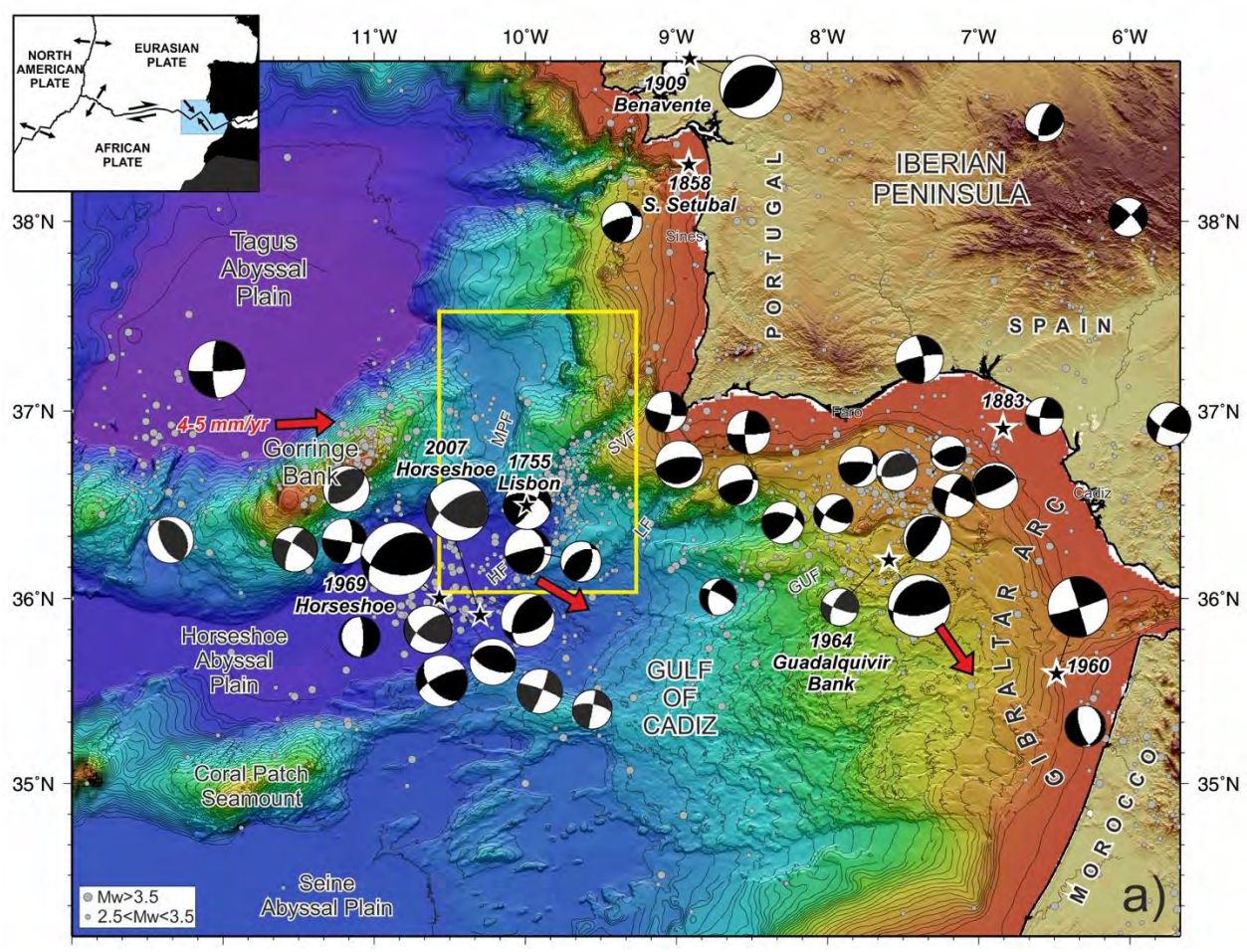

Figure 4.1. *Map of the SW Iberian Margin from SWIM multibeam compilation (Zitellini et al., 2009). Seismicity from the IGN catalogue for the period 1965 to 2015. Small grey dots are epicentres of earthquakes for 2.5<M_w<3.5, and large grey dots are earthquakes of M_w>3.5. Black stars correspond to epicenters of historical and instrumental earthquakes of M_w≥6. Fault plane solutions are also depicted (Stich et al., 2005a,b, 2007, 2010). Red arrows: direction of EUR-AFR convergence. Inset: Plate-tectonic setting of the SW Iberian Margin.*

Main structures and active faults are also located (Gràcia et al., 2003a, 2003b; Zitellini et al., 2009; Terrinha et al., 2003, 2009). The black outlined box depicts the study area presented in Figure 2. GF: Gorringe Fault; MPF: Marques de Pombal Fault; HF: Horseshoe Fault; SVF: Sao Vicente Canyon Fault; LF: Lagos Fault; GUF: Guadalquivir Fault. Inset: Plate tectonic setting of the southwest Iberian Margin along the boundary between the Eurasian and African Plates. The black outlined rectangle corresponds to the area depicted in Figure 1.

Fault investigations have focused on the active structures located at the external part of the Gulf of Cadiz, which correspond to active NE-SW trending west-verging folds and thrusts of the Marquês de Pombal Fault, Horseshoe Fault and Coral Patch Ridge Fault (Gràcia et al. 2003a; Zitellini et al., 2004; Terrinha et al., 2009; Martínez-Loriente et al., 2013). In addition,

long WNW-ESE dextral strike-slip faults referred as SWIM Lineations have recently been identified (Zitellini et al., 2009; Terrinha et al., 2009; Bartolome et al., 2012) (Fig. 4.2).

During the cruise, we focus on specific structures, such as: a) The **Marques de Pombal Fault and slides** (MPF), a 50 km long west verging monocline thrust cutting through the Plio-Quaternary. This fault and associated landslide has been suggested as a potential source of the 1755 Lisbon earthquake (e.g., Gràcia et al., 2003b; Zitellini et al., 2004; Vizcaino et al., 2006); b) The **deep segment of the Lineament South (West)** is a seismogenic, WNW-ESE trending dextral strike-slip fault (Bartolome et al., 2012). It has been further explored in the frame of the COST Action "FLOWS" where we found the presence of deep (>4 km) mud volcanoes, evidence of rising deep fluids and formation of gas hydrates along the fault (Hensen et al., 2015); c) The **shallow segment of the Lineament South** is on the Moroccan Margin and shows the presence of pull-apart basins related to salt structures; and d) The large **mud volcanoes** Ginsberg and Yuma also on the Moroccan margin (Toyos et al., 2016) will allow us to image the 3D geometry of the faults and fault –fluid conduits.

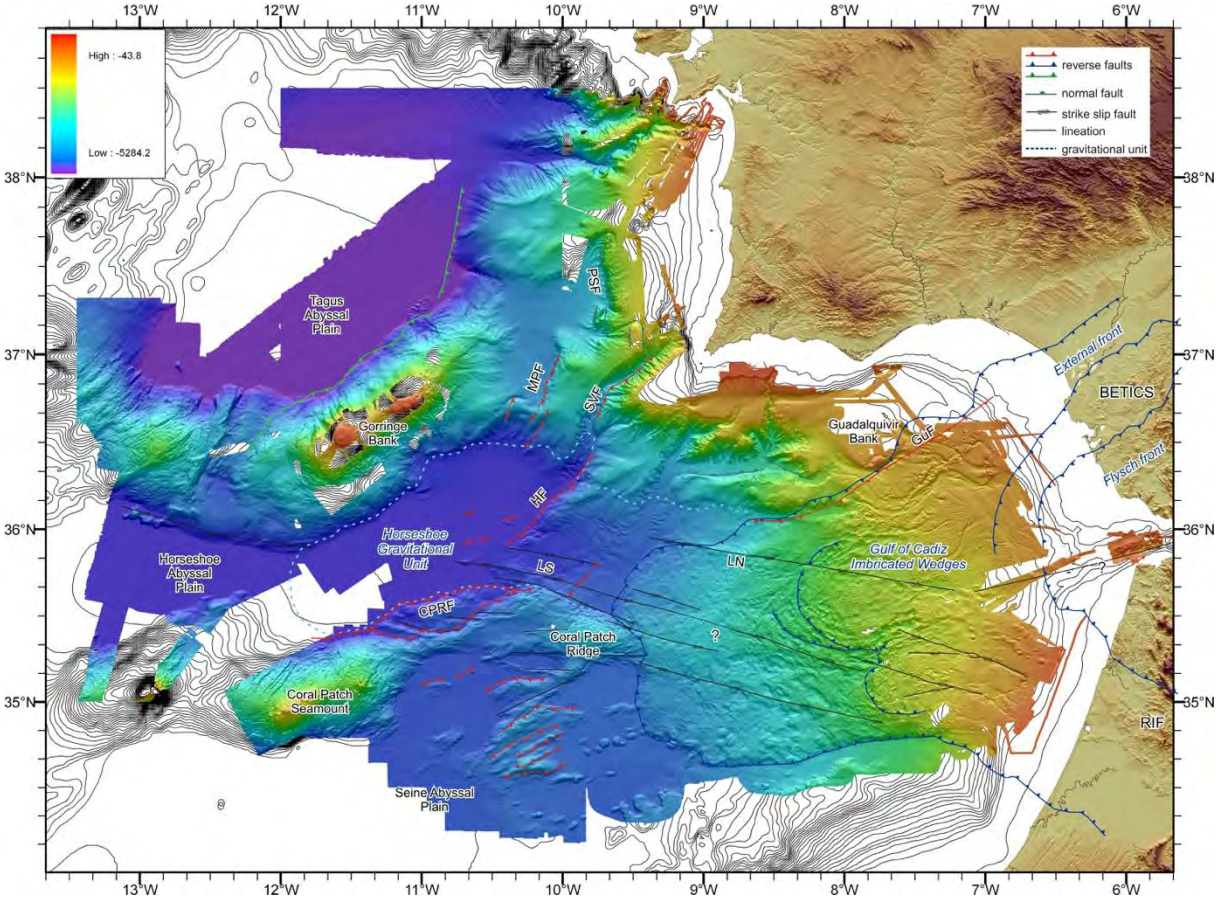

Figure 4.2. *Fault map of the Gulf of Cadiz area. During the INSIGHT-Leg1 cruise we focused on the Marques de Pombal fault and slides (MPF), Lineament South West (LSW), Lineament South East (LSE), Mud volcanoes of the Moroccan Margin and salt diapir.*

5. Objectives of the INSIGHT-Leg 1cruise

The main objective of the INSIGHT-Leg 1 cruise is to investigate with the highest possible resolution the active structures (faults and landslides) recognized in the Gulf of Cadiz, corresponding to Portuguese and Moroccan waters. We will focus specially in the large seismogenic structures, such as the Marques de Pombal Fault and Lineament South (parts West and East), which accommodate part of the AFR-EUR plate convergence. These faults may be the sources of large destructive events, such as the historical 1755 Lisbon earthquake (Mw 8.5) or the 1969 Horseshoe Earthquake (Mw 8.0). Detailed surveys will be carried out in specific areas, such as mud volcanoes in the Moroccan margin, large submarine landslides in the Marques de Pombal block and salt diapirs (e.g. Lolita diapir).

5.1. Specific objectives

The INSIGHT-Leg1 cruise will be the first AUV investigation of active fault systems and submarine landslides in the Gulf of Cadiz. The specific objectives of this cruise are threefold:

1. **Determine the fault seismic parameters of large faults.** The rate at which a fault slips fundamentally determines the seismic hazard that it represents because average earthquake recurrence intervals tend to decrease as slip rates increase. For this reason, it is essential to understand the physical phenomena and definition of the fault seismic parameters regarding: a) Fault geometry (e.g. length, dip, max. seismogenic depth, segmentation) and b) Parameters that control rupture nucleation and dynamics (e.g. rigidity, slip-rate, rupture propagation velocity, frictional behavior). We will use AUV "Abyss" micro-bathymetry to map fault escarpments at unprecedented resolution and the 2D high resolution seismics to accurately obtain dip- and strike-slip rates, depending on the fault kinematics.

2. **Characterizing submarine landslides.** To understand the tsunami potential of submarine landslides we need a better understanding of the dynamics (e.g. velocity and early acceleration history) and geometry (e.g. depth, volume, failure excavation, slope gradient, typology). We will establish parameter distributions for submarine landslides related to the geometry and those that control landslide motion. The mobility of submarine landslides can be analyzed from their vertical and horizontal runout as well as their respective volume. Data may indicate which landslide types are more mobile and their apparent friction coefficients. A regionalization of landslide source parameters will be defined based on comprehensive understanding of the Gulf of Cadiz landslides.

Landslide trigger mechanism/s according to this regionalization will also link to landslide recurrence rates.

3. **Determine the presence of active fluid seepage and characterize its relationship with the occurrence of geohazard-related features.** The occurrence of earthquakes and submarine landslides is strongly dependent on the build-up of pore pressure in the deep and shallow subsurface respectively. Occurrence of pockmarks, mud volcanoes and salt diapirs at the seafloor evidence fluid flow systems and presence of overpressures at various depths. In the Gulf of Cadiz abundant salt and shale diapirism exists it has been shown that there is a close relationship between mud volcanoes, diapirs and tectonic structures (Medialdea et al. 2009) (Fig. 5.1). However, the relationship between fluid seepage, faulting and submarine landsliding is not well constrained in the external Gulf of Cadiz. We will characterize in detail the occurrence of these focused fluid flow systems and determine their relationship to active faulting. We will determine whether the origin of the fluids is deep or relatively shallow, which might result in significantly different types of geohazards (earthquakes vs. landslides). We will also investigate if fluids seep at locations where earthquakes nucleate at depth. Water column imaging capabilities of modern multibeam echosounders (shipboard and AUV) may also reveal active venting of fluids in the water column.

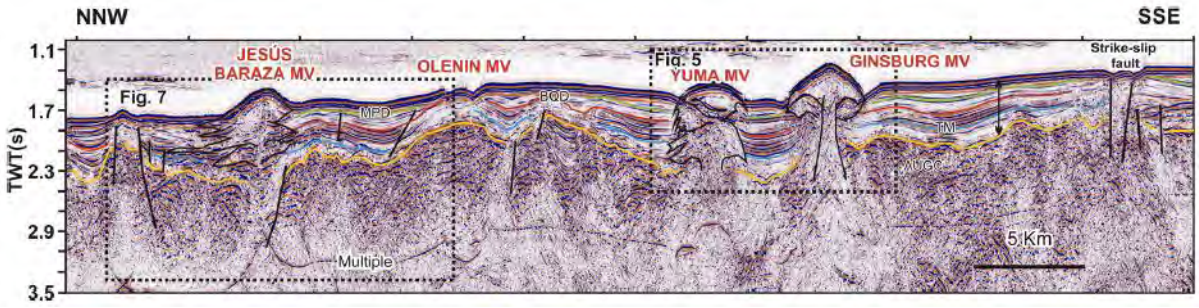

Figure 5.1. *Multichannel seismic profiles across the mud volcano field in the Moroccan Margin of the Gulf of Cadiz (Toyos et al., 2016). During the INSIGHT-Leg1 cruise we devoted a dive to map Ginsburg MV using the AUV "Abyss".*

5.2. Methods

The following methodologies were used during the INSIGHT-Leg1 cruise:

- The AUV "Abyss". This system from GEOMAR- Kiel (Germany) has been used during the first part of the cruise in the frame of an OFEG exchange. This is an autonomous operated vehicle able to dive down to 6000 m depth, an essential requirement to work in the Horseshoe

Abyssal Plain that reaches a maximum depth of almost 5000 m. The AUV can be equipped with the following systems: multibeam echosounder 200/400kHz, high-resolution sidescan sonar 120/410 kHz, 20.2 mega-pixel electronic still camera and other standard sensors (e.g. SBE 49 CTD, fluorimeter and turbidity sensor). Abyss glides at a speed of 4 knots and each dive takes up to 20 hours. The AUV comprises also a Launch and Recovery System (LARS) with a deployment frame installed on the port side or at the stern. During independent AUV data acquisition, we will collect shipboard bathymetry (Atlas Hydrosweep DS), parametric echosounder (Atlas Parasound) and 2D-high resolution seismic data.

The hull-mounted swath-bathymetry system will allow to map un-surveyed areas while the sub-bottom profiler and very high-resolution seismic profiling system will allow to image the shallow sediments below the seafloor. We will also collect sediment samples (gravity/pison corer) to correlate with the sub-bottom profiler and bathymetric data. All these data will be collected using the marine geosciences acoustic instrumentation on board the RV "Sarmiento de Gamboa", which includes:

- Multibeam echosounder ATLAS Hydrosweep DS available on the RV *"Sarmiento de Gamboa"* and characterized by an emission frequency range between 14.5 to 16 kHz. It can collect data at depths between 200 to 11000 m. Swath-bathymetric data and backscatter will be acquired. Acquisition at low speed (2-3 knots) will generate data redundancy allowing to generate grids of a few m cell-size. Hull mounted.

- Parametric sub-bottom profiler ATLAS Parasound P35 is also available on the RV *"Sarmiento de Gamboa"*. It uses a primary frequency of 18-20 kHz and a secondary frequency of 1.5 to 4 kHz. It is simultaneously acquired with the multibeam, it will allow obtaining depth sections with high sediment penetration (> 50 m) and metric vertical resolution. Hull mounted.

- **High-resolution 2D-seismic system** is composed by a 450 m long (9 sections, 50 m long each) near-surface streamer, with 96 channels spaced at 6.25 m. The streamer is towed behind the vessel at a survey speed of 5 knots. The source will be composed by a small volume Ggun-II airgun-array or a Sparker GeoSpark 7000 XF + Geo Source 400 Dual system Towed behind the vessel.

- **Corer system**, using a gravity corer with a pipe up to 5 m long we will be able to collect sediment cores of 10 cm diameter in selected areas where micro-bathymetry and seismics will be acquired. Over the side during sample stations.

6. Navigation and cruise plan

During the INSIGHT-Leg 1 cruise in the Gulf of Cadiz (Figure 6.1), which took place from the 29th April (Vigo) to 17th May (Cádiz), AUV dives, high-resolution multichannel seismic profiles, gravity cores, swath-bathymetry (seafloor and water column) and parametric sub-bottom profiler data has been acquired.

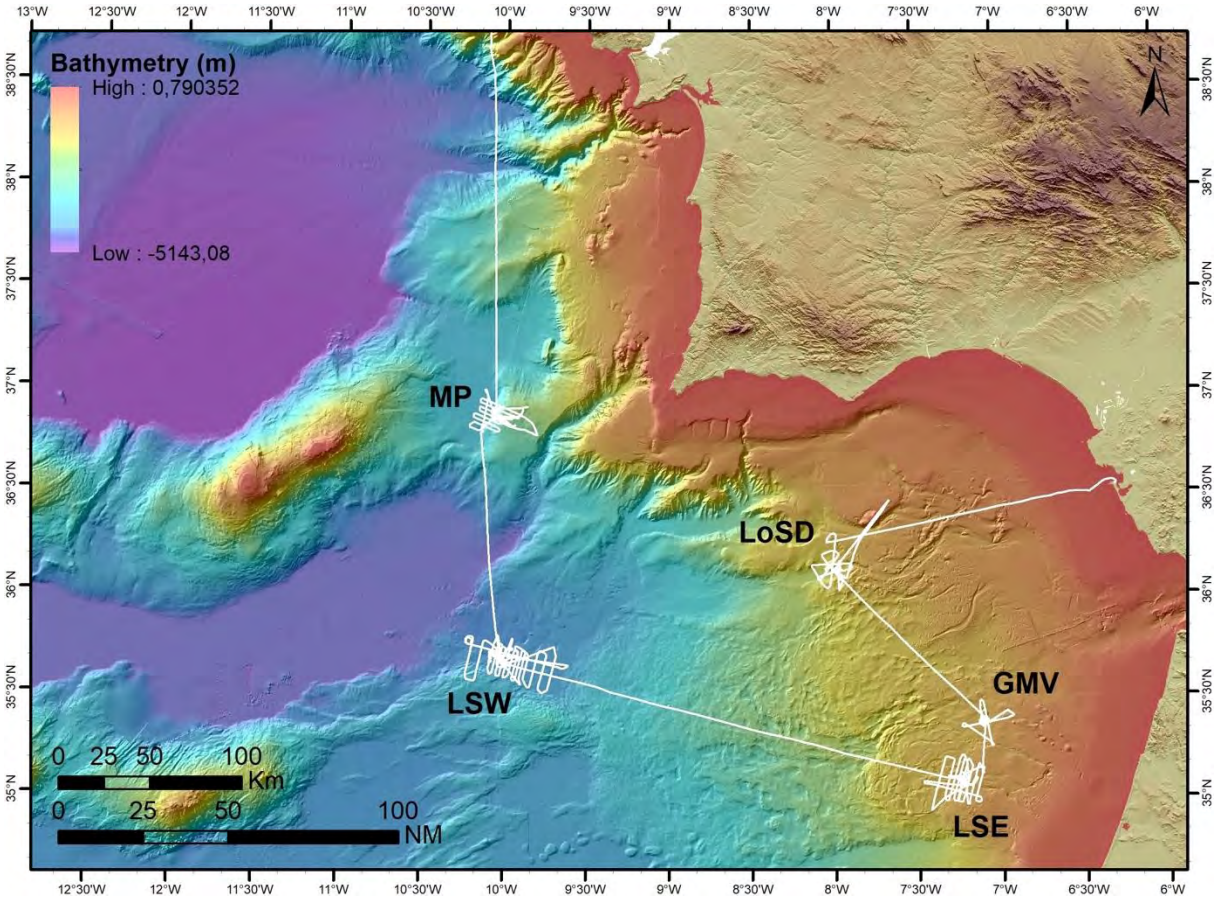

Figure 6.1. *Navigation carried out during the INSIGHT-Leg1 in Gulf of Cadiz.*

A total of 12 AUV dives were done and swath-bathymetry, multichannel seismics profiles, parametric echosounder and 16 gravity cores were acquired along and across the main faults, slides and mud volcanoes of the Gulf of Cadiz. The AUV Abyss (alias "Tiffany") from GEOMAR (Germany) was used to acquire high-resolution bathymetry data (12 dives) in the following localities: a) Marques de Pombal Fault & slide (2 dives), b) Lineament South West (4 dives), c) Lineament South East (3 dives), d) Ginsburg mud volcano (1 dive) and e) Lolita salt diapir and slide (2 dives). The new high-resolution bathymetry and acoustic backscatter covers 9538 km^2 of new data acquired and a total of 3600 km of parametric ehosounder across different environments. The MCS profiles totalize 704 km corresponding to 44 profiles (42902 shots) of new high-resolution seismic data in the Gulf of Cadiz.

6.1. The Marques de Pombal Fault and Slides

The Marques de Pombal Fault and Slides (MPFS) is located in the outer part of the Gulf of Cadiz (between 36º20'N to 37º20'N), in the area between the Gorringe Bank and Cape São Vicente (Fig. 6.2). The MPF is an active 50 km long west verging thrust cutting through the Plio-Quaternary units as evidenced by MCS data (Gràcia et al., 2003a, Terrinha et al., 2003, Zitellini et al., 2001, 2004; Cunha et al., 2010). This fault, together with the Horseshoe Fault was suggested as a potential source of the 1755 Lisbon earthquake (e.g. Gràcia et al., 2003a; Zitellini et al., 2004). Associated to the MPF, mass transport deposits have been recognized at the foot of the MPF block (Gràcia et al., 2003a; Vizcaino et al., 2006). Geotechnical measurements (shear strength and ring shear tests) and pore water analyses were carried out in four cores along on the slides of the MPF (Minning et al., 2006). Turbidite paleoseismology has been carried out at the external part of the SW Iberian margin (Gràcia et al., 2010).

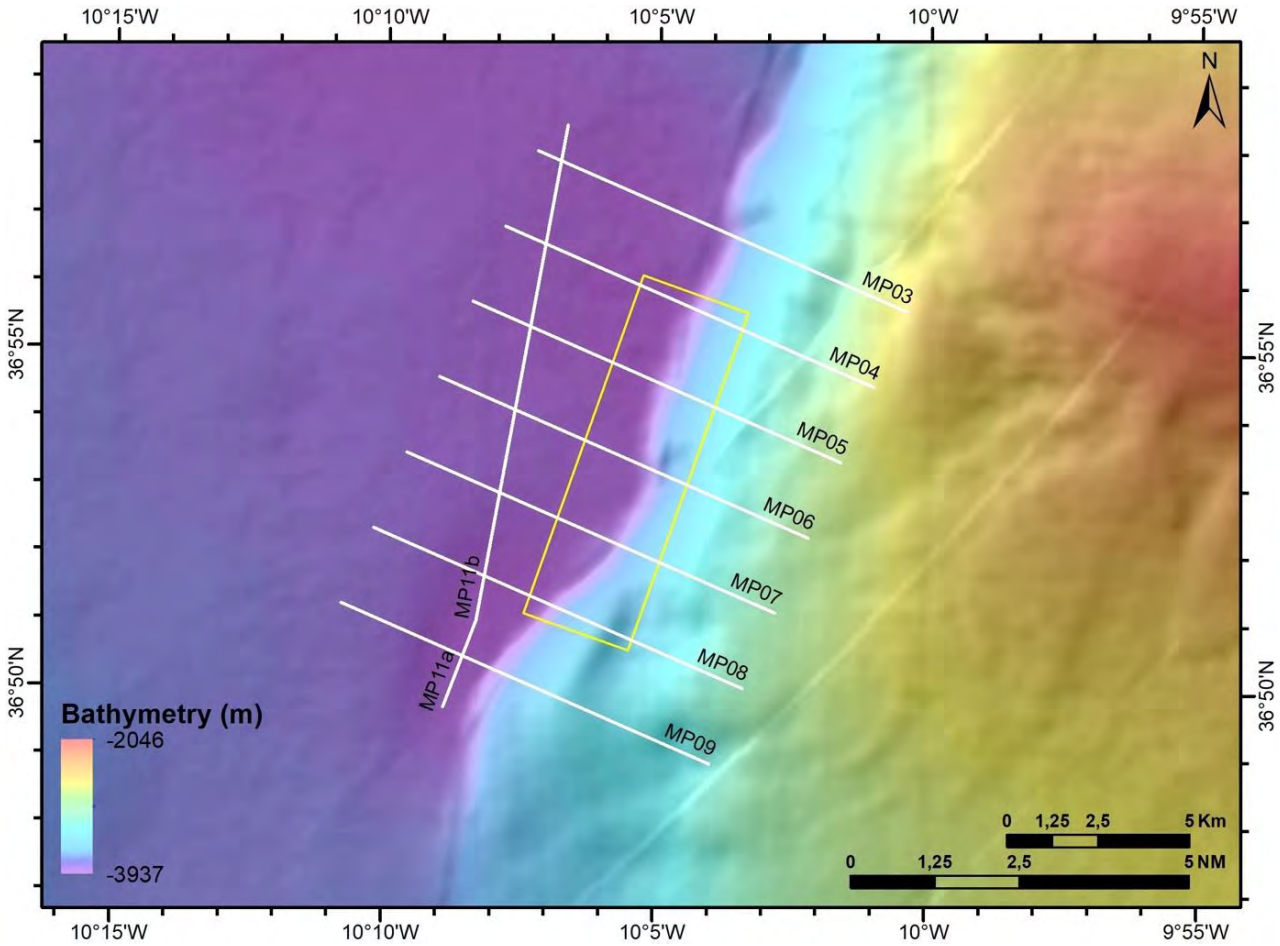

Figure 6.2. *Map of the Marques de Pombal Fault and Slides, with the location of the AUV survey and the HR-MCS profiles acquired.*

6.2. The Lineament South West

The Lineament South West (LSW) is a WNW-ENE–trending (average strike 105° ± 2°) linear morphological feature that extends for 150 km across the Horseshoe Abyssal Plain and the Gulf of Cadiz imbricated wedge (GCIW) (Fig. 6.3). In the MCS profiles, the LSW corresponds to a 2–3-km-wide fault zone. It is associated with a transparent seismic facies bounded by subvertical faults and cuts across the entire sedimentary sequence, which ranges from Mesozoic to Quaternary age. The LSW is a deep-seated subvertical fault that roots in the basement to at least a depth of ~10 km (Bartolome et al., 2012). The lineament south has been conseiderd as the plate boundary between the Eurasian and African Plates (Zitellini et al., 2009). Associated to LSW, deep mud volcanoes located at ~4500 m water depth, outside of their typical geotectonic environment, have been discovered (Hensen et al., 2015). The position of the MVs along the LS fault coincides with a seismically active zone with earthquakes of magnitudes Mw ≤6 nucleating in the upper mantle between 40 km and 60 km depth (Geissler et al., 2010).

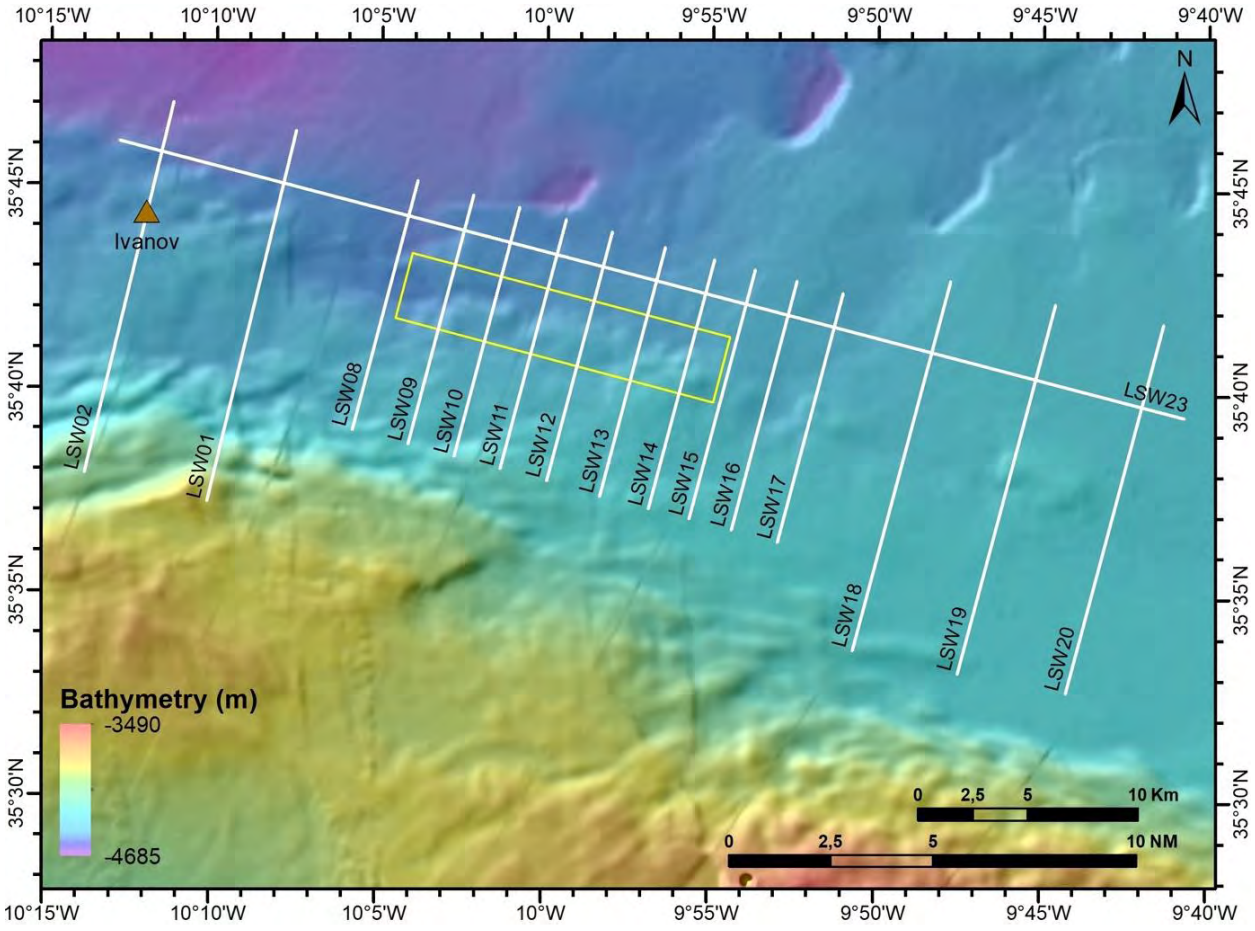

Figure 6.3. *Map of the Lineament South West, with the location of the AUV survey and the HR-MCS profiles acquired.*

6.3. The Lineament South East

The Lineament South East corresponds to the easternmost end of the Lineament South, plate boundary, located in the Moroccan Margin. This lineament cuts across the south lobe of the Gulf of Cadiz Accretionary Wedge. North of this structure there is the Hermes fault (Crutchley et al., 2011), where a 3D high-resolution seismic cube was acquired in a pull-apart basin within the frame of the HERMES project. Geometrical relationships between an array of faults and associated basins show evidence for both dextral and sinistral shear-sense in the Southern Lobe of the Gulf of Cadiz Accretionary Wedge. Strike-slip faulting within the lobe may provide a link between frontal accretion at the deformation front and extension and gravitational sliding processes occurring further upslope. The Lineament South East shows a well-developed pull-apart basin and a fault trace with different branches. On the MCS profiles we recognized abundant salt layers and domes.

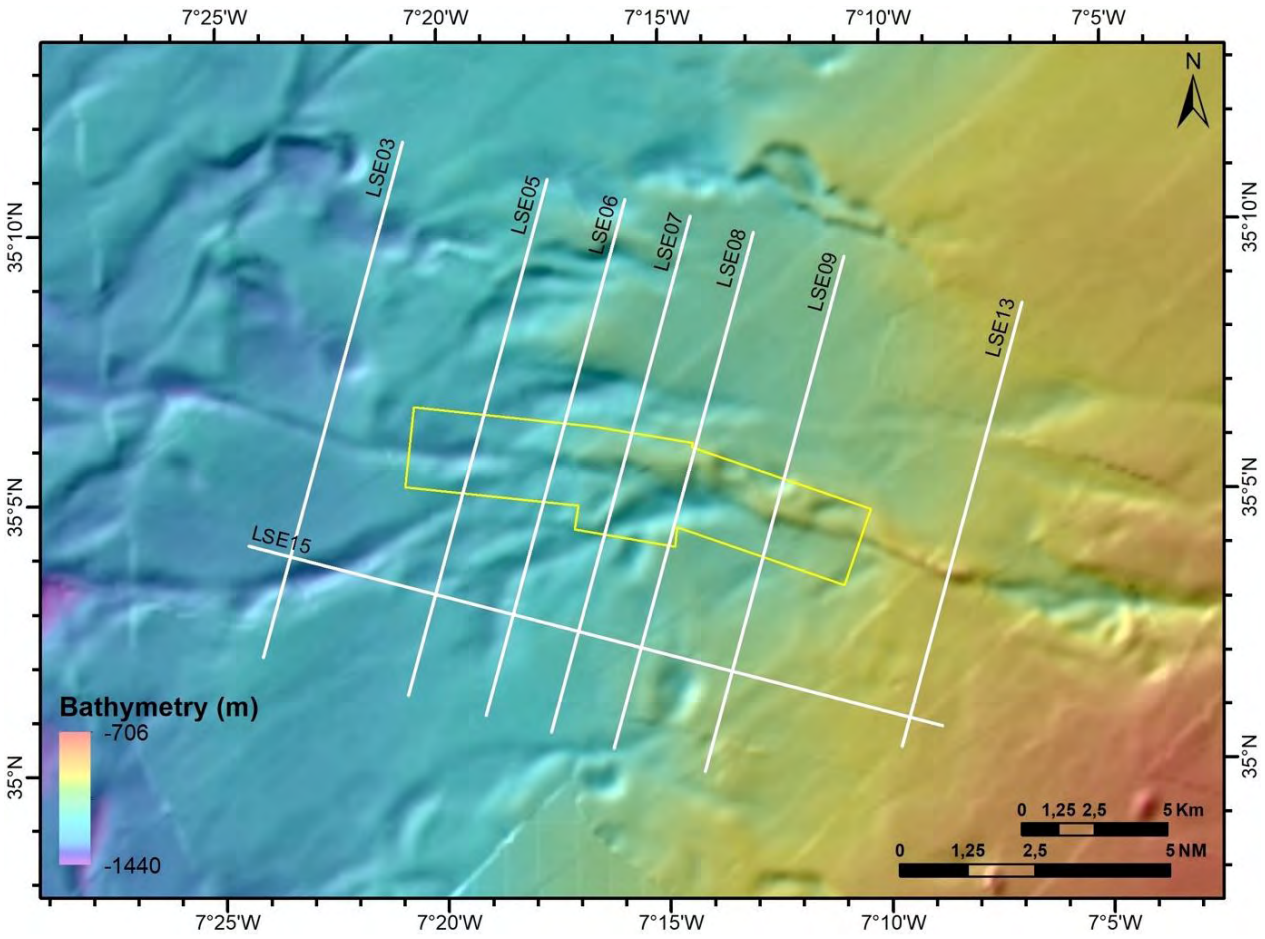

Figure 6.4. *Map of the Lineament South East, with the location of the AUV survey and the HR-MCS profiles acquired.*

6.4. The Ginsburg Mud Volcano

The Gulf of Cádiz has become an area of increased interest for the scientific community due to the presence of widespread seabed fluid venting-related features indicative of intense hydrocarbon seep activity along the continental slope of the Iberian and African margins (Mascle et al. 2014). The most prominent are numerous mud volcanoes (MVs), together with large pockmark fields and carbonate-mud mounds bearing authigenic carbonates (e.g. Somoza et al., 2003; Van Rensbergen et al., 2005; Medialdea et al., 2009; León et al., 2012). Submarine mud volcanoes were first identified in the Gulf of Cádiz in 1999 west of Morocco (Somoza et al. 2003). Since then, more than 60 mud volcanoes have been investigated on this margin in water depths of 350 to 4000 m. The Ginsburg MV is a circular, cone-shaped NNW–SSE elongated cone 280 m high and 3,860 m in maximum diameter. The edifice is topped by a dome (33 m high, 715 m in diameter) located at 909 m water depth, which shows high backscatter values (Toyos et al., 2016), and is surrounded by an irregular rimmed depression. Three lobes can be distinguished related to outflow mud pulses.

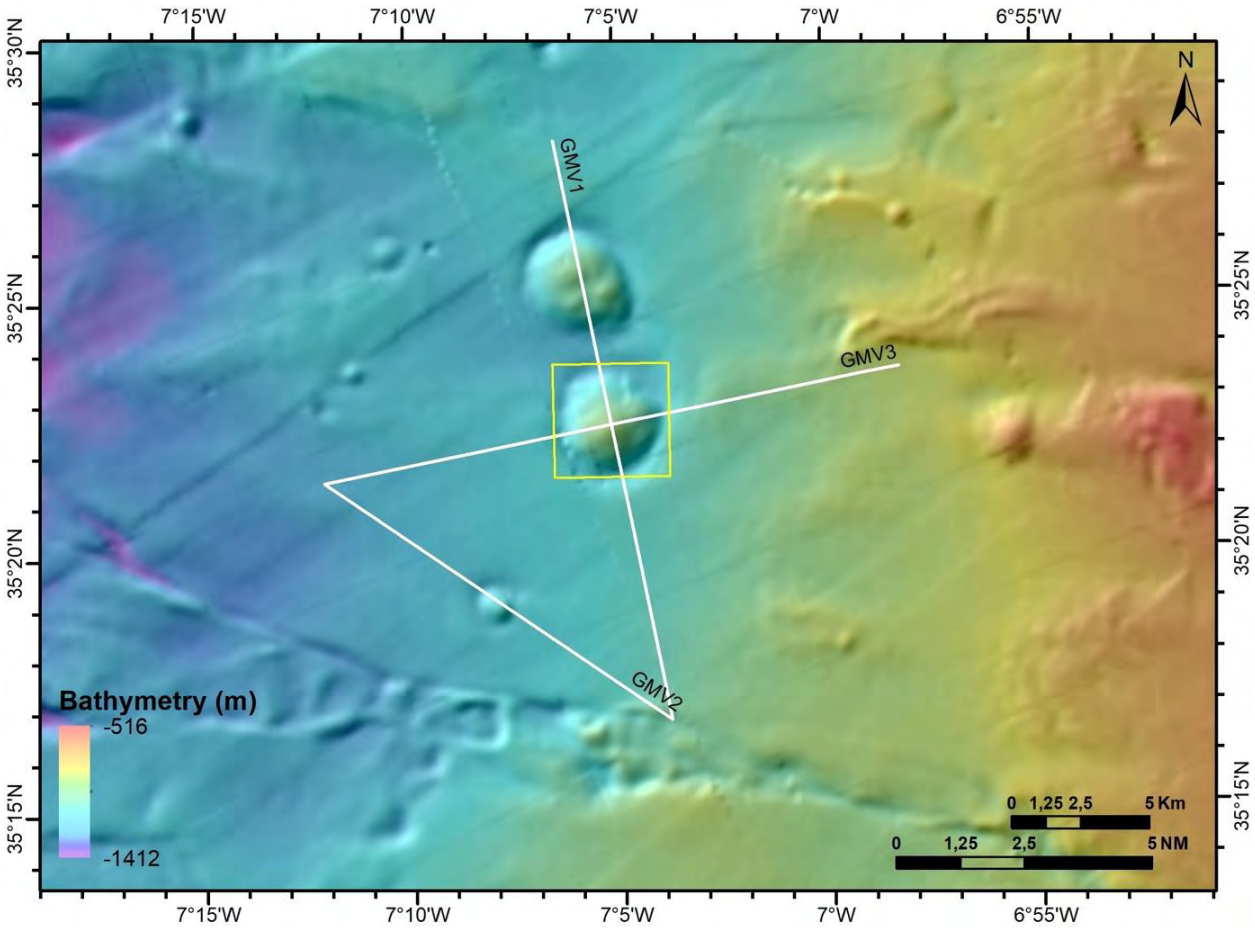

Figure 6.5. *Map of the Ginsburg Mud Volcano, with the location of the AUV survey and the HR-MCS profiles acquired.*

6.5. The Lolita Salt Diapir

A series of morphological structures, such as scars and escarpments related to seafloor instabilities, have been observed in the Gulf of Cadiz. According to the geometry of the slide scars, the slope angle, the surrounding seafloor morphology and the mechanical parameters of the sediment, we suggest the likely mechanisms initiating the failures for the different types of observed structures. Most of the small-scale sediment failures ($\leq$ 2 km^2) seem directly related to dome-like structures (where slopes are steep) or are located in the vicinity of such structures (fluid flows). It appears that progressive deformation or fluid flow related to the growing of domelike structures may have weakened the sediments sufficiently to bring steep slopes to metastable conditions. Our study case is the Lolita Salt Diapir, located in the Cadiz Valley. The Lolita Salt Diapir is a large structure (diapiric structure related to salt dynamics) located in the Cadiz Valley (Portuguese waters) and consists of a rounded dome, which has collapsed due to diverse processes, such as gravitational forces, mud eruption or small tremors. Steep slopes likely associated with fluid transfer in sensitive layers of mud volcanoes may be the triggering mechanism (Toyos et al., 2016).

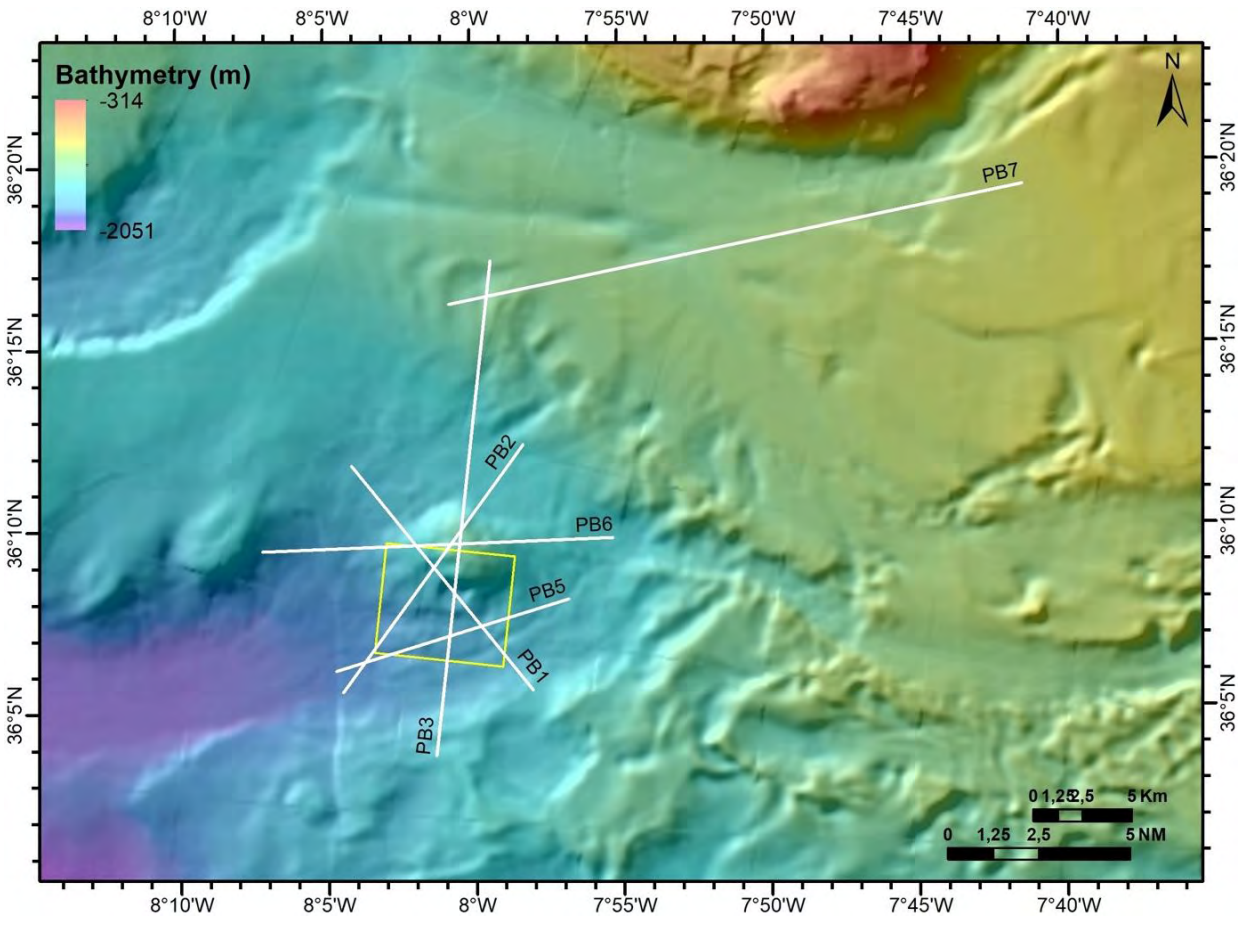

Figure 6.6. *Map of the Lolita Salt Diapir, with the location of the AUV survey and the HR-MCS profiles acquired.*

7. Multibeam bathymetry

7.1. Introduction

During the INSIGHT Cruise Leg-1 the swath bathymetry MB data were acquired with the ATLAS Hydrosweep DS multibeam echosounder. The ATLAS DS works at a frequency ranging between 14.5 and 16 kHz. It operates between 10 to 11000 m, with a maximum vertical resolution of 6.1 cm, and 0.5 m of accuracy. The maximum angular coverage is 5.5 times the water depth (140º), with up to 141 hardware beams, 1ºx1º, corresponding to 345 beams with High Order Beam forming. The echosounder also acquires acoustic backscatter, whose processing was still in a preliminary stage during the creation of this Cruise Report. All beams are calibrated in real time for the ship attitude (roll, pitch, yaw, heave) and dynamic beam focusing is applied. The ATLAS Hydrosweep DS is operated by a standard commercial computer through the ATLAS Hydrosweep Control software, which include controls for the main acquisition and visualization settings (swath, backscatter, frequency, coverage, main acquisition filters).

The echosounder has four interfaces: the motion and position correction sensor Applanix POS-MV, the EIVA NaviScan navigation software, a surface water velocity sensor and the acquisition system Teledyne PDS. The acquired swath-bathymetric data were eventually processed onboard through the CARIS HIPS and SIPS software (Ver. 10.3).

7.2. The multibeam echosounder ATLAS Hydrosweep DS

The ATLAS Hydrosweep DS echosounder software is composed of three main modules, each one with specific functions:

1. HYDROSWEEP Control: it allows for the control of the multibeam acquisition settings. Once the configuration for the working scenario is loaded, it is recommended to change only the depth range for the forced bottom search, source power (lower for shallower areas) and swath angle (determining the spatial coverage of the emitted swath). The Display Cross Profile window allows for the visualization of the raw data in real time and a first quality control of the data. The best observed results were obtained with a navigation velocity of 3.5 knots and setting the swath angles covering from 200% to 150% of water depth. Data achieved at greater angles showed considerable artefacts in the acquired external pings. These errors have been minimized as much as possible in order to make easier the subsequent data processing.

2. ATLAS PARASTORE: this module controls the hard disk data storage.

3. TELEDYNE PDS: it allows for the real time visualization and control of acquired bathymetric data (Fig. 7.1). This module shows graphical display for all ship motion sensors, as depth and sidescan profiles. Moreover, a preliminary real-time coverage map is created after gridding the acquired data. The software also supports the display of the ship and the track along with background graphical layers, which are useful to control the acquisition over previously surveyed areas. It produces the raw data in the .s7k format (new Teledyne-ATLAS format).

The EIVA NaviScan software allowed for visualization of the MB acquisition (surface maps), setting of navigation and planning of runlines and waypoints during the cruise. The visualization of MB coverage in the new NaviScan version required the settings to be included in the old version. This is the reason to run both versions in the same time (Fig. 7.1).

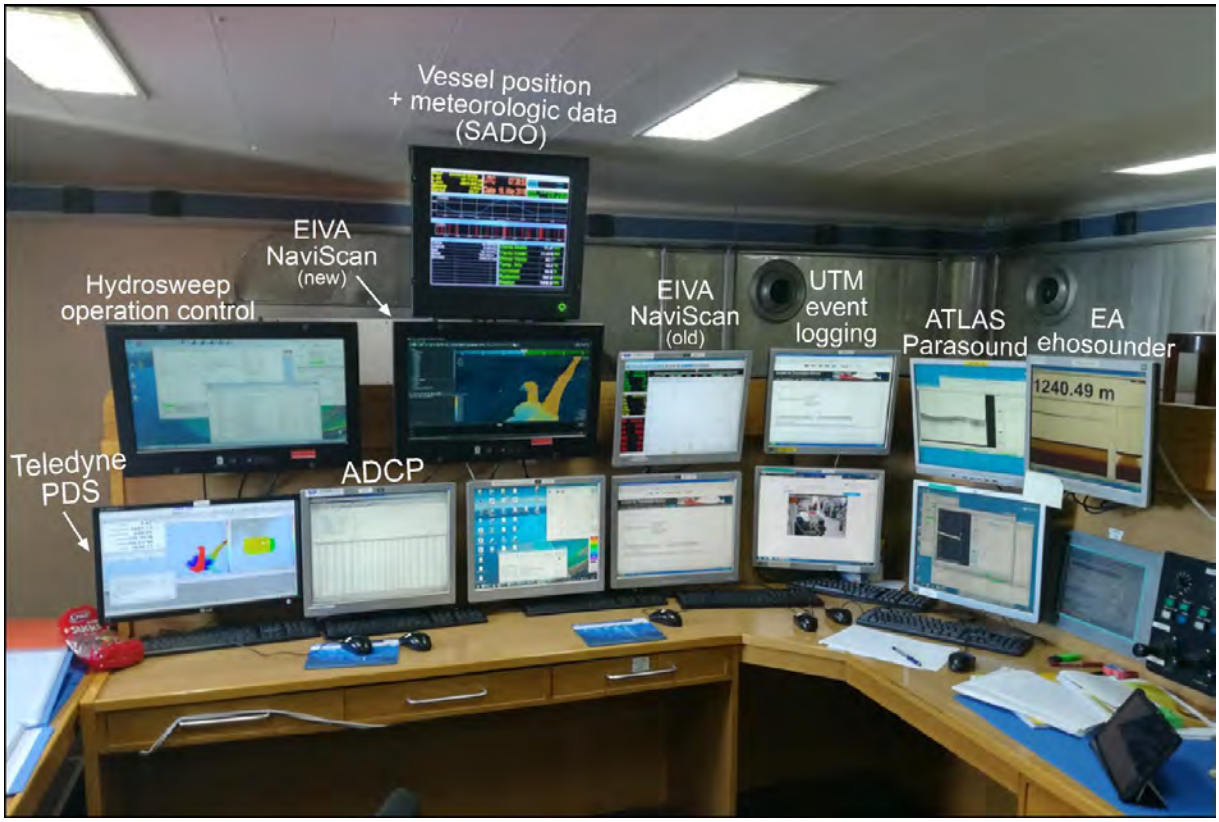

Figure 7.1. T*he MB acquisition work-station, as set during the INSIGHT-Leg 1 cruise.*

7.3. Multibeam echosounder calibration

At the start of the expedition, the attitude sensors were specifically calibrated for the INSIGHT Cruise, mainly regarding the pitch and roll errors. Roll calibration was performed acquiring MB data at the maximum swath width (open angles) along a single line on a sub-horizontal sector, towards the two opposite directions. Pitch calibration was performed acquiring MB data at the minimum swath width (close angles) along a single line on a steep sector, towards the two opposite directions.

The calibration lines were:
2018504_070621_Gamboa.s7k; 2018504_080621_Gamboa.s7k;
2018504_090406_Gamboa.s7k; 2018504_095821_Gamboa.s7k;
2018504_103152_Gamboa.s7k.

After attitude calibration, the resulting roll and pitch values were **-0.75** and **2.38,** respectively.

SVP CALIBRATION: The sound velocity was calibrated by means of the CTD probe installed on the AUV ABYSS (Seabird SBE49). CTD data were extracted from each AUV dive, performed in the different surveyed areas. Data were subsequently processed and included in the CARIS project (see below "MB data processing flow"). The main reason for using the AUV CTD data in the SVP calibration instead of the standard XBT probes was the incorrect functioning of the XBT acquisition (an issue that has been solved only at the end of the Cruise. See the UTM technical report). Furthermore, the operational depth of the XBT probes is by far shallower than the surveyed depth in part of the INSIGHT study areas. This implies that the sound velocity across the deepest water column should be extrapolated from the shallower data, with consequent possible errors in the velocity calibration.

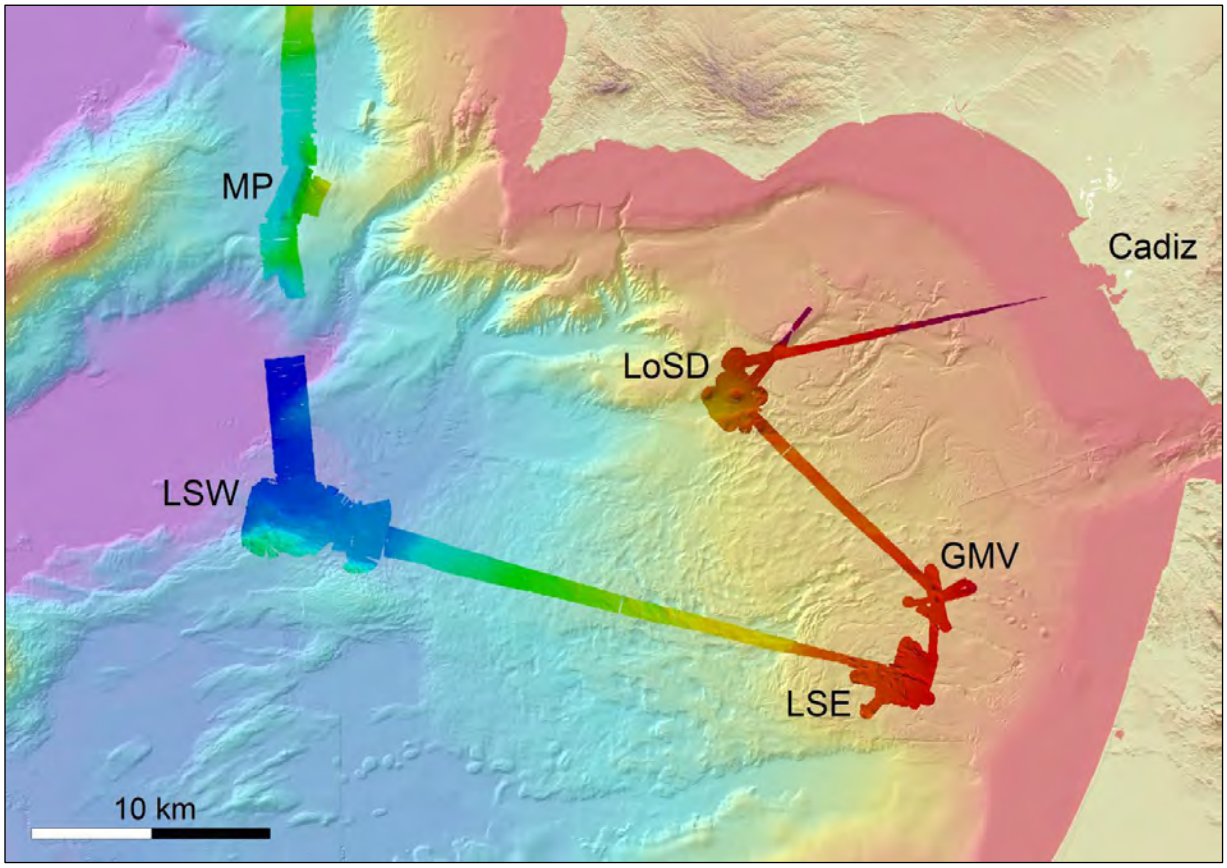

Figure 7.2. *Shipboard bathymetric data acquired in the Gulf of Cadiz during INSIGHT-Leg1 cruise*

7.4. Multibeam maps of the INSIGHT-Leg 1 cruise study areas

Five main areas were mapped during the INSIGHT-Leg 1 cruise (Figs. Xx.2 -xx.9):

- The Marques de Pombal area – MP (from 1 to 3 May; depth range: 2200-3950 m)
- The Lineament Sur – West sector area – LSW (from 4 to 8 May; depth range: 3700-4720 m)
- The Lineament South -East sector area – LSE (from 9 to 12 May; depth range: 805 – 1830 m)
- The Ginsburg Mud Volcano – GMV (from 12 to 13 May; depth range: 710 – 1230 m)
- The Lolita Salt Diapir area – LoSD (from 13 to 17 May; depth range: 460 – 2340 m)

MB data were acquired in parallel with the acquisition of the multichannel seismic lines, at an average navigation speed of 3.5 knots. Data acquisition was interrupted during the AUV deployment and recovery operations and during the collection of gravity cores. Below we present

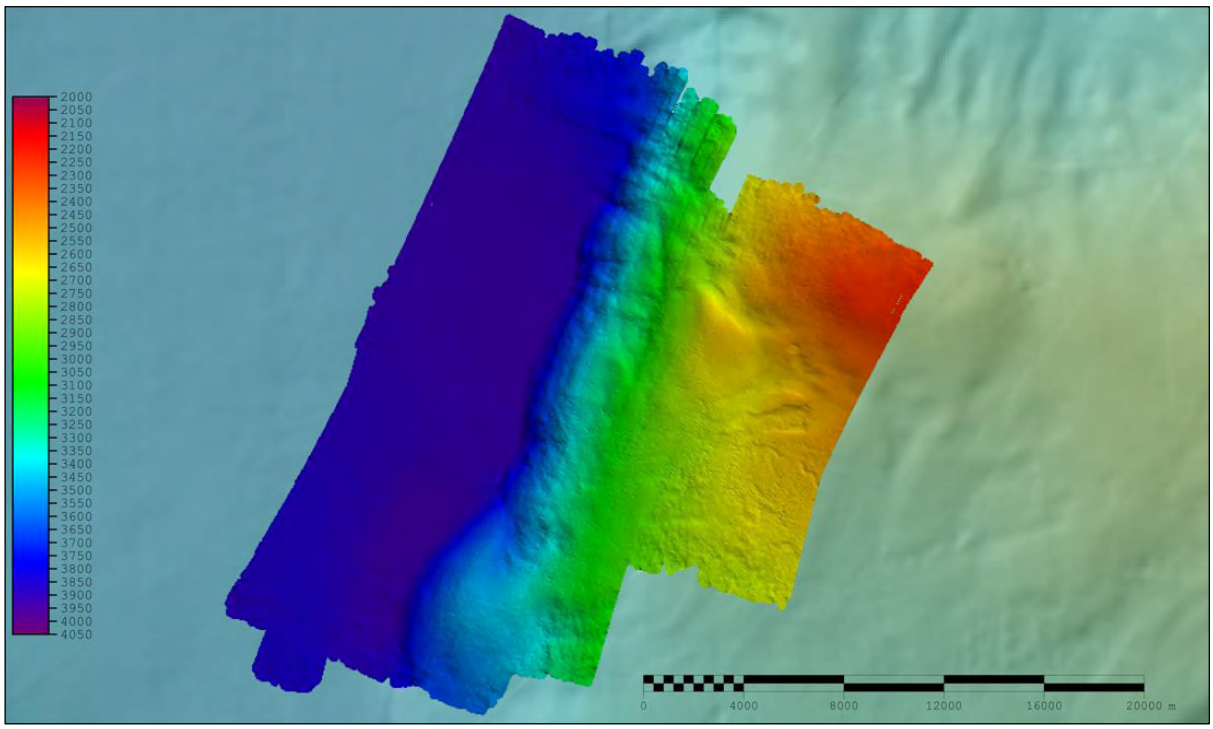

Figure 7.3. *Bathymetric map of the Marques de Pombal area (MP). Pixel resolution: 50m.*

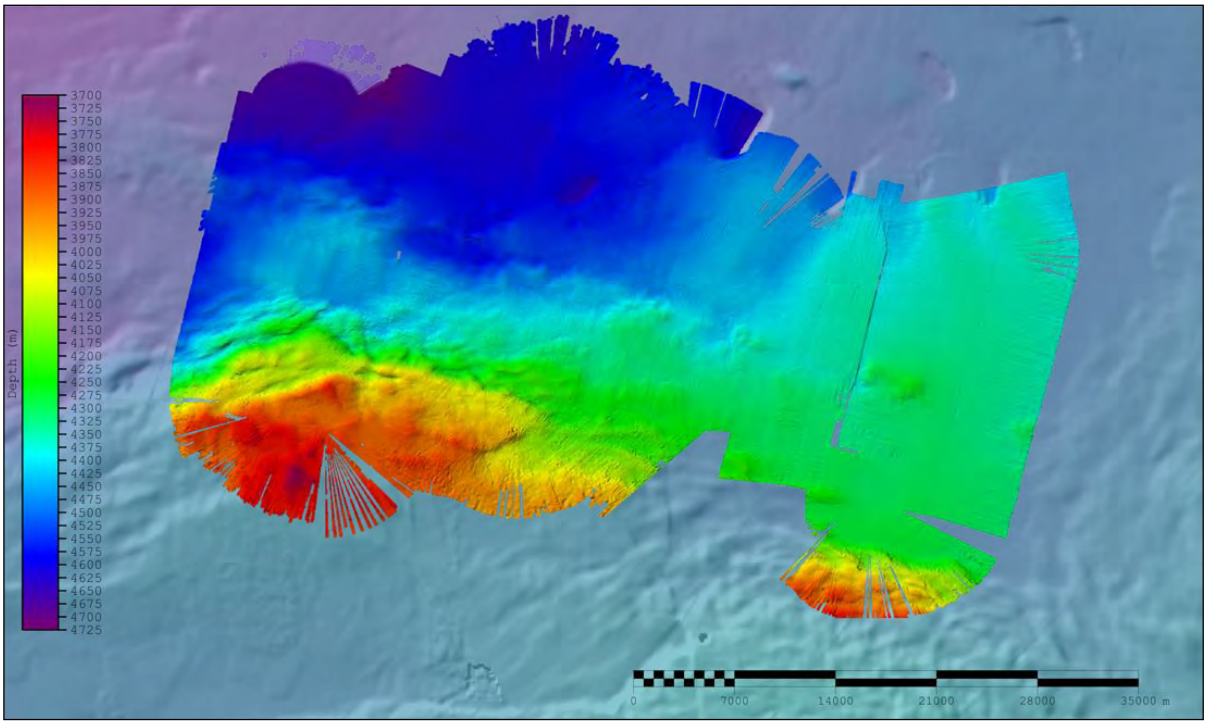

Figure 7.4. *Bathymetric map of the Lineament South – Western sector (LSW). Pixel resolution: 50m.*

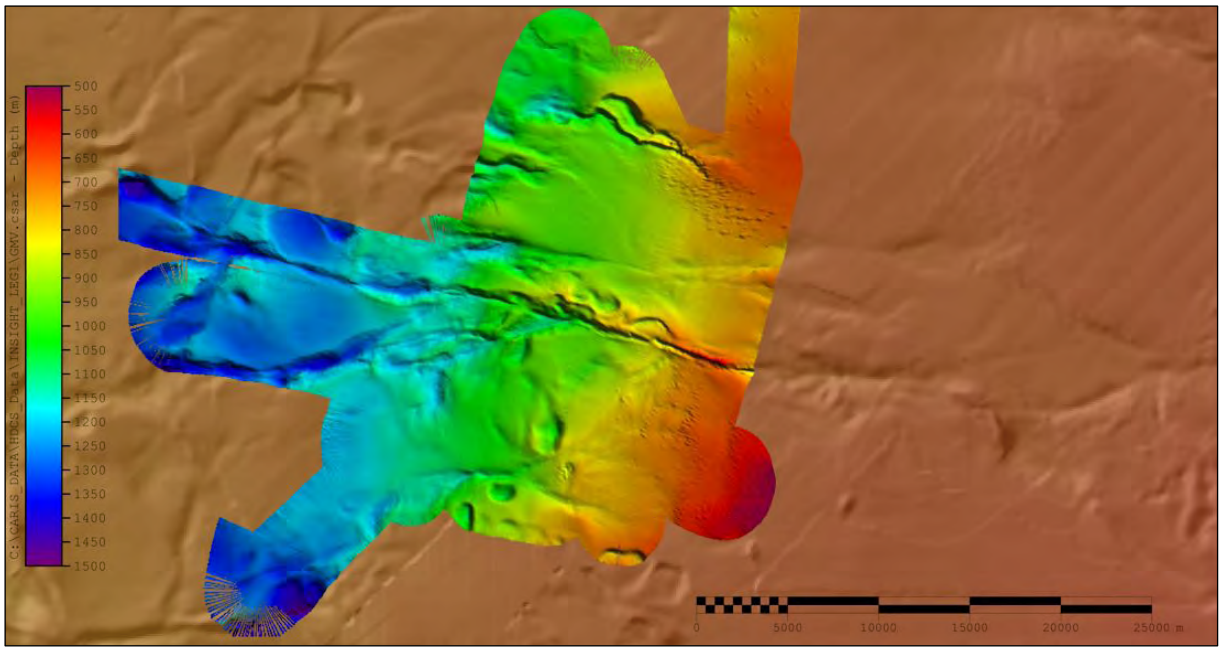

Figure 7.5. *Bathymetric map of the Lineament South – Eastern sector (LSE). Pixel resolution: 50m.*

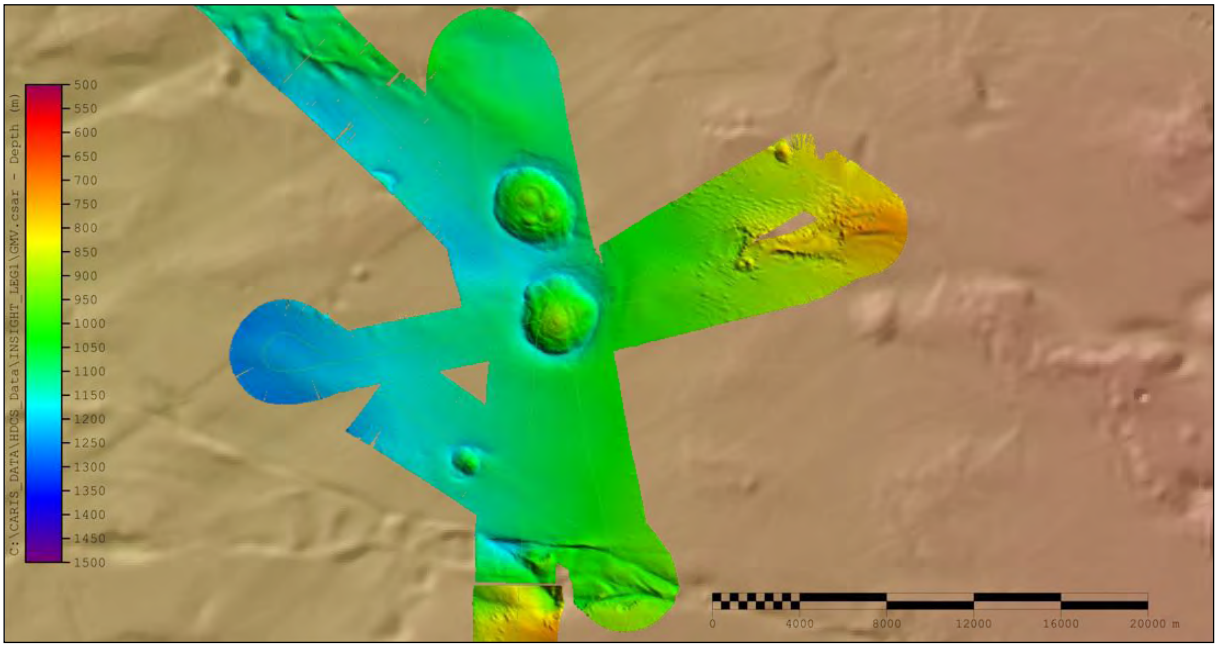

Figure 7.6. *Bathymetric map of the Ginsburg (south) and Yuma (north) Mud Volcanoes (GMV). Pixel resolution: 50m.*

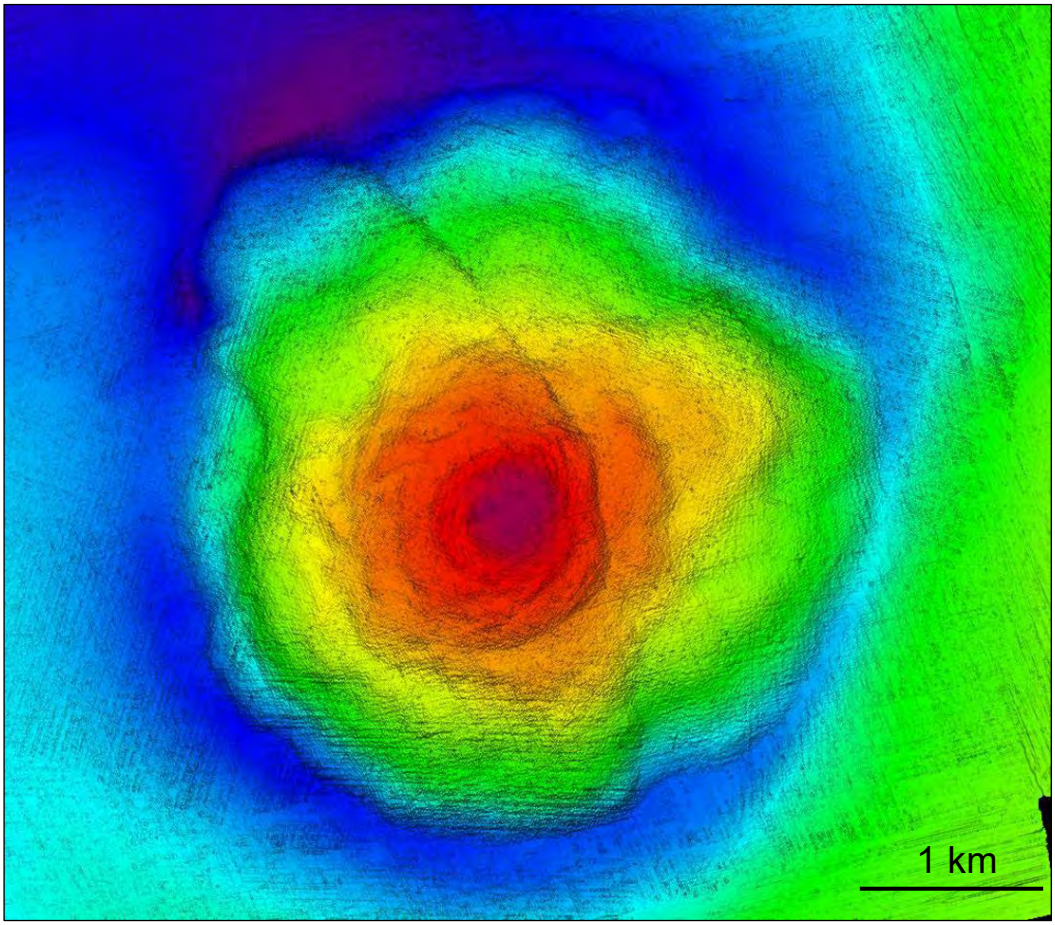

Figure 7.7. *High-resolution hull-mounted MB map of the Ginsburg Mud Volcano. Pixel resolution: 10 m. Approx depth range: 920 – 1200 m. Note the full coverage map at high spatial resolution despite the depth of the surveyed area, due to the increased density of the beams produced by the DS ATLAS Hydrosweep.*

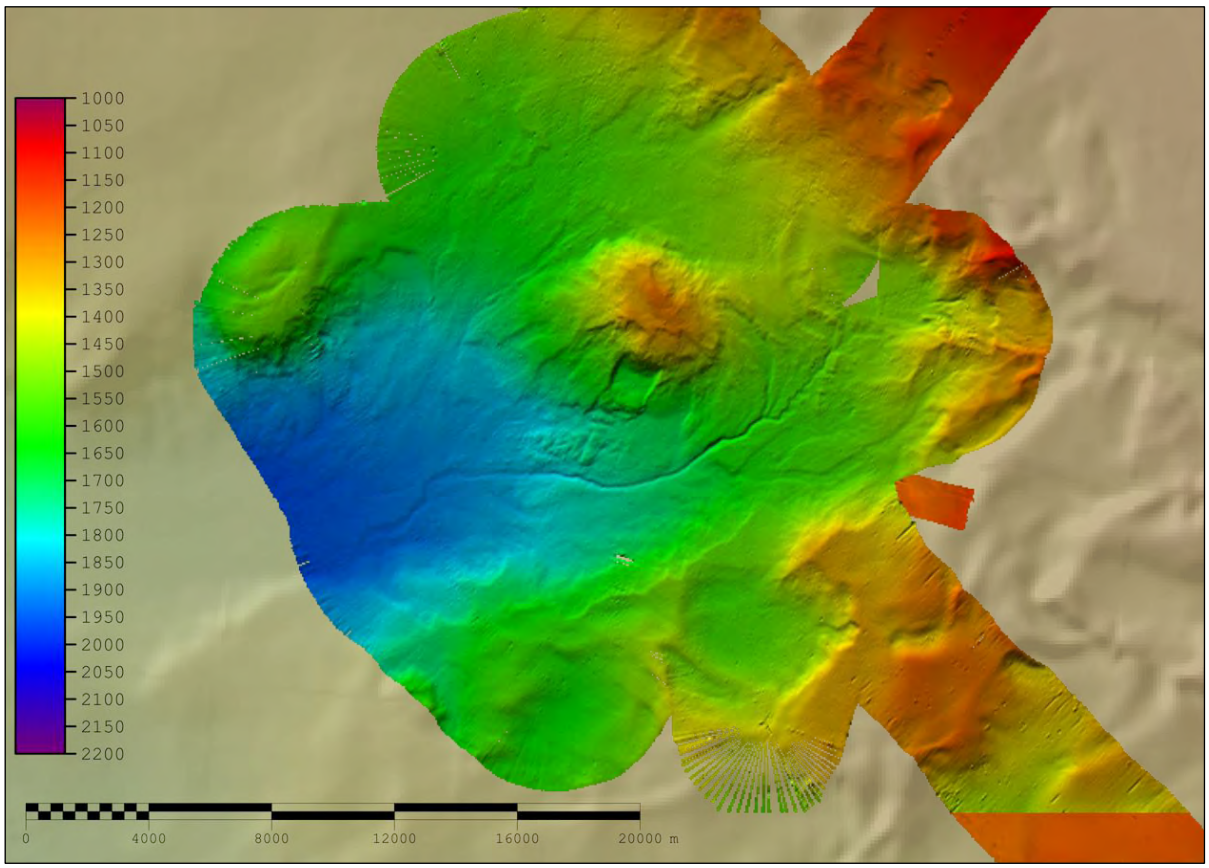

Figure 7.8. *Bathymetric data acquired of the Lolita Salt Diapir region (LoSD). Pixel resolution: 50m.*

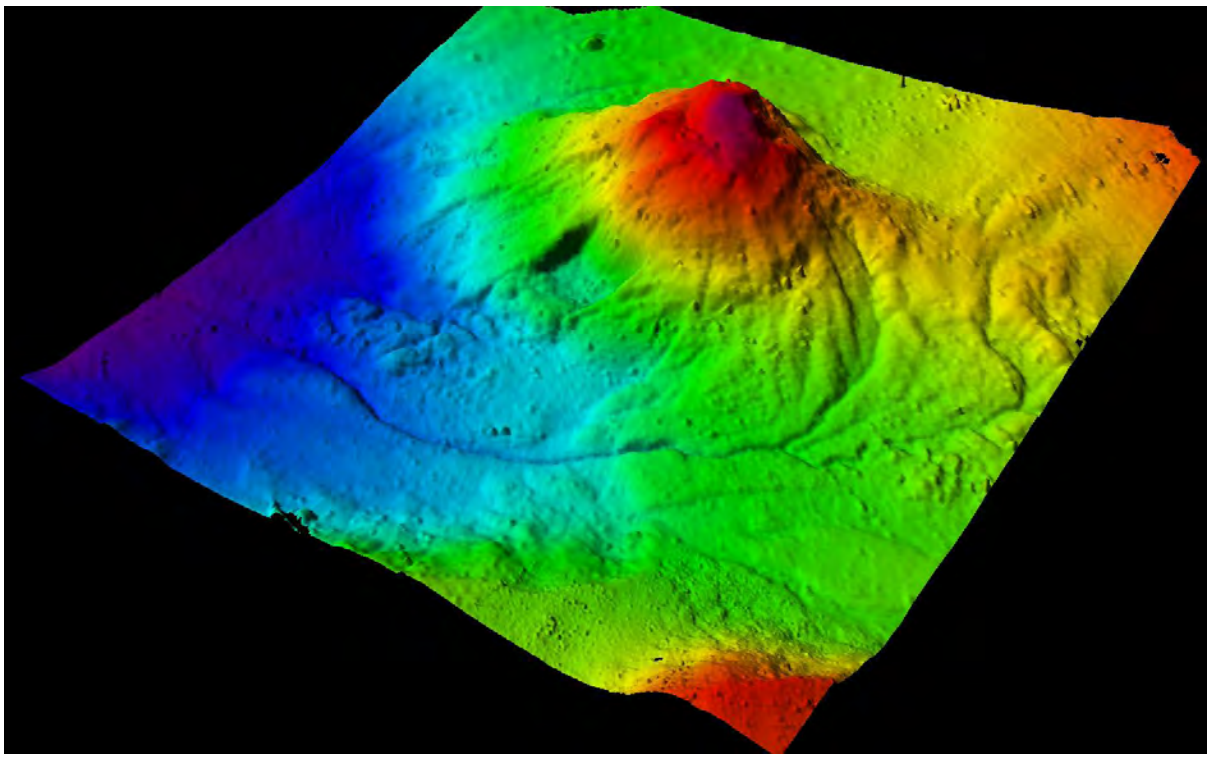

Figure 7.9. *High-resolution hull-mounted MB map of the Lolita Salt Diapir. Pixel resolution: 10m. Note the full coverage map at high spatial resolution despite the depth of the surveyed area, due to the increased density of the beams produced by the DS ATLAS Hydrosweep.*

7.5. Multibeam echosounder data processing flow

Bathymetric data were processed with the program CARIS HIPS&SIPS, version10.3. The adopted vessel file "SdG-DS-plantilla20180418.hvf" accounted in CARIS for the calibrated roll and pitch values and for the offsets between the position of the MB echosounder installed on the hull of the ship and the GPS antenna (Fig. 7.10).

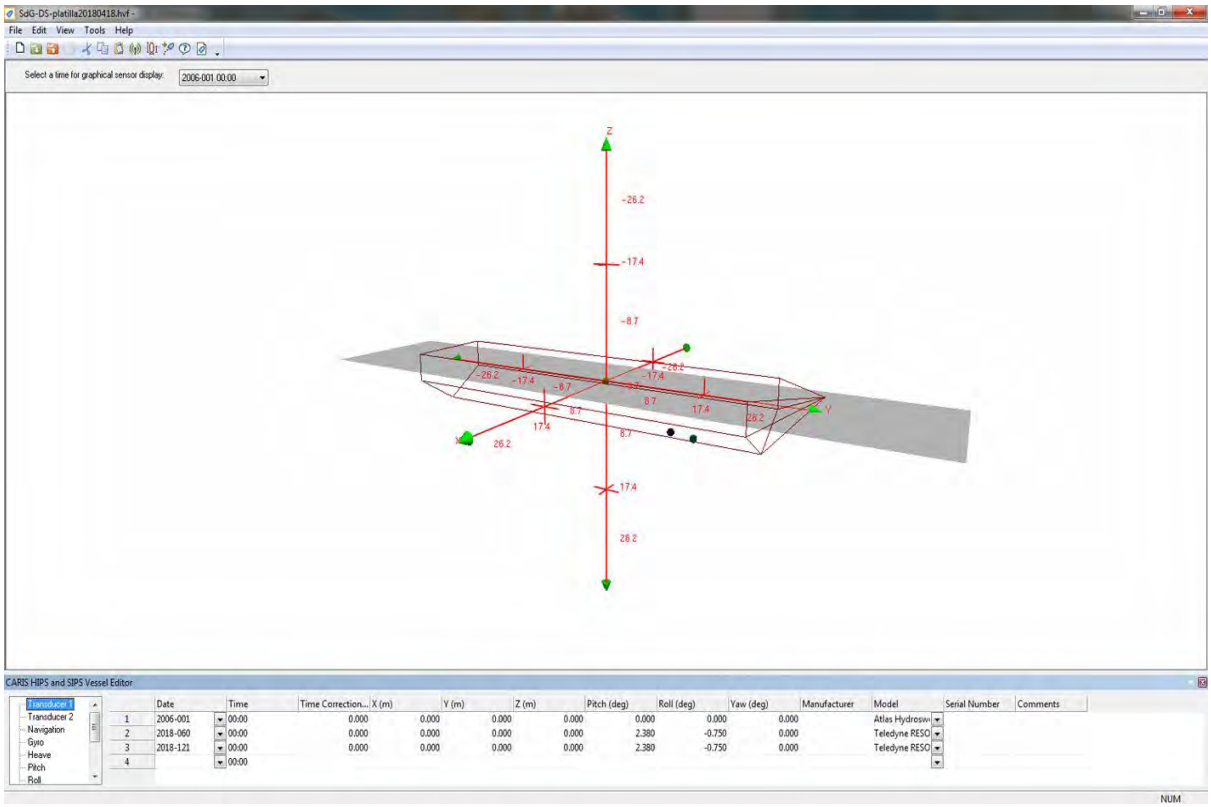

Figure 7.10. *Configuration of the CARIS vessel file "SdG-DS-plantilla20180418".*

The SVP calibration file for the CARIS project is the "ABYSS_AUV_16 May.svp", which included sound velocity profiles extracted from the AUV CTD probe. A sound velocity profile was created from each AUV dive and included in the above CARIS svp file (Table 1; Fig. 7.11).

Table 7.1. ***(next page)*:** *Characteristics of the CTD profiles included in file "ABYSS_AUV_16 May.svp" for the sound velocity calibration in CARIS.*

Day	Time	Lat (North)	Long (West)	Max Depth (m)	Area	AUV dive
01-May	14:13	36° 53' 63''	-10° 04' 24''	3912	MP	279
02-May	15:27	36° 52' 49''	-10° 06' 40''	3900	MP	280
04-May	13:56	35° 41' 43''	-10° 00' 26''	4530	LSW	281
05-May	15:23	35° 41' 44''	-09° 58' 31''	4578	LSW	282
06-May	20:53	35° 39' 27''	-09° 52' 19''	4509	LSW	283
07-May	16:47	35° 37' 25''	-09° 42' 22''	4538	LSW	284
09-May	11:49	35° 06' 04''	-07° 22' 31''	1102	LSE	285
10-May	10:49	35° 04' 40''	-07° 15' 16''	1105	LSE	286
11 May	03:05	35° 03' 37''	-07° 09' 58''	1220	LSE	287
12-May	14:17	35° 22' 36''	-07° 06' 04''	1113	GMV	288
14-May	01:19	36° 08' 59''	-08° 00' 44''	1727	LoSD	289
15-May	02:05	36° 06' 57''	-08° 01' 14''	1766	LoSD	290

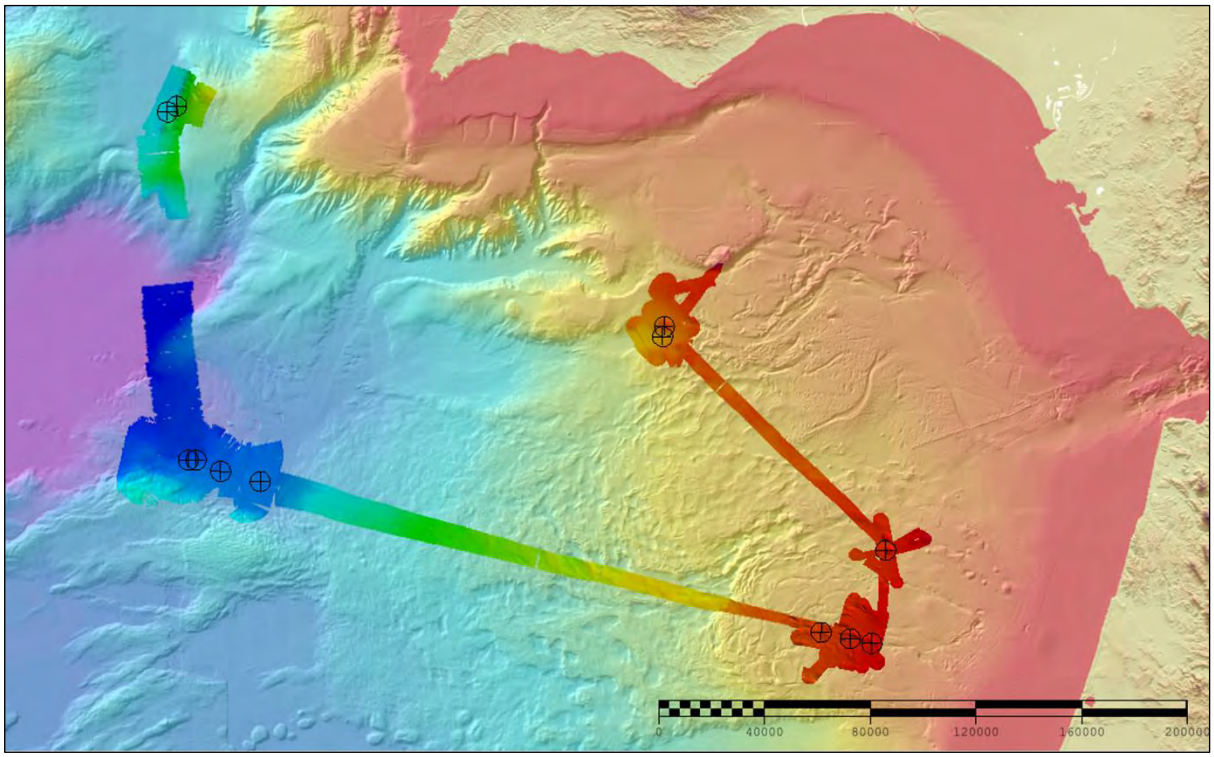

Figure 7.11. *Location of the CTD profiles used for the sound velocity calibration during the cruise.*

Once the calibration values (roll and pitch) were included in the vessel file (Fig. 7.10), the following workflow was adopted to calibrate and process the data and finally create the bathymetric maps:

1. Import the raw MB data (.sk7 format) into CARIS HIPS&SIPS.
3. A file with a constant zero value of tide was applied to all lines.
4. Lines were calibrated for the sound velocity profile.
5. Lines were eventually merged with the corresponding navigation and attitude data.
6. Navigation was cleaned in order to avoid some of the loops.
7. Across track surface coverage of each line was reduced automatically in order to remove the noise of the external beams (filter "across track", Fig. 7.12).
8. Noisy outliers beams were partially removed automatically using a standard deviation value of depth as a filtering threshold (filter "processed depths – St Dev", Fig. 7.13).
9. Spike cleaning: two methods were eventually adopted to remove the noise manually:

• Swath editor: remove spikes from each single line.

• Subset editor: manual filtering with more detailed observation from the surface data ("subset editor").

10. DTM creation: a 50m cell size DTM was eventually created for the each area (Figs. 7.2 to 7.9). High resolution DTMs were also created in specific areas of interest (Figs. 7.7 and 7.9).
11. Export the processed data as a Geotiff images and ASCII ArcGis rasters.

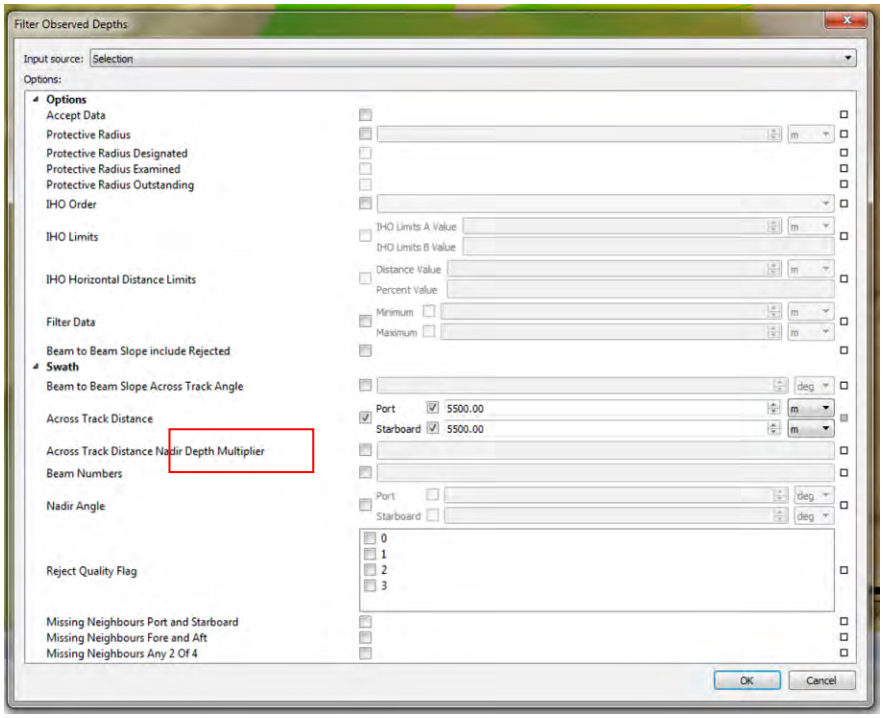

Figure 7.12. *Window of the "across track" filter in CARIS.*

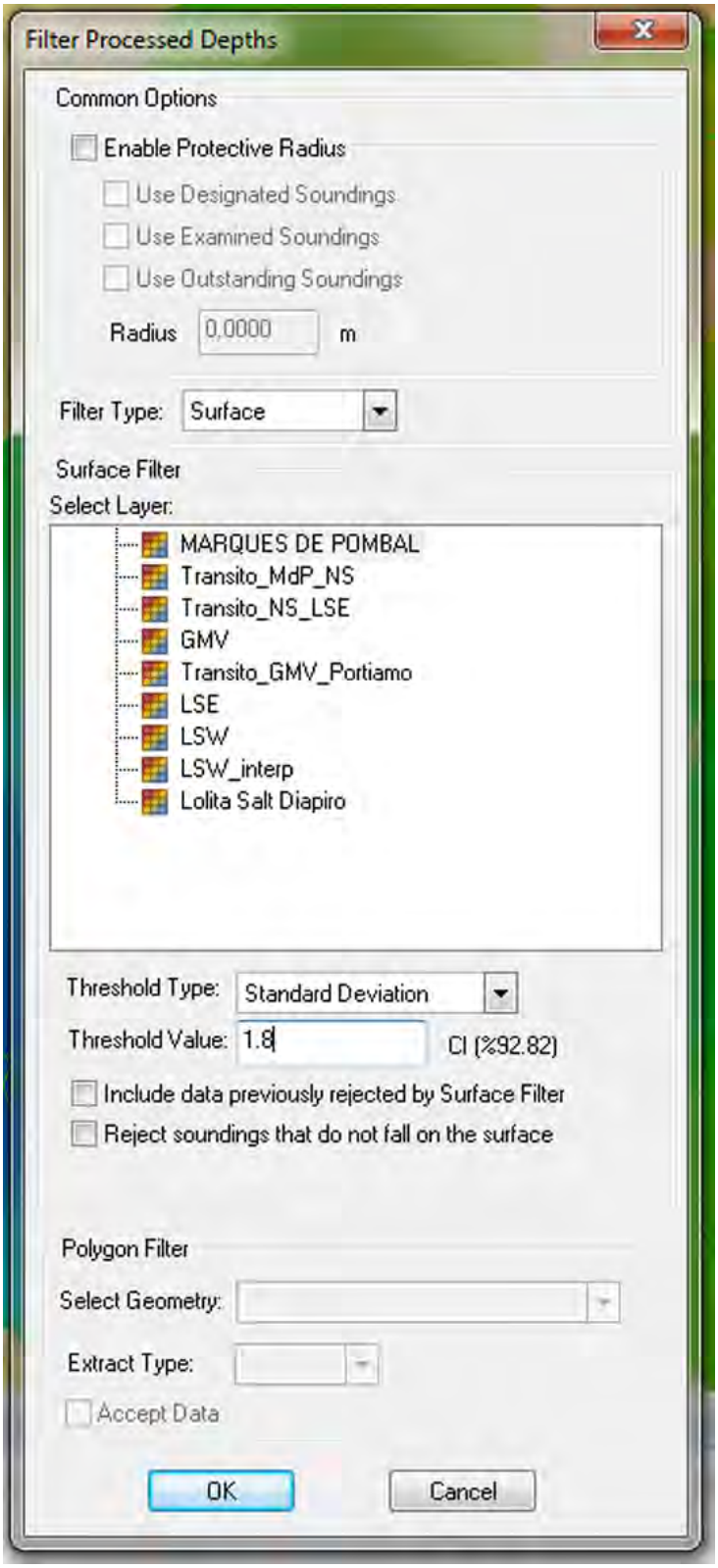

Figure 7.13. *Window of the applied standard deviation filter for the processed depths.*

8. Parasound sub-bottom profiler

8.1. Technical description of the ATLAS Parasound sub-bottom profiler

The ATLAS Parasound P35 is a narrow beam parametric sub-bottom profiler with high sediment penetration. It uses a primary frequency of 18-39 kHz, and a secondary frequency of 0.5 to 6 kHz, yielding a survey depth range up to 11,000 m and a theoretical maximum bottom penetration of > 150 m. The system offers a high degree of customization through its different software interfaces and special attention should be taken during initial setup and operation. Transmission/Reception parameters are configured through the Atlas Hydromap Control Software (Fig. 8.1), and parameters chosen will affect the recorded data and cannot be changed on post-processing.

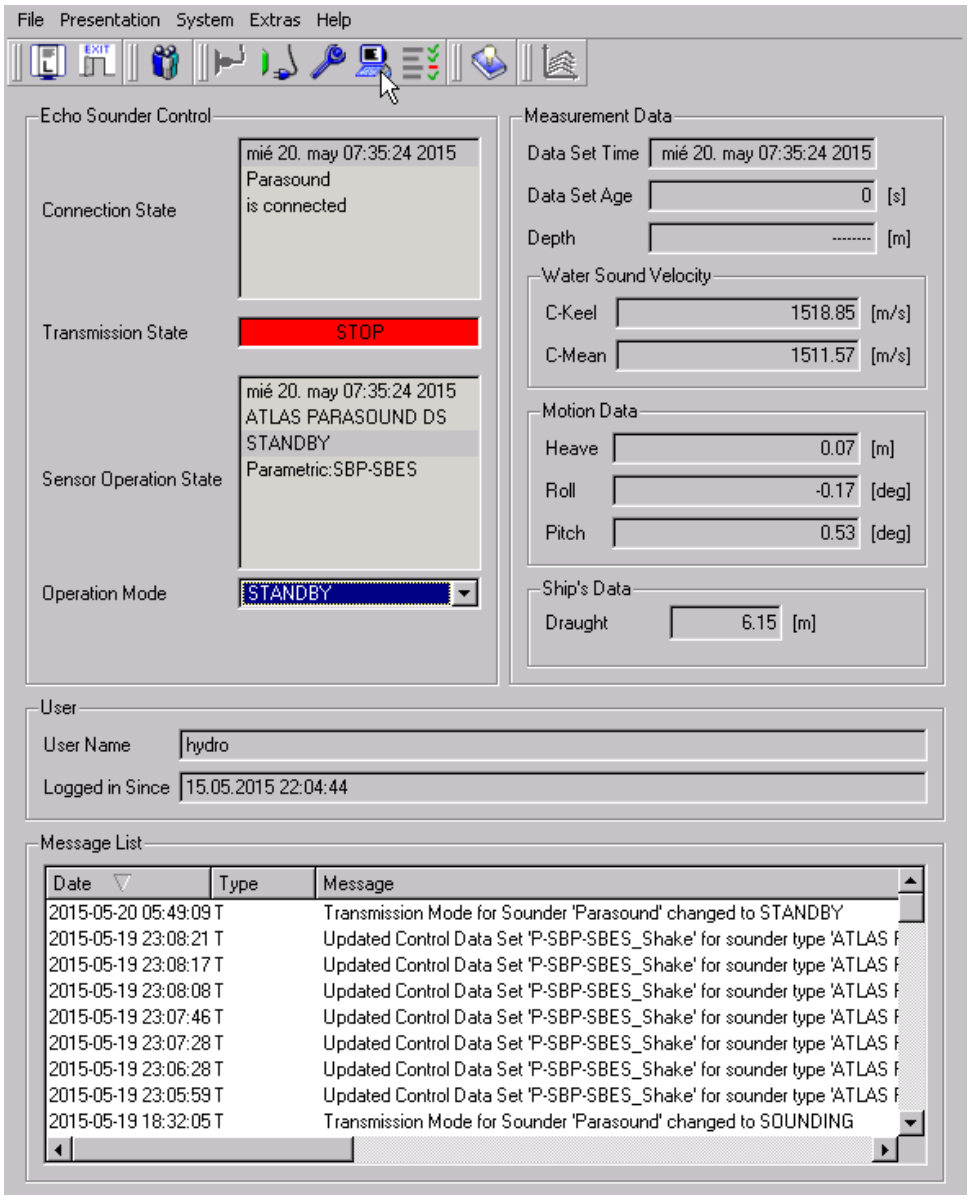

Figure 8.1. *The Atlas Hydromap Control Software.*

8.2. ATLAS Parasound acquisition parameters

During the INSIGHT-Leg 1 cruise a Chirp pulse around a center frequency of 4 kHz was used from April 30 to May 7 while a Continuous wave pulse with a center frequency of 3.5 kHz was used from this same date to the end of the cruise. The pulse length was 0.57 ms. Data were recorded at a sampling rate of 6.1 kHz.

The Atlas PARASTORE software controls data recording, processing and visualization. The Software's Echogram (Fig. 8.2) window displays real time processed data. However the only processing step recorded in the output SEG-Y files was envelope generation. As PARASOUND raw ASD data is also recorded, we regenerated the carrier frequency data for processing with RadexPro using an acquisition window of 267 ms and navigation in UTM zone 29 coordinates. ASD data can be reexported again using PARASTORE for future additional processing if needed.

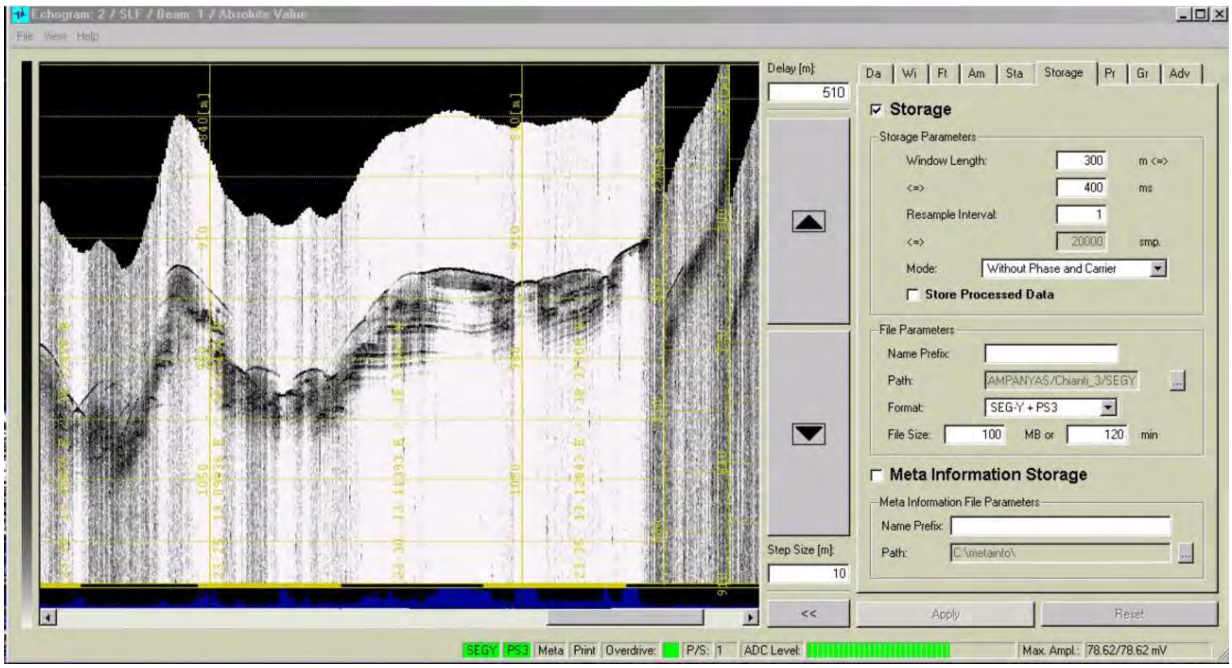

Figure 8.2. *The Atlas PARASTORE Echogram view.*

8.3. Parametric sub-bottom profiles processing flow

Data processing carried out during the INSIGHT cruise was done outside the Atlas PARASTORE software as it was found that the processed output option produces blank SEG-Y files. The workaround solution found was to output the Carrier Frequency data as SEG-Y (Fig. 8.3, 8.4) and process the data with RadexPro.

The processing steps taken in RadexPro are the following:

A. Extract the source wavelet for later use in deconvolution (Fig. 8.5)

1. Input SEG-Y data
2. Automatically pick the seafloor and store the value in a header value
3. Subtract the pick to flatten the seafloor (Apply static correction)
4. Define an ensemble on the FFID trace header
5. Stack all traces on the section to remove the geology and leave the trace signature.
6. Output the trace for use in deconvolution (Fig. 8.5)

B. Subbottom profiler processing steps (Figs. 8.6, 8.7)

1. Input SEG-Y data
2. Remove burst noise
3. Automatically pick the seafloor and store the value in a header value
4. Average the seafloor picks (41 picks) to avoid areas of bad seafloor detection
5. Generate picks parallel to the seafloor at 50 and 100 msec below the seafloor
6. Apply a time variable Gain with slopes of 1 (above the seafloor), 1 (between the seafloor and 50 msec below the seafloor), 3 (between 50 msec below the seafloor and 100 msec below the seafloor), and 8 below that reflector
7. Apply a new exponential amplitude correction starting at the seafloor
8. Bring the picked seafloor up 3 msec for latter mute of the water column and to account by shift during deconvolution
9. Deconvolve with the source wavelet (step taken for Chirp pulses)
10. Equalize all traces
11. Generate Envelope
12. Trace mixing with three traces
13. Mute the water column above the seafloor with the seafloor picked in step 8
14. Output SEG-Y data.

Finally, profiles were imported to The Kingdom Suite software for displaying and interpretation.

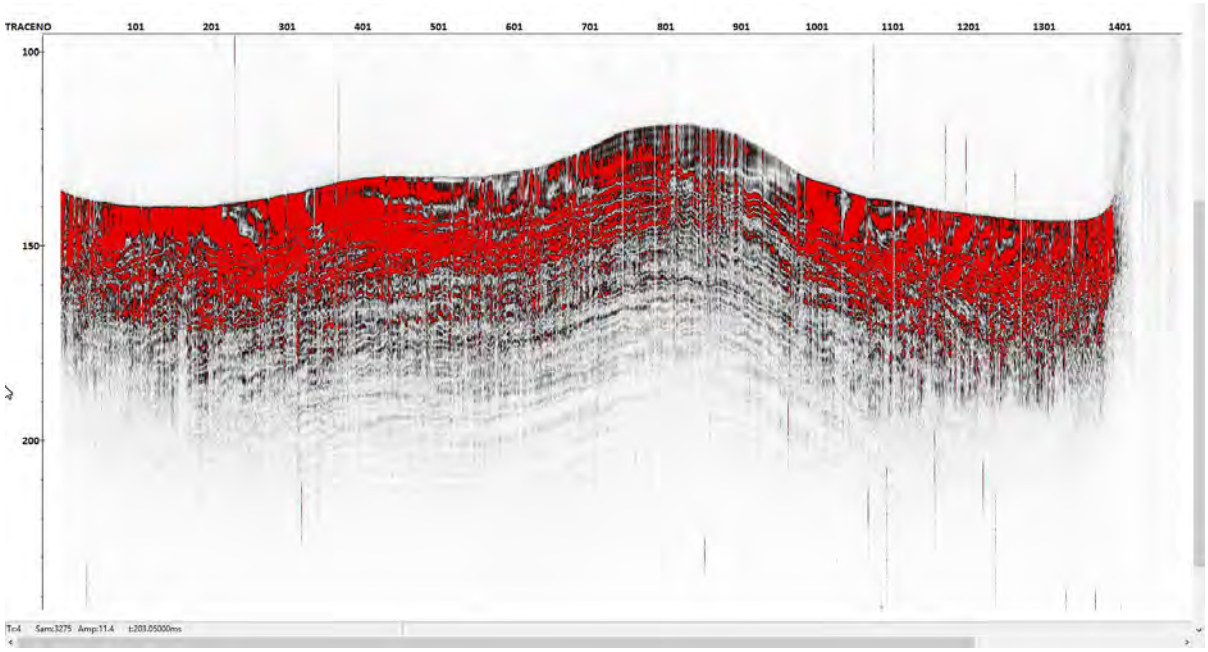

Figure 8.3. *Raw data with envelope*

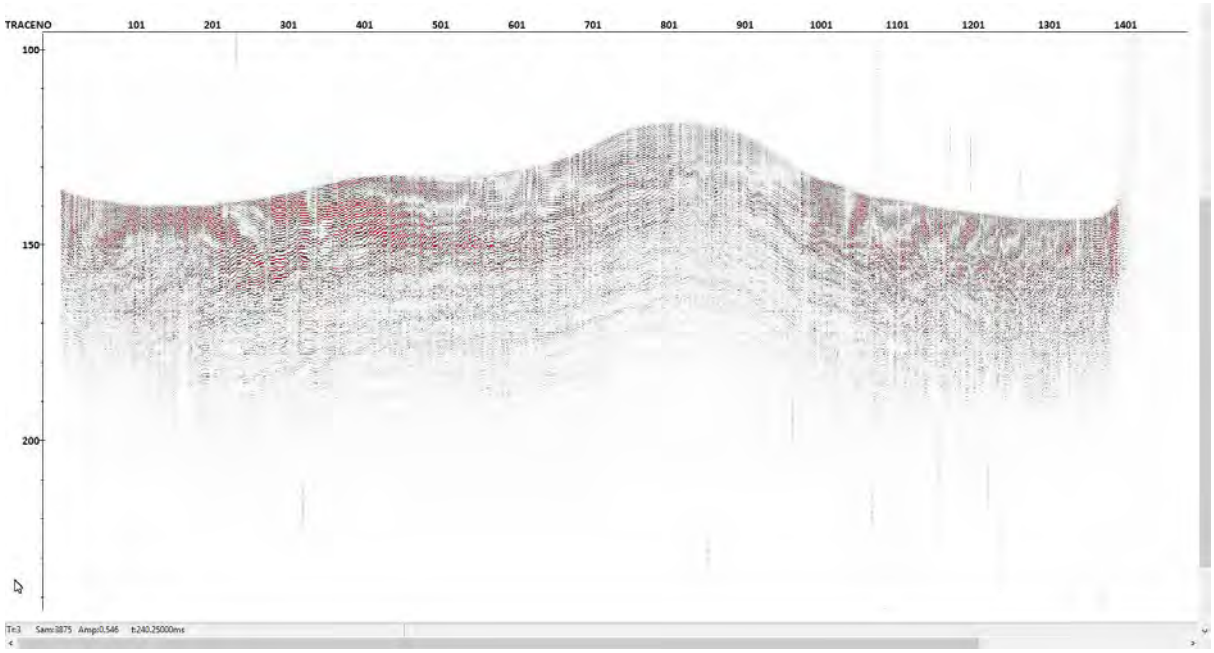

Figure 8.4. *Carrier Frequency data*

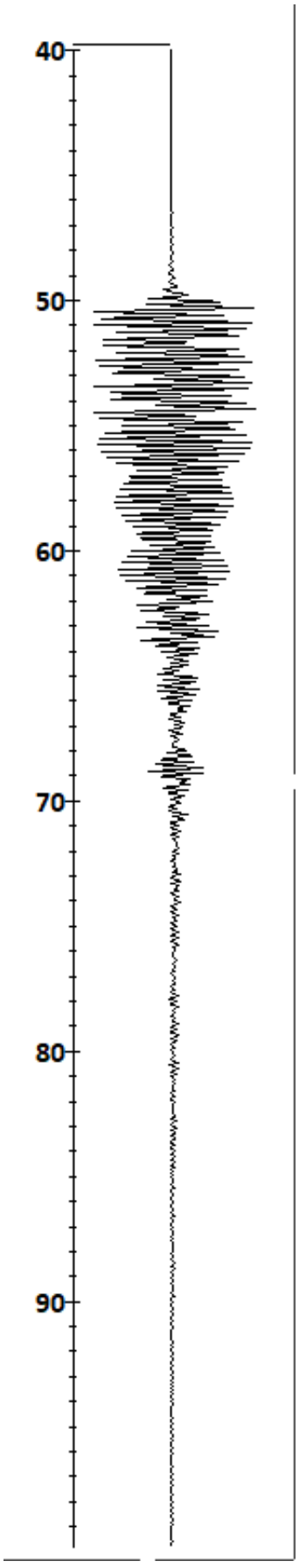

Figure 8.5. *Extracted source wavelet used in deconvolution.*

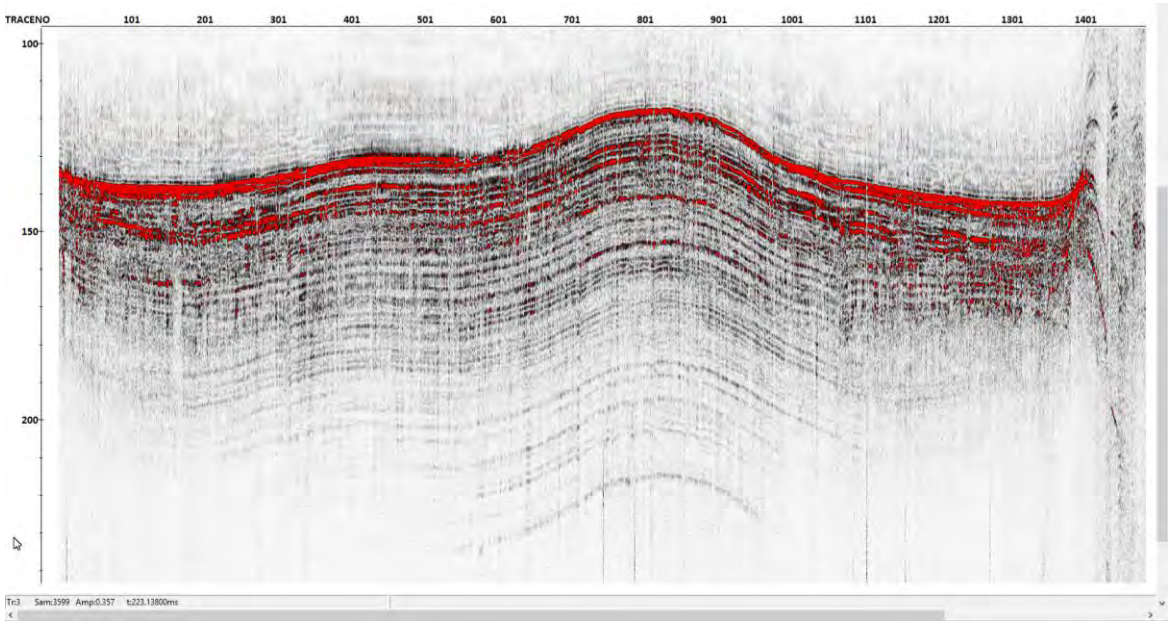

Figure 8.6. *Fully deconvolved data with envelope.*

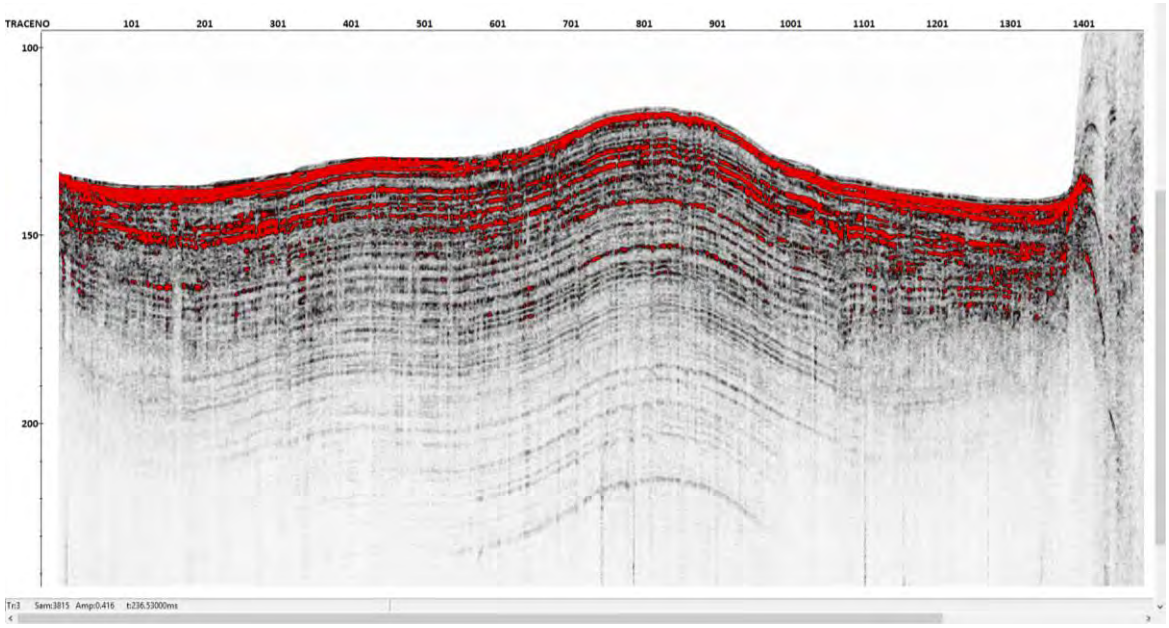

Figure 8.7. *Fully deconvolved data with envelope, trace mixing (3) and mute above the seafloor.*

8.4. Preliminary results: Parametric sub-bottom profiles

During the cruise, five areas have been covered where parametric sub-bottom profiles have been acquired in parallel with seismic, shipboard bathymetry and AUV microbathymetry. These areas are the Marques de Pombal thrust, Lineation South West, Lineation South East, the Ginsburg mud volcano and the Lolita Salt diapir (Fig 8.8). A total of 3813 km of subbottom parametric data were collected. Most of the profiles were collected at a speed of 3.5 kn, however, during transits data were collected at relatively high speeds of 8 knots.

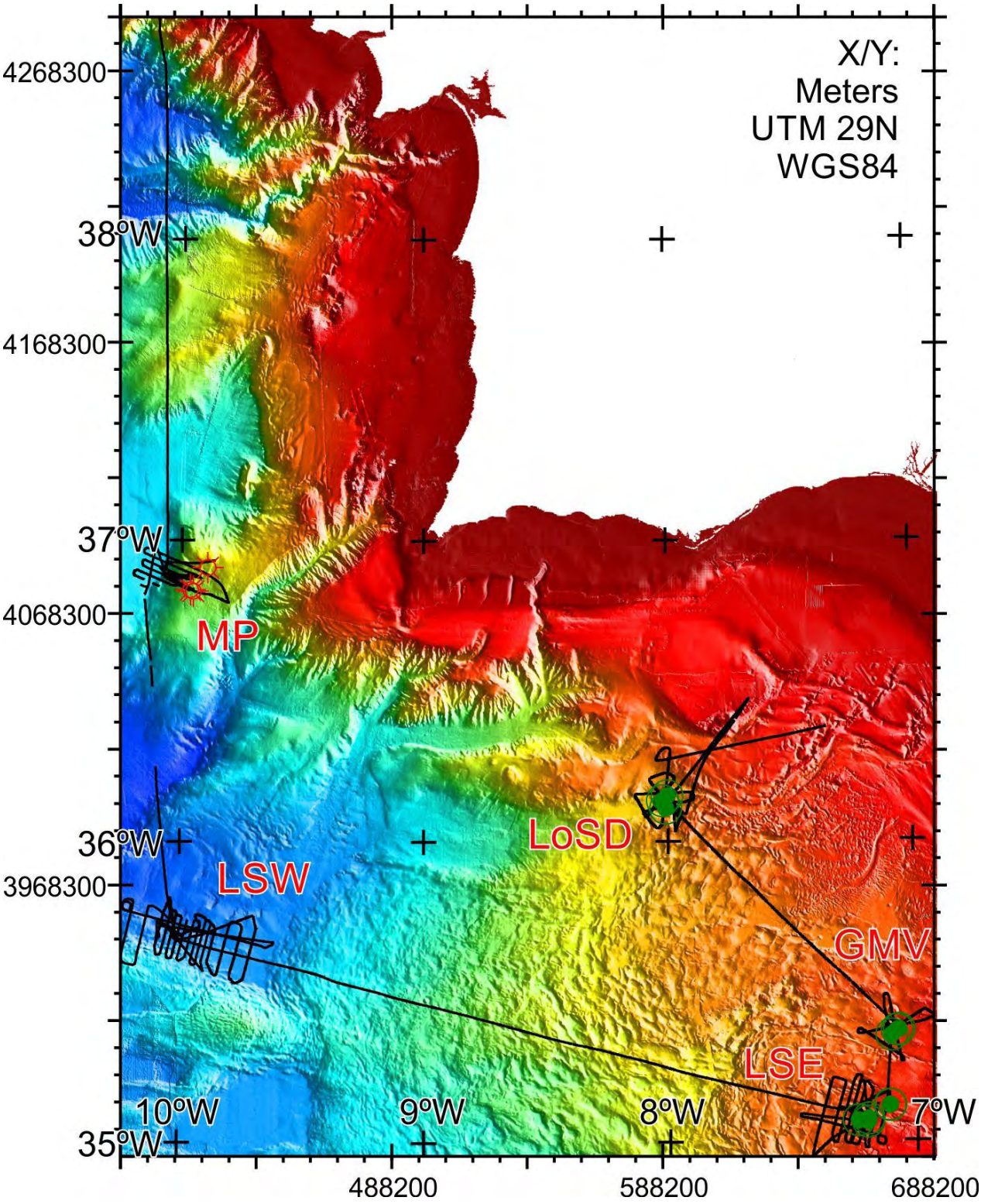

Figure 8.8. *Tracks of the parametric sub-bottom profiles acquired in the Gulf of Cadiz during the INSIGHT cruise. MP: Marques de Pombal thrust, LSW: Lineation South West, LSE: Lineation South East, GMV: Ginsburg mud volcano and LoSD: Lolita Salt diapir.*

The ATLAS Parasound parametric data show detailed stratigraphic information of the uppermost tens of meters below the seafloor (up to 100 m at an assumed sediment velocity of 1.5 km/s). These new data provide insights into the structural controls, late Quaternary

deformation related with diapirs, slope failure processes and growth/decay of deep water coral mounds in the Gulf of Cadiz. The best results have been obtained in flat areas with highly penetrative sediments, while abrupt slope areas and rock outcrops display very low penetration.

The Marques de Pombal thrust area is characterized by parallel stratified facies, with penentration up to 100 ms on the basin that develops on the footwall of the thrust. Interbedded with those sediments are transparent lenses, which likely originate from slope failures on the hanging wall (Fig. 8.9a). The slopes an high reliefs upslope from the thrust display opaque facies or stratified facies with penetrations not exceeding 50 msec. The parallel facies are often disrupted by scarps from the Marques de Pombal landslide (Fig. 8.9b).

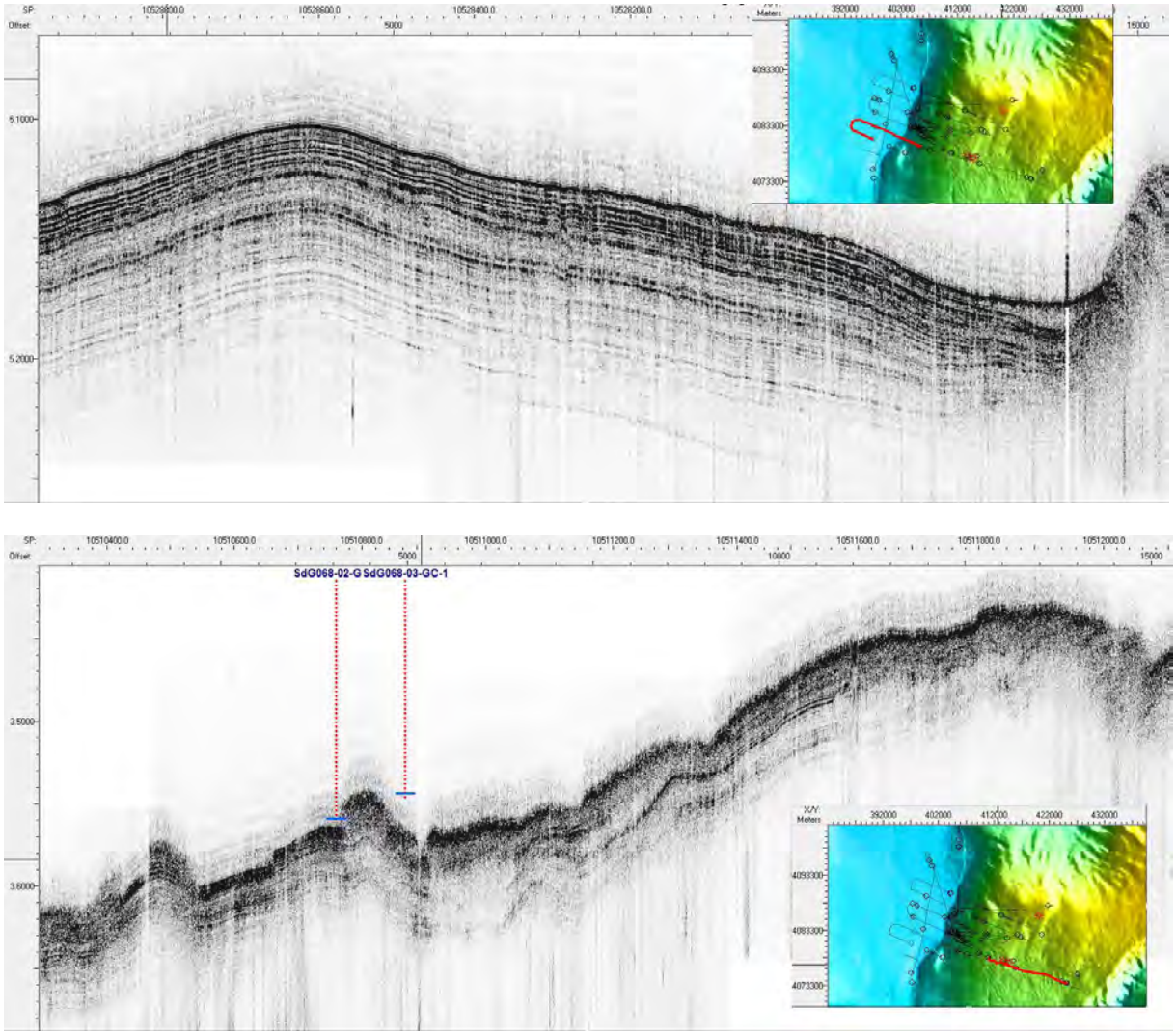

Figure 8.9. *Parametric SBP acquired on the Marques de Pombal area: (a) thrust footwall with laminated sediments and transparent lenses (debris flows). (b) Transparent and truncated laminated reflectors showing sediments involved in the Marques de Pombal landslide. Cores SdG068-02-GC-1 and SdG068-02-GC-1 are projected on the line.*

The profiles collected on the western deep part of the Lineament South show hyperbolic opaque or slightly stratified response on the southern side of the fault, with penetrations in subseafloor sediments not exceeding 50 msec (Fig. 1.10a). To the north of the fault the seafloor displays penetration up to 100 msec with parallel to parallel-undulated response. Strata north of the fault show abundant evidence of erosion and internal discontinuities (Fig. 1.10b). Slope failures have been also identified from which lenses with acoustic transparent facies develop. The fault itself appears most of the time as a scarp or north-facing slope (particularly in the 2/3 western part of the area), but it may also appear as a depression , a south facing slope or be totally concealed (Fig. 8.10a).

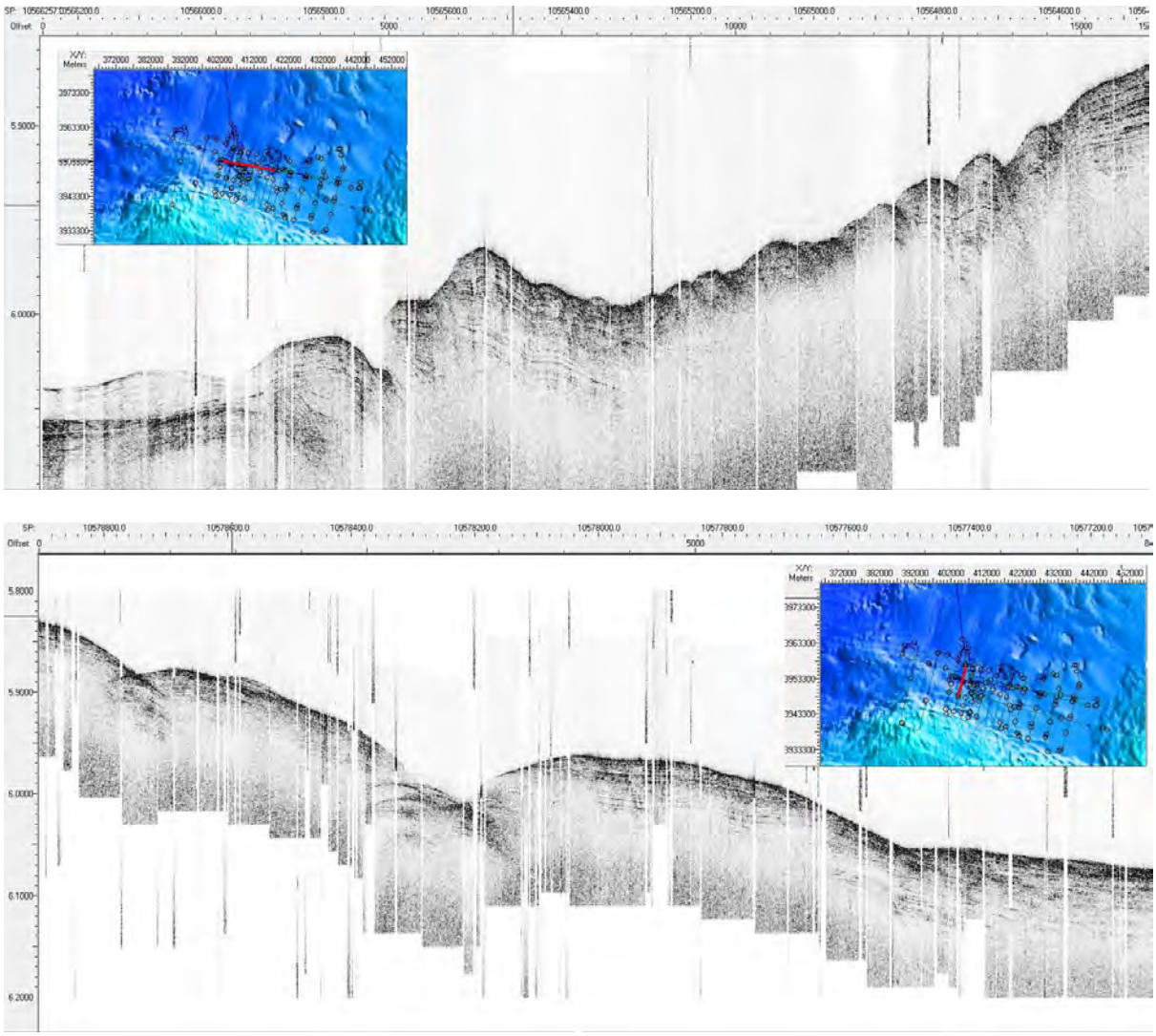

Figure 8.10. *Examples of parametric sub-bottom profiles acquired on the western deep-water area of Lineation South: (a) Near-surface expression of the fault and surrounding sediments, (b) Sediments on the northern flank of the fault showing evidence of erosion and various truncations within the sequence.*

The same Lineament South has a quite distinct character in the eastern shallower part, in Moroccan waters. There the fault is associated with more than 100 m deep depressions and/or 100 m high ridges adjacent to the fault. The sediments surrounding the depressions, interpreted as pull-apart basins, are well stratified in general and present truncations at the edge of the basin and evidences of recent faulting (Figs. 8.11a,8.11c). Patches of transparent sediment have been observed in the sediment, often associated to hyperbolae generating mounds (Fig. 8.11b). These have been interpreted respectively as fossil cold-water coral mounds. Some of the ridges surrounding Lineament South are also built by cold-water corals.

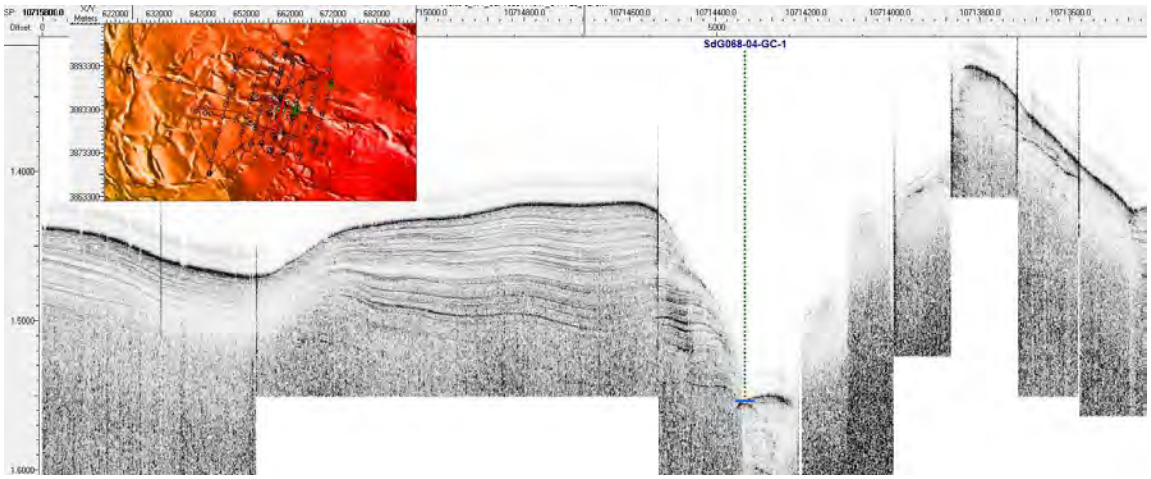

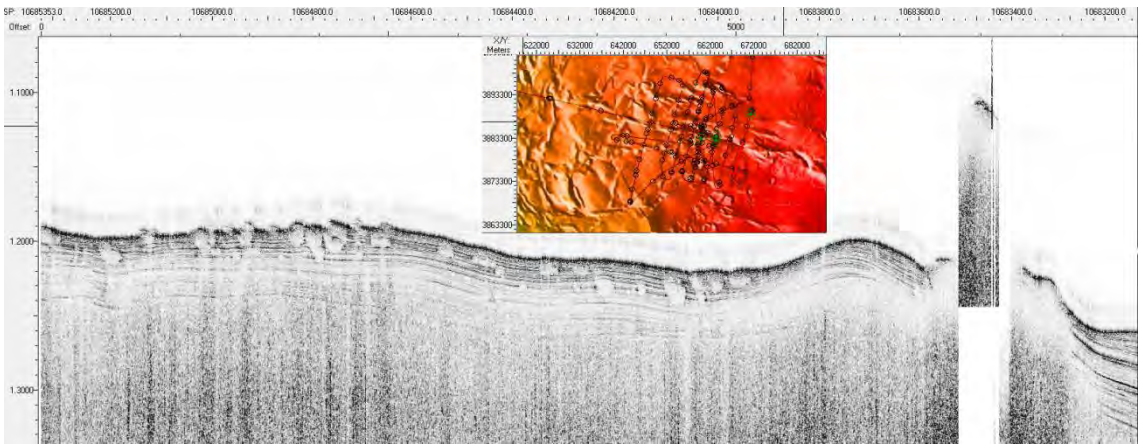

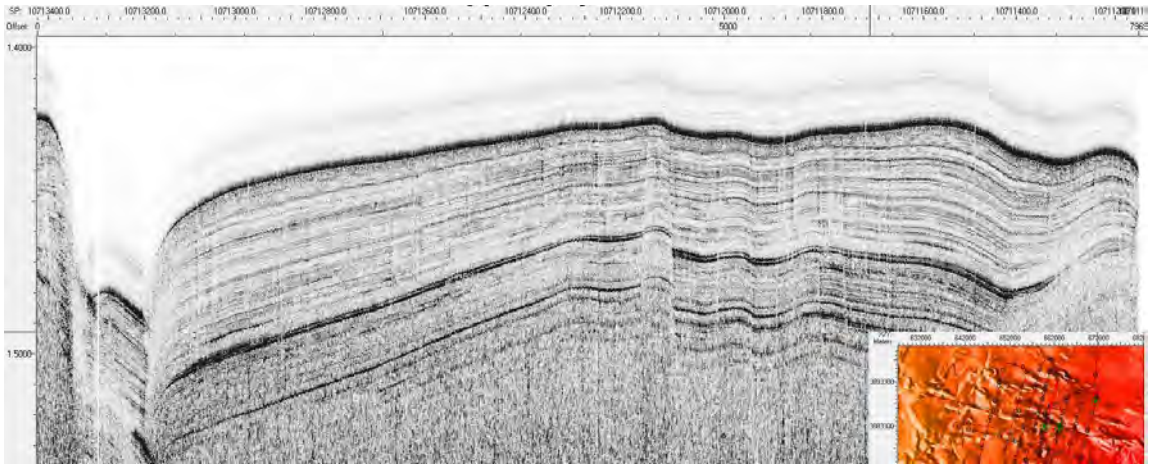

Figure 8.11. *Examples of parametric sub-bottom profiles acquired on the eastern shallow-water area of Lineation South: (a) Near-surface expression of the fault with pull-apart basin and surrounding sediments. Core SdG068-04-GC-1 is projected on the line, (b) The expression of the fault further to the north is a positive relieve, likely enhanced by the growth of cold-water coral mounds. Buried smaller scale mounds appear as transparent patches within the sedimentary record, c) Evidence of faulting in near surface sediments near Lineation South*

The Yuma and Ginsburg Mud Volcanoes display opaque to chaotic facies, while the sediments surrounding these features most often display parallel laminated acoustic facies. In proximity of the moat surrounding the mud volcanoes reflectors may display truncations and wedge geometries. Upslope from the mud volcanoes patches displaying transparent facies are also found within the sediment, in a smilar manner to those of the Lineament South shallow area described above. These are interepreted to form part of the same cold-water coral mound field.

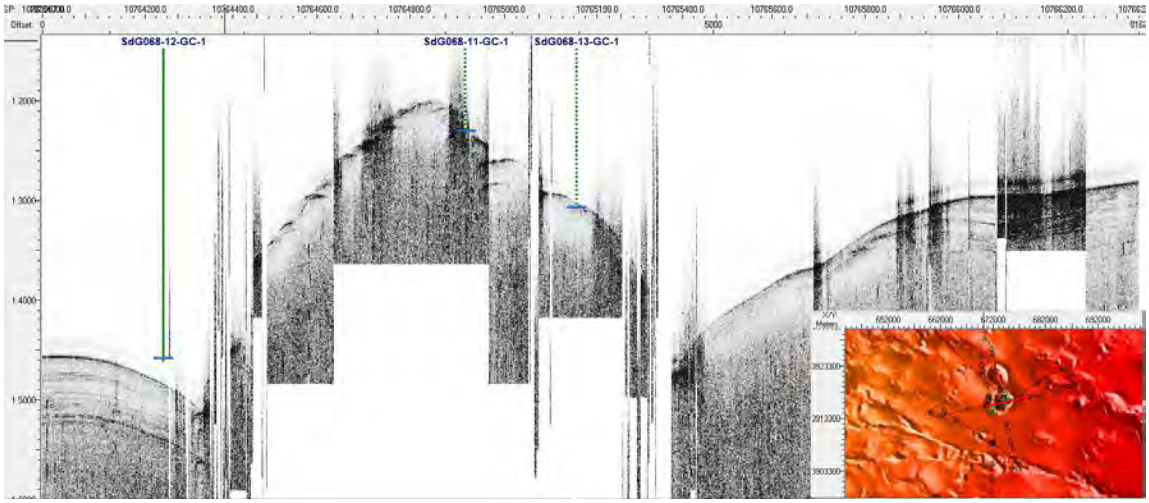

Figure 8.12. *Example of parametric sub-bottom profiles acquired along the Ginsburg mud volcano showing the moat and surrounding stratified sediments. Cores SdG068-11-GC-1, SdG068-12-GC-1 and SdG068-13-GC-1 are projected on the line, but are not necessarily located on the line.*

The Lolita salt diapir is characterized by stratified facies at its top (Fig. 8.13a) that evolve into hyperbolic, opaque and transparent facies moving from its top to the deep basin (Fig. 8.13b). The transparent facies onlap onto the stratified deep basin sediments. At the top of the diapir, stratified sediments display evidence of cracking (Fig. 8.13a). North of the diapir the basin sediments display signs of erosion and cross bedding (Fig. 8.13c).

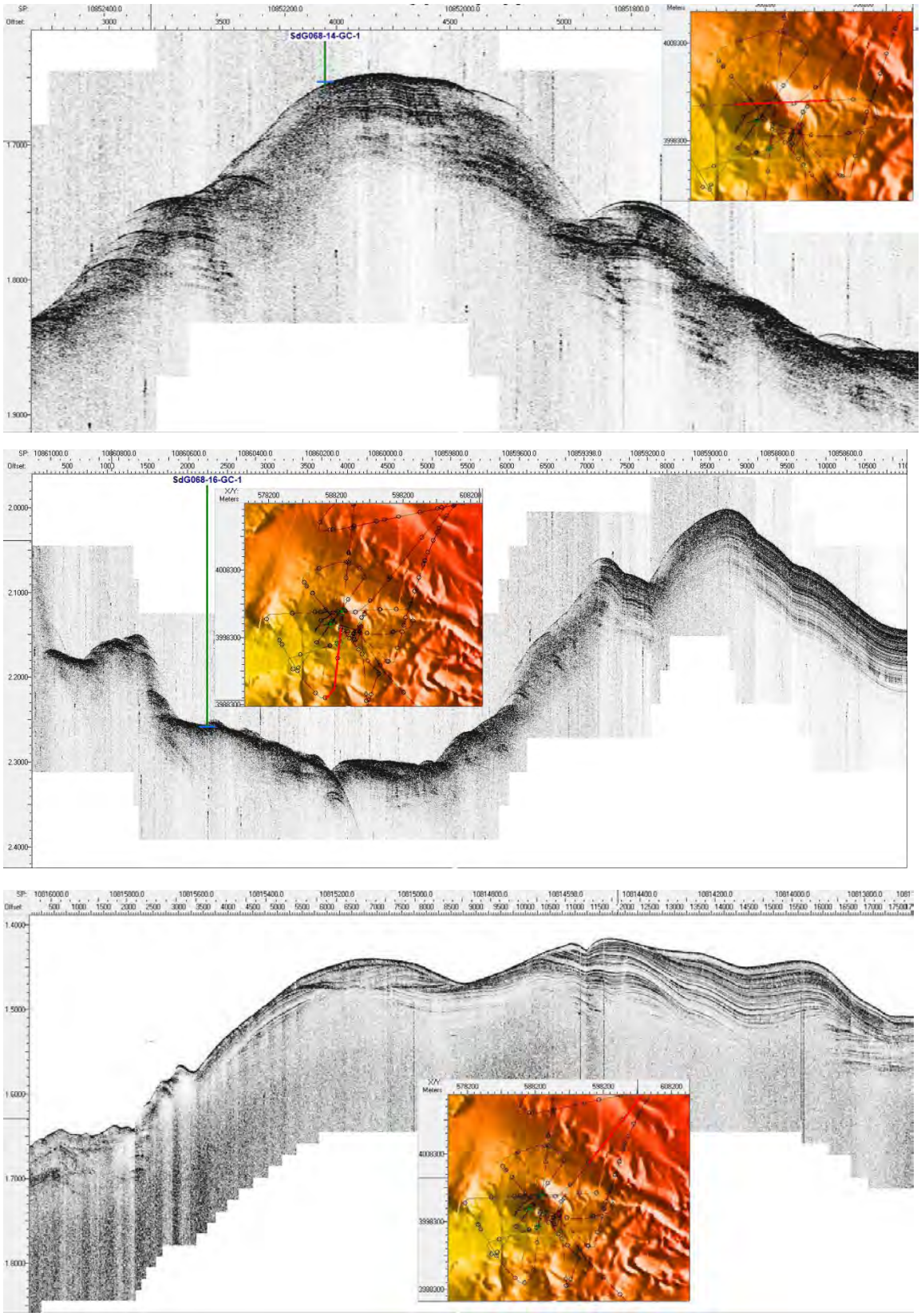

Figure 8.13. *Examples of parametric profiles acquired on Lolita salt diapir: (top) Opaque to hyperbolic facies associated to collapse of the diapir southern flank & onlap onto the stratified sediments; (middle) Stratified sediments with evidence of cracking on top of the diaper; (bottom) Evidence of erosion and cross-bedded sediments north of the diapir. Cores SdG068-14-GC-1 and SdG068-16-GC-1 are projected on the line.*

9. AUV "Abyss" surveys

9.1. Introduction

The Abyss device is an Autonomous Underwater Vehicle (AUV) dedicated to the scientific recognition on margins and deep basins up to 6000 m deep. Their missions are devoted to study the seabed or the water column with multiple scientific objectives through various payloads (e.g. multibeam sonar, sidescan sonar, ADCP, photo, etc). Abyss is a modular AUV designed to survey the ocean combining geophysical studies of the seafloor with oceanographic investigations of the overlying water column. The basic mission of Abyss is deep-sea exploration, 55ery55fically in volcanically and tectonically active parts, such as mid-ocean ridges, active faults and submarine landslides. With a maximum mission depth of 6000 meters, the AUV uses several technologies to map the seafoor accurately and determine its geological structure with applications from geology to biology to mineral exploration (Linke and Lackschewitz, 2016).

Figure 9.1. *Manu and Torje ultimating preparations before a new dive of the AUV.*

The Autonomous Underwater Vehicle (AUV) Abyss was built in 2008 by the US company HYDROID Inc., and was funded by the German Research Foundation to GEOMAR. The torpedo-shaped autonomous underwater vehicle maps areas of the seafloor in high resolution

using its various sonars (Haase et al., 2009; Hensen et al., 2015; Speckbacher et al., 2011, 2012; Yeo et al., 2016). Additionally, it can collect data from the water column with its physical sensors (Tippenhauer et al., 2015). The Abyss system comprises the AUV itself, a control and workshop container, and a mobile Launch and Recovery System (LARS) with a deployment frame that was installed in the afterdeck, port side of R/V Sarmiento de Gamboa. The self-contained LARS was developed by WHOI to support ship-based operations so that no Zodiac or crane is required for launch and recovery of the AUV. The LARS is mounted on steel plates, which are screwed to the deck of the ship, and is stored in a 20ft. container during transport. The LARS is configured in a way that the AUV can be deployed over the stern or port/starboard side on medium and and large size research vessels. The AUV Abyss can be launched and recovered at weather conditions with a swell up to 2.5 m and wind speeds of up to 6 Beaufort. For the recovery, the nose float pops off when triggered through an acoustic command. The float and the ca. 17 m recovery line drift away from the vehicle so that a grapnel hook can snag the line. The line is then connected to the LARS winch, and the vehicle is pulled up. Finally, the AUV is brought up on deck and secured in the LARS. The AUV missions were planned on the basis of ship bathymetry.

The AUV Abyss glides close to the ocean floor (up to 6000 m) with a speed of up to 4 knots while autonomously avoiding obstacles. It can be deployed from middle to large research vessels and uses a specially designed LARS for lowering it to the side or the stern of a vessel. Before each use, a scientist programs the autonomous vehicle with a destination, course and research task. Each dive takes up to 20 hours and then the AUV Abyss surfaces alone and is brought on board, lithium batteries are charged for the next dive and data is downloaded. The data is used to create three-dimensional, high-resolution maps of the seafloor (Linke and Lackschewitz, 2016).

9.2. Technical data

9.2.1. The AUV "Abyss"

• Owner and Operator: GEOMAR Helmholtz Centre for Ocean Research Kiel, Year: 2008
• Dimensions: Length 3.98 m, diameter 0.66 m
• Weight in air: 880 kg
• Max. depth: 6000 m
• Speed: up to 4 knots, operating time: up to 20 hrs
• Energy and Power: 11 kWh lithium-ion batteries (12 hrs charging time)

• Max range: Up to 100 km

• Standard sensors: SBE 49 CTD, fluorometer and turbidity sensor, side scan sonar 120/410 kHz, multibeam echosounder 200/400 kHz

• Optional sensors: 20.2 Megapixel electronic still camera (Canon 6D) with 15mm fish-eye lens (Kwasnitschka et al., 2016), sub-bottom profiler (4-24 kHz), eH sensor (by Dr. K. Nakamura, AIST, Japan), microstructure sensor

• LARS (Launch and Recovery System) with a hydraulically operated A-frame.

• Transport: Two 20-foot containers

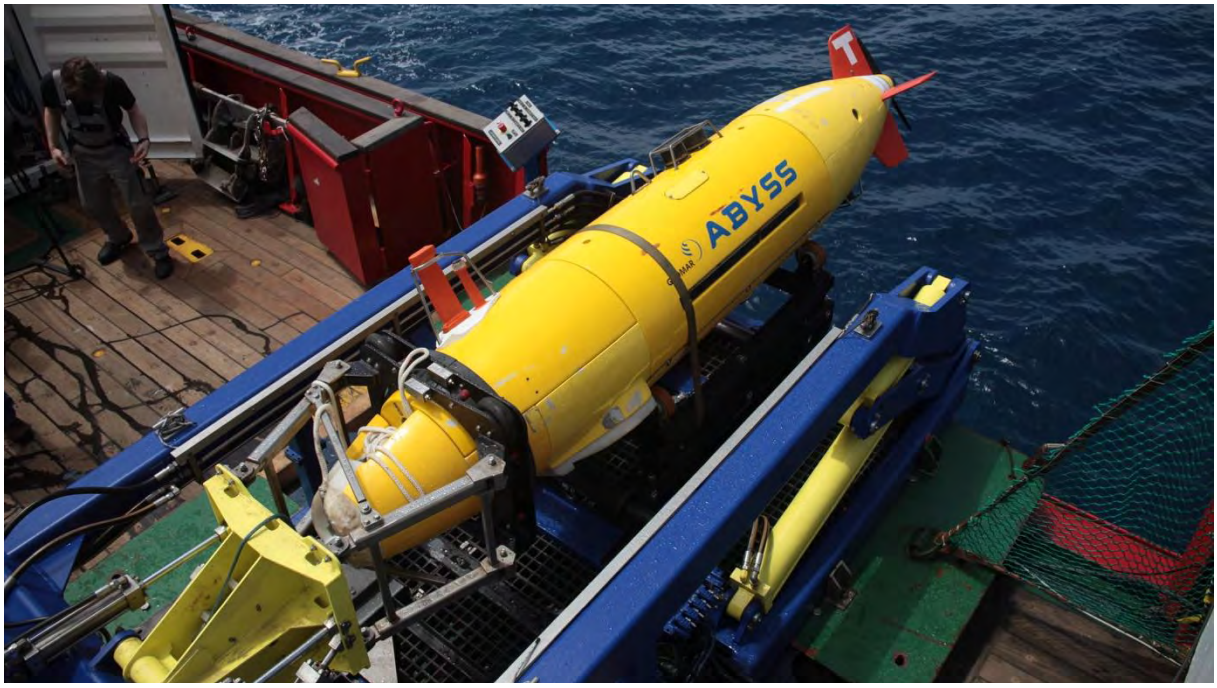

Figure 9.2. *The AUV Abyss and LARS system installed on the RV Sarmiento de Gamboa.*

The vehicle consists of a tapered forward section, a cylindrical midsection and a tapered tail section. An internal titanium strongback, which extends much of the vehicle length, provides the structural integrity and a mounting platform for syntactic foam, equipment housings, sensors and release mechanisms. The maximum vehicle diameter is 0.7 meters and the overall length is 3.95 meters. Vehicle weight is, depending on the payload, approximately 850 kilograms. A rectangular compartment in the midsection of the vehicle contains three pressure housings and an oil-filled junction box. Two of the pressure housings contain each one 5.75 kWhr 29-Volt lithium-ion battery pack. The third pressure housing contains the vehicle and sidescan sonar electronics. The vehicle's Inertial Navigation System (INS) and Acoustic Doppler Current Profiler (ADCP) are housed in two other independent housings that are mounted forward of the 3 main pressure housings. The propulsion and control systems are located in the tail assembly, which bolts to the aft face of the vehicle's strongback. The tail

assembly consists of a pressure housing with motor controller electronics, and an oil-compensated motor housing. Propulsion is generated with a 24 VDC brushless motor driving a two-bladed propeller. Control is achieved with horizontal and vertical fins driven by 24 VDC brushless gear motors. The vehicle velocity range is 0.25 to 2.0 m/s, although best control is achieved at velocities above 1.0 m/s. The AUV dives descent with about 1 m/s whereas the ascent time is about 0.7 m/s or 1m/s if the ascent weight is dropped. Together with the deployment/recovery procedure the descent to the seafloor and the ascent back to the vessel takes about 3 hours at a water depth of 3500 m. Based on the sensor configuration in use the dive time varies between 16 and 20 hours. After a full dive the batteries have to be recharged, which needs approximately 12-14 hours.

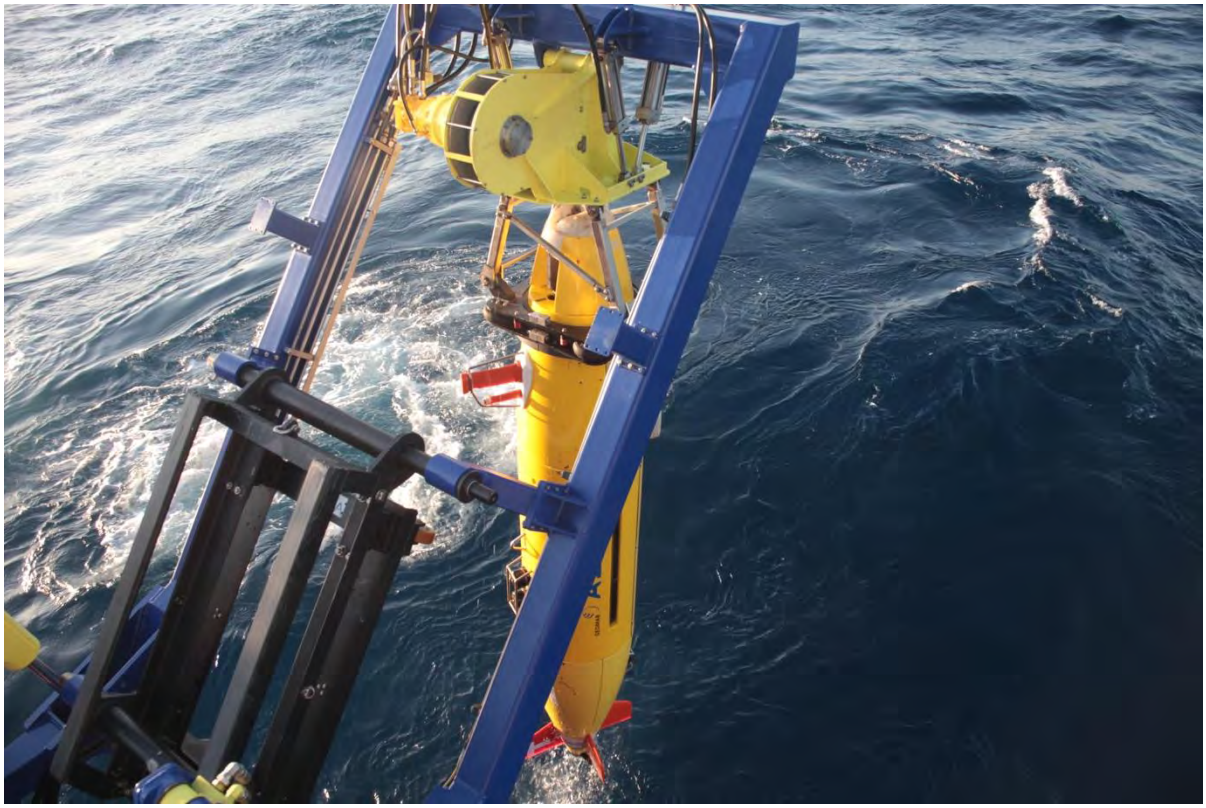

Figure 9.3. *Recovering the AUV Abyss with the LARS system after a dive.*

9.2.2. Navigation sensors

The vehicle navigates autonomously using a combination of navigation methods which depend on the mission objectives, conditions, and optional equipment enabled.

• GPS -Works only on the surface, GPS determines the vehicle's location on Earth. GPS determines the "initial position" before the vehicle submerges, and 58ery_es or corrects the vehicle's position when it surfaces during the mission. GPS also plays a critical role during INS alignment.

• Inertial Navigation System (INS) – After alignment on the surface, INS continuously integrate acceleration in 3 axes to calculate the vehicle's position. It uses input from the DVL and the GPS to maintain its alignment.

• Doppler Velocity Log (DVL) – Continuously measures altitude and speed over ground whenever the vehicle can maintain bottom-lock. The DVL receives temperature and salinity data from the CT Probe to calculate sound speed. The DVL must be within range of the bottom to measure altitude and provide bottom-track for the INS.

• Long Baseline Acoustic Navigation (LBL) – The vehicle navigates using Long Baseline (LBL) navigation by computing its range to a two (or more) moored acoustic transponder array covering the area of each mission. The deployment and calibration of each transponder takes approximately 2-3 hours at a water depth of 3000 m.

Figure 9.4. *Moving Abyss into the cointainer to change batteries and data recovery.*

9.3. Main sensors

All of the 12 missions were flown using exclusively the multibeam-configuration. The primary sensor of those dives was the RESON Seabat 7125 (multibeam echosounder) 200 kHz. More details are found in Tables 9.1 to 9.4. The turbidity sensor (WetLabs ECO FLNTU Fluorometer and Turbidity sensor; S/N FLNTURTD-939), the REDOX potential sensor (by Ko-ichi Nakamura) and the CTD (Seabird SBE49 FastCAT; S/N 4948793-0198) ran

simultaneously and served as secondary sensors. All data have a time stamp and/or are related to a position of the vehicle. Please consider that those positions are the original and not navigational adjusted positions.

9.3.1. Multibeam echosounder Reson SeaBat 7125

The AUV has a Reson SeaBat 7125 echo sounder (Table 9.1). Main frequency is 200kHz, although 400 kHz is also available on request. Multibeam bathymetry and sidescan sonar can be obtained. Sidescan sonar and camera were not used duing the cruise.

Multibeam

Vendor	Reson	
Typ	SeaBat 7125 Receiver EM7216 PN:85002184 SN:1713118 200kHz Projektor TC2163 PN: 85000327 SN: 3710027	
Last calibration	September 2017	
Exported data	S7k files	
Unit	-	
Notes	The following specifications are taken from the general datasheet	
Frequency	200kHz (400kHz available on request)	
Along-track transmit beamwidth	2.2° (± 0.5°) at 200 kHz / 1° (± 0.2°) at 400 kHz	
Across-track receive beamwidth	1.1° (± 0.05°) at 200 kHz / 0.54° (± 0.03°) at 400 kHz	
Max ping rate	50 Hz (± 1 Hz)	
50 Hz (± 1 Hz)	33 µsec to 300 µsec	
Number of beams	256EA*/256ED* at 200kHz 256EA*, 512EA*, 512ED* at 400kHz	* EA= Equi-angle / ED= Equi-distant
Max Swath angle	128°	
Depth resolution	6mm	
	Bathymetry, sidescan & snippets 7K data format Gbit Ethernet	

Table 9.1. *Characteristics of the multibeam echosounder Reson SeaBat 7125.*

9.3.2. Sidescan sonar Edgetech 2200-M

Side Scan Sonar

Vendor	Edgetech
Typ	2200-M
Last calibration	September 2017
Exported data	.jsf
Unit	-
Notes	The following specifications are taken from the general datasheet
Frequency	120kHz & 410 kHz

Table 9.2. *Characteristics of the sidescan sonar Edgetech 2200-M.*

9.3.3. Camera Cannon 6D

Camera

Vendor	Cannon
Typ	6D
Lens	CANON EF 8-15mm f/4L Fisheye USM
Exported data	.jpeg
Frequency	Max 1Hz

Table 9.3. *Characteristics of the camera Cannon.*

9.4. Integrated vehicle sensors

ADCP

Vendor	RDI Teledyne
Typ	Model WHN300 S/N
Serial number	11436
Last calibration	
Exported data contains	• Latitude (degrees) • Longitude (degrees) • Altitude (meters) • Depth (meters) • Forward velocity over the bottom (meters/sec) • Starboard velocity over the bottom (meters/sec) • Error velocity • Temperature (degrees C) • Ensemble number • Heading (in degrees) • Stbd water velocity in mm/sec • Forward water velocity in mm/sec • Water velocity away from the transducer face (mm/sec) • Coordinate transform mode. The MSB (0x80) of this value indicates whether the water velocities are from the upward (set) or downward (cleared) looking beams.
Sample rate	-

CTD

Vendor	Seabird
Typ	SBE 49 FastCAT
Serial number- [CTD1] or [CTD2]	4955482-[0198] or [0168]
Last calibration	03.07.2017
Exported data contains	latitude, longitude, mission_time, depth, conductivity, temperature, salinity, sound_speed
Unit	[deg],[deg],[HH.MM.SS.F],[m],[S/m],[°C],[psu],[m/s]
Sample rate	4Hz

ECO (Combination Fluorometer and Turbidity Sensor)

Vendor	Wetlabs
Typ	FLNTU / 0712017
Serial number	FLNTURTD-939
Last calibration	-
Exported data contains	latitude, longitude, mission_time, depth, version, chl_ref(lambda), chl_sig, chlorophyll_a, turbidity_ref, turbidity_raw, turbidity
Unit	[deg],[deg],[HH.MM.SS.F],[m],[],[nm],[count],[µg/l],[nm],[count],[NTU]
Sample rate	1Hz

Preassure/Depth

Vendor	Paroscintific
Typ	Digiquartz Intelligent Depth Sensor
Model	8BT7000-I
Range	7000m
PN	1537-001-0
Serial number	109773
Last calibration	-
Exported data contains	
Unit	
Sample rate	1Hz

Tables 9.4. *Characteristics of the integrated sensors in the Abyss vehiucle, which comprises ADCP, CTD, ECO (optional) and Preassure/Depth.*

9.5. AUV acquisition, processing and positioning

9.5.1. AUV data acquisition, processing and display

During the cruise INSIGHT-Leg 1, one AUV dive was performed almost every day, resulting in a total of 12 missions. Each mission was done in the multibeam configuration (RESON Seabat 7125 200 kHz). All data were properly recorded except of dive 280, for which the receiver of the multibeam was mounted in an incorrect way (180° heading offset). Next, we describe the procedure of handling and post-processing of the data during this cruise. This workflow is not a strict way to follow and is altered when needed, modified from Caress (2014):

1. The download of the data started as soon as the AUV was brought inside the container after the completion of a mission. The data were downloaded directly onto the AUV server.
2. The raw data of the RESON Seabat 7125 are logged in the proprietary format .s7k. A file of this format consists of several records with specific contents. During this cruise, the following records were logged: 1003, 1006, 1008, 1012, 1013, 7000, 7001, 7004, 7007,

7017, 7022, 7027, 7028, 7200, 7503. That means bathymetric, backscatter and so called snippets data were recorded, but no water column information.

3. A first check of the data is performed in order to verify that the multibeam was working properly, that all the files are correctly logged and that the appropriate multibeam parameters were set. These points have to be checked in order to decide if a dive has to be re-done or not. This brief checkout was done by using the software package Qinsy/Qimera. This software tool allows a quick import even of a large data set.
4. As a next step a working map was created, which is normally used as a base for further scientific work during a cruise. The proper post-processing takes too long especially if the data are disturbed or the navigation adjustment is difficult. This base map was also created in Qinsy/Qimera. The imported data were roughly cleaned using specific preset filters. These prepared data were handed over to the scientific party in a format they require. In this case all the data were exported ungridded in an ASCII format (latitude/longitude/depth). During missions 290 and 291, small add-on mission legs for the calibration of the multibeam were planned. To find proper areas for a calibration like this is not easy, as the planning has to be done based on ship-based bathymetric maps that usually have a resolution of more than 25 meters. The application of the calibration data is done using the software PDS2000.
5. For the next processing steps, the software MB Systems is used. There were several software problems in different versions of this processing software during this cruise. This lead to a much longer lasting post-processing phase.

   5a) The raw files (*.s7k) are copied in a *mbdatalist* as a preparation of the processing.

   5b) Next is the command *mb7kpreprocess*, it was applied to all data inside the data list. This command creates new files with the extension *.mb88 while leaving the original s7k files intact. It creates a set of ancillary files, which are used to speed up processing. This tool also interpolates the asynchronous navigation and attitude data and synchronizes it with the multibeam data, the output files *.mb88 contain correctly embedded information.

   5c) The new created *.mb88 files have been copied in an separate folder (*mbdatalist*).

   5d) The position of the multibeam transducer heads has to be referenced in the vehicle coordination and the attitude biases have to be considered. This happened by using the *mbset* command. It creates or modifies the *mbprocess* parameter files. The parameters contained in these files have been applied to the multibeam data with the

command *mbprocess*. In case of mission 280 a heading offset of 180° was applied (see above).

5e) Usually, the adjustment of the navigation would be the next step and followed by an editing cleaning of the data could be done with a corrected navigation in a later step and maybe with another tool. This was not a feasible approach on this cruise since most of the dives acquired very disturbed data. The exact reasons for this are unknown. So, instead of the renavigation we used the *mbedit/mbeditviz* tool to clean the data as a preparation for the navigation adjustment. Here, data points are marked or flagged if they not represent the sea floor. This bathymetry edit flags are saved in a specific ancillary file format. The flags are applied again by using the *mbprocess* command.

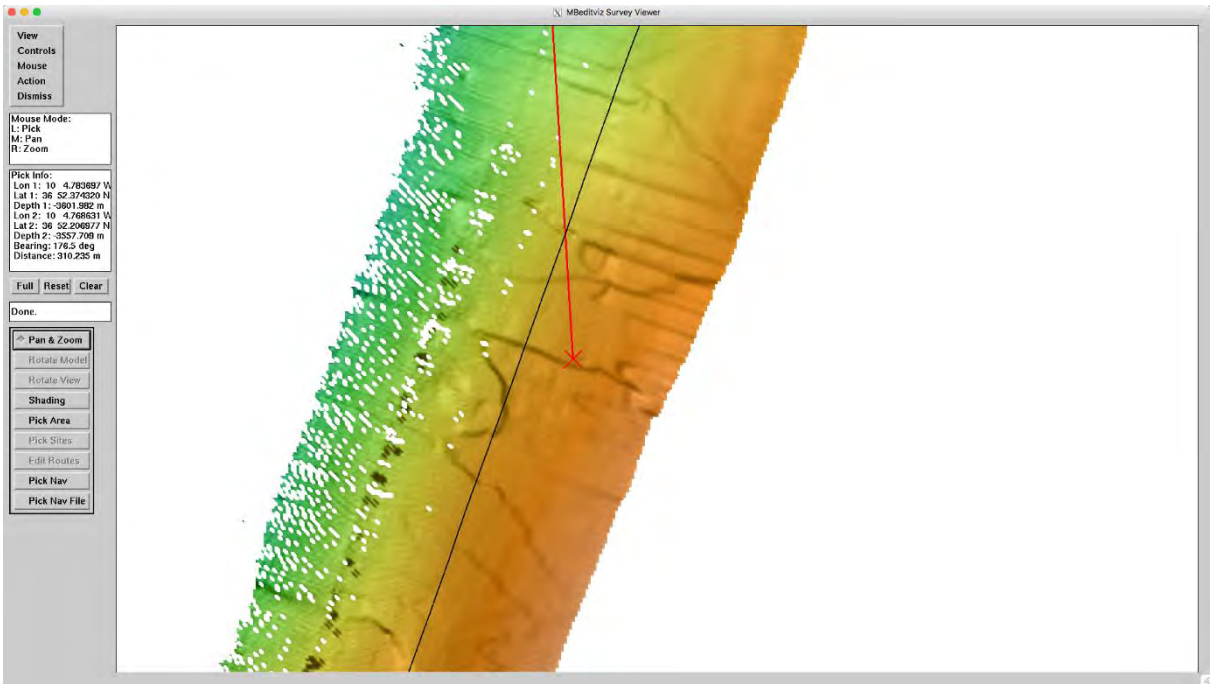

Figure 9.5. *Example on how the data was cleaned using mbedit/mbeditviz tool of MBsystem.*

5 f) As mentioned before time lags were figured out in all of the dives. Since this can be only seen during this process, the latency cannot be correct during the first *mb7kpreprocess* step. We checked the time lag either by using *mbeditviz* or by calculating the time lag with *mbrolltimelag*. That is why this command is used a second time to apply this specific time lag. The result is applied by using *mbpre7kprocess* and *mbprocess*.

5 g) During this cruise, one of the last steps of the data processing is the adjustment of navigation offsets using the tool *mbnavadjust*. This tool allows to adjust poorly

navigated surveys by matching topographic features in overlapping swaths. In this case, the slowly increasing drift of the inertial navigation can be compensated. The tool divides the files in sections of user-defined size. MB Systems generates contour lines of each section and compares them against each other. The overlapping areas will be shown in a window of *mbnavadjust* for manual adjustment using tie points in both sections. The adjustments are saved in a specific file, which is applied with a further *mbprocess*.

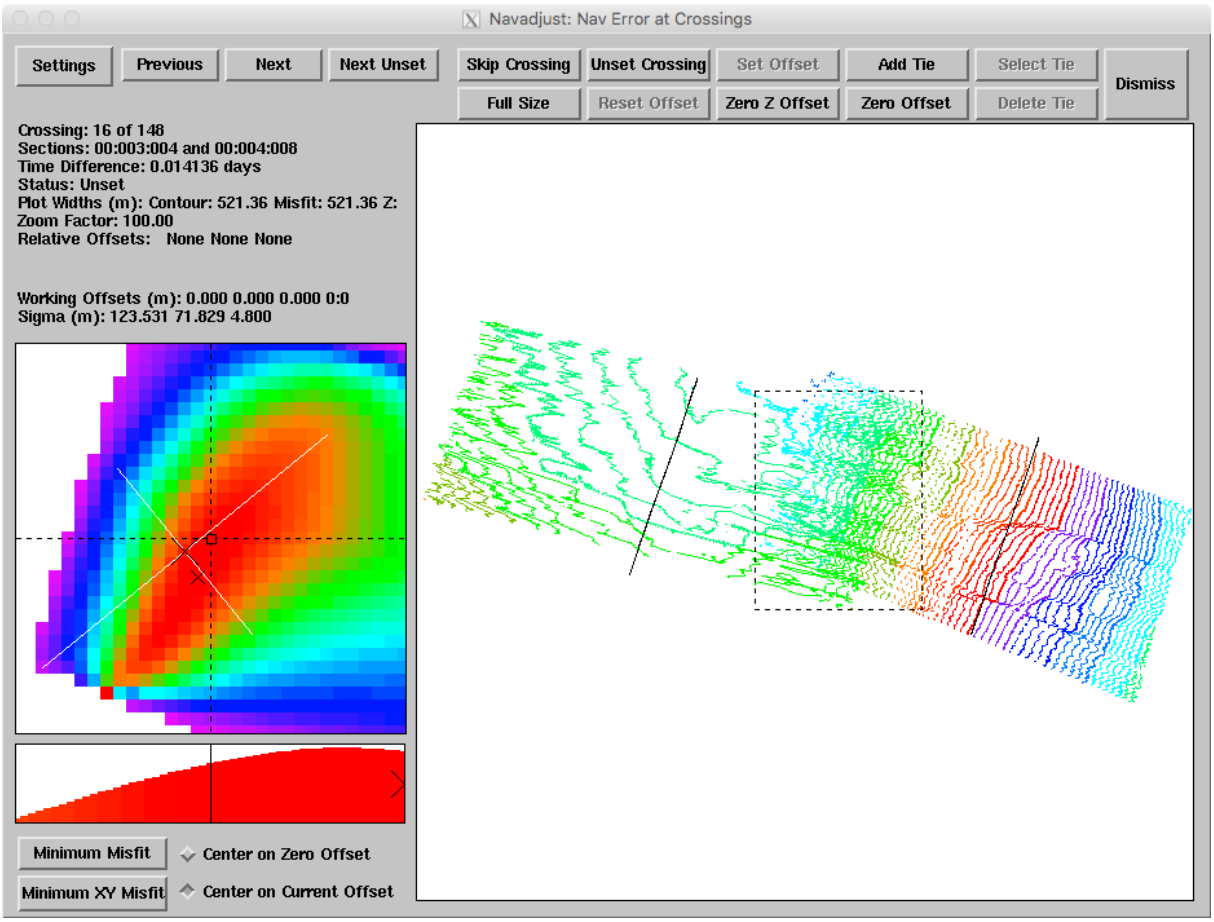

Figure 9.6. *Example on how the different datasets have been manually adjusted using mbnavadjust tool of MBsystem.*

5 h) After the treatment of the various sections or dives, they are brought together by the help of *mbnavadjustmerge*. That means a merging of the *mbnavadjust* projects and it leads to a combined map.

5 i) The internally consistent, navigation-edited data requires a correction to an absolute position. This is usually done be adjusting the AUV map to topographic features in the ship-based bathymetry.

As soon as the adjustment of the navigation was conducted successfully and the final data

show no anomalies, the data were exported according to the needs of the scientific party. In the present case the ungridded data was exported in an ASCII format by using *mblist* (latitude, longitude, depth). Those data are imported into Qinsy and gridded. The conversion of the data into required data formats in Qinsy is unproblematic and quickly done (e.g. geotiff, FM scenes, etc.)

9.5.2. Transponders

The AUV Abyss uses a LBL (Long Baseline) system to support its navigation. Each of the five working areas during the INSIGHT cruise had a set of transponders, which the vehicle used to get a navigation update after the descent phase. The type of Long Baseline transponders, which is part of the REMUS 6000 system works with frequencies between 9 and 12 kHz. The AUV uses only two transponders for triangulating its position. The following table enlists the details of each used transponders during the INSIGHT cruise.

Table 9.5. *Table including the working area, positioning, transducer dept., deployments, releasing and recovery of the transponders used during INSIGHT-Leg 1 cruise.*

Transponder	Type	Working area	Position	Transducer depth (m)	Deployment	Released	Recovered
1C	DT4C-LF	M. Pombal	36° 52,762' N 010° 03,731' W	3300	01.05.2018 11:40 UTC	03.05.2018 18:26 UTC	03.05.2018 20:07 UTC
2D	DT4C-LF	M. Pombal	36° 53,319' N 010° 03,573' W	3310	01.05.2018 11:50 UTC	03.05.2018 17:58 UTC	03.05.2018 19:45
4A	DT4C-LF	LSW	35° 40,687' N 010° 01,243' W	4396	04.05.2018 07:52 UTC	08.05.2018 15:52 UTC	08.05.2018 17:00 UTC
3C	DT4C-LF	LSW	35° 40,564' N 010° 00,413' W	4388	04.05.2018 07:27 UTC	08.05.2018 14:52 UTC	08.05.2018 16:10 UTC
5A	DT4C-LF	LSE	35° 06,530' N 007° 15,000' W	1086	09.05.2018 07:15 UTC	11.05.2018 20:24 UTC	11.05.2018 21:09 UTC
6C	DT4C-LF	LSE	35° 06,271' N 007° 14,016' W	1043	09.05.2018 07:30 UTC	11.05.2018 19:50 UTC	11.05.2018 20:35 UTC
7A	DT4C-LF	Ginsburg MV	35° 23,106' N 007° 07,058' W	1113	12.05.2018 11:33 UTC	13.05.2018 09:50 UTC	13.05.2018 10:30 UTC
8C	DT4C-LF	Ginsburg MV	35° 22,405' N 007° 07,089' W	1090	12.05.2018 11:45 UTC	13.05.2018 10:26 UTC	13.05.2018 10:55 UTC
9A	DT4C-LF	Lolita	36° 08,441' N 007° 58,782' W	1487	13.05.2018 21:17 UTC	15.05.2018 15:20 UTC	15.05.2018 15:50 UTC
10C	DT4C-LF	Lolita	36° 07,792' N 007° 58,778' W	1558	13.05.2018 21:04 UTC	15.05.2018 15:55 UTC	15.05.2018 16:25 UTC

9.6. Abyss AUV dives

During cruise INSIGHT 12 missions were carried out by the AUV Abyss (Table 9.6). The missions were done using exclusively the multibeam-configuration. The primary sensor was the RESON Seabat 7125 (multibeam echosounder) 200 kHz. The turbidity sensor (WetLabs ECO FLNTU Fluorometer and Turbidity sensor; S/N FLNTURTD-939), the REDOX potential sensor (by Ko-ichi Nakamura) and the CTD (Seabird SBE49 FastCAT; S/N 4948793-0168) ran simultaneously and served as secondary sensors. All data have a time stamp and/or are related to a position of the vehicle. Please consider that those positions are the original and not navigational adjusted positions. More detailed information about the dives is found in Table 9.6.

Table 9.6. *Table including the 12 dives carried out during the cruise, working area, date, maximum depth (m), travelled distance (km), time in water (h), time for each mission (h) and survey time (h) during INSIGHT-Leg 1 cruise.*

	Dive	Working area	Date	Max. Depth (m)	Travelled distance (km)	Water time (h)	Mission time (h)	Survey time (h)
1	Abyss0279	M. Pombal	01. May 18	3852	64055	17,9	12,8	9,4
2	Abyss0280	M. Pombal	02. May 18	3841	97386	27,1	17,5	15,0
3	Abyss0281	Lineament SW	04. May 18	4450	63168	19,7	11,6	7,9
4	Abyss0282	Lineament SW	05. May 18	4505	97770	27,1	17,6	14,1
5	Abyss0283	Lineament SW	06. May 18	4435	61465	16,1	11,1	7,9
6	Abyss0284	Lineament SW	07. May 18	4470	97887	21,4	17,7	14,3
7	Abyss0285	Lineament SE	09. May 18	1100	99165	19,0	17,9	16,9
8	Abyss0286	Lineament SE	10. May 18	1100	65575	13,8	11,8	10,8
9	Abyss0287	Lineament SE	11. May 18	1210	98606	19,0	17,8	16,0
10	Abyss0288	Ginsburg MV	12. May 18	1107	97948	19,3	17,5	16,1
11	Abyss0289	Lolita Diapir	13. May 18	1710	105609	20,7	19,0	17,4
12	Abyss0290	Lolita Diapir	15. May 18	1750	60582	13,6	10,9	9,4
	Total dives: 12					**234,7**	**183,3**	**155,2**

AUV Statistics during cruise INSIGHT/ Leg 1

(Survey time = time spent mapping on the seafloor; Mission time = time including descent, survey and ascent phase; Water time = time between launch and recover; Distance travelled = total distance during mission)

9.6.1. Dive 279-Marques de Pombal Fault (North)

Dive 279 was devoted to map the northern half of the Marques de Pombal Fault scarpment.

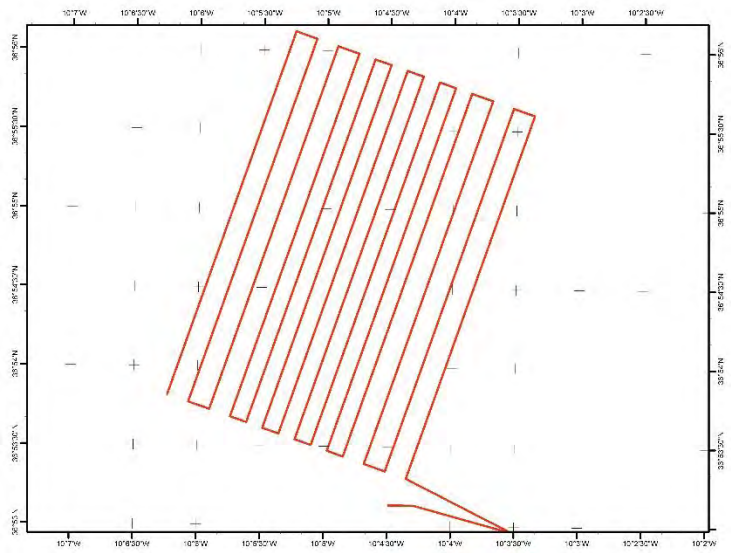

Figure 9.7. *AUV track corresponding to dive 279 on the north of Marques de Pombal Fault.*

Dive 279 shows the frontal part of the Marques de Pombal Thrust fault, with a bathymetric relief ranging from 3450 m to 3900 m (Fig. 9a). We observe the sharp boundary between the steep slope and the fault area of the Infante Don Henrique Basin. The slope map (Fig. 9b), clearly shows the boundary betwen the 2 domains presented above. Mapped area: 12.7 km^2.

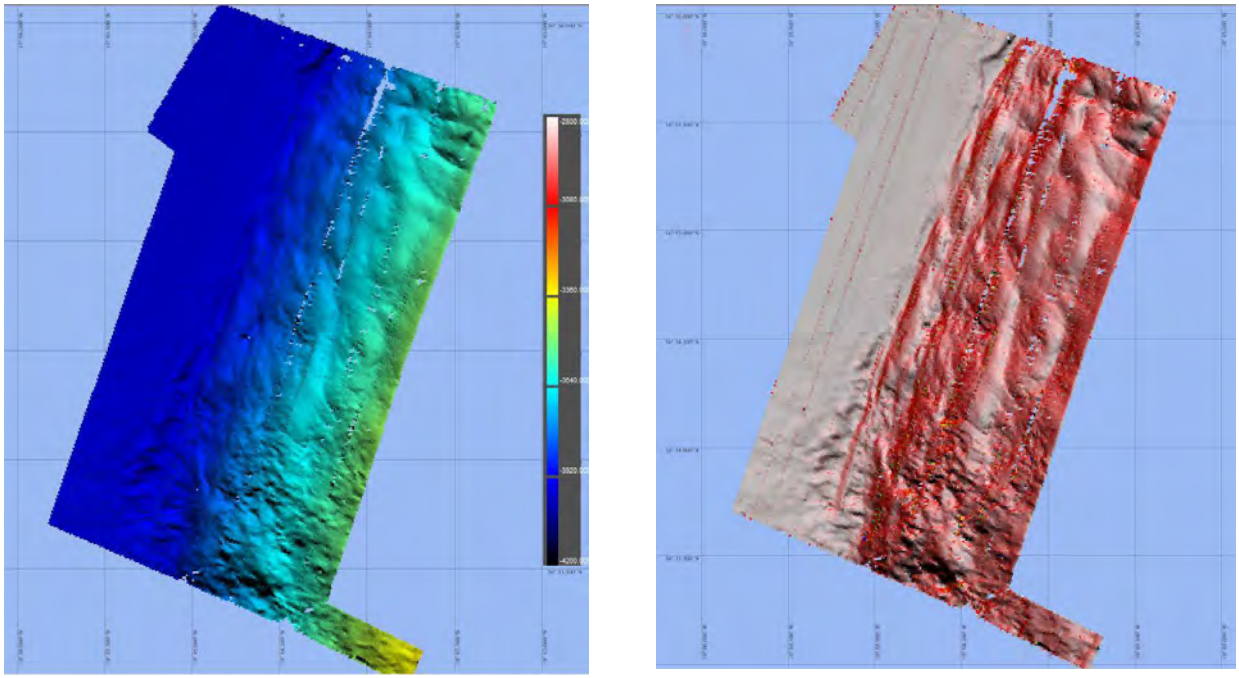

Figure 9.8. *a: AUV bathymetric map corresponding to dive 279, on the northern part of the Marques de Pombal Fault. b: AUV slope map of the same area.*

9.6.2. Dive 280-Marques de Pombal Fault (South)

We do not have available yet the processed data of dive 280. Mapped area: 16.7 km^2.

9.6.3. Dive 281-Lineament South West Fault (central W)

Dive 281 was devoted to map the cental part of the Lineament SouthWest Fault (Fig. 9.9).

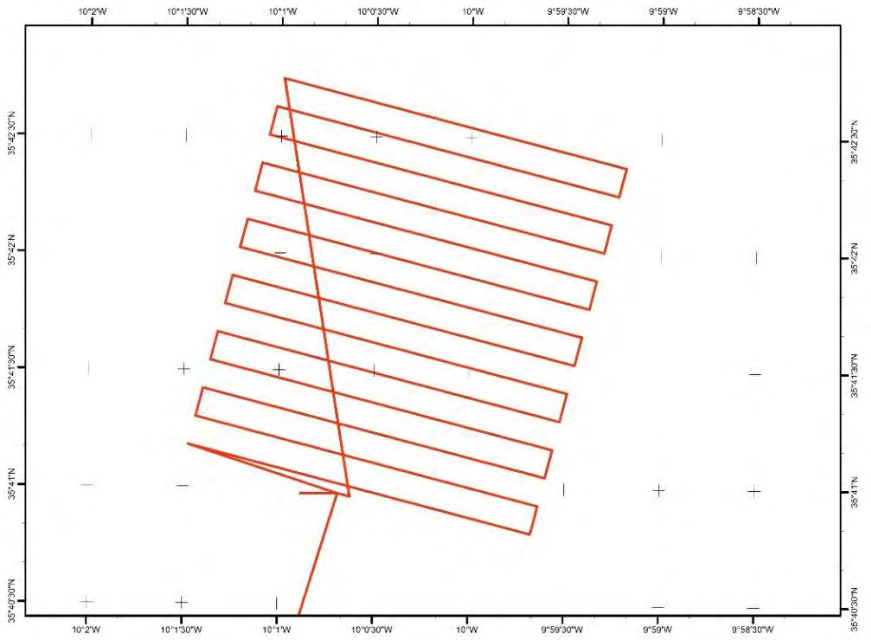

Figure 9.9. *AUV track of dive 281 on central –west part of the Lineament South-West fault, where the transponders were located.*

Dive 281 depicts the central part of the Lineament SouthWest Fault, with a bathymetric relief ranging from 4410 m to 4500 m (Fig. 9.10). We can observe the sharp boundary that represents the LSW fault. Mapped area: 8.3 km^2.

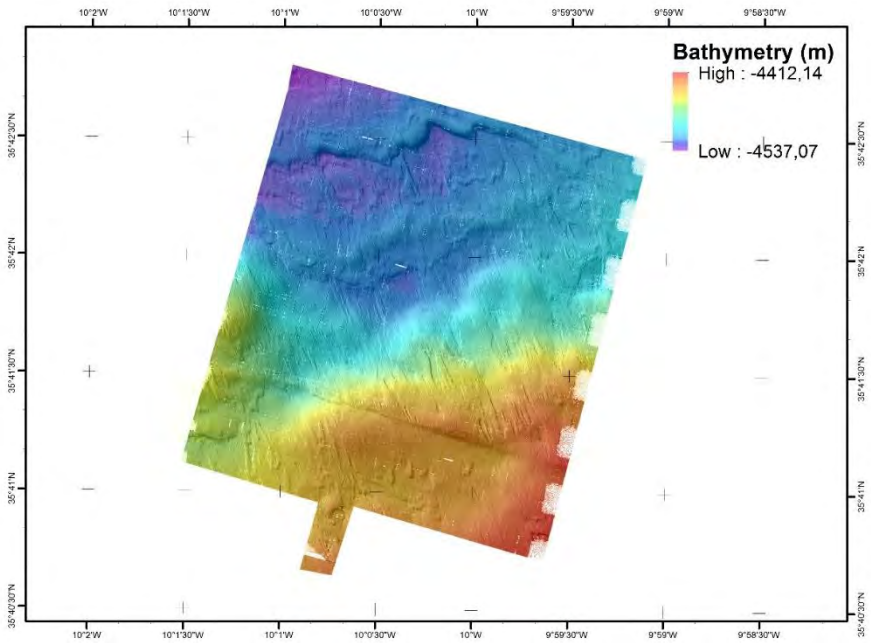

Figure 9.10. *AUV bathymetric map corresponding to dive 281, on the central-west part of LSW fault.*

9.6.4. Dive 282-Lineament South West Fault (extreme W)

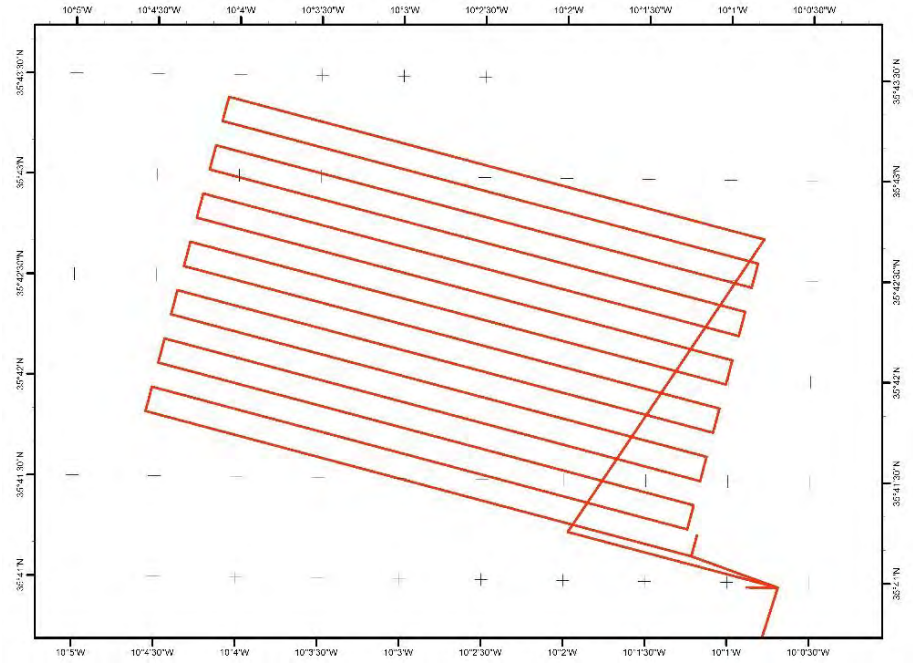

Figure 9.11. *AUV track corresponding to dive 282 on northwestern part of the Lineament SouthWest Fault.*

Dive 282 depicts the northwestern part of the Lineament SouthWest Fault, with a bathymetric relief ranging from 4400 m to 4500 m (Fig. 9.12). We can observe the trace of the fault on both sides and a small pressure ridge at the middle. Numerous seafloor structures, probably related to bottom currents are observed, all following a NW-SE trend. The gap in the middle of the image was acquired during dive 284. Mapped area: 15.4 km^2.

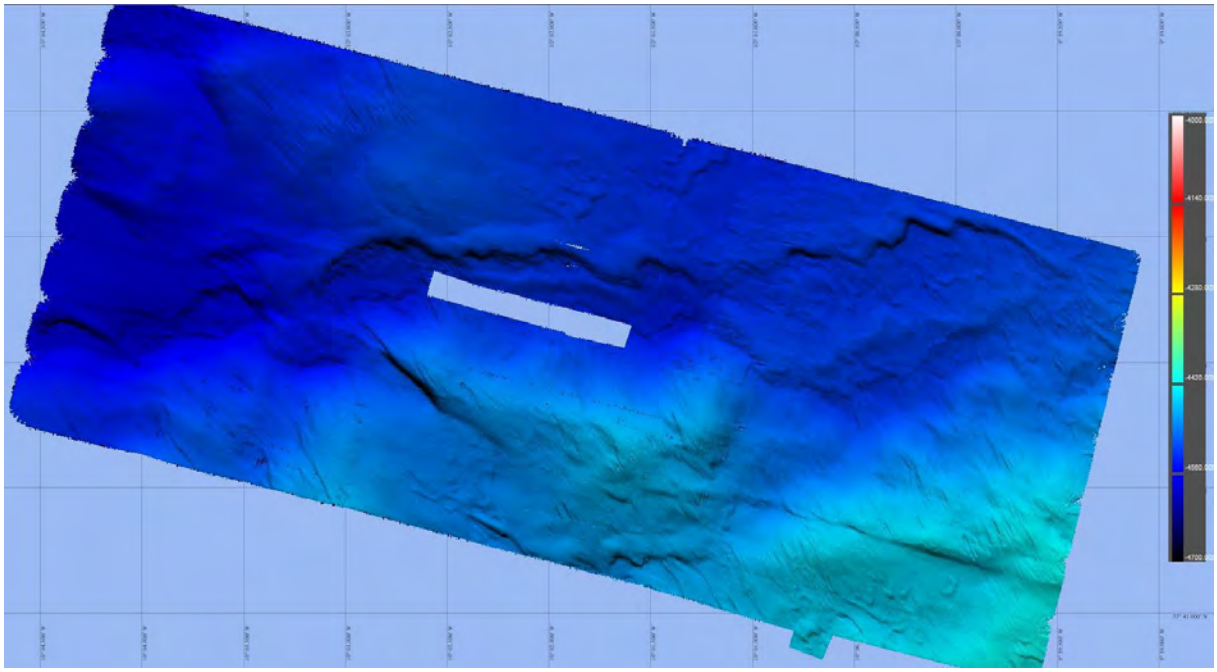

Figure 9.12. *AUV bathymetric map corresponding to dive 282, on the northwestern part of LSW Fault.*

9.6.5. Dive 283-Lineament South West Fault (central E)

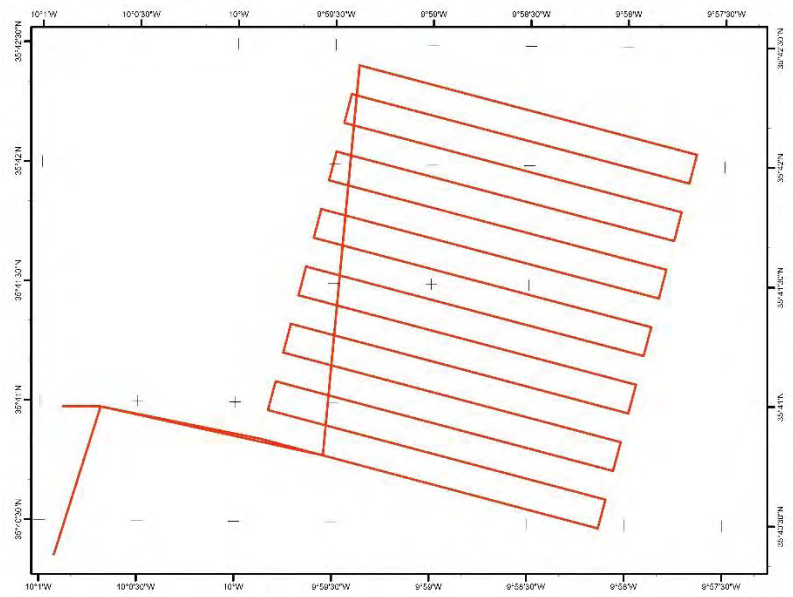

Figure 9.13. *AUV track corresponding to dive 283 on central-east part of the Lineament SouthWest Fault.*

Dive 283 depicts the continuation of dive 281, at the central-east part of the Lineament SouthWest Fault, with a bathymetric relief ranging from 4350 m to 4550 m (Fig. 9.14). We barely observe the trace of the fault at the bottom of the image and again, the numerous traces of bottom currents, as well as scarps. Mapped area: 8 km^2.

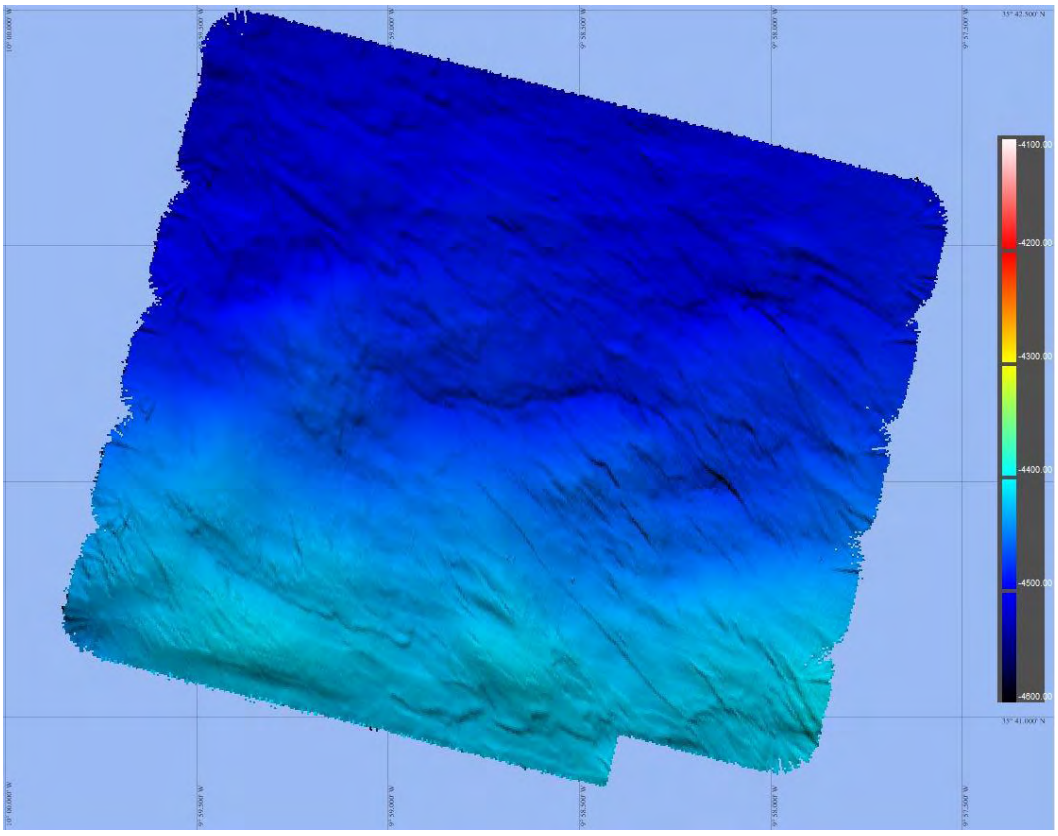

Figure 9.14. *AUV bathymetric map of dive 283, on the central–east part of LSW fault.*

9.6.6. Dive 284-Lineament South West Fault (extreme E)

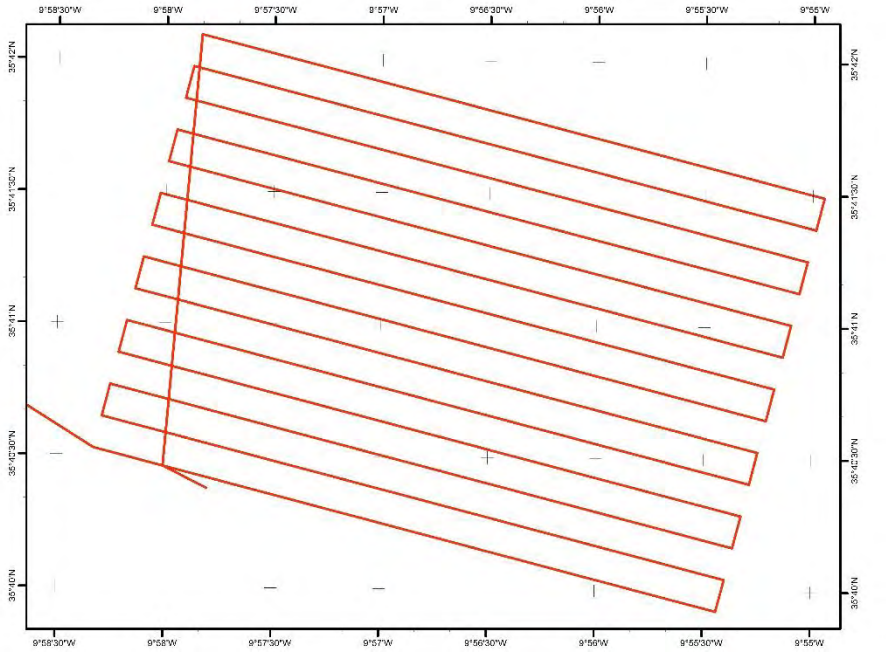

Figure 9.15. *AUV track corresponding to dive 284 on southeastern part of the Lineament SouthWest Fault.*

Dive 284 depicts the termination of the surveyed area, at the easternmost part of the Lineament SouthWest Fault, with a bathymetric relief ranging from 4300 m to 4550 m (Fig. 9.15). We observe the fault trace at the bottom of the image with a prominent fault scarp, fault discontinuities, and ENE-WSW traces associated to the fault system. Mapped area: 13.8 km^2.

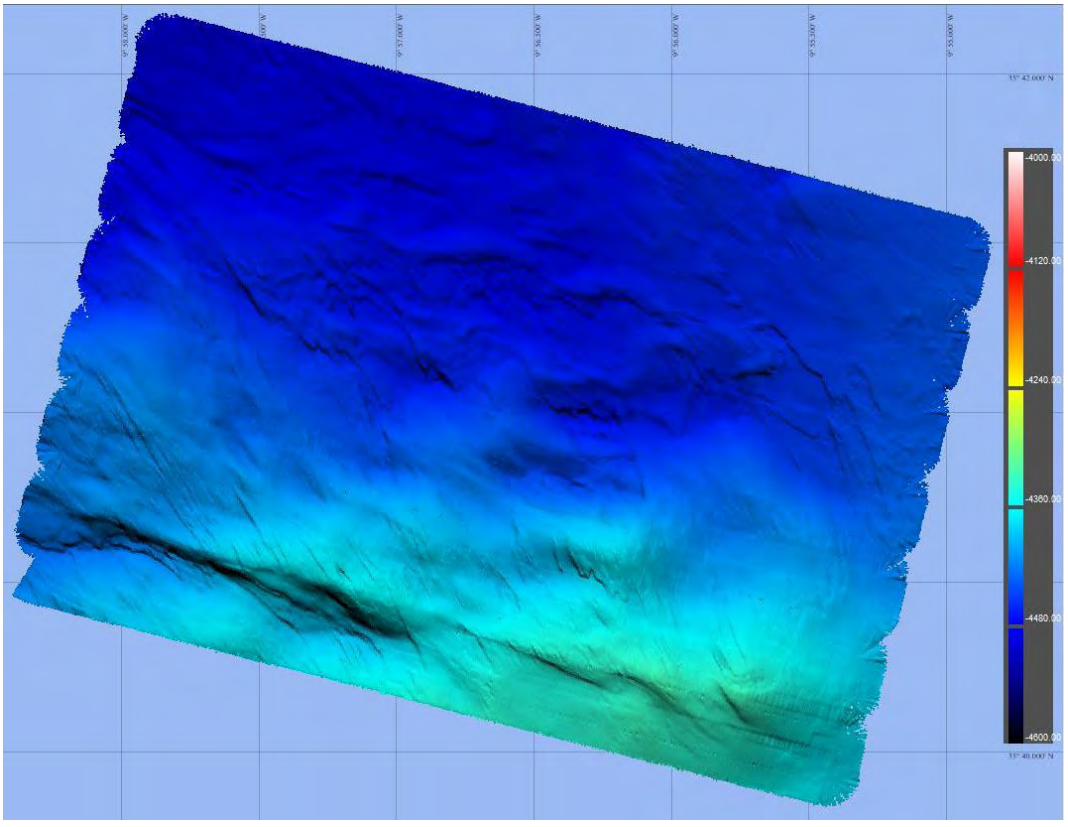

Figure 9.16. *AUV bathymetric map of dive 284, on the easternmost part of LSW fault.*

9.6.7. Dive 285-Lineament South East Fault (extreme E)

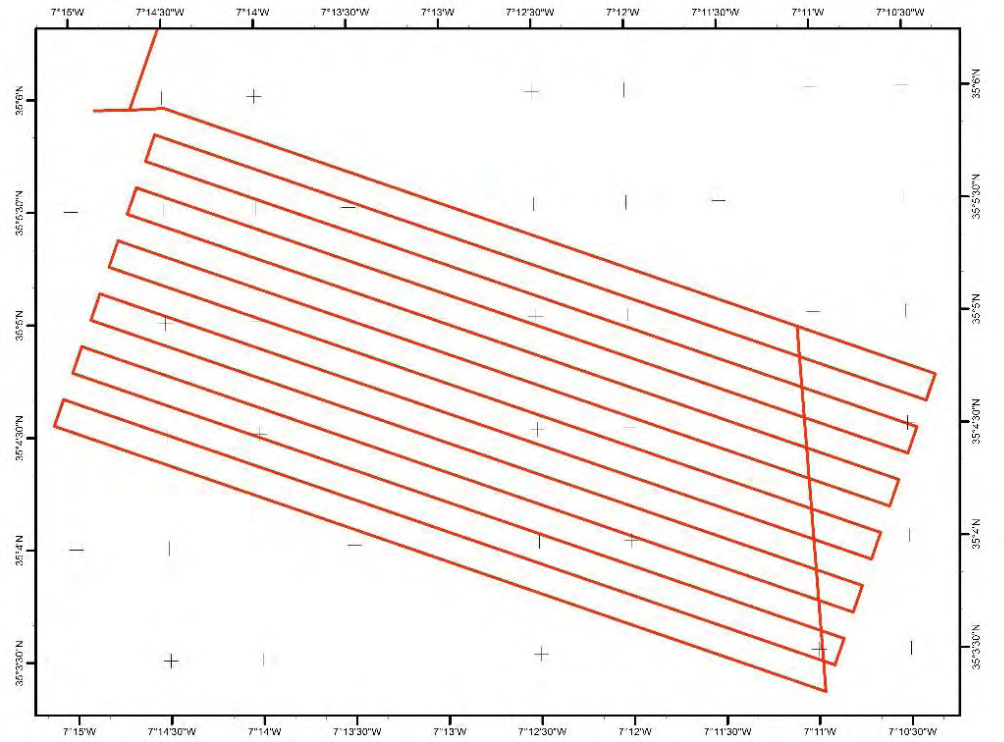

Figure 9.17. *AUV track corresponding to dive 285 on southeastern part of the Lineament SouthEast Fault.*

Dive 285 depicts the easternmost termination of the area surveyed in the Lineament SouthEast Fault, in the Moroccan Margin. Bathymetric relief ranges from 900 m to 1200 m (Fig. 9.18). On the image, we observe the main fault trace and the presence of structures probably related to salt collapses, which often are rimmed by alignments of mounds, probably related to fossil deep-water corals. Towards the SE end of the image, we observe a NE-SW trending fault bounding a pull-apart basin > 1200 m depth. Mapped area: 14.4 km^2.

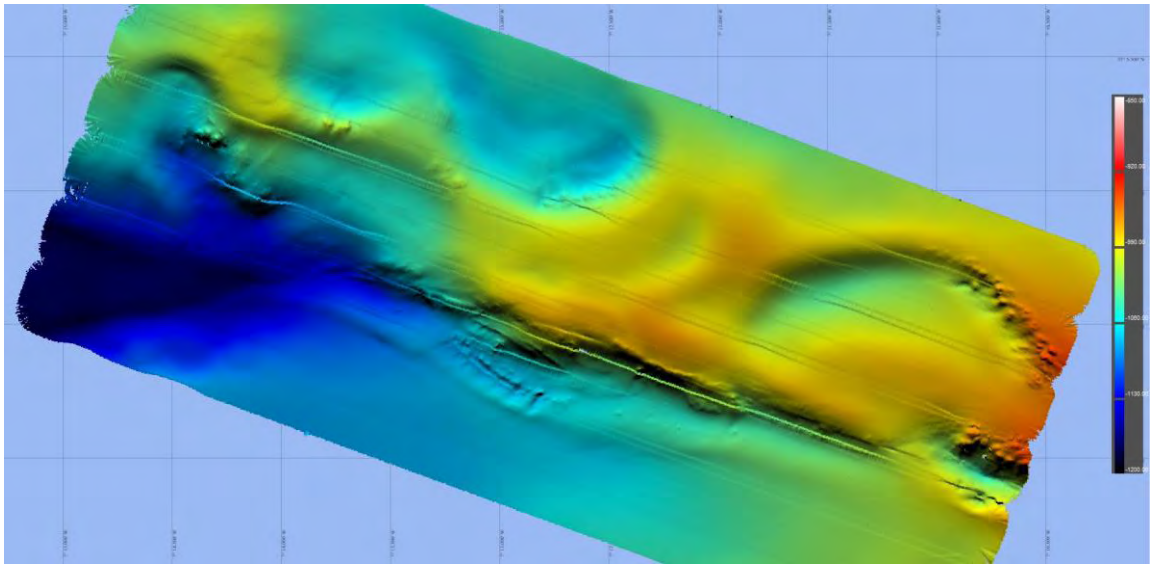

Figure 9.18. *AUV bathymetric map of dive 285, on the easternmost part of LSE fault.*

9.6.8. Dive 286-Lineament South East Fault (central)

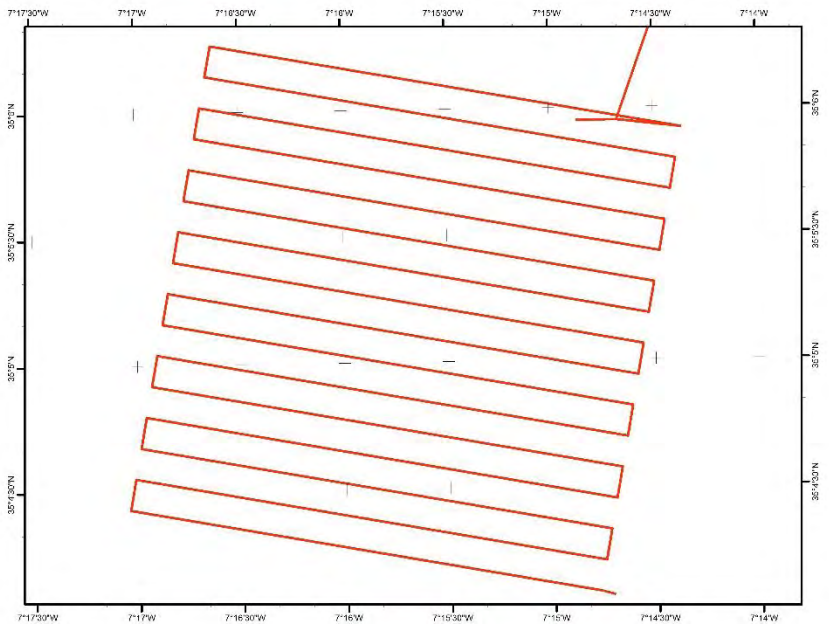

Figure 9.19. *AUV track corresponding to dive 286 on central part of the Lineament SouthEast Fault.*

Dive 286 depicts the central part of the area surveyed in the Lineament SouthEast Fault. Bathymetric relief ranges from 1020 m to 1200 m (Fig. 9.20). On the image below, we observe the main trace, which is about 100 m wide, very continuous showing small elongated ridges and basins. A collapse basin (north side) is confronted to a small N45 trending wide ridge (south side) denoting a clear dextral strike-slip displacement. Mapped area: 12.2 km^2.

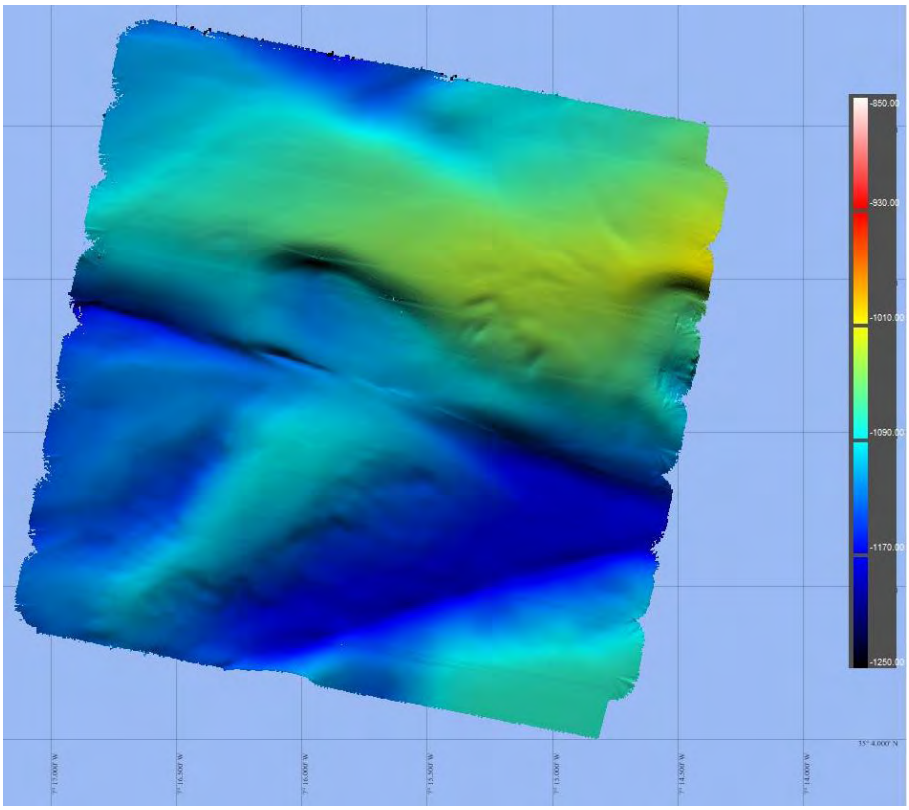

Figure 9.20. *AUV bathymetric map of dive 286, on the central part of LSE fault.*

9.6.9. Dive 287-Lineament South East Fault (extreme W)

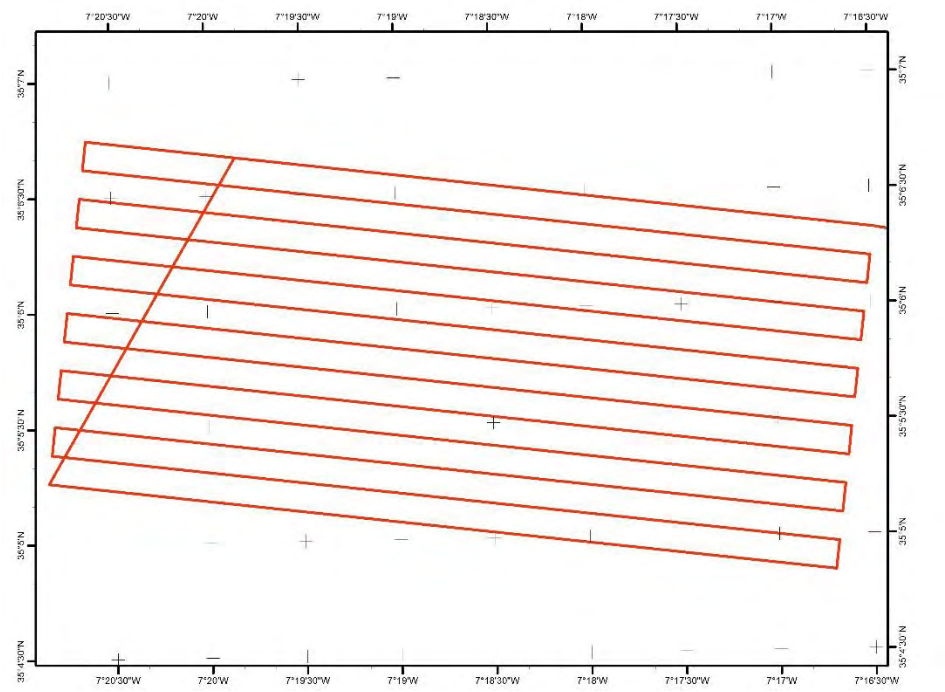

Figure 9.21. *AUV track corresponding to dive 287 on eastern part of the Lineament SouthEast Fault.*

Dive 287 depicts the western part of the area surveyed in the Lineament SouthEast Fault. Bathymetric relief ranges from 1050 m to 1250 m (Fig. 9.22). On this map, we observe the presence of a small, elongated pressure ridge in between the west and east fault traces, which is about 350 m wide and 2 km long. Towards the east, a pull-apart basin of 400 m wide and 4.2 km long is also observed. Numerous slide scars are bounding the pull-apart basin. The fault continues for 15 km to the west, until it reaches the accretionary wedge and the fault trace is difficult to be identified. Mapped area: 17.5 km^2.

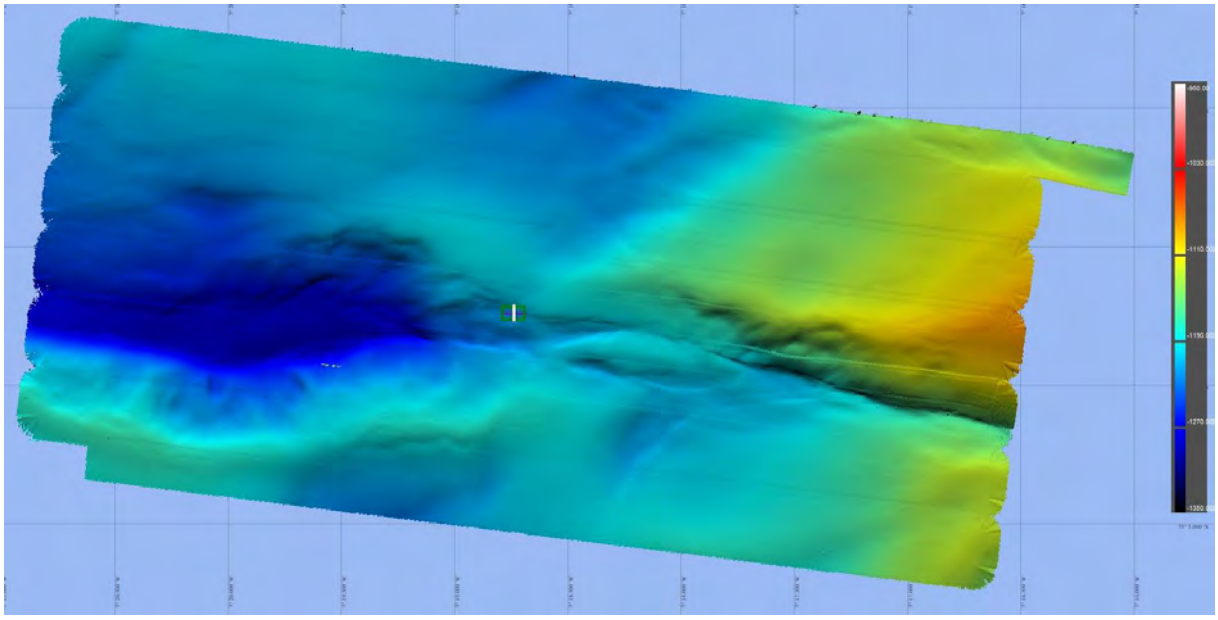

Figure 9.22. *AUV bathymetric map of dive 287, on the westernmost part of LSE fault.*

9.6.10. Dive 288-Ginsburg Mud Volcano

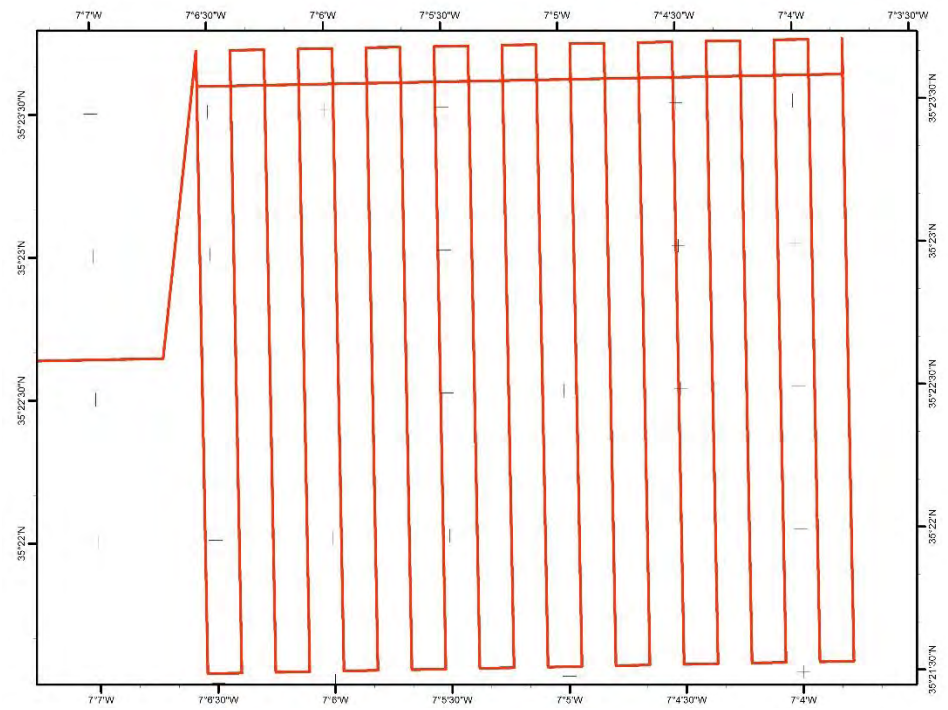

Figure 9.23. *AUV track of dive 288 corresponding to the Ginsburg mud volcano.*

Dive 288 was devoted to the mapping of the Ginsburg Mud Volcano, also in the Moroccan margin. This structure is associated to a twin mud volcano located just to the north of Ginsburg, named Yuma mud volcano. Bathymetric relief of Ginsburg MV ranges from 900 m to 120 m (Fig. 9.24). On the maps below, we observe the AUV bathymetric mapping as well as the slope. These maps show a series of concentrical features on the center and top of the mud volcano, as well as a clear a mud flow on the NW side of the Ginsburg mud volcano. Around the MV feature, a clear moat is observed. Mapped area: 16.8 km^2.

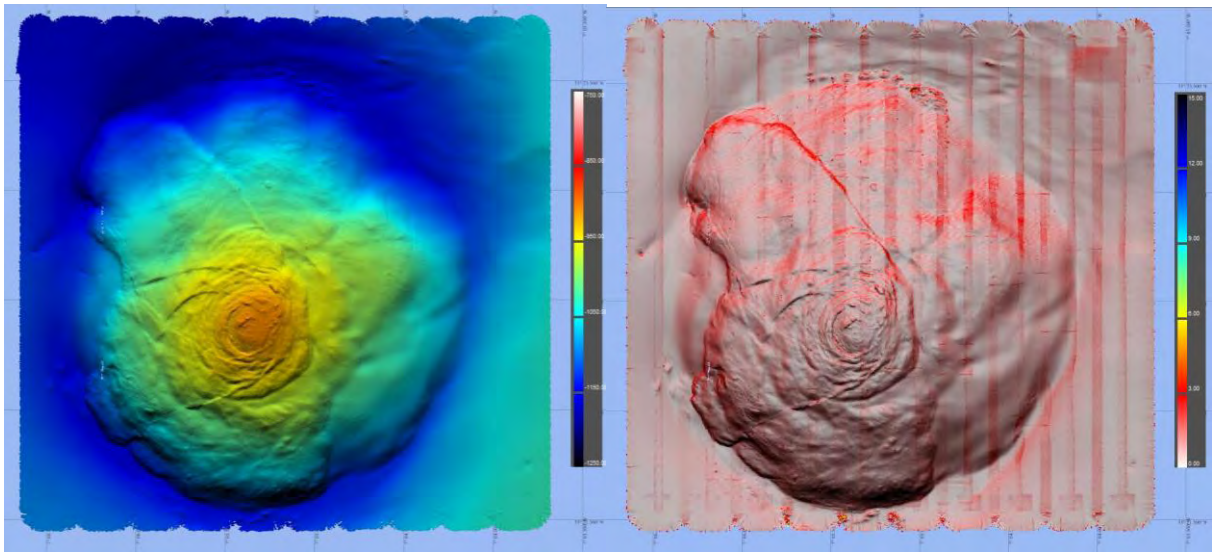

Figure 9.24. *AUV bathymetric map and slope map of dive 288, corresponding to the Ginsburg mud volcano.*

9.6.12. Dive 289-Lolita Mud Diapir (Northern part)

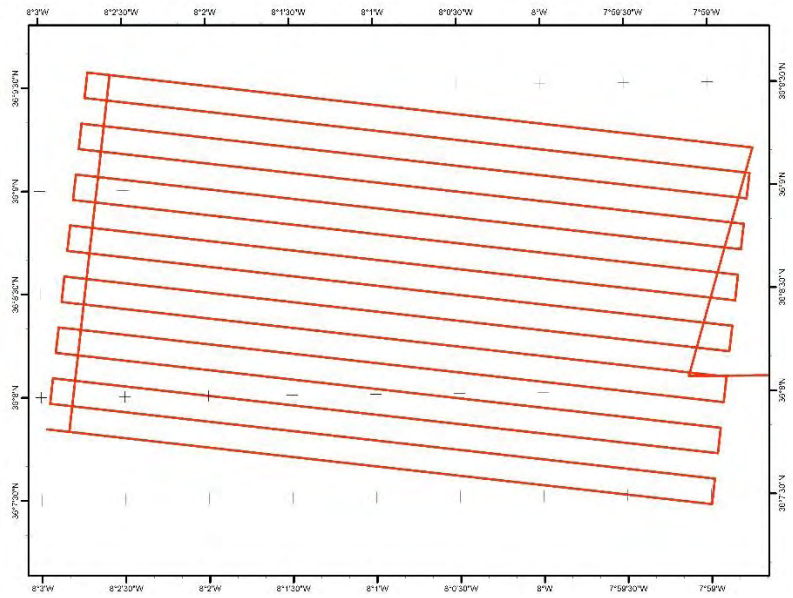

Figure 9.25. *AUV track of dive 289 corresponding to the northern half of the Lolita salt diapir structure.*

Dive 289 focused on the northern half of the Lolita salt diapir, in Portuguese waters. It is located on the western rim of the Portimao Bank, where successive diapiric structures are located, north of the accretionary wedge. Bathymetric relief of Lolita salt diapir ranges from 1250 m to 1750 m (Fig. 9.26). We observe a 4.5 km long fault main scarp from where numerous mass transport deposits and scars are observed, and a free surface of 400 m long, with a main large translational slide of about 1.6 km^2. Mapped area: 19.1 km^2.

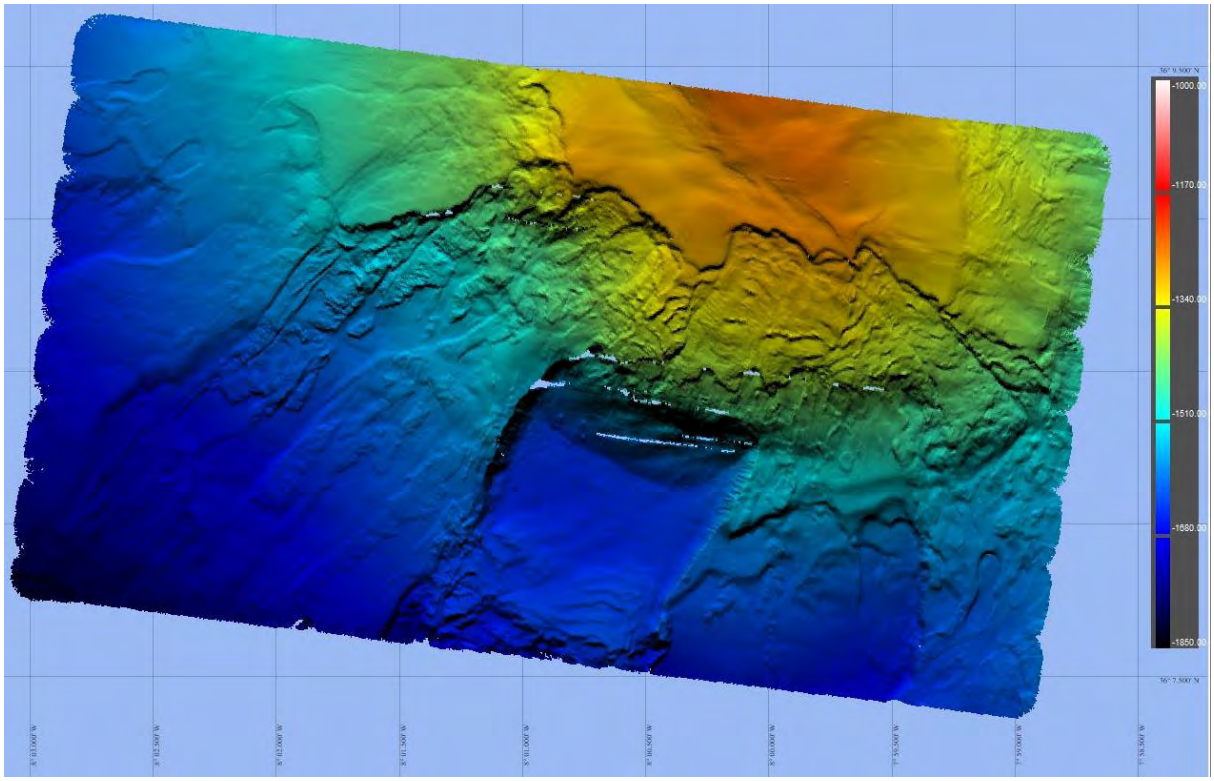

Figure 9.26. *AUV bathymetric map of dive 289, corresponding to the Lolita salt diapir (top).*

9.6.12. Dive 290-Lolita Mud Diapir (Southern part)

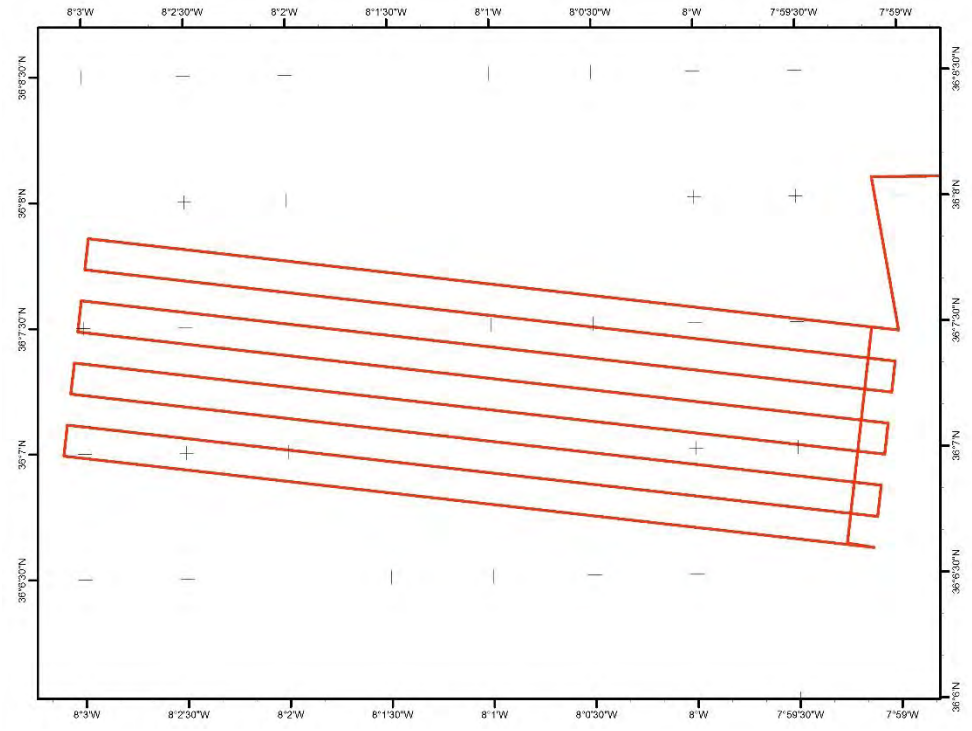

Figure 9.27. *AUV track of dive 290 corresponding to the southern half of the Lolita salt diapir structure.*

Dive 290 focused on the southern half of the Lolita salt diapir. Bathymetric relief of this part of the Lolita salt diapir ranges from 1600 m to 1850 m (Fig. 9.28). We observe a lower fault scarp with numerous mass transport deposits, disaggregated and accumulated the foot of the structure.Towards the east of the lower part of the slide, a scar of 1.9 km is observed Mapped area: 9.6 km^2.

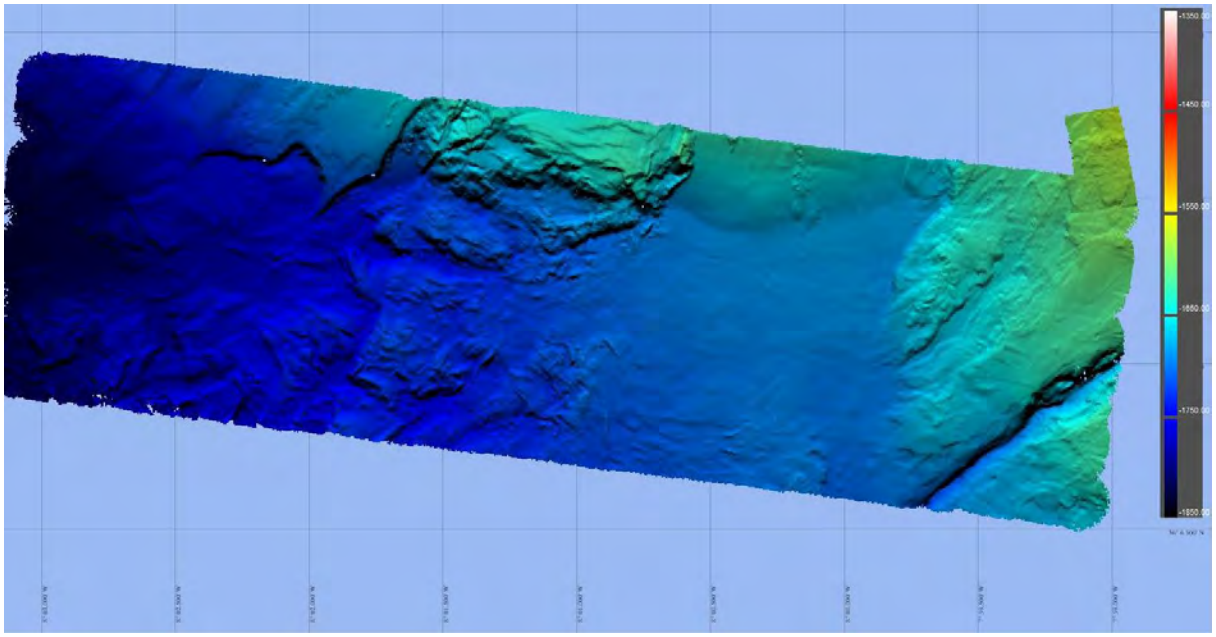

Figure 9.28. *AUV bathymetric map of dive 290, corresponding to Lolita salt diapir (bottom).*

10. High-resolution multichannel seismic data

10.1. Introduction to MCS acquisition

Between 2nd and 16th May 2018, the INSIGHT-Leg 1 survey focused on the acquisition of Multichannel Seismic Reflection (MCS) data using the digital, solid state, 605 m-long streamer and the source airgun system of the Unidad de Tecnología Marina (CSIC) onboard R/V Sarmiento de Gamboa. A total 44 MCS profiles were acquired between -10.3°W and -6.9°W and 34.9°N and 37°N following mainly NE-SW and W-E directions (Fig. 10.1). The objective of the INSIGHT-Leg 1 survey was to image the main tectonic strike-slip structures involved in the Africa and the Eurasian plate, the thrust fault Marques de Pombal fault located west of San Vicente Canyon, a mud volcano of the Moroccan Margin and a salt diapir structures near the Portimao Bank, all in the Gulf of Cadiz area. During this leg, a total of 704 km of MCS were collected. Tables 10.1 and 10.2 provide detailed information of the location and acquisition of MCS lines.

Table 10.1. *Table including the number of MCS profiles, and coordinates of starting (lat, lon) and ending points (lat, lon) of the seismic profiles acquired during the INSIGHT-Leg 1 cruise.*

Area	Line	SOL (Lat)	SOL (Lon)	EOL (Lat)	EOL (Lon)
MPF	MP02	036°52'18.8149"	009°51'55.810"	036°55'31.81571"	-010°00'7.93055"
	MP03	036°55'46.47209"	-010°00'50.46996"	036°58'4.58344"	-010°07'37.71447"
	MP04	036°56'49.74831"	-010°07'48.05036"	036°54'23.85766"	-010°00'44.98421"
	MP05	036°53'23.25764"	-010°01'35.90648"	036°55'48.99879"	-010°08'43.13334"
	MP06	036°54'35.44436"	-010°08'59.96047"	036°52'7.31878"	-010°01'48.83405"
	MP07	036°51'12.74374"	-010°03'2.06302"	036°53'36.52385"	-010°09'58.02698"
	MP08	036°52'14.90075"	-010°09'52.71748"	036°49'56.42087"	-010°03'9.05378"

	MP09	036°48'55.49423"	-010°04'0.65492"	036°51'19.62669"	-010°11'1.48633"
	MP10	036°49'44.79903"	-010°08'52.86043"	036°51'1.51559"	-010°08'17.71963"
	MP11	036°51'27.79608"	-010°08'11.66303"	036°58'37.01937"	-010°06'39.07305"
LSW	LW01	035°44'38.34111"	-010°02'29.03931"	035°46'42.19772"	-010°05'36.21445"
	LW01	035°46'21.64088"	-010°07'34.96034"	035°37'4.39849"	-010°10'11.93185"
	LW02	035°37'56.37562"	-010°13'52.48388"	035°47'22.14483"	-010°11'12.73520"
	LW08	035°39'1.44027"	-010°05'49.04692"	035°45'20.71032"	-010°03'49.80627"
	LW09	035°44'50.73464"	-010°02'12.99033"	035°38'28.19348"	-010°04'12.24603"
	LW10	035°38'23.14691"	-010°02'43.92729"	035°44'47.84894"	-010°00'44.20283"
	LW11	035°44'13.32480"	-009°59'25.04220"	035°37'47.15460"	-010°01'25.10100"
	LW12	035°43'56.18657"	-009°58'1.78289"	035°37'34.33183"	-010°00'1.87863"
	LW13	035°37'28.14631"	-009°58'18.01884"	035°43'46.31017"	-009°56'19.93299"
	LW14	035°43'16.09286"	-009°54'55.40551"	035°36'51.48692"	-009°56'57.40282"
	LW15	035°36'56.90754"	-009°55'36.52516"	035°43'22.00708"	-009°53'35.39039"
	LW16	035°42'46.09368"	-009°52'25.87969"	035°36'23.78930"	-009°54'24.86602"
LSW	LW17	035°42'27.66180"	-009°50'57.09120"	035°36'9.08040"	-009°53'1.07880"
	LW18	035°33'42.08760"	-009°50'40.29600"	035°43'6.77640"	-009°47'39.06840"
	LW19	035°42'16.00860"	-009°44'39.19320"	035°32'52.56120"	-009°47'33.77400"
	LW20		-		-

		035°32'40.00800"	009°44'14.98080"	035°41'58.46760"	009°41'16.91520"
	LW23	035°46'5.53800"	-010°12'57.02800"	035°39'24.152400"	-009°40'30.22000"
LSE	LSE03	035°11'40.89780"	-007°20'46.52040"	035°01'49.55160"	-007°24'13.69140"
	LSE05	035°01'23.95380"	-007°20'51.06240"	035°11'8.78700"	-007°17'26.25120"
	LSE06	035°11'38.29320"	-007°15'22.45560"	035°00'49.43340"	-007°19'10.29420"
	LSE07	035°00'40.47480"	-007°17'39.26340"	035°10'47.82300"	-007°14'6.91980"
	LSE08	035°09'53.35920"	-007°12'53.23980"	035°00'9.23760"	-007°16'18.84900"
	LSE09	034°59'55.21080"	-007°14'11.10420"	035°09'34.98900"	-007°10'46.32720"
	LSE13	035°08'30.73260"	-007°06'50.83500"	035°00'13.71900"	-007°09'46.14360"
	LSE15	035°00'40.43880"	-007°08'48.73680"	035°04'15.74220"	-007°24'39.13800"
GMV	GMV1	035°28'6.18960"	-007°06'27.21540"	035°16'30.67260"	-007°03'48.51720"
	GMV2	035°16'43.13340"	-007°03'49.45500"	035°16'41.54817"	-007°03'47.24837"
	GMV3	035°21'26.65200"	-007°12'4.19820"	035°21'25.81343"	-007°12'7.02045"
LSD	LSD1	036°05'44.31000"	-007°58'11.91240"	036°11'56.37120"	-008°04'16.27260"
	LSD2	036°12'18.74940"	-007°58'16.99140"	036°05'25.97940"	-008°04'34.51680"
	LSD3	036°03'48.30180"	-008°01'19.76340"	036°17'52.65600"	-007°59'17.47380"
	LSD	036°06'7.63440"	-008°04'42.35640"	036°07'27.37500"	-007°59'36.09420"
	LSD	036°09'44.40420"	-007°55'20.70480"	036°09'25.99740"	-008°07'21.27060"
	LSD	036°16'12.41700"	-008°00'47.69940"	036°19'23.86740"	007°41'5.54880"

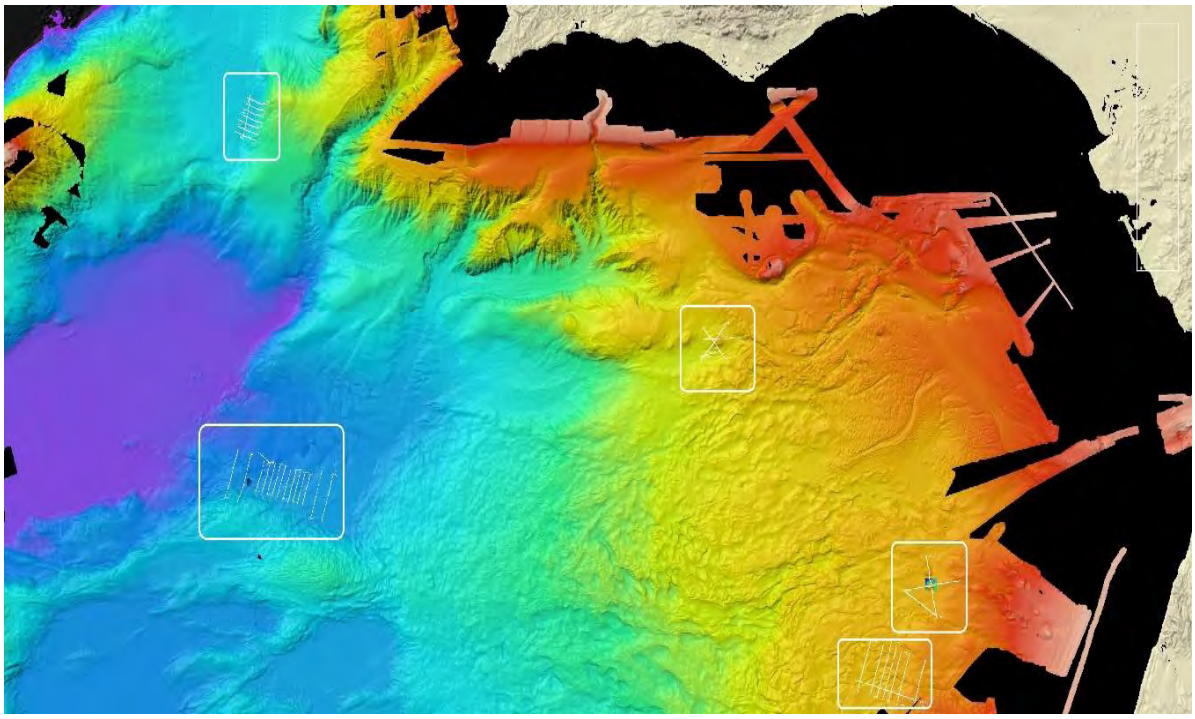

Figure 10.1. *Overview of the multichannel seismic profiles acquired in the five study areas during INSIGHT-Leg 1 survey (position based on the COS location during MCS shooting). MCS profiles are depicted in white lines.*

During the INSIGHT-Leg 1 cruise, we deployed seismic equipment as soon as the AUV Abyss was going down to start its daily mission. Every day, we deployed and recovered the MCS gear (airgun array and GeoEel streamer), and the time of MCS acquisition depended on the duration of the AUV dives, which was from 18 h maximum and 12 h minimum, approximately. To ensure the environmental policy regarding MCS acquisition, we followed established protocols in order to avoid any harm to local marine mammals near the vessel by using a soft-start methodology.

AREA	LINE	LENGTH (m)	SHOTS	SHOT INTERVAL (m)	ACQUIS. WINDOW (s)
Marques de Pombal Fault	MP03b	13554,77	606	18,5	8
	MP03b	10935,48	592	18,5	8
	MP04b	11392,23	613	18,5	8
	MP05b	11487,26	614	18,5	8
	MP06b	11607,51	634	18,5	8
	MP07b	11211,77	607	18,5	8
	MP08b	10870,12	585	18,5	8

	MP09b	11331,61	617	18,5	8
	MP11b	2519,39	138	18,5	8
	MP11c	13424,83	738	18,5	8
Lineation South Western Part	LSW01	6054,74	255	25	10
	LSW01	17617,31	727	25	10
	LSW02	17889,13	729	25	10
	LSW08	12064,09	498	25	10
	LSW09	12161,83	515	25	10
	LSW10	12229,20	523	25	10
	LSW11	12275,14	469	25	10
	LSW12	12146,50	503	25	10
	LSW13	12023,76	498	25	10
	LSW14	12240,48	508	25	10
	LSW15	12249,73	508	25	10
	LSW16	12128,36	500	25	10
	LSW17	12073,66	489	25	10
	LSW18	17985,12	723	25	10
	LSW19	17906,41	729	25	10
	LSW20	17779,25	716	25	10
	LSW23	50458,96	1928	25	10
Lineation South Eastern Part	LSE03	18961,39	1524	12,5	5,8
	LSE05	18752,48	1506	12,5	5,8
	LSE06	20809,95	1670	12,5	5,8
	LSE07	19472,46	1563	12,5	5,8
	LSE08	18737,83	1504	12,5	5,8
	LSE09	18603,72	1493	12,5	5,8
	LSE13	15946,83	1281	12,5	5,8
	LSE15	24982,74	1999	12,5	5,8
Ginsburg Mud Volcano	GMV1	21820,97	1747	12,5	5,8
	GMV2	15637,22	1252	12,5	5,8
	GMV3	21935,08	1754	12,5	5,8

Lolita Salt Diapir	PB1	14640,66	1171	12,5	5,8
	PB2	15836,11	1276	12,5	5,8
	PB3	26196,31	2102	12,5	5,8
	PB5	8041,71	647	12,5	5,8
	PB6	18013,88	1443	12,5	5,8
	PB7	30072,67	2408	12,5	5,8

Table 10.2. *Acquisition parameters of successfully acquired MCS lines.*

10.2. MCS acquisition

10.2.1. Seismic energy source

A total of 10 G-Gun II® (Fig. 10.2), one air compressor LMF and a laboratory equipment to control the firing and synchronization of guns were used during the MCS acquisition of the INSIGHT survey. The firing procedure starts with an electric signal sent from the source controller software to active the solenoid valve installed on each gun. The subsequent opening of the piston that hold the air in the gun chamber triggers the release of the compressed air and the emission of the discrete pulse of acoustic energy into the water.

SOURCE PARAMETERS	
Source controller	Big Shot®
Source type	G-GUN II®
Air pressure	2000 psi
Volume	930 cu.in (TS01 – TS04)
Compressors	1 x LMF®
Number of arrays	1
Total number of guns	10
Gun synchronization	+/- 0.1 ms
Deployment depth	3.6 m (3.5 theoretical)
Shot interval	12.5 / 18.5 / 25 m
Aiming point	50 ms

Table 10.3. *General details of seismic source used during MCS data acquisition.*

The source array was designed to maximize the energy concentrated at the 90 Hz frequency range. The shooting interval was defined as a compromise between maximum redundancy of data (CMP fold), capacity of the air compressors (Table 10.3) and depth of the seafloor.

Figure 10.2. *Array of 10 G-GUNII® airgun deployed in the survey (930 c.i.).*

The configuration of the source composed by one array of 10 guns was designed to work at a total volume of 930 cu.in, using five clusters of two guns. Guns configuration of 150 x 2, 110 x 2, 90 x 2, 70 x 2 and 45 x 2 cu.in. were deployed from the stern of the boat (Fig. 10.3) and towed off at starboard side of the boat. The purpose of mixing different volume guns improve the signal characteristics of the seismic source increasing its power and leads to a constructive summation of the primary peak and destructive summation of the bubble (secondary peaks) amplitudes of the individual airguns. The separation between guns was 2.5 meters between plates (Fig. 10.3). All the airguns worked at theoretical depth of 3.5 meters (3.6 m in practice). The air used by the guns, at 138-bars pressure (2000 psi), was supply by one LMF compressor. The distance from the stern to the COS of the arrays was 35 meters for seismic lines.

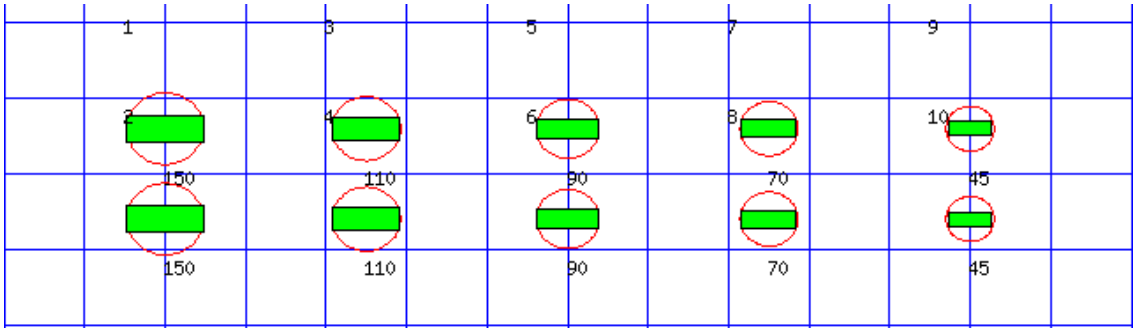

Figure 10.3. *930 cu.in. configuration of the gun array used during the acquisition of MCS.*

The design of seismic source was done using Gundalf® commercial software.The main characteristics of the signal (Table 10.4) generated by the array are:

Table 10.4. *Statistics for a seismic source signature of 930 cu.in. deployed at 3m depth. Seismic source was finally deployed at 3.5 m*

PARAMETERS OF THE ARRAY	VALUES FROM SIMULATION
Number of guns	10
Total volume (cu.in).	930 cu.in. (15.2 liters)
Peak to peak pressure (bar-m)	51.6 +/- 0.818 (5.16 +/- 0.0818 MPa, ~254 db re 1 muPa. at 1m)
Zero to peak pressure (bar-m)	29.4 (2.94 MPa, 249 db re 1 muPa. at 1m)
RMS pressure in bar-m.	1.89 (0.189 MPa, 226 db re 1 muPa. at 1m)
Primary-bubble (peak to peak)	55 +/- 2.48
Bubble period to first peak (s)	0.0835 +/- 0.00772
Maximum spectral ripple (db): 10.0 - 50.0 Hz.	8.86
Maximum spectral value (db): 10.0 - 50.0 Hz.	197.00
Average spectral value (db): 10.0 - 50.0 Hz.	195
Total acoustic energy (Joules)	27775.5
Total acoustic efficiency (%)	13.2

The predicted signature of the wavelet of the seismic airgun array of 930 cu.in. as well as its amplitude spectrum was calculated (Fig. 10.4) in the time domain. It shows a good relationship between first and second bubbles, and the concentration of the energy at frequencies ranging 90 to 120 Hz.

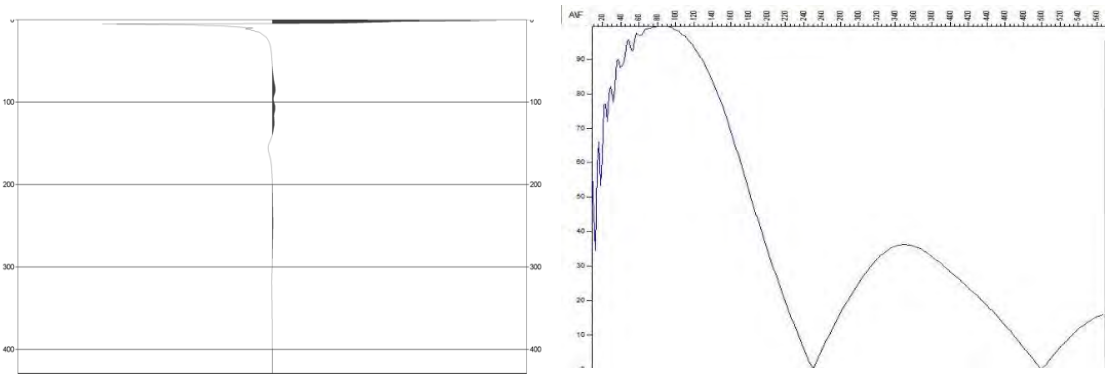

Figure 10.4. *Predicted signature of the source wavelet corresponding to the 930 cu.in. array at 3m depth, very similar to the one used during acquisition of lines (3.5 m depth). Close up of amplitude spectrum of the source wavelet (right).*

No major problems arise with this source configuration and no failed of the guns during the acquisition were detected

10.2.2. Streamer configuration

The receiver used during the acquisition of seismic profiles was a 443.75 meters-long streamer with 72 channels (Table 10.5). The distance between channels was 6.25 m; therefore, the CMP distance was 3.125 meters. The near offset (distance COS – 1st channel) was 104.9 meters and the far offset (distance COS – 72nd channel) 551.5 meters (Fig. 10.5).

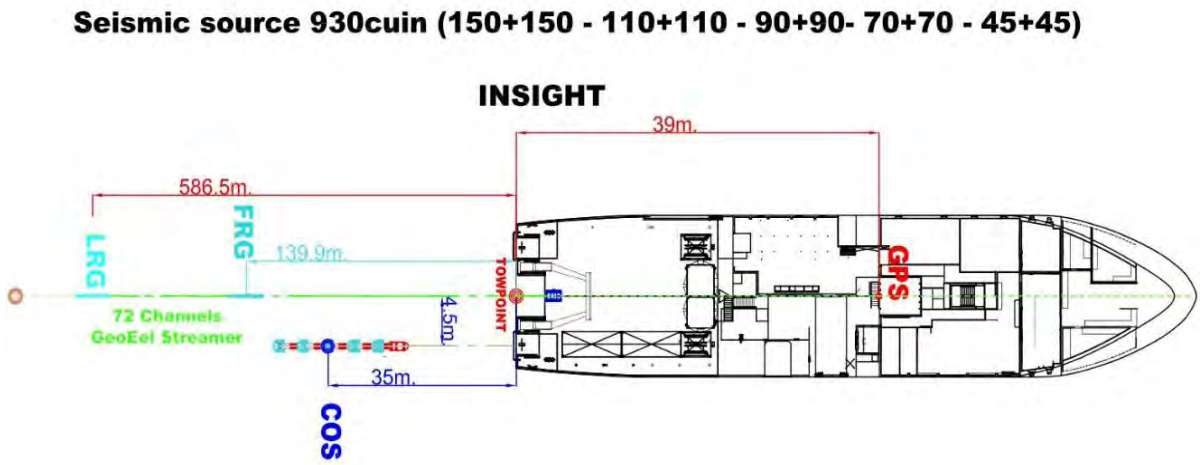

UTM
UNIDAD DE TECNOLOGÍA MARINA

UTM Code	Cost (€)	Streamer, 72 Ch. from 1 ms to 0.500 ms sample rate Digicourse Birds/compass-birds + GEOSPACE Retreivers	Remarks	Length	Offset from Winch	Offset from Towpoint (Bow)	Offset from MRU (0,0)
0057519-01SP	4166.7	50 m 2D DECK CABLE	(apart stored)	50.00			
57558-02SP	9074.1	RIGHT-ANGLE REPEATER MODULE		0.35			
24341-05	12037.0	SLIP RING ASSEMBLY, ETHERNET, for Signal Cable winch		3.30			
57516-21SP	10185.2	70 m Tow Cable, SINGLE WET-END s/n TC-1189	10 loops in drum	70.00	19.8	10.8	53.8
61225-025SP1B	8333.3	Stretch Section, 50m GEL	s/n: S01189	10.00	29.8	20.8	63.8
57625-01SP	11111.1	IN LINE TENSION GAUGE/REPEATER	In line tension gauge (New)	0.37	30.1	21.1	64.1
61225-010SP1B	9259.3	Vibration isolation section, 10 m	s/n: VIS-040	10.00	40.1	31.1	74.1
57516-22SP	12037.0	70 m. DMS Tow Cable Two Wet Ends	s/n: TC01196	70.00	110.1	101.1	144.1
57550-20SP	12037.0	Stretch Section, 25m GEL	s/n: S-01189	25.00	135.1	126.1	169.1
57558-01SP	8333.3	GeoEel Repeater Module	s/n: RP-01180	0.30	135.4	126.4	169.4
61225-010SP1B	9259.3	Vibration Isolation Section, 10m	s/n: VIS0026	10.00	145.4	136.4	179.4
57550-20SP	12037.0	2D A/D MODULE	s/n: DG02106	0.35	145.8	136.8	179.8
60236-050SP	25000.0	GEOEEL ACTIVE SECTION	COLLAR on tail coil s/n GS-0595	50.00	195.8	186.8	229.8
57550-20SP	12037.0	2D A/D MODULE	s/n: DG02050	0.35	196.1	187.1	230.1
60236-050SP	25000.0	GEOEEL ACTIVE SECTION	SIN COLLARES s/n GS-0594	50.00	246.1	237.1	280.1
57550-20SP	12037.0	2D A/D MODULE	s/n: DG02051	0.35	246.5	237.5	280.5
60236-050SP	25000.0	GEOEEL ACTIVE SECTION	COLLAR on tail coil s/n GS-0627	50.00	296.5	287.5	330.5
57550-20SP	12037.0	2D A/D MODULE	s/n: DG02052	0.35	296.8	287.8	330.8
60236-050SP	25000.0	GEOEEL ACTIVE SECTION	SIN COLLARES s/n GS-0624	50.00	346.8	337.8	380.8
57550-20SP	12037.0	2D A/D MODULE	s/n: DG02053	0.35	347.2	338.2	381.2
60236-050SP	25000.0	GEOEEL ACTIVE SECTION	SIN COLLARES s/n GS-0626	50.00	397.2	388.2	431.2
57550-20SP	12037.0	2D A/D MODULE	s/n: DG02025	0.35	397.5	388.5	431.5
60236-050SP	25000.0	GEOEEL ACTIVE SECTION	COLLAR on tail coil s/n GS-0595	50.00	447.5	438.5	481.5
57550-20SP	12037.0	2D A/D MODULE	s/n: DG02027	0.35	447.9	438.9	481.9
60236-050SP	25000.0	GEOEEL ACTIVE SECTION	SIN COLLARES s/n GS-0593	50.00	497.9	488.9	531.9
57550-20SP	12037.0	2D A/D MODULE	s/n: DG02026	0.35	498.2	489.2	532.2
60236-050SP	25000.0	GEOEEL ACTIVE SECTION	SIN COLLARES s/n GS-0592	50.00	548.2	539.2	582.2
57550-20SP	12037.0	2D A/D MODULE	s/n: DG02055	0.35	548.6	539.6	582.6
60236-050SP	25000.0	GEOEEL ACTIVE SECTION	COLLAR on tail coil s/n GS-0628	50.00	598.6	589.6	632.6
57536-02SP	463.0	GeoEel Swivel+Rope		15.00	613.6	604.6	647.6
		Tail Buoy		0.00	613.6	604.6	647.6

Figure 10.5. *Acquisition diagram.*

STREAMER PARAMETERS	
Streamer model	GeoEel®
No. of hydrophones per channel	8
Depth	3.5 m
Active channels	72
Active length	443.75 m
Group interval	6.25 m
No. birds (all of them with compasses)	4
CMP distance	3.125 m
Auxiliary channels	4

Table 10.5. *General acquisition parameters of the streamer used during INSIGHT-Leg1 seismic profiles.*

The streamer tow depth was 3.5 m on the basis of the high-resolution (high frequency) targets, and it was decided as a compromise between the need to isolate the streamer from the noise sources and the water layer necessary to obtain an appropriate bandwidth of the data and record length. A total of four birds (Fig. 10.6) were deployed along the streamer to accurately control and ensure the tow depth.

Figure 10.6. *Example of a bird and a section of the streamer deployed during the survey.*

Due to a malfunction of the acquisition system, the number of active channels had to be reduced to 40 for all the lines within the Lolita Salt Diapir area (MCS lines PB1 to PB7). The last five sections of the streamer were derigged resulting in a 354 meters long streamer. The near offset did not change.

10.2.3. Navigation and processing

The software used on board the RV Sarmiento de Gamboa for the integrated navigation acquisition is the seismic package Eiva®, property of UTM-CSIC. Because EIVA do not provide the real positions of CMP gathers, we used the GPS coordinates to calculate them through RadexPro processing software. EIVA provides the position of the center of source (COS) as well, using the GPS data and the offsets of the experiment for the calculation. Nevertheless, because the number of errors in the distance calculation between subsequent COS is larger than the same calculation with the GPS data antenna acquired in the middle of the vessel, we decided to use GPS antennae data and offsets instead of COS during processing.

Shot events, time and positioning were extracted from the NaviEdit (NT) Interpreter Format file (*_S.NPD) generated by the EIVA® integrated navigation system. Shot events were positioned in UTM system and geographical coordinates and the streamer information was recorded for each shot event including the (x,y) coordinates of the Center of Source (COS). The entire information of the raw EIVA navigation system is: header information, date, time, shot number, vessel position, tow point position, first receiver group position, common mid-point position, center of source position.

10.2.4. MCS processing description: Data quality control

A total 44 MCS profiles covering about 704 km and 42902 shots were processed on board the R/V Sarmiento de Gamboa during the INSIGHT-Leg 1 survey (see Table 10.2).

Raw seismic data were acquired in individual shot records (SEG-D format), corrected from the aiming time of 50 ms (record window starts before the shot explosion), geometry was introduced into the trace headers and profiles were written out after processing to SEG-Y. The processing flow used to improve the signal-to-noise ratio of the data and generate a first-pass interpretable section is explained in the next sections, by area of exploration, and the parameters and menus have been exported and imaged from the processing software using screen shots. The example of processing flow applied to MCS profiles corresponds to profile LSW12 in the lineation south.

Processing flow includes:

1. Reformat of the data: SEG-D raw data is changed to Radexpro format. 72 channels were output with at 1 ms sampling interval.

2. Positive (upward) 50 ms shift of data. A bulk shift correction of -50 ms was applied in order to compensate the time delay existed in the acquisition system between the opening of the acquisition time window and the shooting gun time. This positive

(upward) shift was applied to the whole data, in order to correct the existing lag between shot triggering and data recording window (Fig. 10.7).

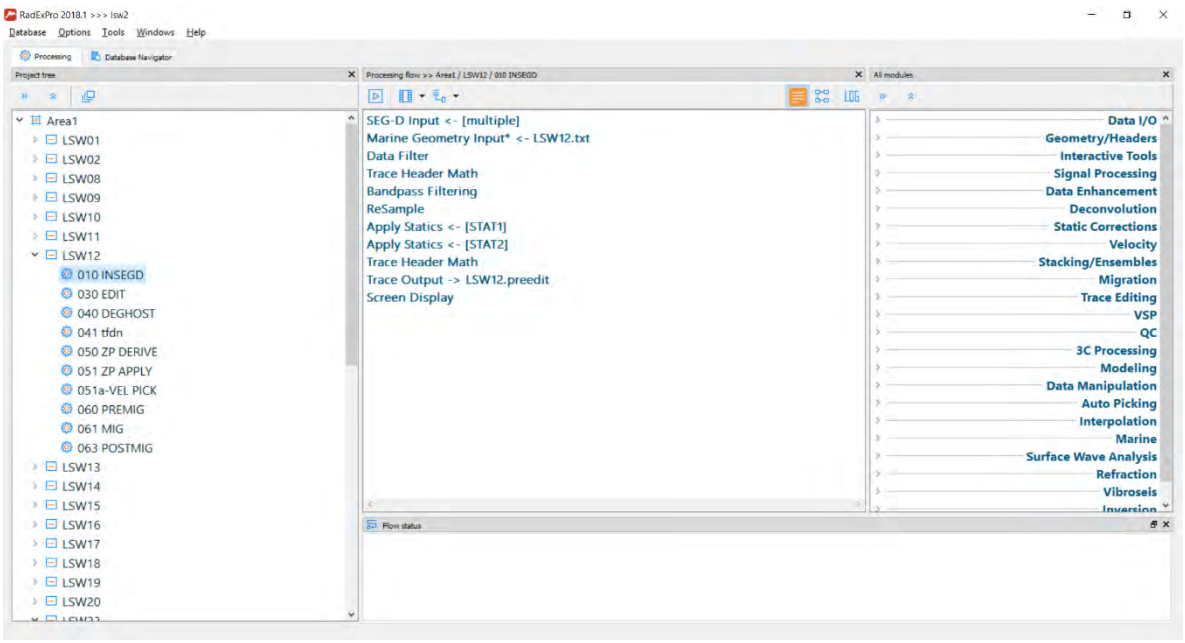

Figure 10.7. *Flow processing step for reformatting and shift applying traces.*

3. **Shot displaying** in order to check bad shots and traces identified in the observer's logs.

Bandpass filtering A gentle zero phase Ormsby filter was applied to the data to remove low frequency noise and avoid anti-aliasing. We used a (5-10-420-480 Hz with some small variations between profiles.

4. **Plotting and checking trace headers** in order to verify an optimal recording (Fig. 10.8)

5. **Offset checking** (distance source-first channel). Checking the time corresponding to the aiming time (selected to -50 ms in the technical specifications) from the first break of the direct arrival and multiple arrivals, for instance, checking if the time of first multiple is double of the first arrival. Picking first break and input into a trace header (Fig. 10.9).

Trace edition: Constant noisy channels and/or random bad traces were identified and subsequently edited and/or muted. It was not necessary to mute refraction waves during the survey.

Geometry definition: Real geometry of the experiment was calculated and added to trace headers, using the original positioning information obtained from EIVA navigation files. That includes: GPS (x,y) coordinates and offsets.

Top mute: Automatic top mute was applied from the zero time to the seafloor

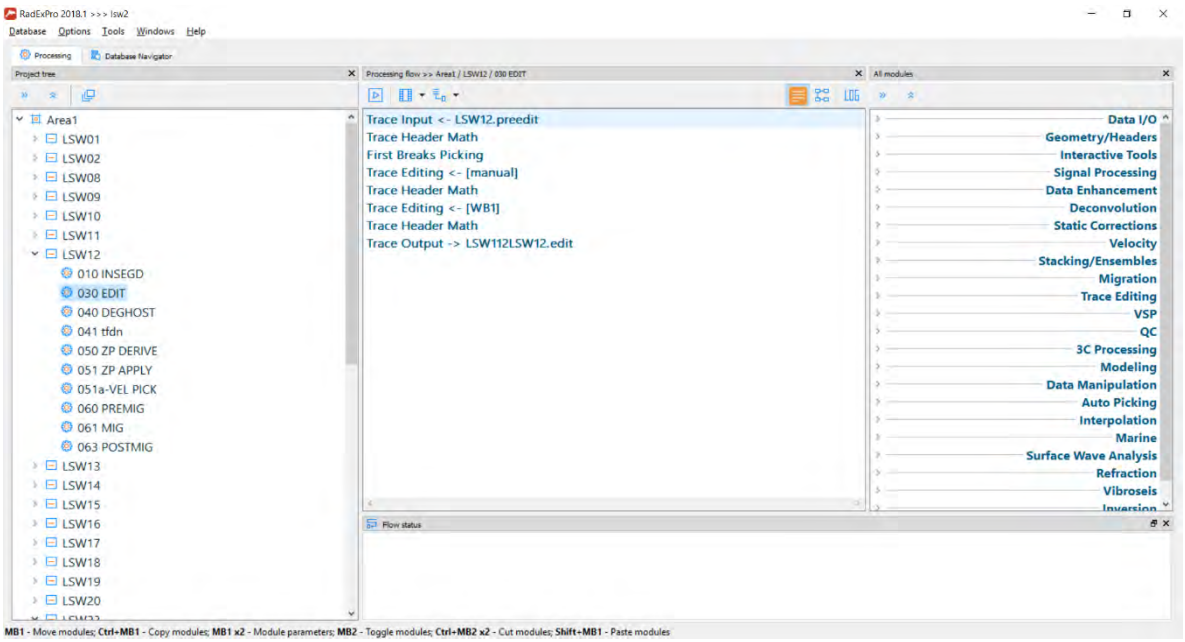

Figure 10.8. ***Flow processing step for editing and first break picking the traces.***

6. Deghost of the source. Deleting the ghost of the source and streamer in the recod sections (Fig. 10.9).

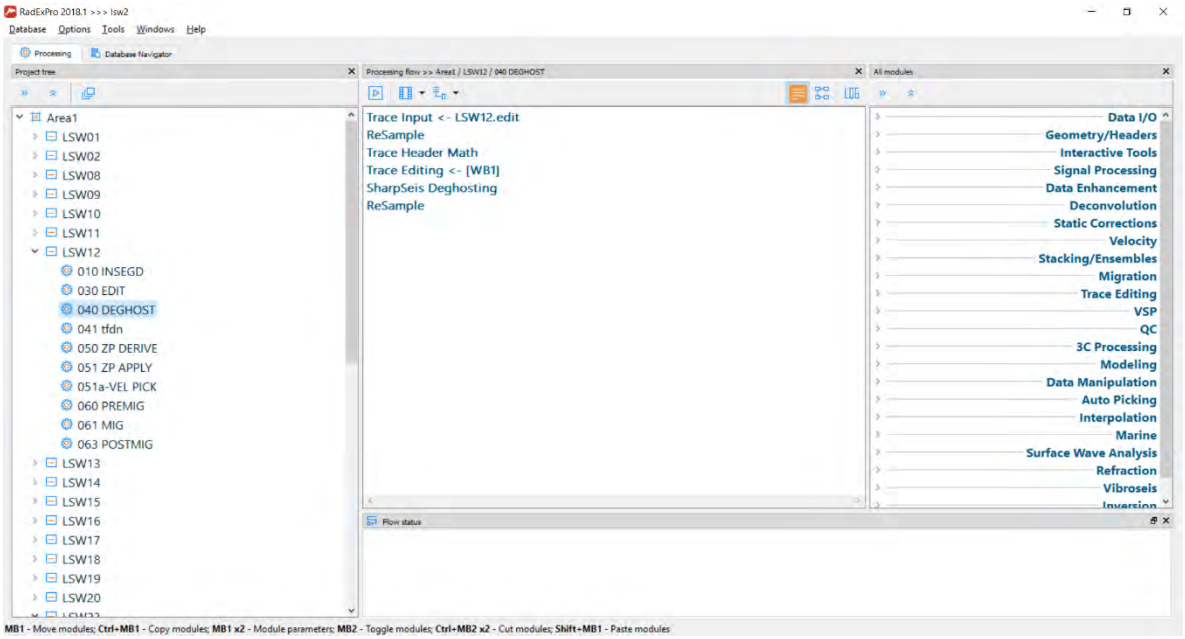

Figure 10.9. *Flow processing step for deghosting the source and the streamer.*

7. TFDN. Time-frequency domain denoise, in order to delete noise of the data in the shot domain (Fig. 10.10).

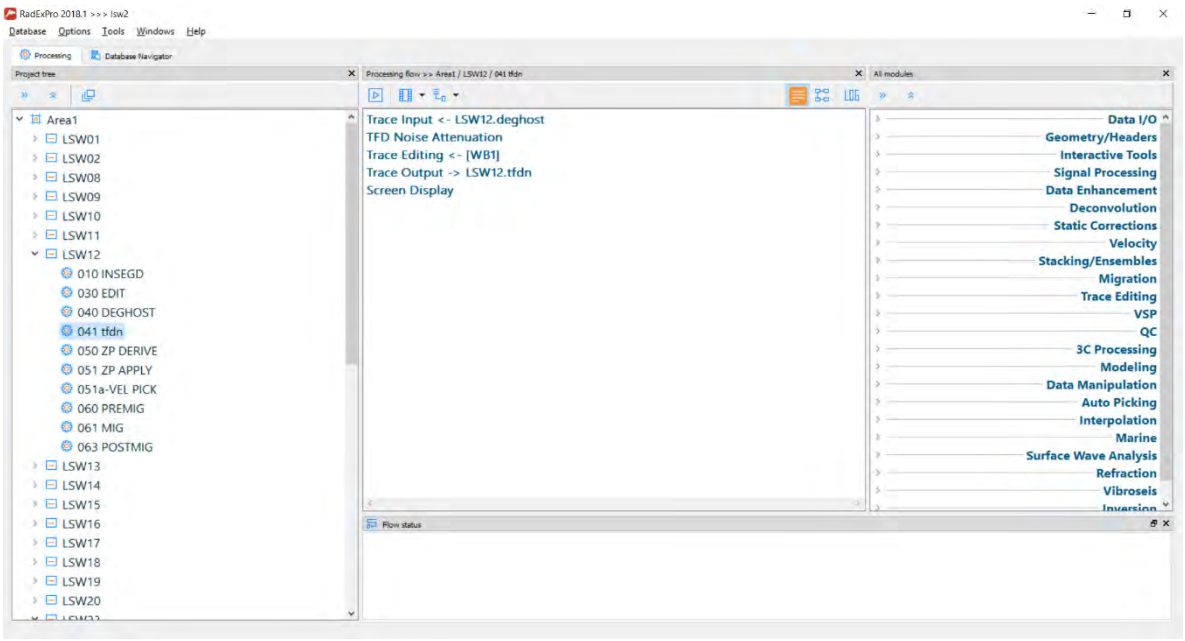

Figure 10.10. *Flow processing step for deghosting the source and the streamer.*

8. **Zero phase derive:** Extract the source from the data to deconvolve and eliminate the source contribution from the data (Fig. 10.11).

CDP-gather generation: Traces were re-ordered in CDP gathers.

Final stacking using RMS velocities picked along the profile

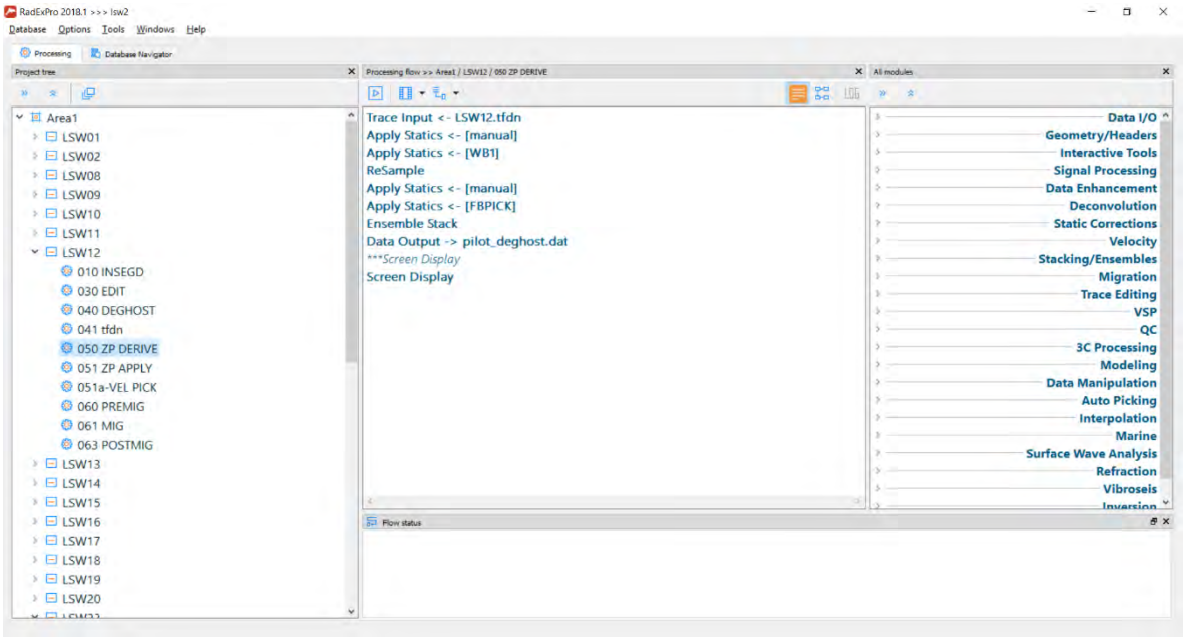

Figure 10.11. *Flow processing step for derive the source to deconvolve the data and stack the data.*

9. Zero phase apply and deconvolution: We applied the source wavelet extracted in 8. to the data using a predictive deconvolution (Fig. 10.12). Predictive deconvolution tests shown good compression of the original wavelet and optimal reverberation removal with some specific prediction operator length and prediction lag and whitening of 10%.

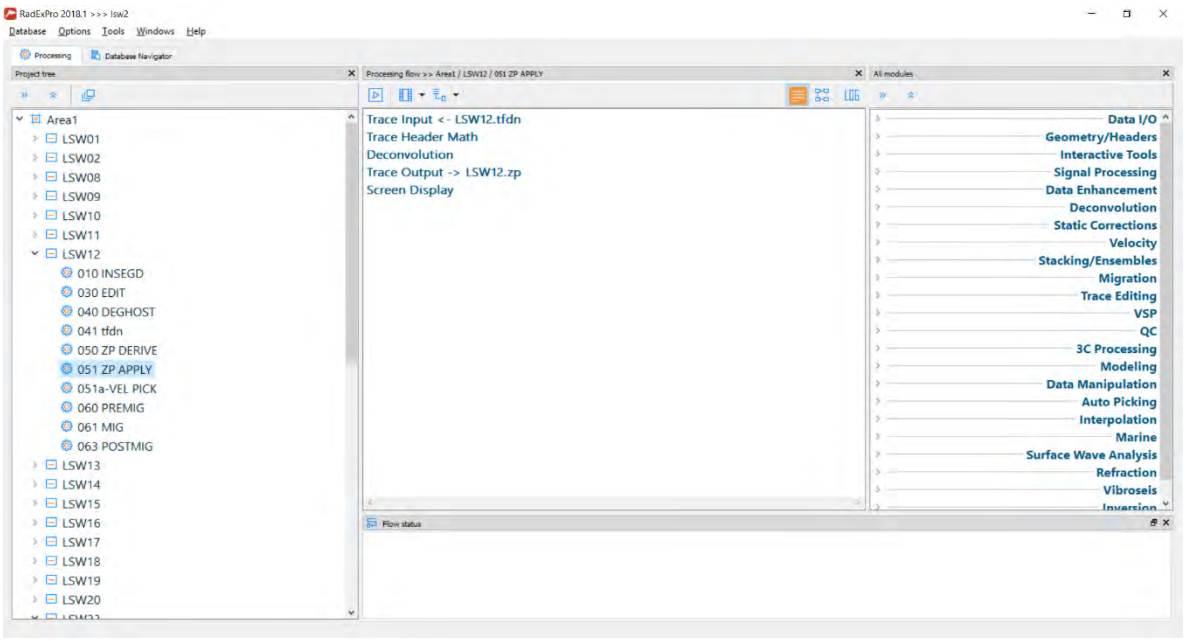

Figure 10.12. *Flow processing step to deconvolve data using predictive deconvolution.*

10. Velocity model: An rms-velocity model was refined using the Radexpro Velocity Analysis interactive application. After picking, the velocities for each line were checked using the NMO corrected CDP gathers (Fig. 10.13).

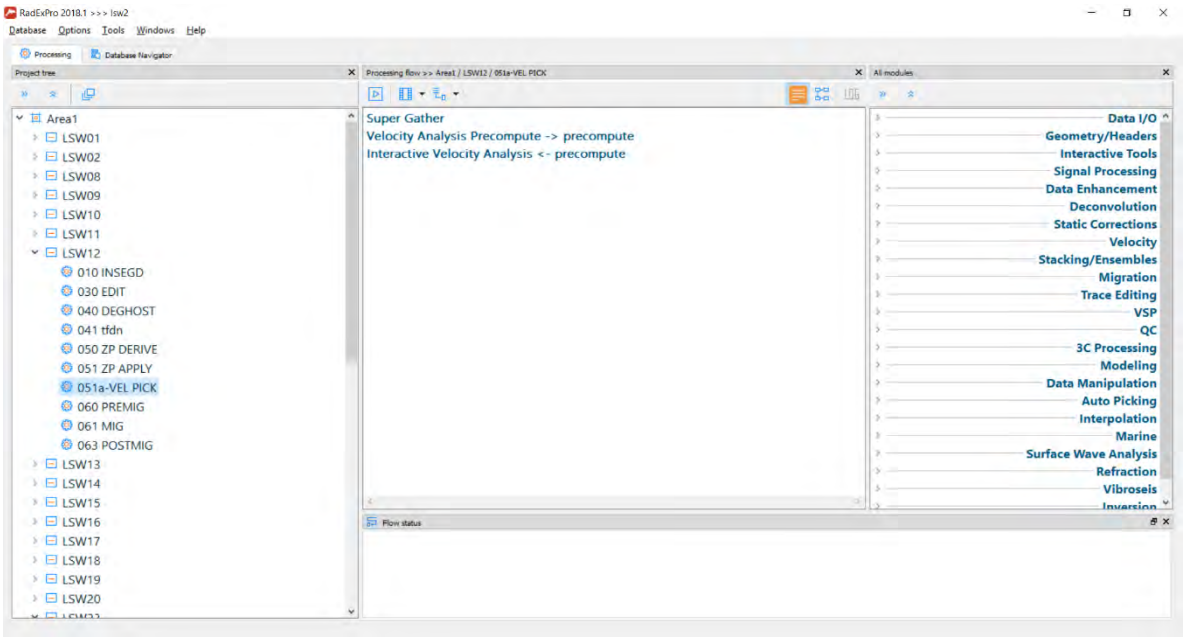

Figure 10.13. *Flow processing step to build supergathers and pick velocities for stack.*

11. Amplitude Recovery: A gain recovery proportional to RMS velocities was applied to the data to account for geometric spreading loss of energy.

Amplitude average: The amplitude of the data was averaged using the average amplitude of each trace and smoothed along the profile to equalize the profile (Fig. 10.14).

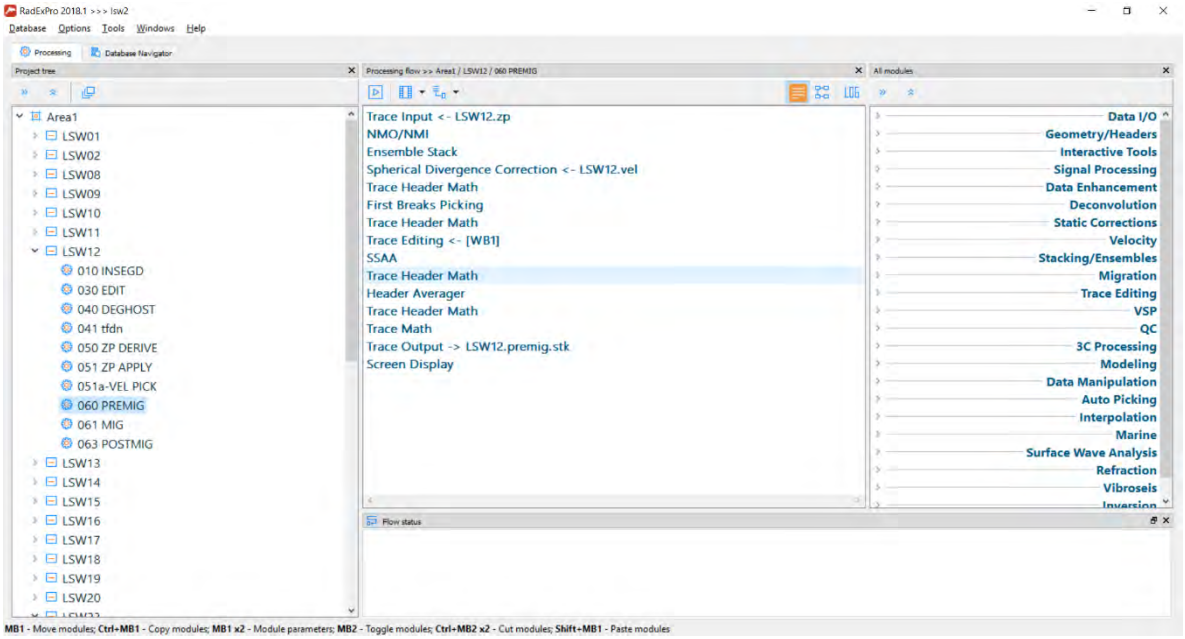

Figure 10.14. *Flow processing step to apply spreading divergence correction and trace equalization.*

12. Migration: A gain recovery proportional to RMS velocities was applied to the data to account for geometric spreading loss of energy (Fig. 10.15).

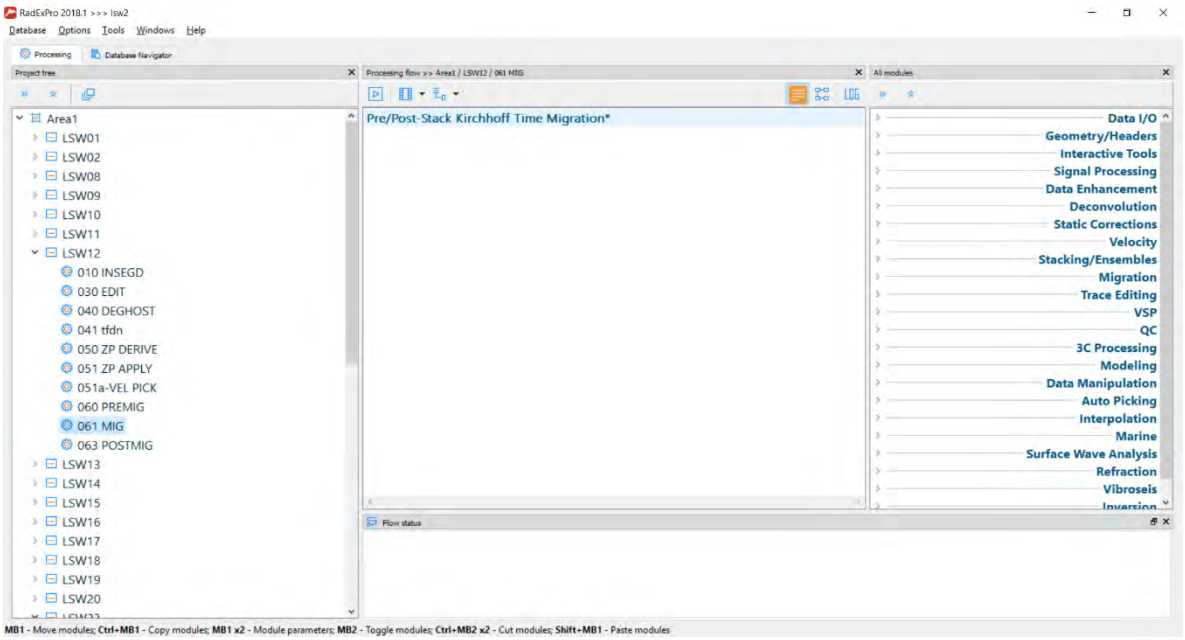

Figure 10.15. *Flow processing step to migrate the section using RMS stack velocities.*

13. Amplitude correction, band-pass filtering, editing traces, segy-output: Flow to balance and filter trace amplitudes for the plotting and representation of the final migrated sections. Data have been exported to segy format and is lastly imaged using a combination of seismic UNIX and GMT software jobs (Fig. 10.16).

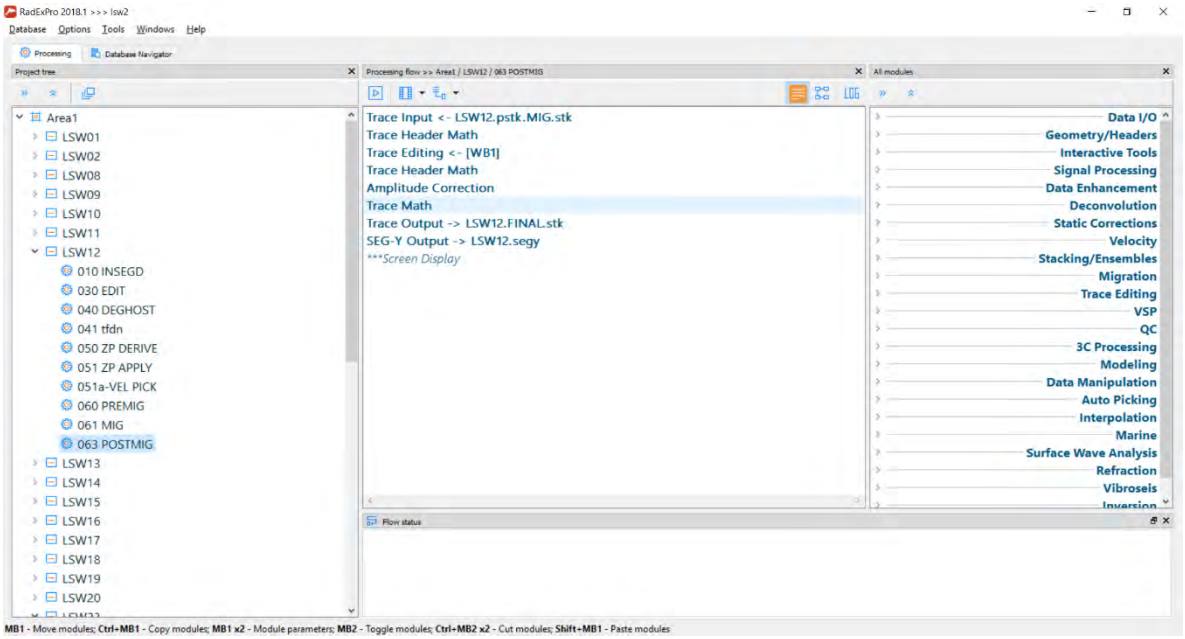

Figure 10.16. *Flow processing step to final balance amplitude and export of the data into seg-y format after migration.*

On the next pages, we show a figure of all the MCS line processed duinrg the INISIGHT-Leg 1 cruise. They are presented by each of the 5 areas of investigation. MCS profiles were generated using The Generic Mapping Tools software (GMT, http://gmt.soest.hawaii.edu) after processing with RadexPro

The Marques de Pombal Fault (MCS profiles):

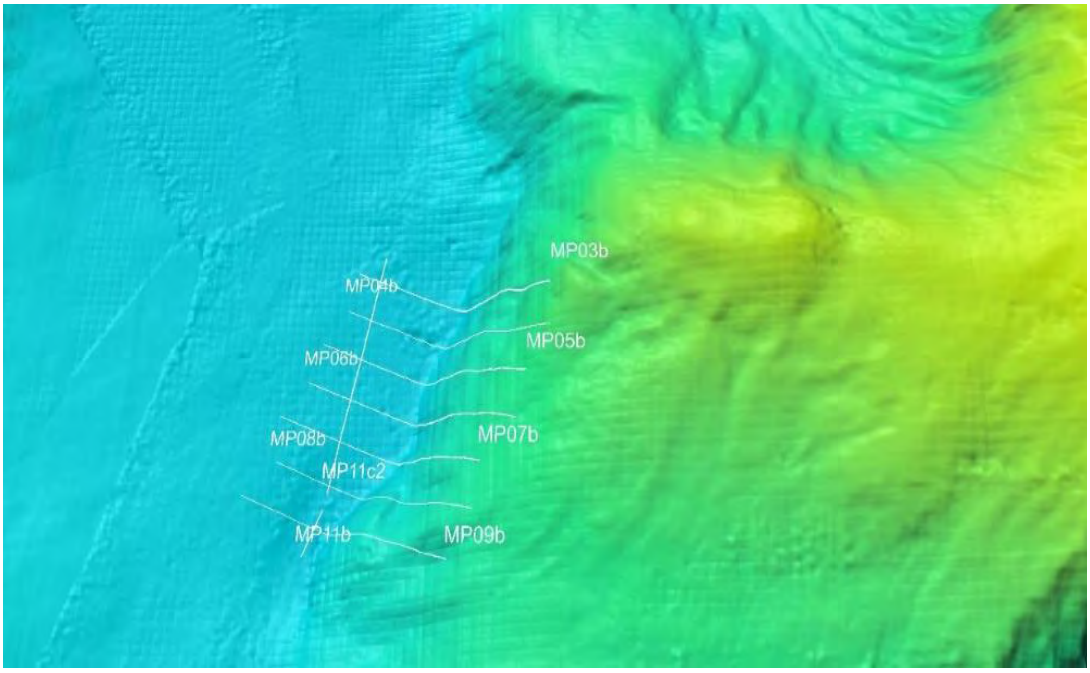

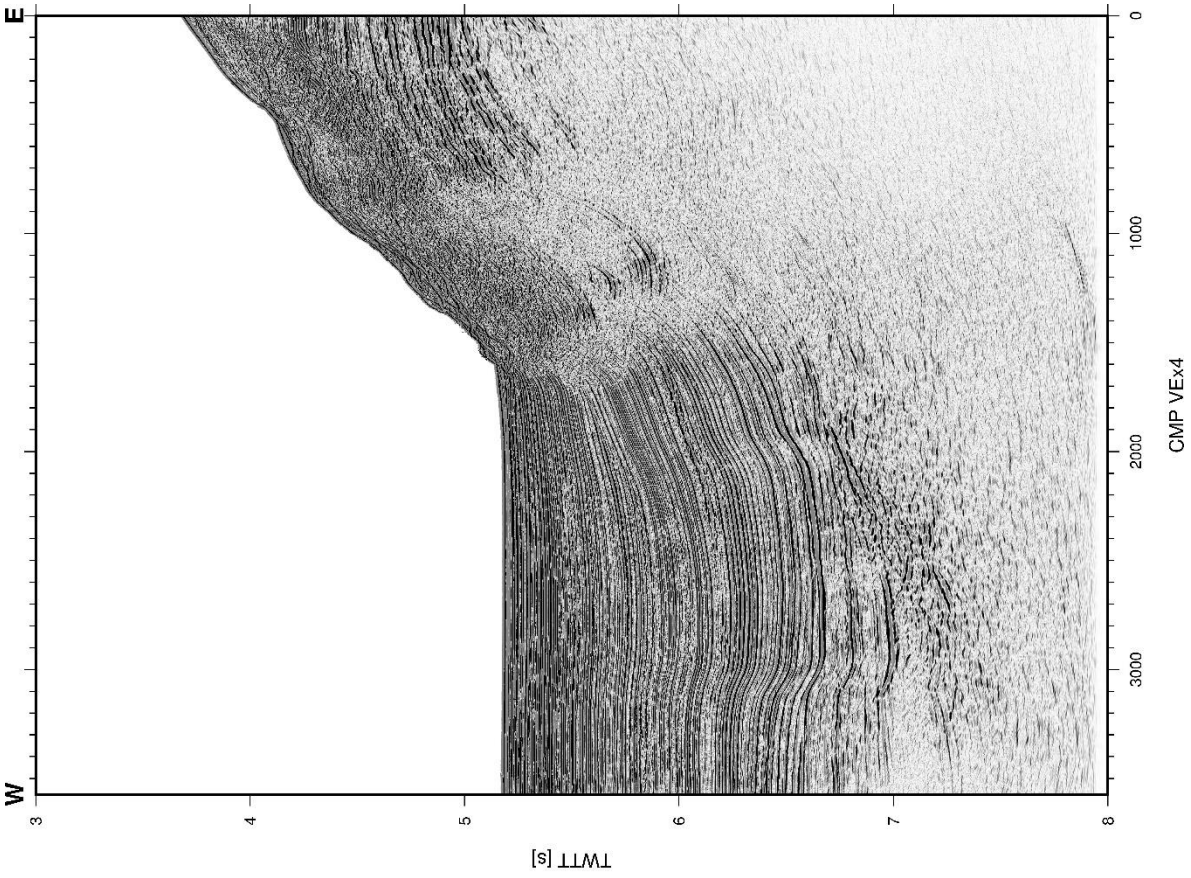

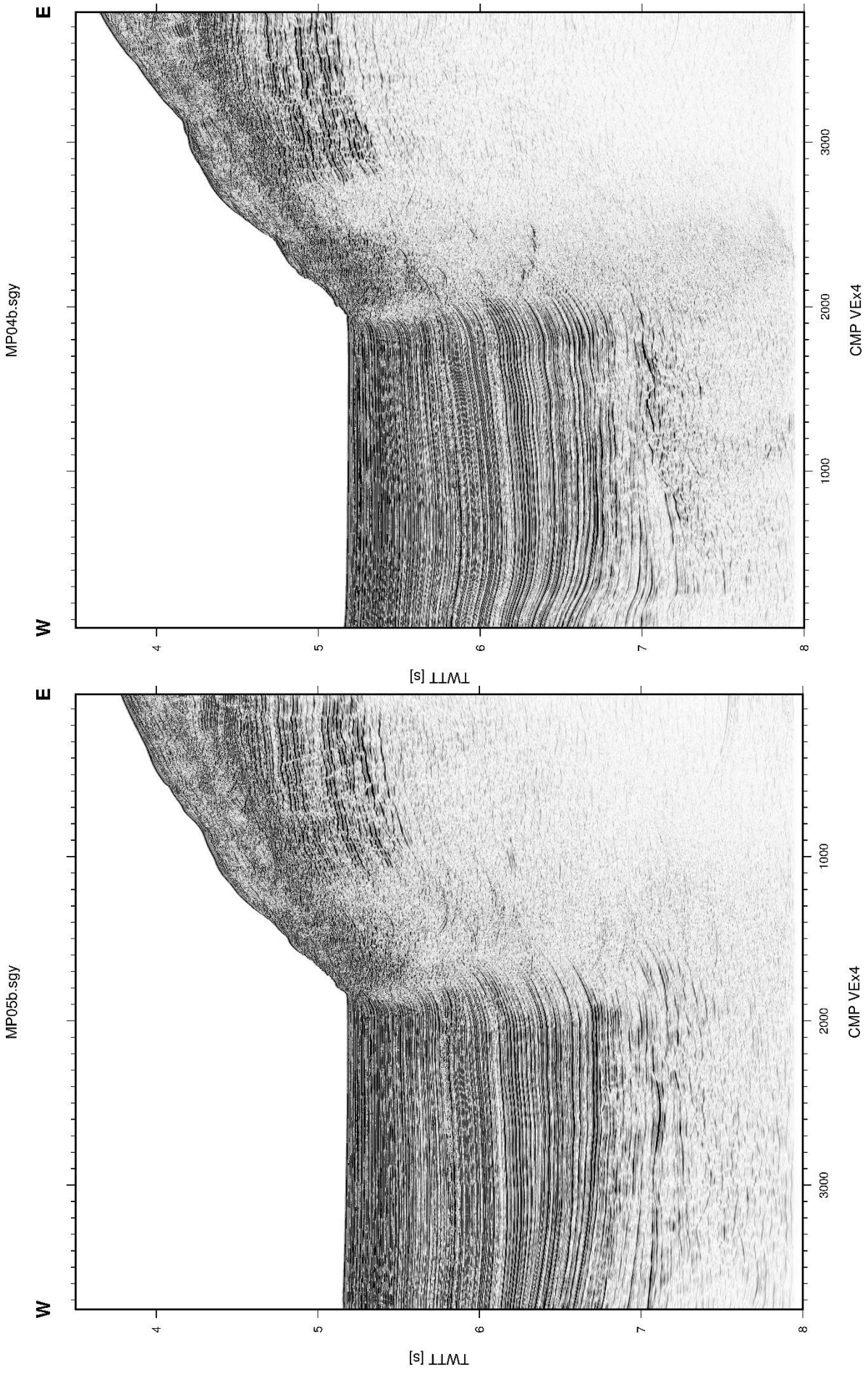
MP04b.sgy
W
E
TWTT [s]
4
5
6
7
8
1000
2000
3000
CMP VEx4
MP05b.sgy
W
E
TWTT [s]
4
5
6
7
8
1000
2000
3000
CMP VEx4

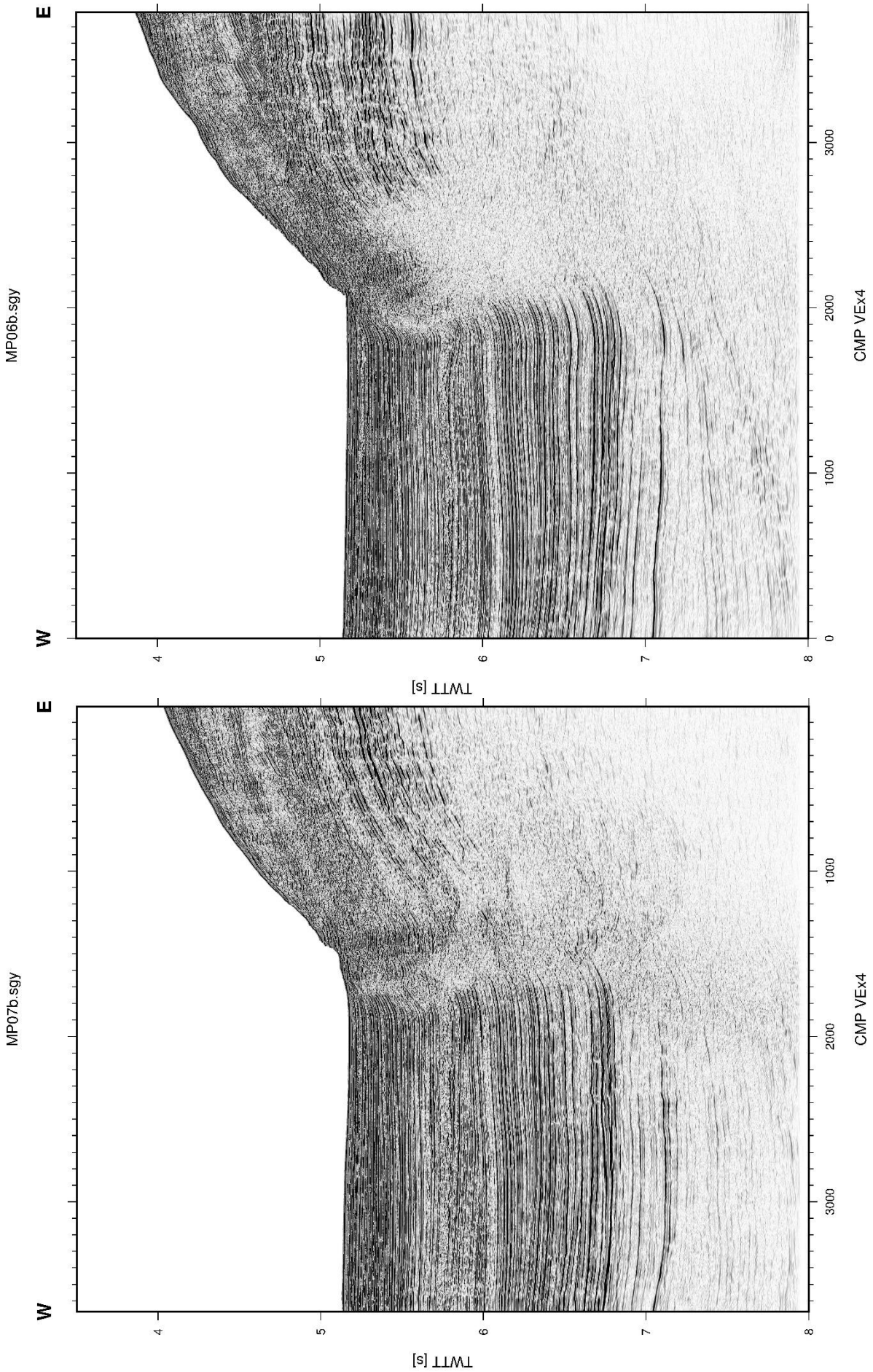
MP06b.sgy
W
E
TWTT [s]
4
5
6
7
8
0
1000
2000
3000
CMP VEx4
MP07b.sgy
W
E
TWTT [s]
4
5
6
7
8
1000
2000
3000
CMP VEx4

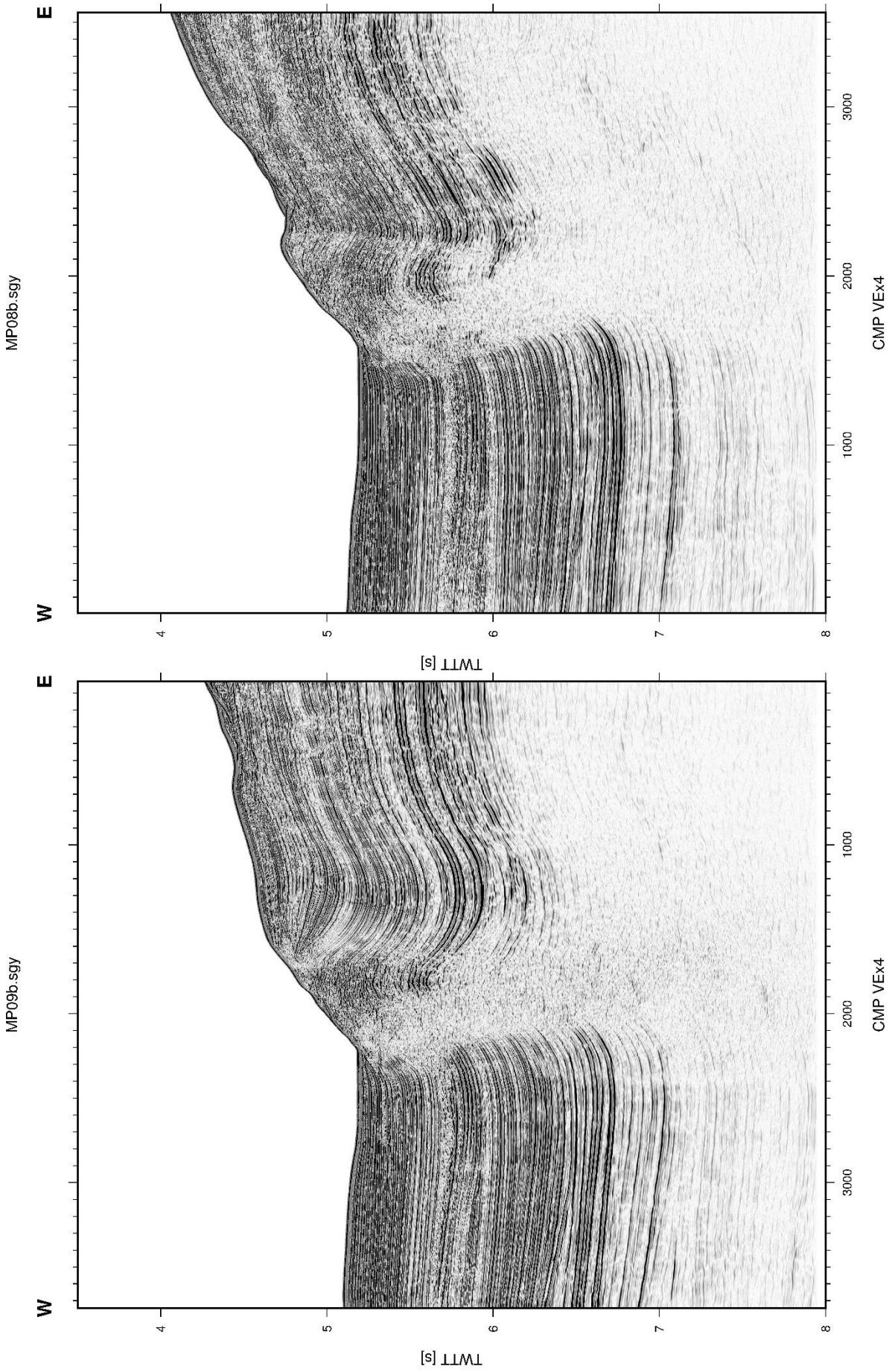
MP08b.sgy
W
E
TWTT [s]
4
5
6
7
8
1000
2000
3000
CMP VEx4
MP09b.sgy
W
E
TWTT [s]
4
5
6
7
8
1000
2000
3000
CMP VEx4

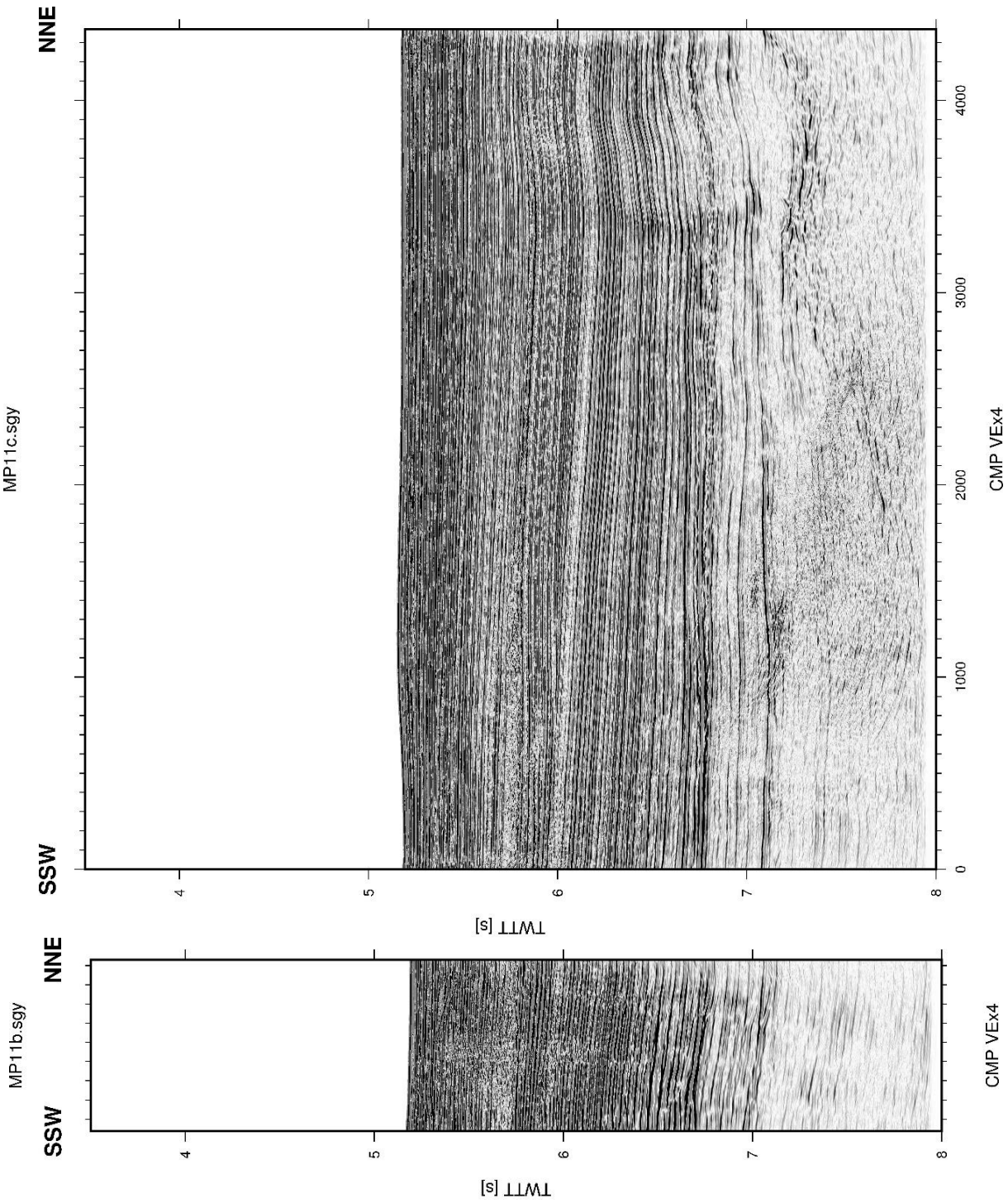
MP11c.sgy
SSW
NNE
TWTT [s]
CMP VEx4
MP11b.sgy
SSW
NNE
TWTT [s]
CMP VEx4

The Lineament South West Fault (MCS profiles):

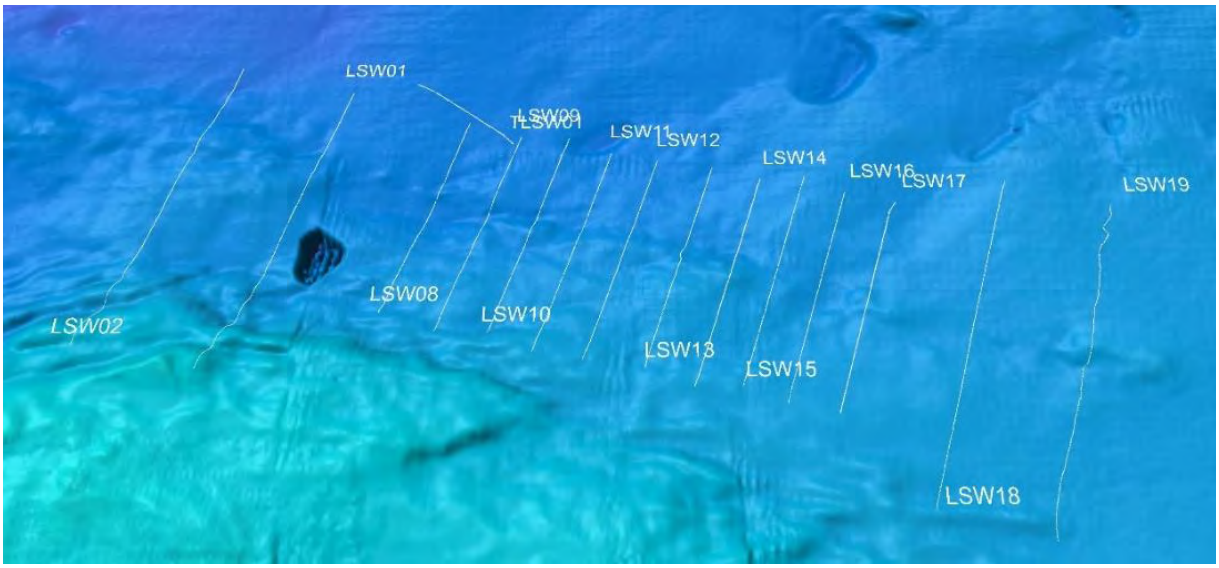

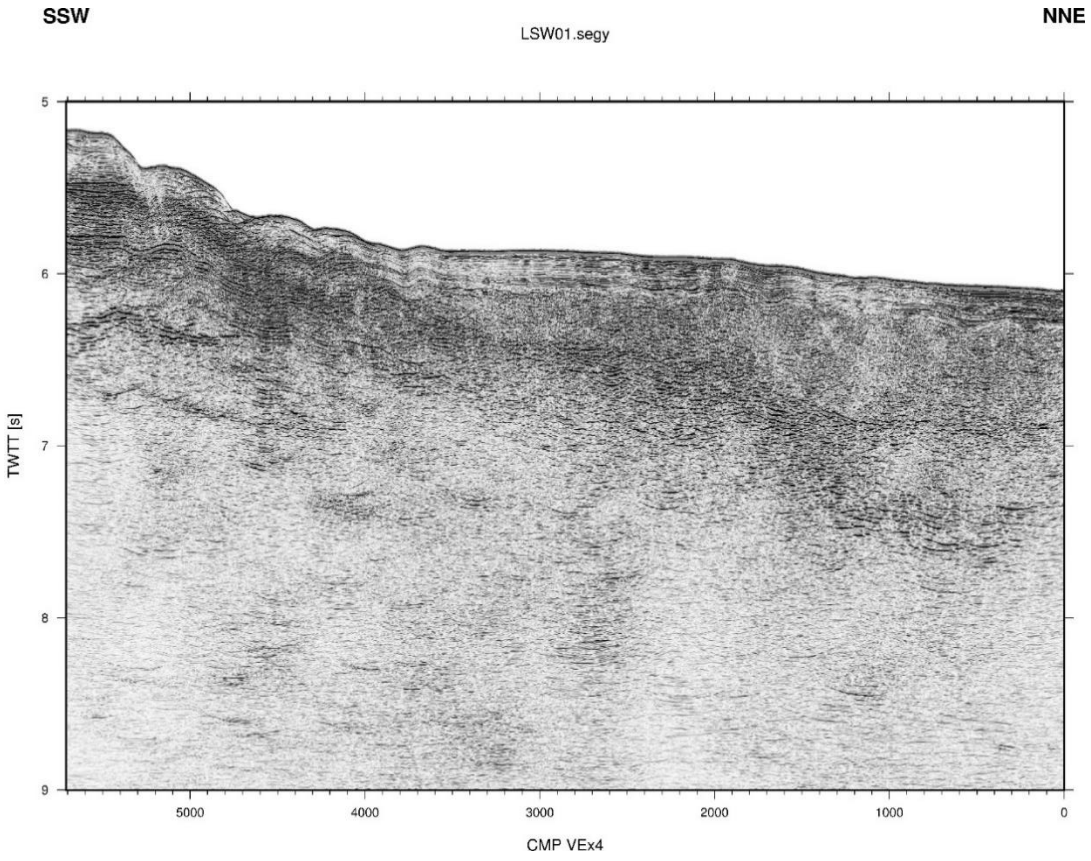

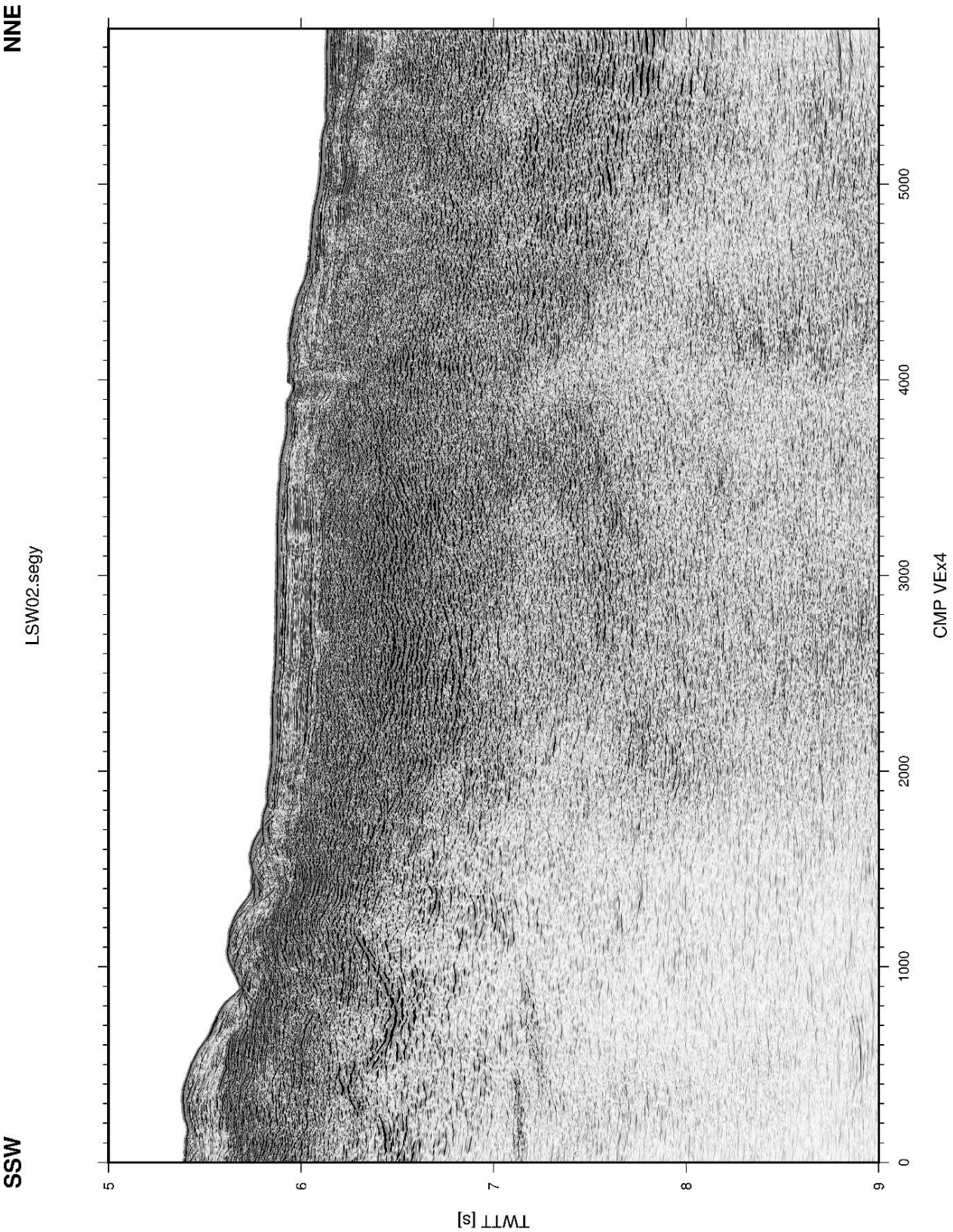
NNE
SSW
LSW02.segy
TWTT [s]
5
6
7
8
9
0
1000
2000
3000
4000
5000
CMP VEx4

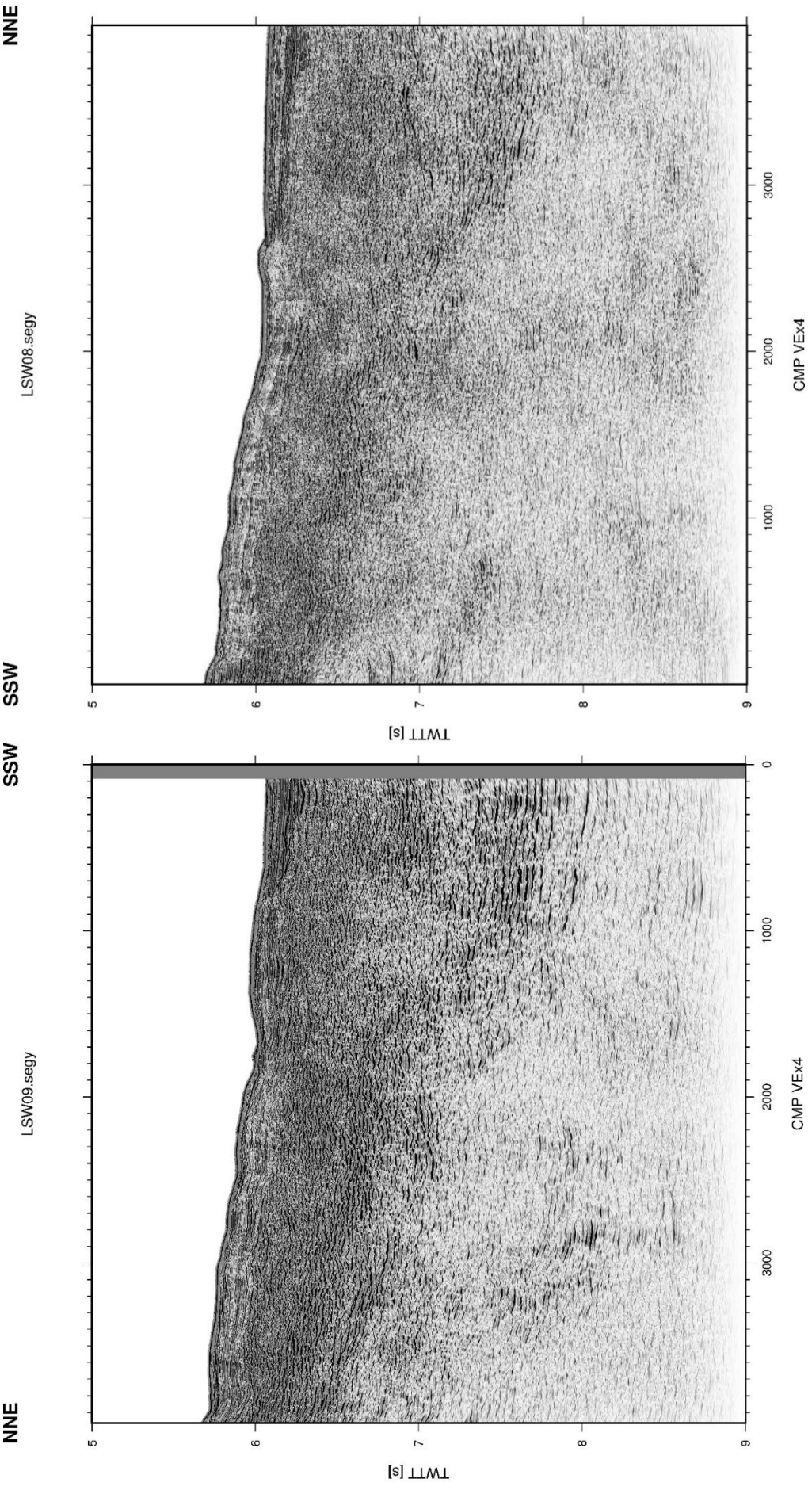
NNE
SSW
LSW08.segy
CMP VEx4
TWTT [s]
SSW
NNE
LSW09.segy
CMP VEx4
TWTT [s]

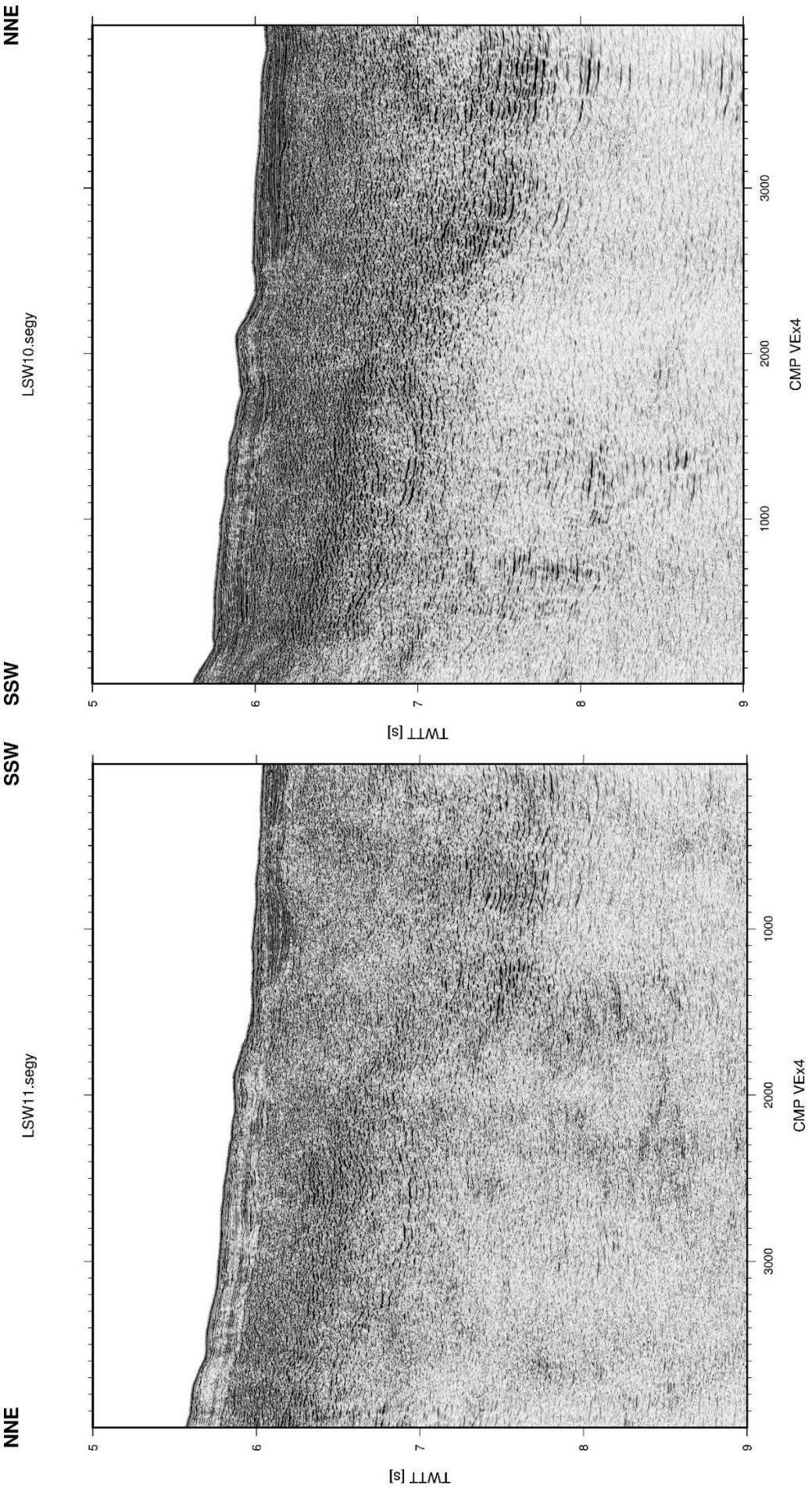
NNE
SSW
LSW10.segy
TWTT [s]
CMP VEx4
SSW
NNE
LSW11.segy
TWTT [s]
CMP VEx4

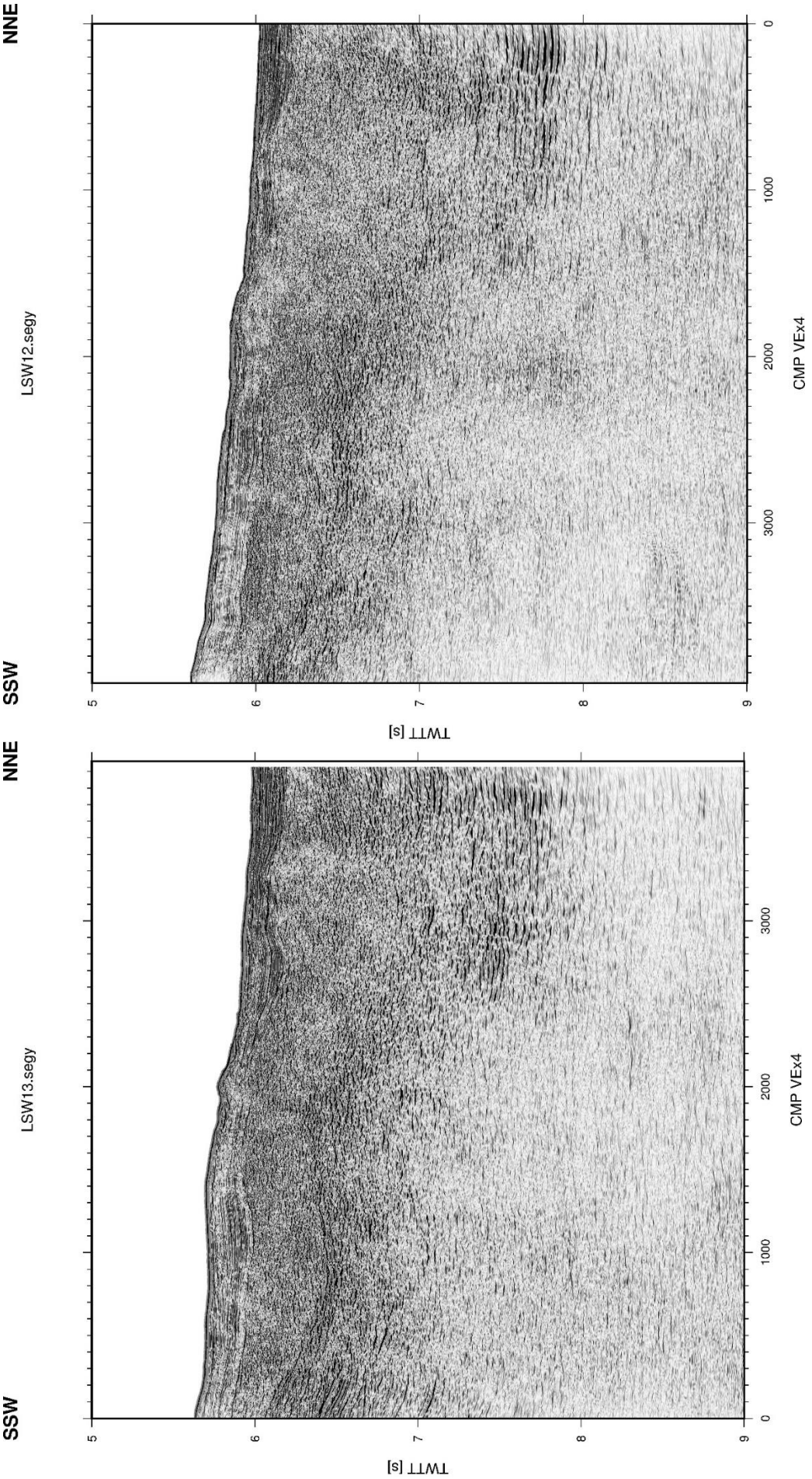
NNE
SSW
LSW12.segy
TWTT [s]
CMP VEx4
NNE
SSW
LSW13.segy
TWTT [s]
CMP VEx4

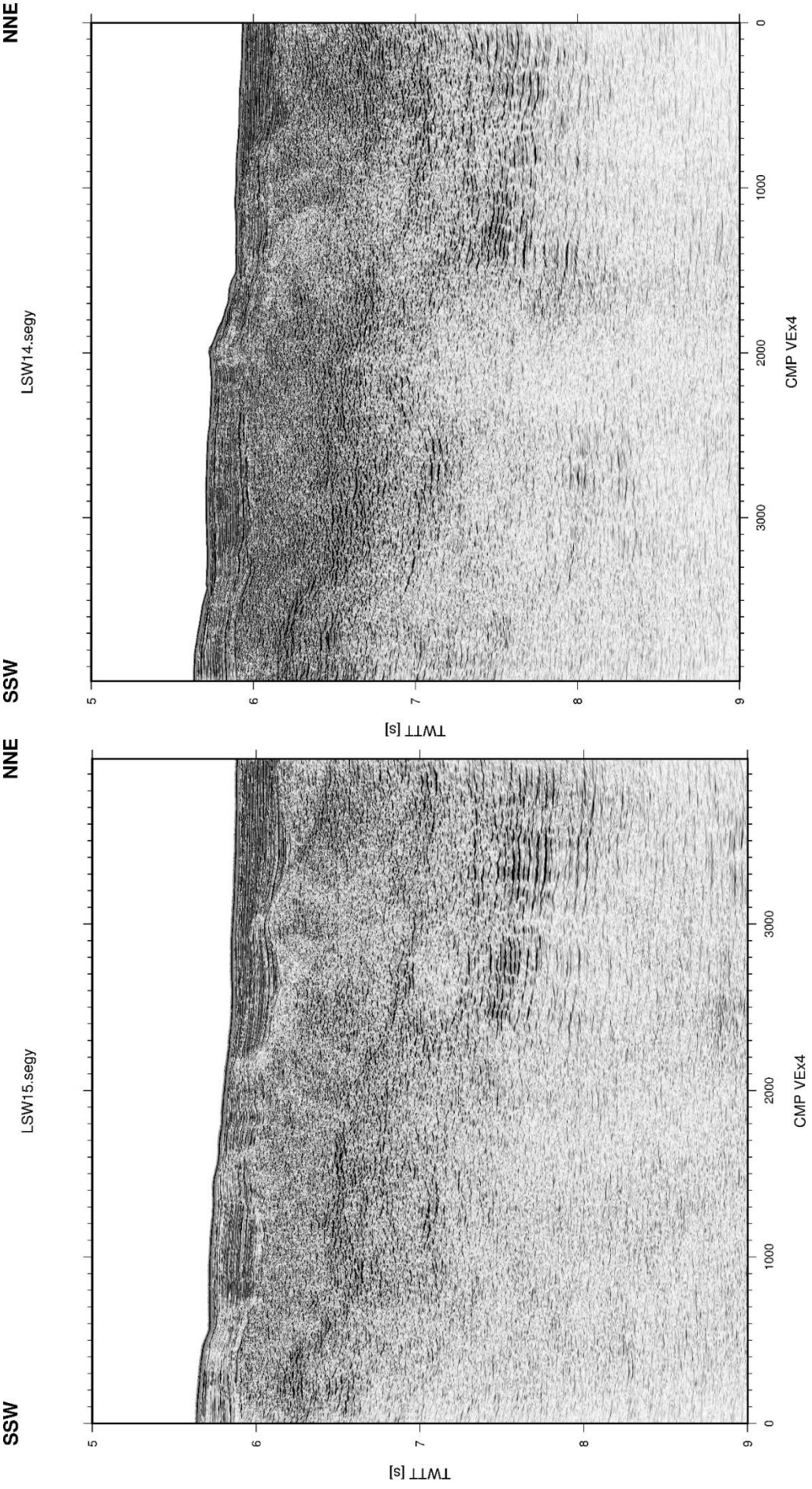
NNE
SSW
LSW14.segy
TWTT [s]
CMP VEx4
NNE
SSW
LSW15.segy
TWTT [s]
CMP VEx4

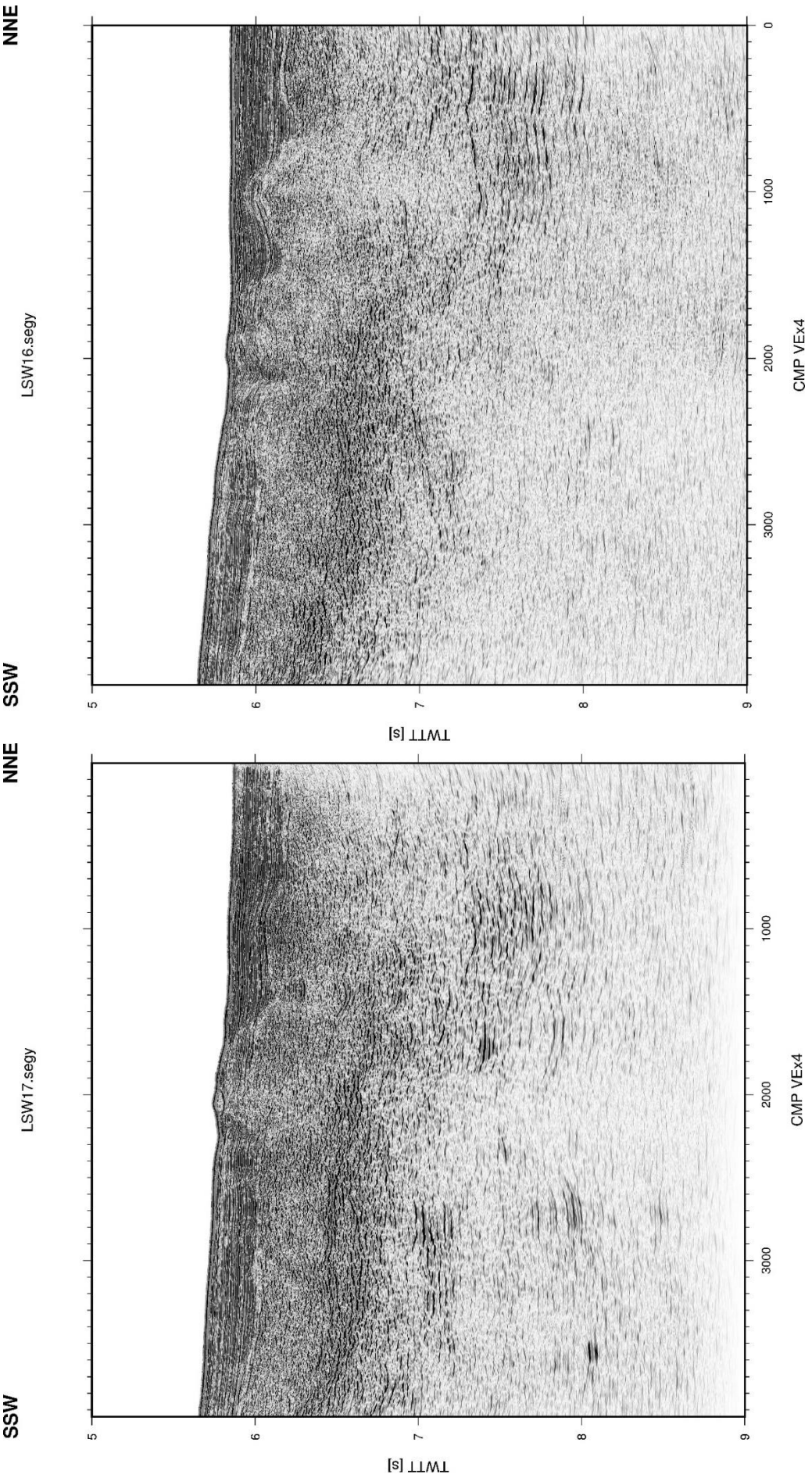
NNE
SSW
LSW16.segy
TWTT [s]
CMP VEx4
NNE
SSW
LSW17.segy
TWTT [s]
CMP VEx4

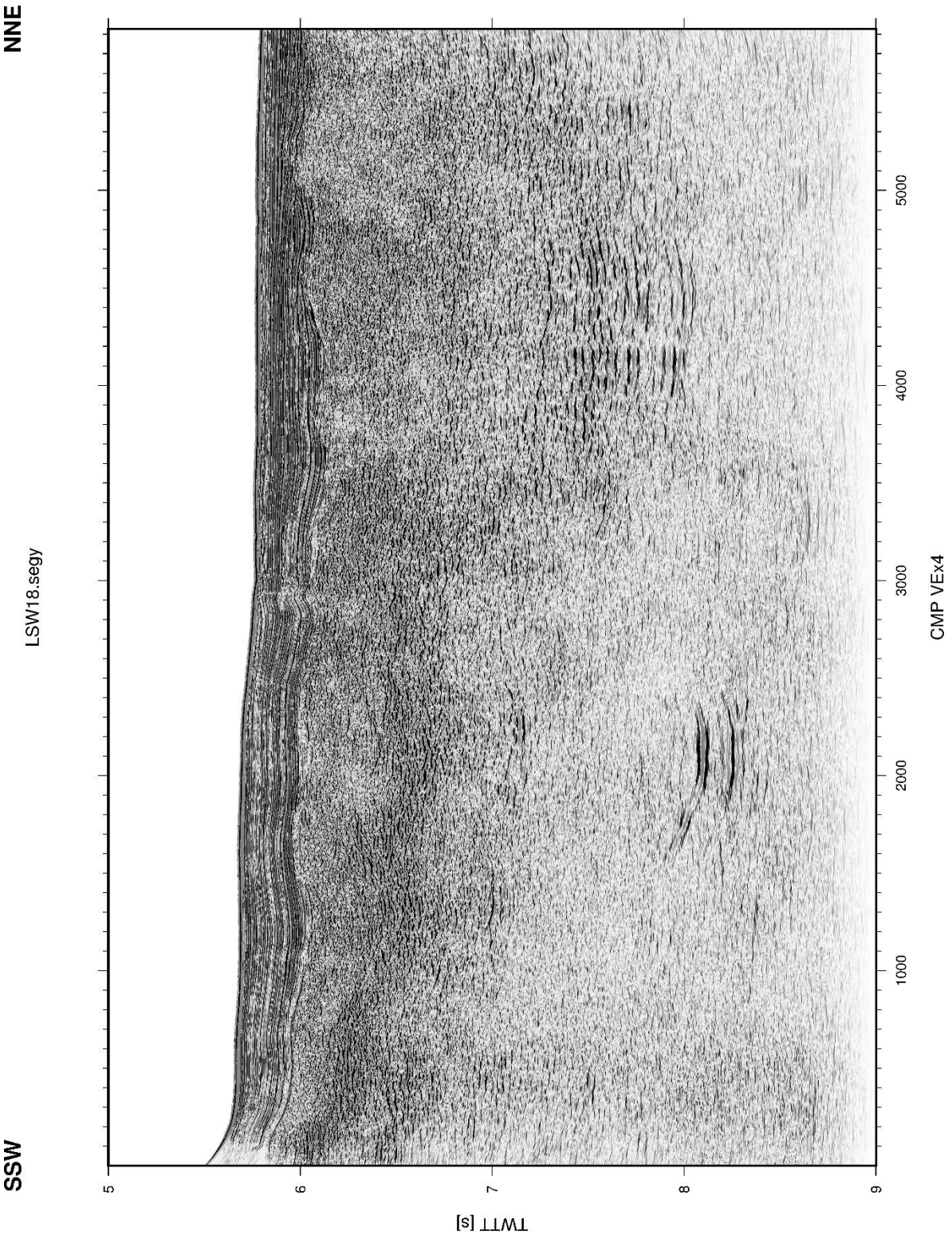
NNE
SSW
LSW18.segy
CMP VEx4
1000
2000
3000
4000
5000
5
6
7
8
9
TWTT [s]

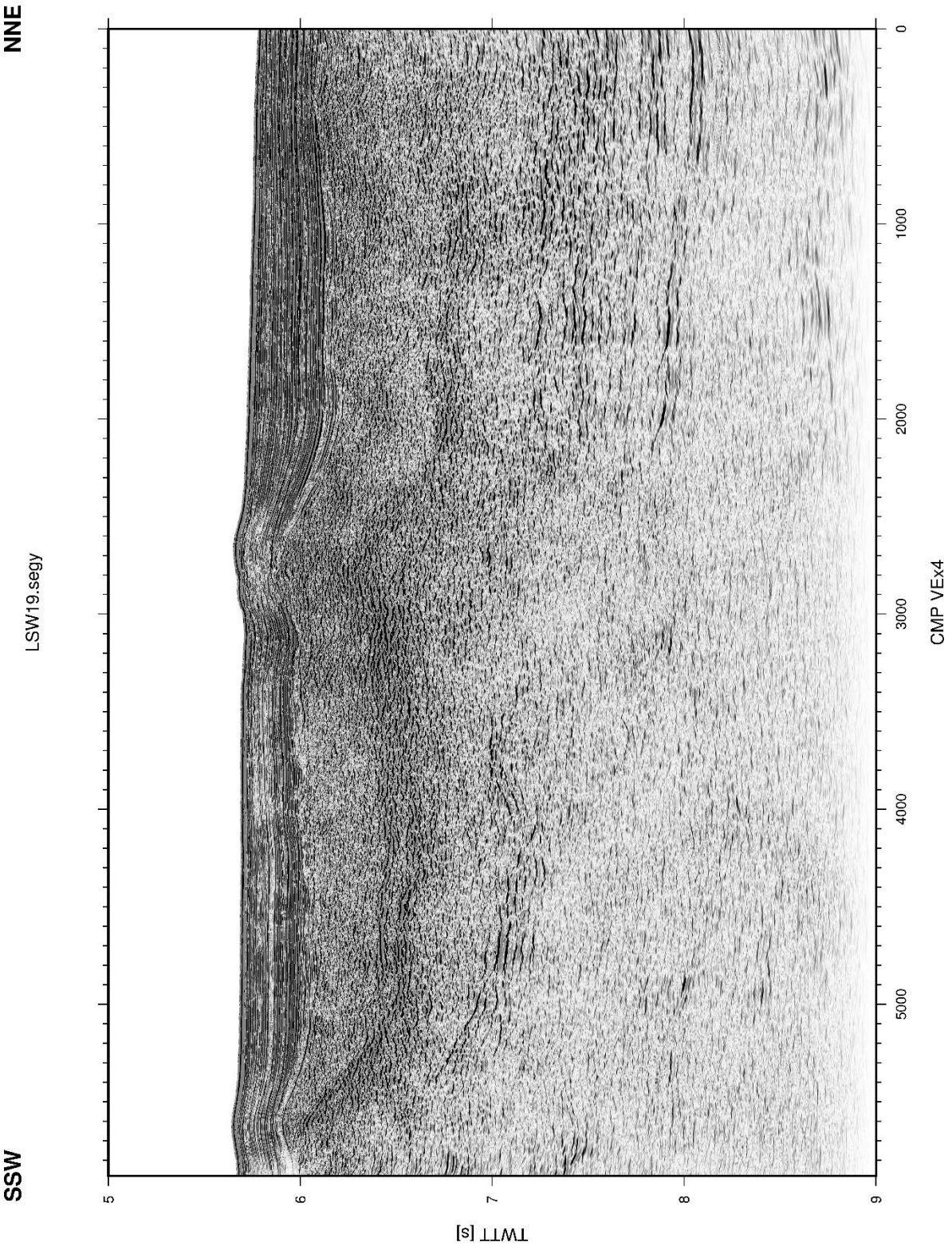
NNE
SSW
LSW19.segy
CMP VEx4
0
1000
2000
3000
4000
5000
5
6
7
8
9
TWTT [s]

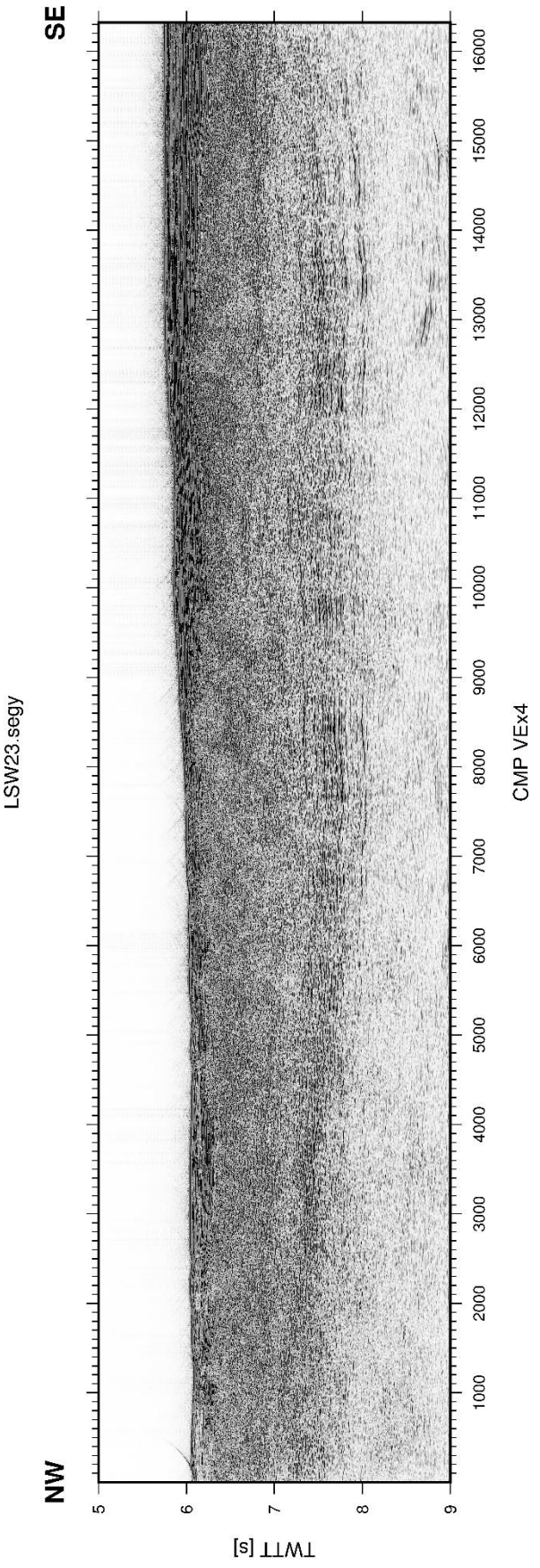
NW
SE
LSW23.segy
CMP VEx4
TWTT [s]
5
6
7
8
9
1000
2000
3000
4000
5000
6000
7000
8000
9000
10000
11000
12000
13000
14000
15000
16000

The Lineament South East Fault (MCS profiles):

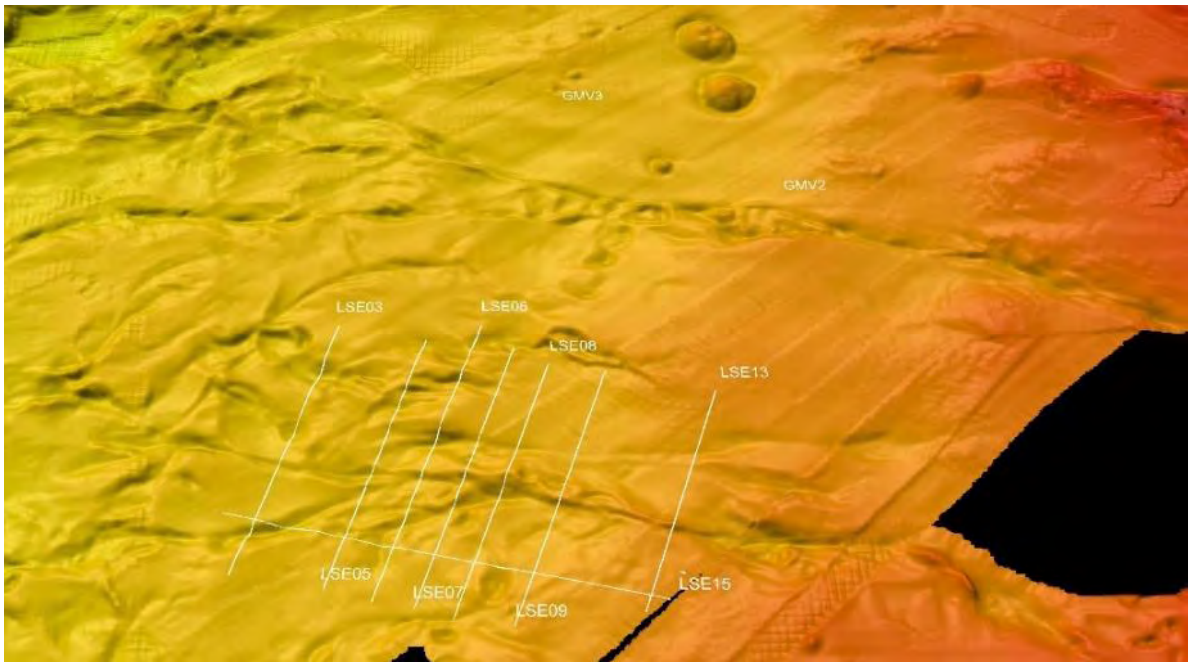

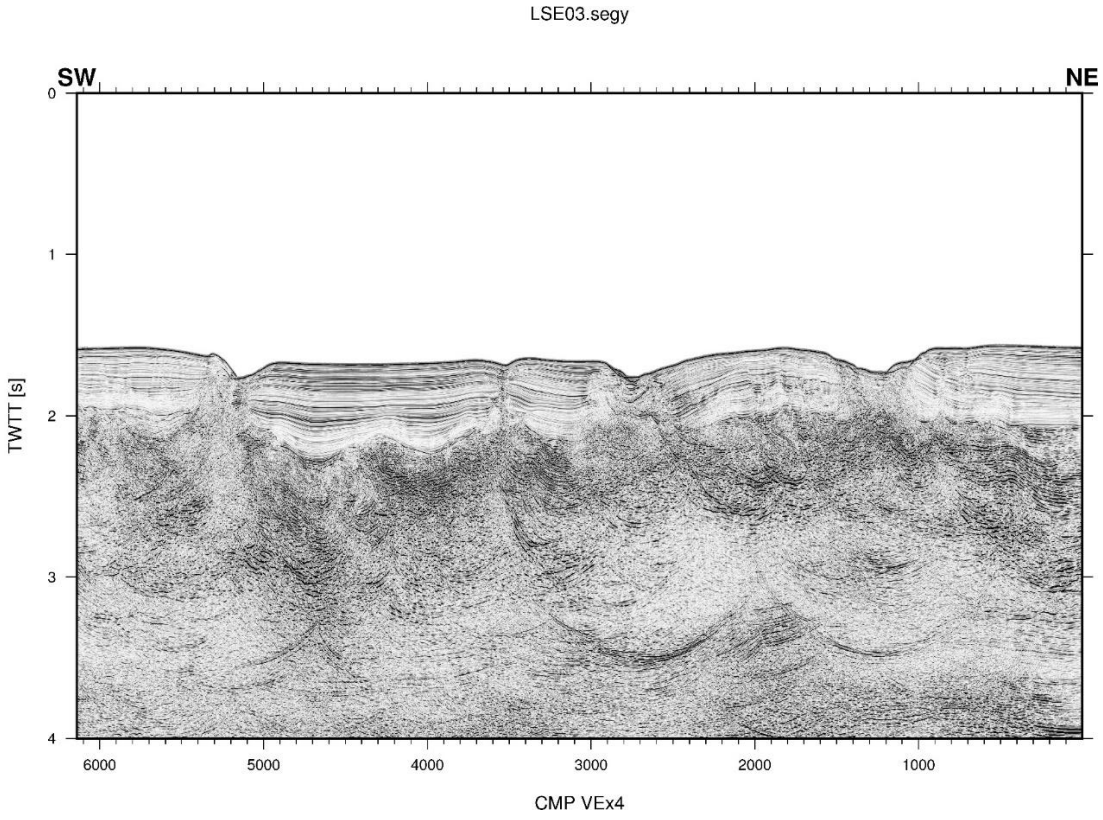

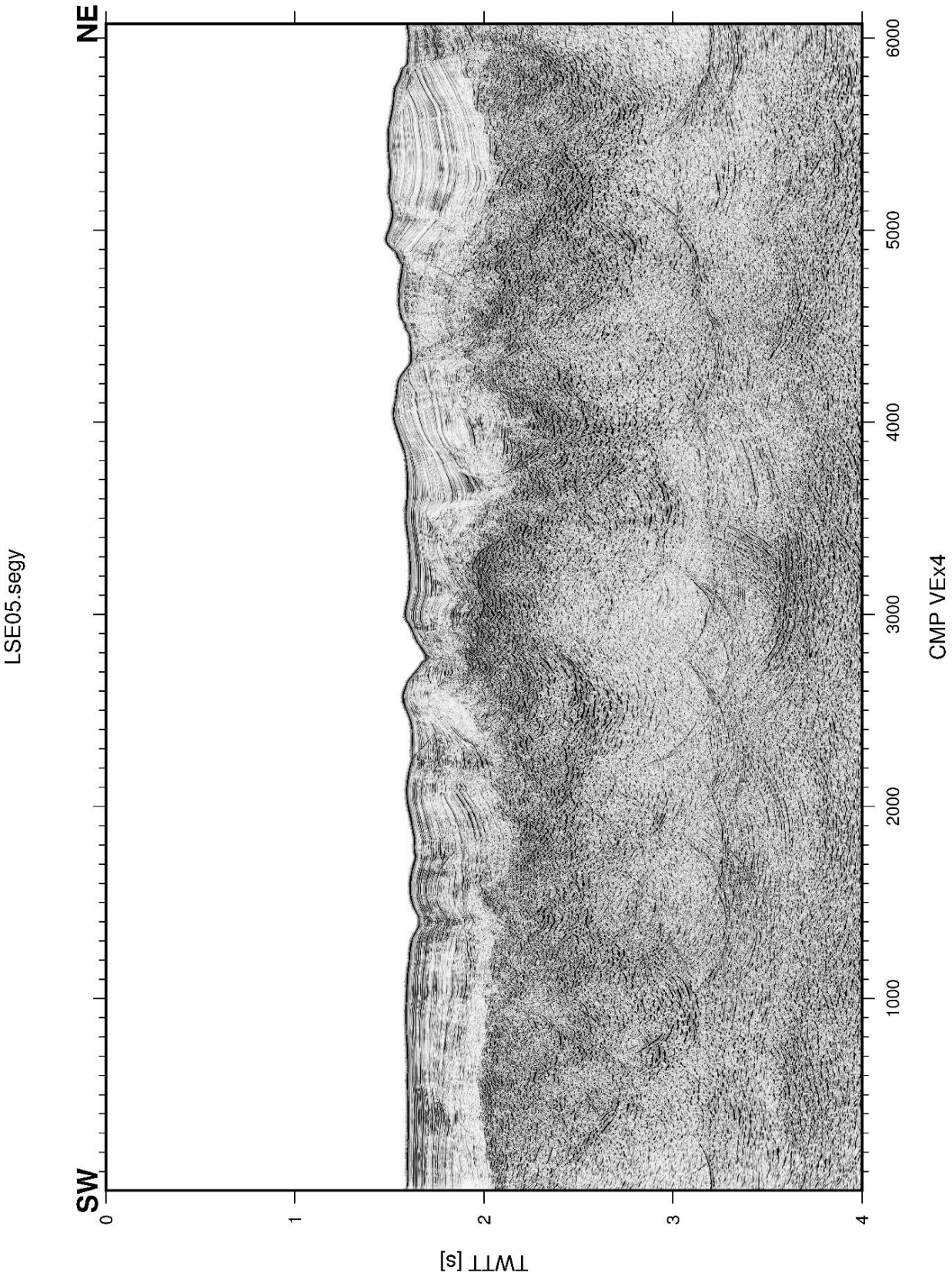
NE
SW
LSE05.segy
TWTT [s]
0
1
2
3
4
1000
2000
3000
4000
5000
6000
CMP VEx4

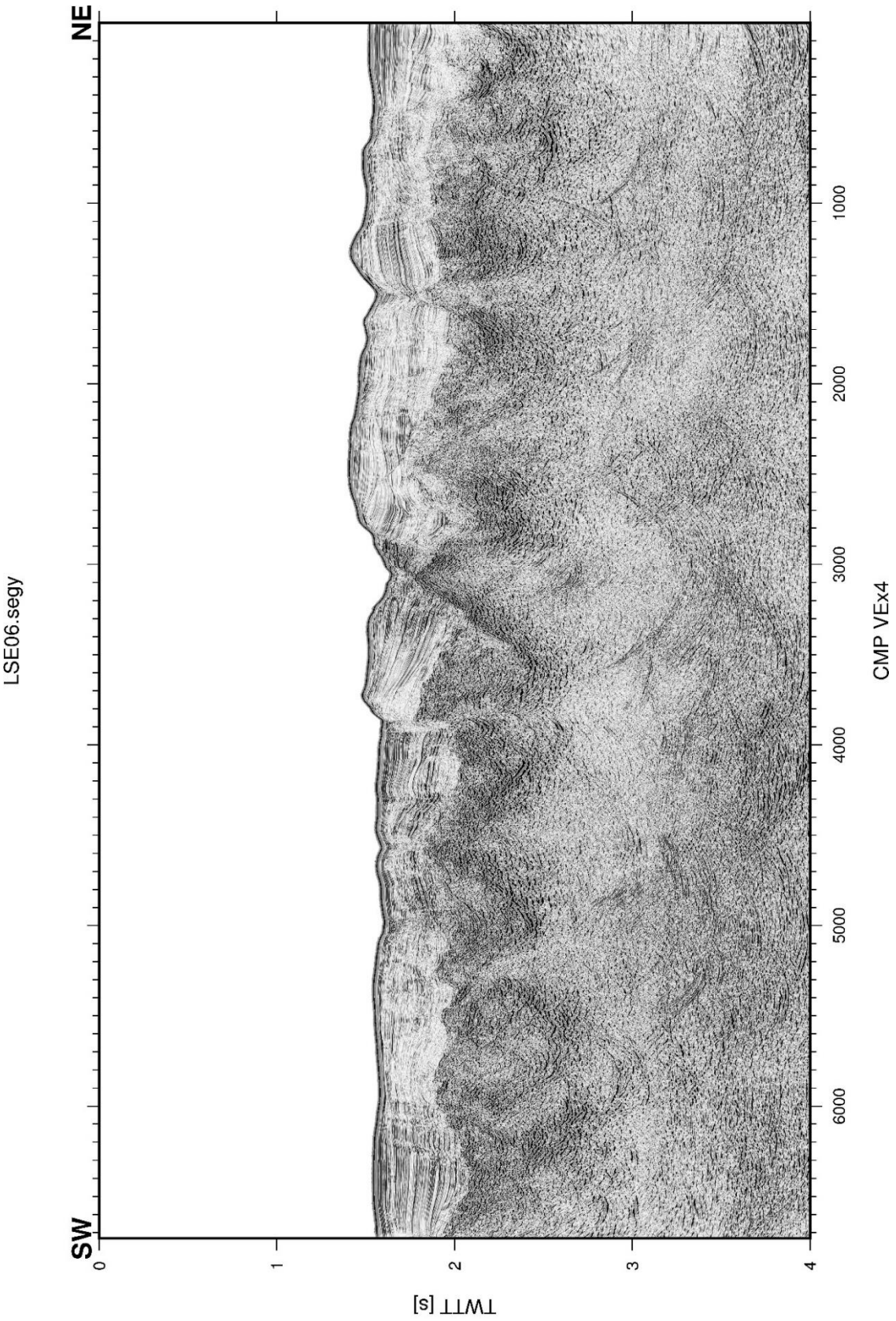
NE
SW
LSE06.segy
TWTT [s]
0
1
2
3
4
1000
2000
3000
4000
5000
6000
CMP VEx4

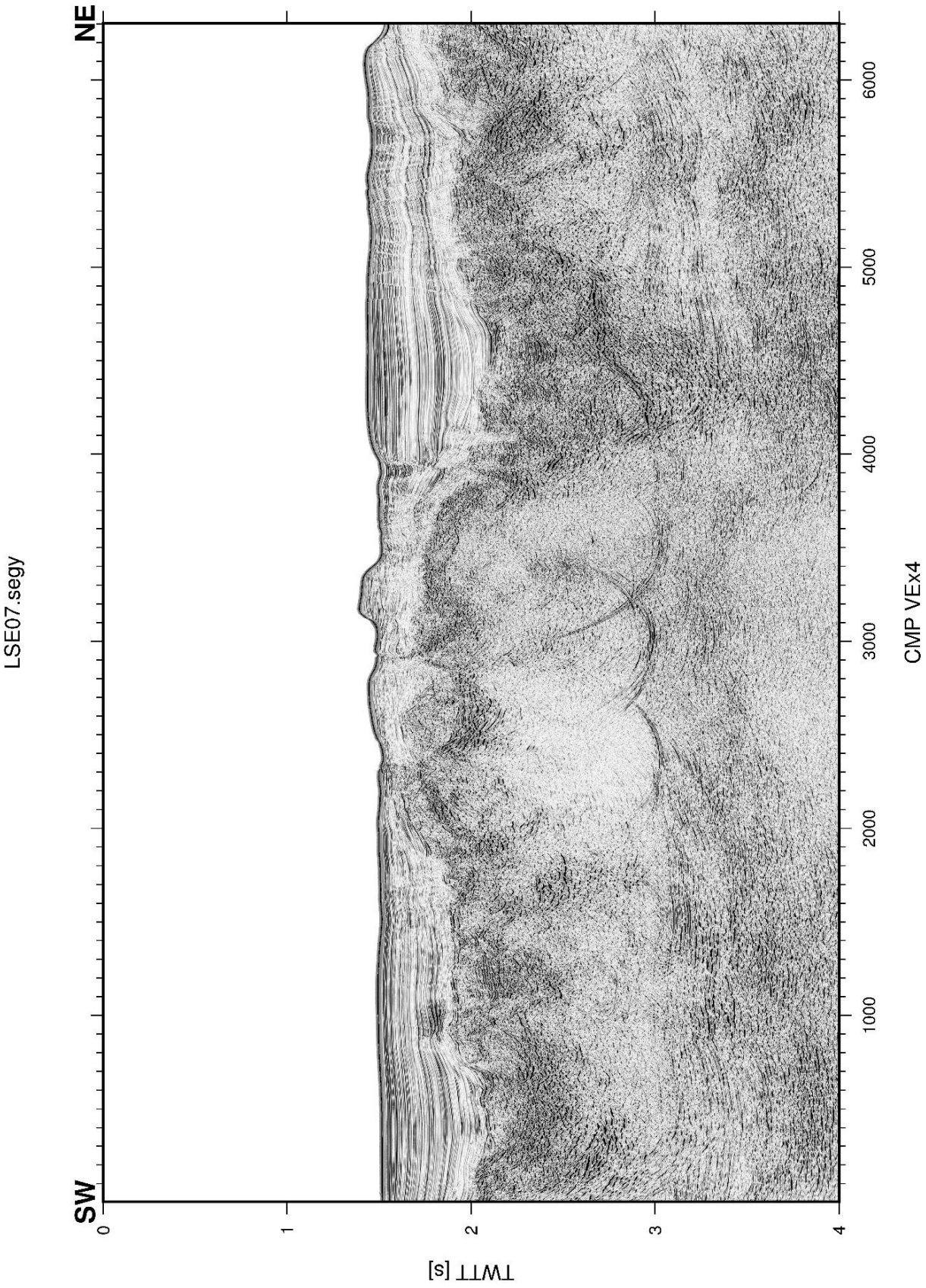
NE
SW
LSE07.segy
CMP VEx4
TWTT [s]
0
1
2
3
4
1000
2000
3000
4000
5000
6000

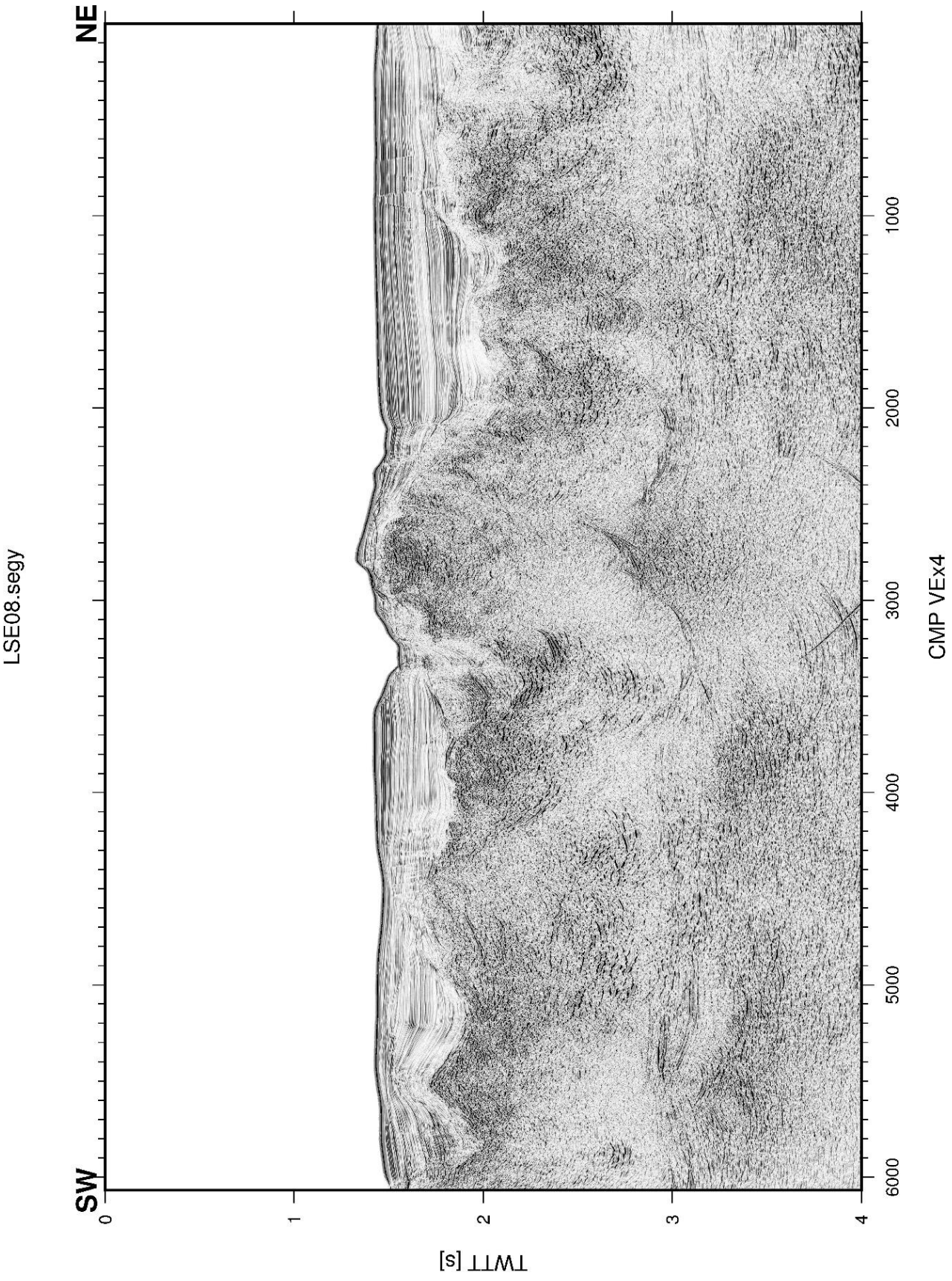
NE
SW
LSE08.segy
TWTT [s]
0
1
2
3
4
1000
2000
3000
4000
5000
6000
CMP VEx4

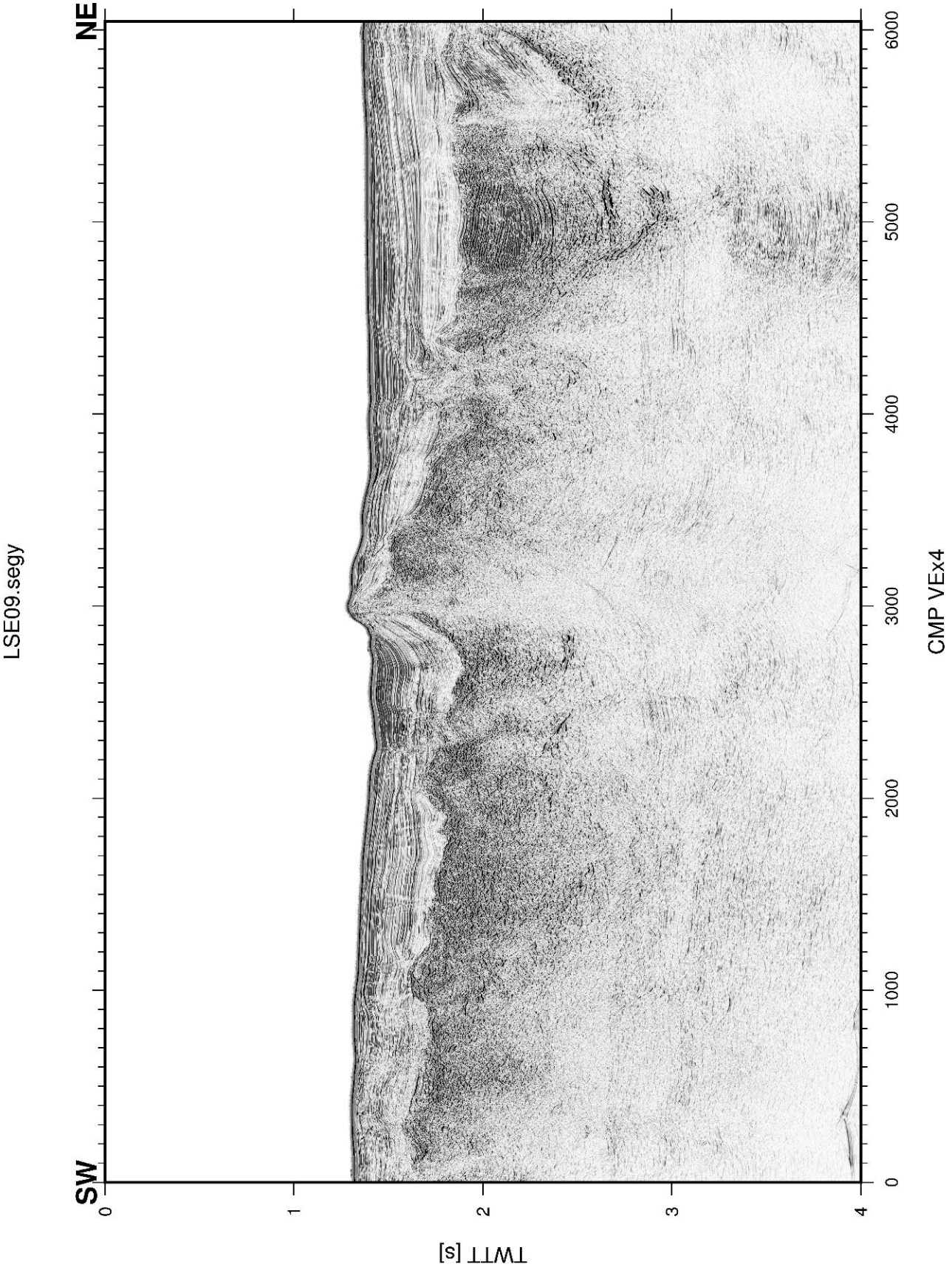
NE
SW
LSE09.segy
TWTT [s]
0
1
2
3
4
0
1000
2000
3000
4000
5000
6000
CMP VEx4

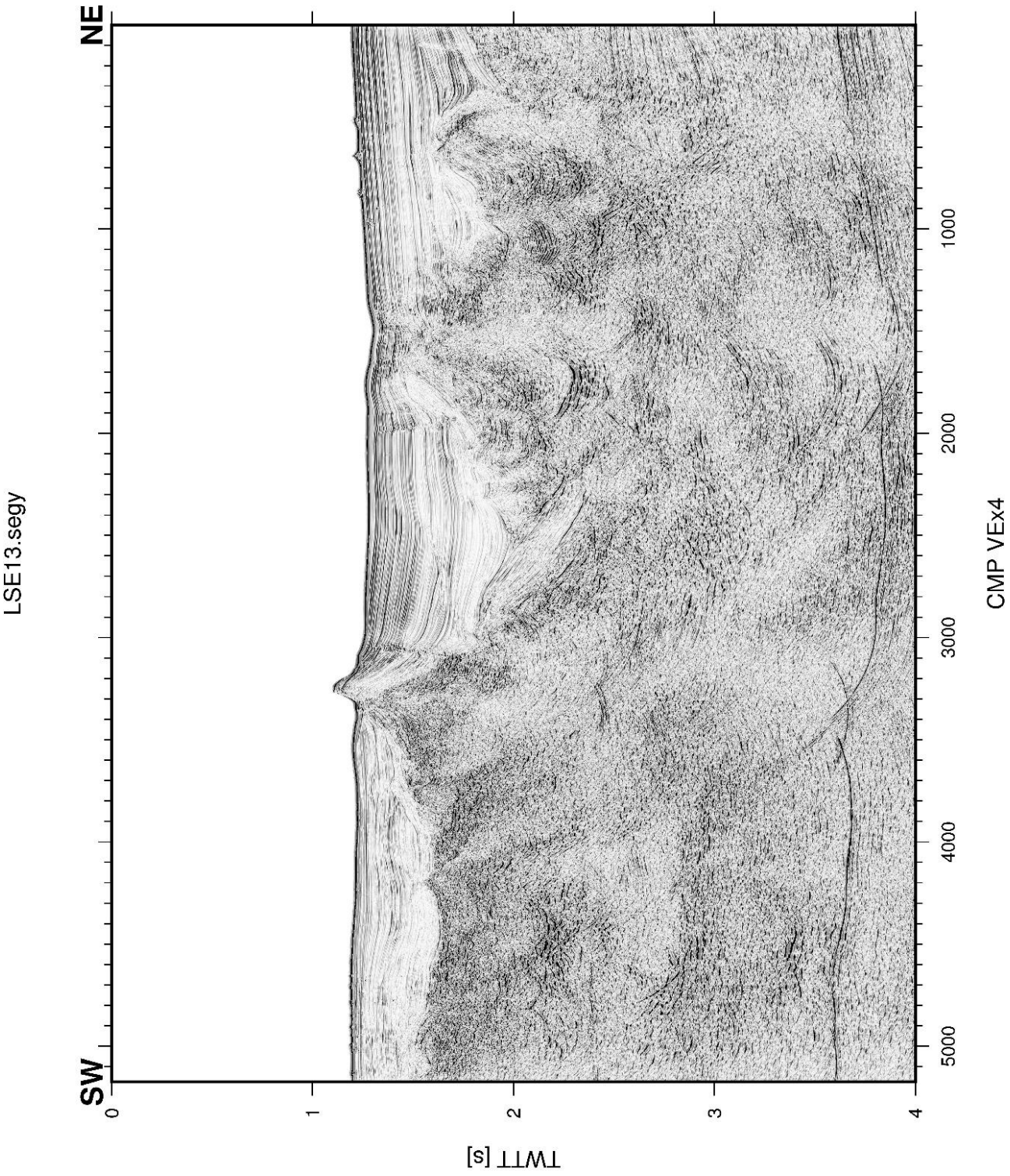
NE
SW
LSE13.segy
CMP VEx4
TWTT [s]
0
1
2
3
4
1000
2000
3000
4000
5000

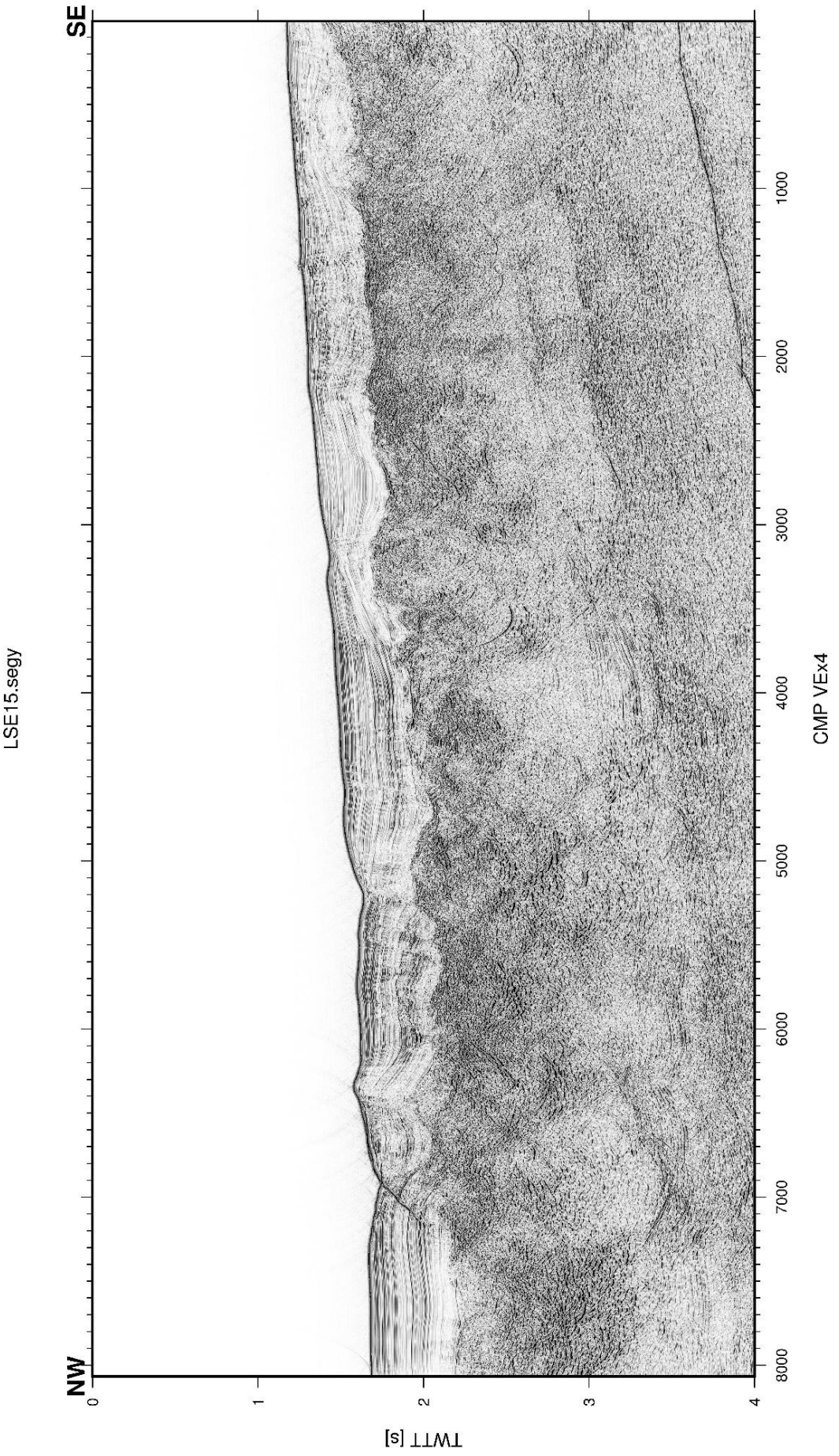
SE
NW
LSE15.segy
TWTT [s]
0
1
2
3
4
1000
2000
3000
4000
5000
6000
7000
8000
CMP VEx4

The Ginsburg Mud Volcano (MCS profiles):

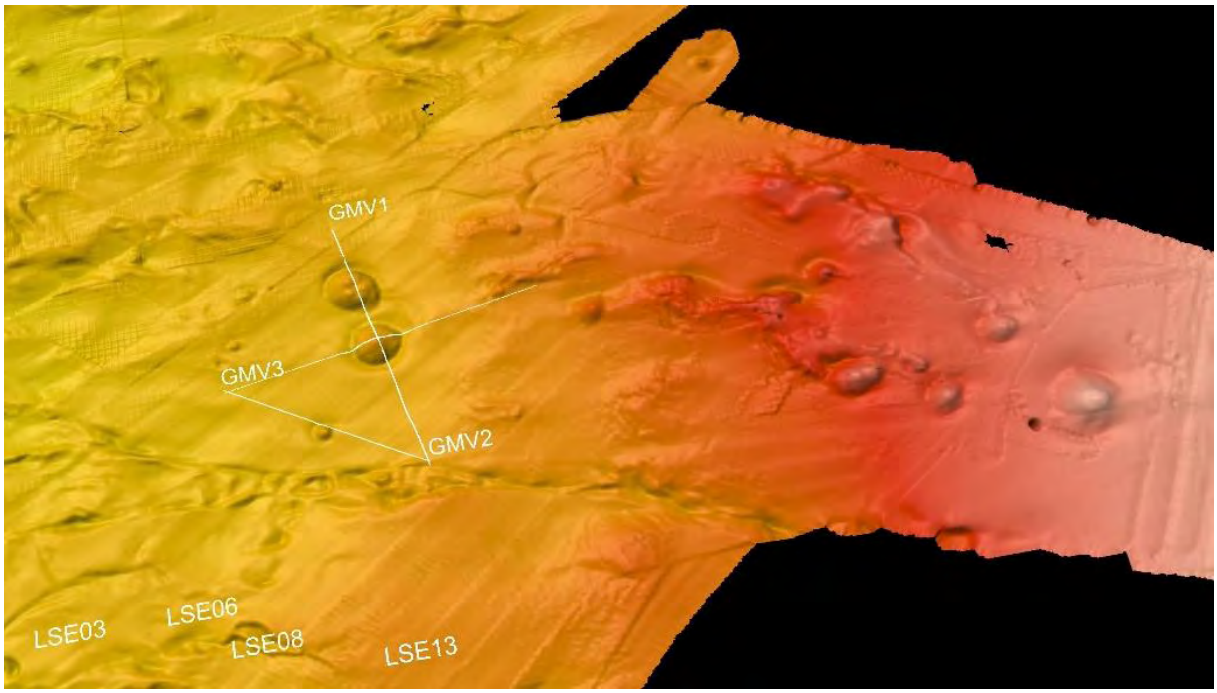

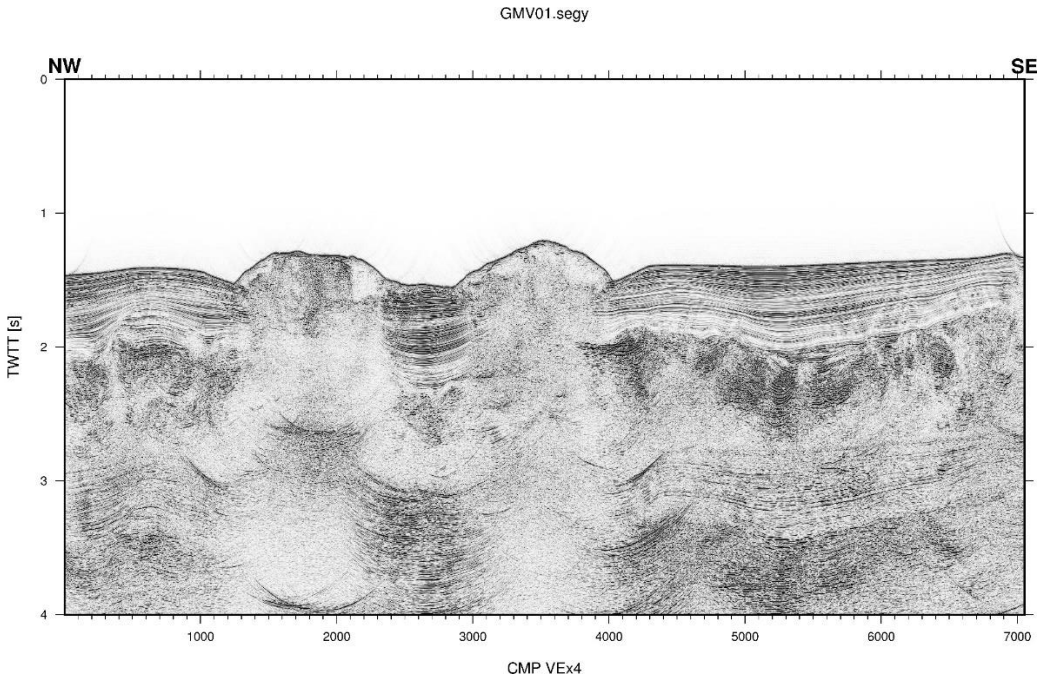

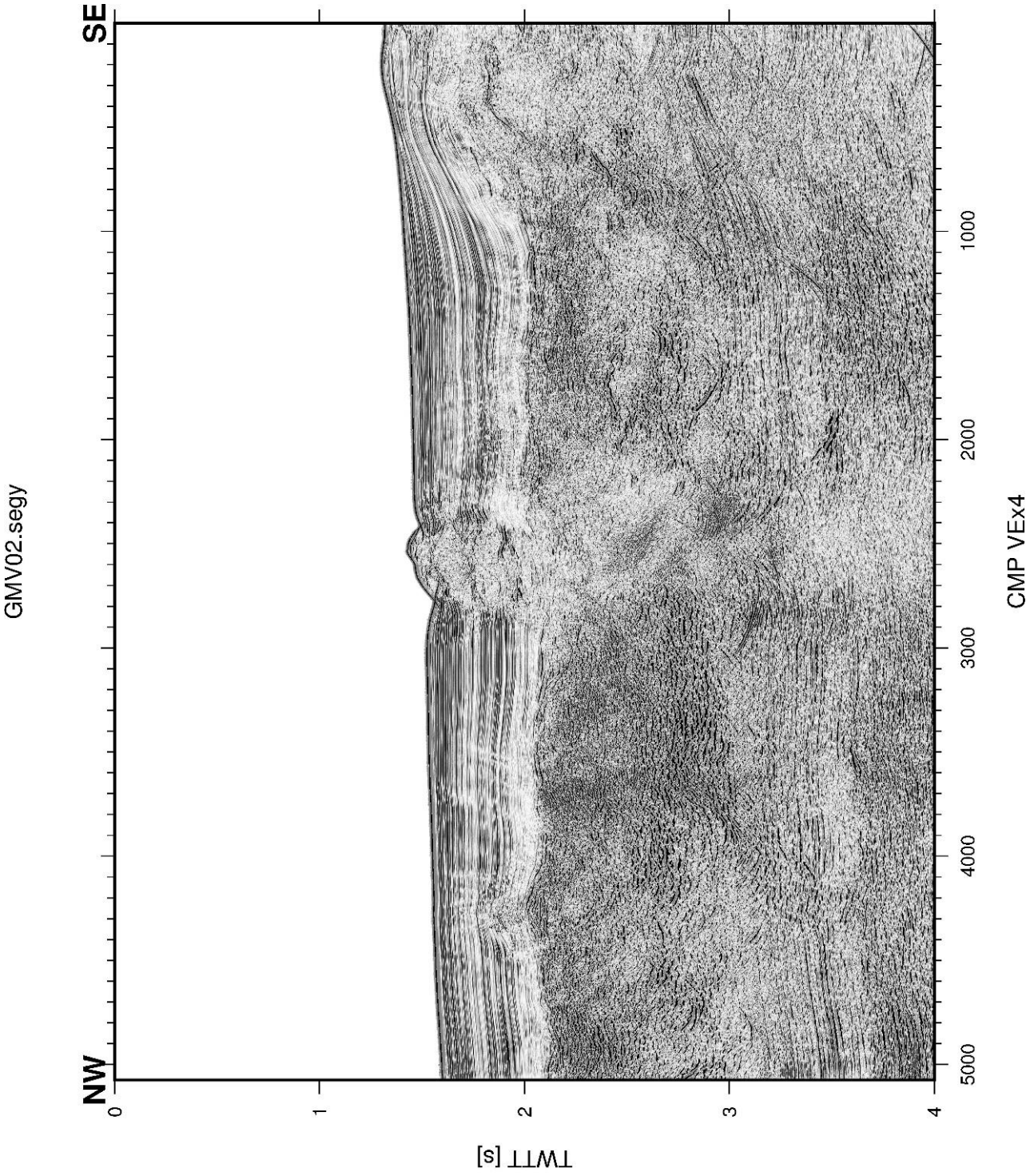
SE
NW
GMV02.segy
TWTT [s]
0
1
2
3
4
1000
2000
3000
4000
5000
CMP VEx4

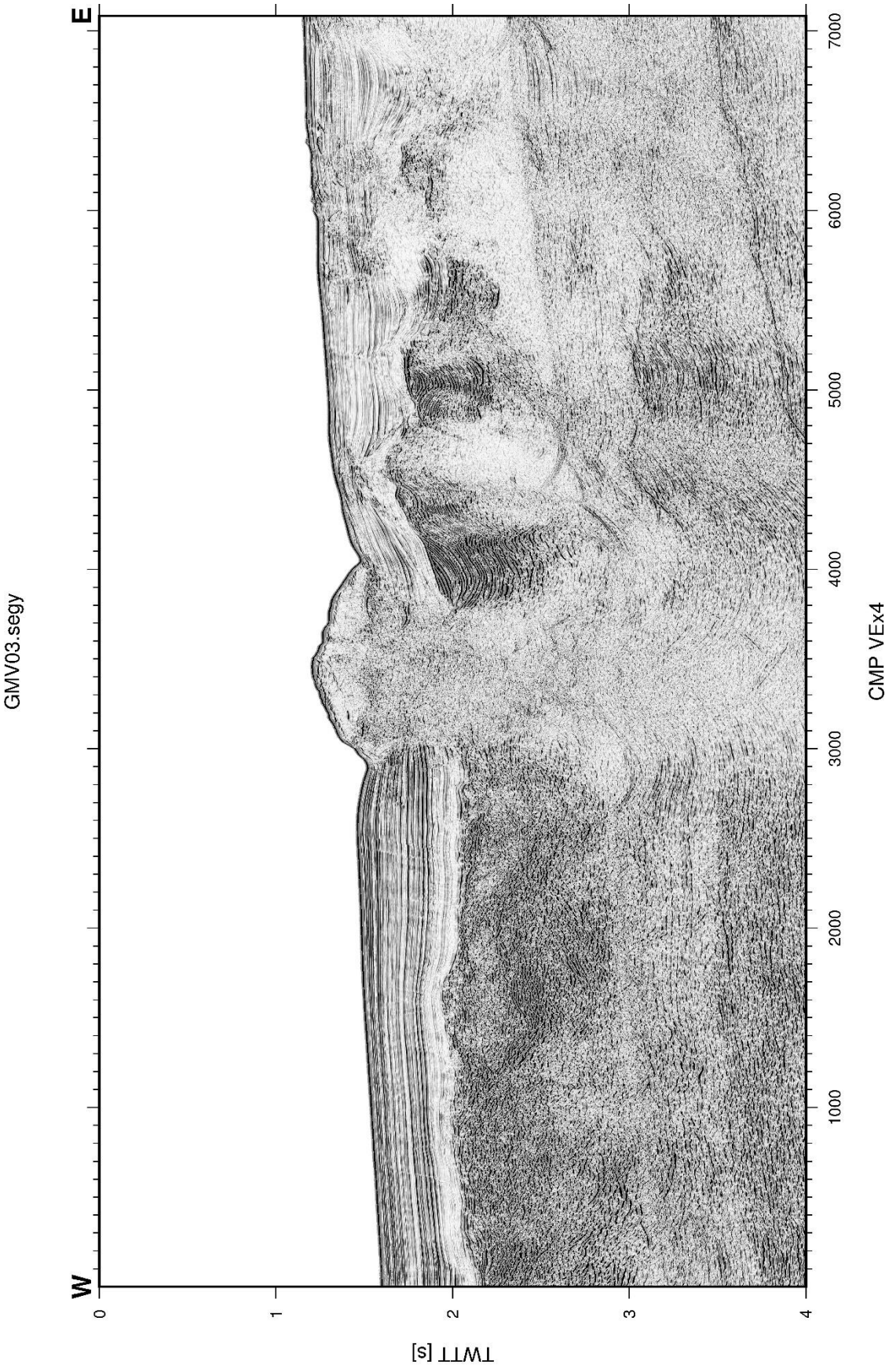
W
E
GMV03.segy
TWTT [s]
0
1
2
3
4
1000
2000
3000
4000
5000
6000
7000
CMP VEx4

The Lolita Salt Diapir (MCS profiles):

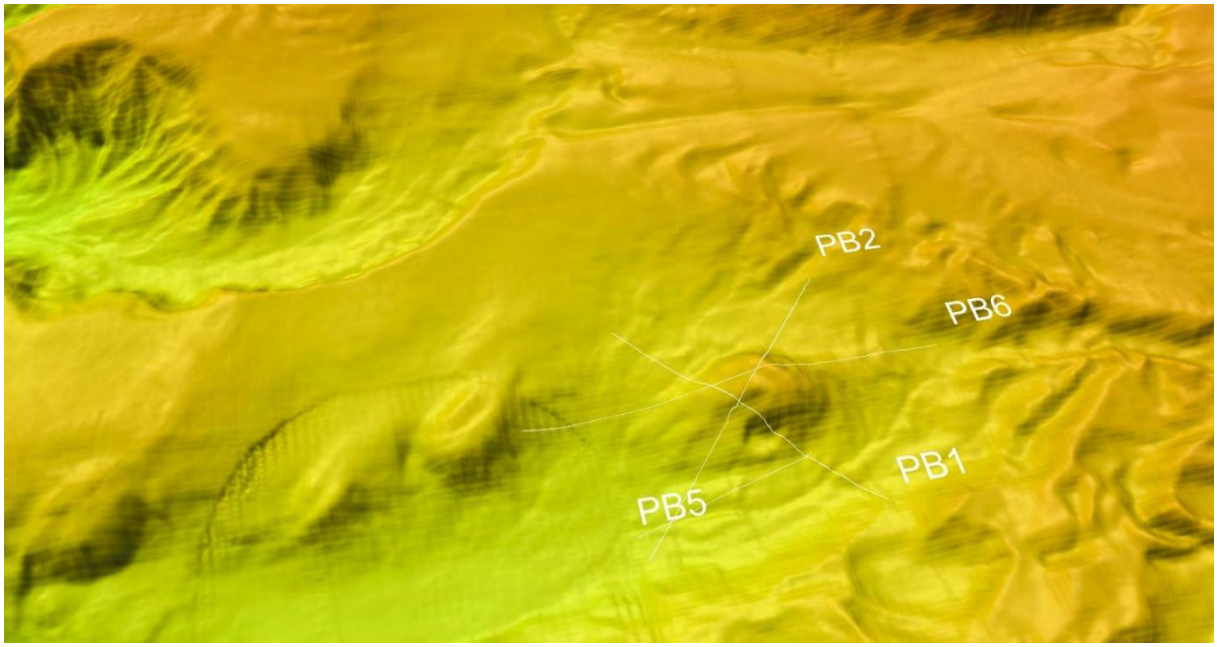

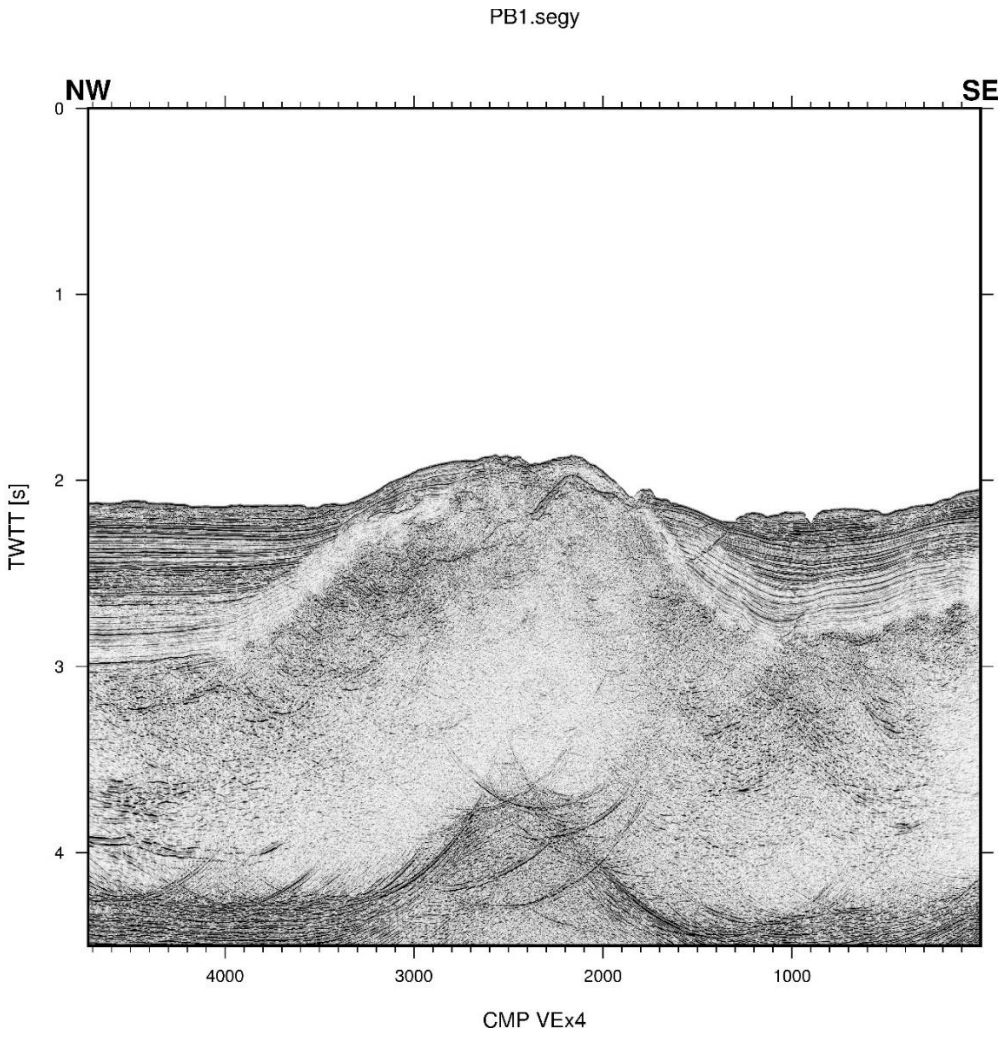

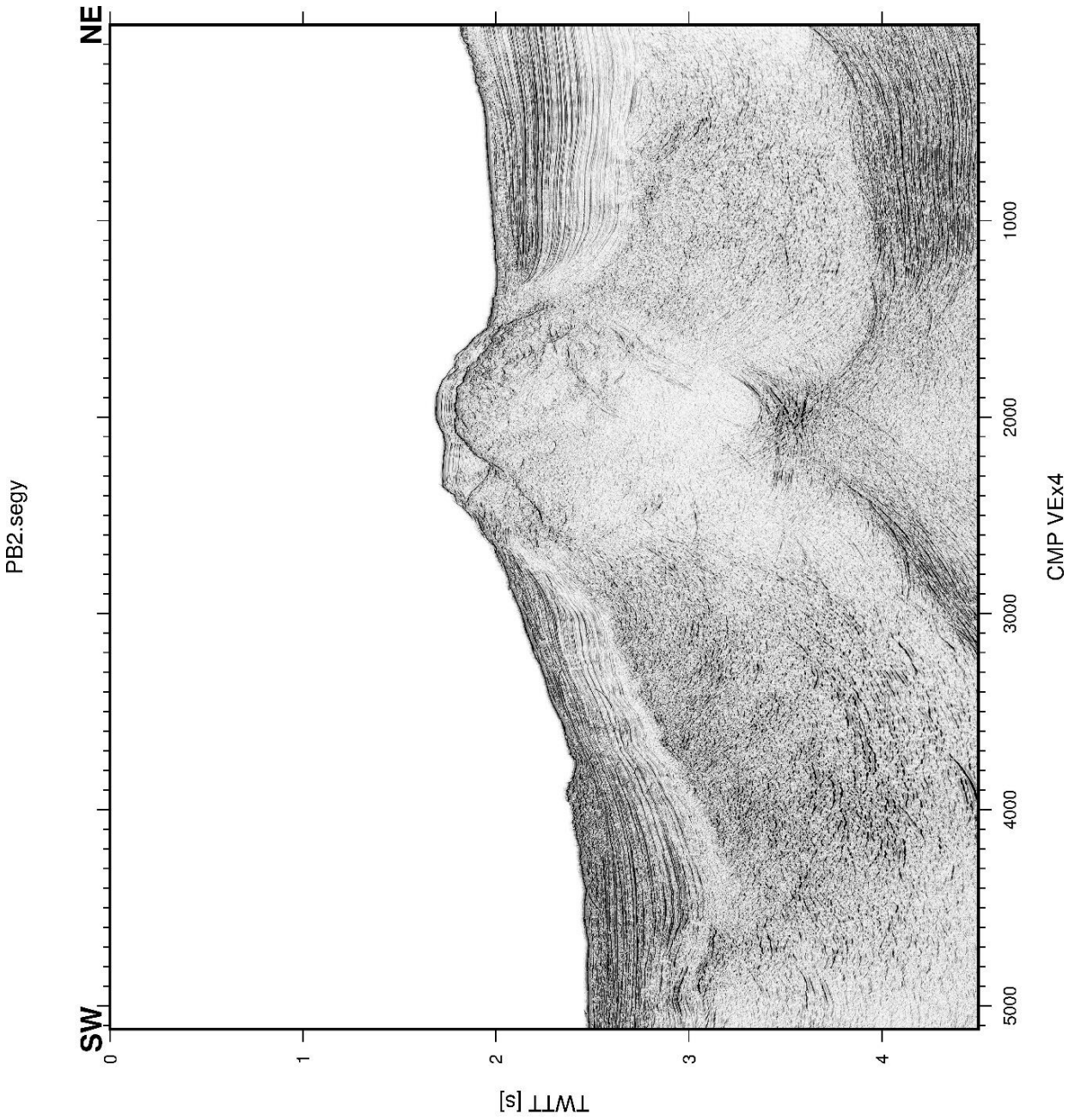
NE
SW
PB2.segy
TWTT [s]
0
1
2
3
4
1000
2000
3000
4000
5000
CMP VEx4

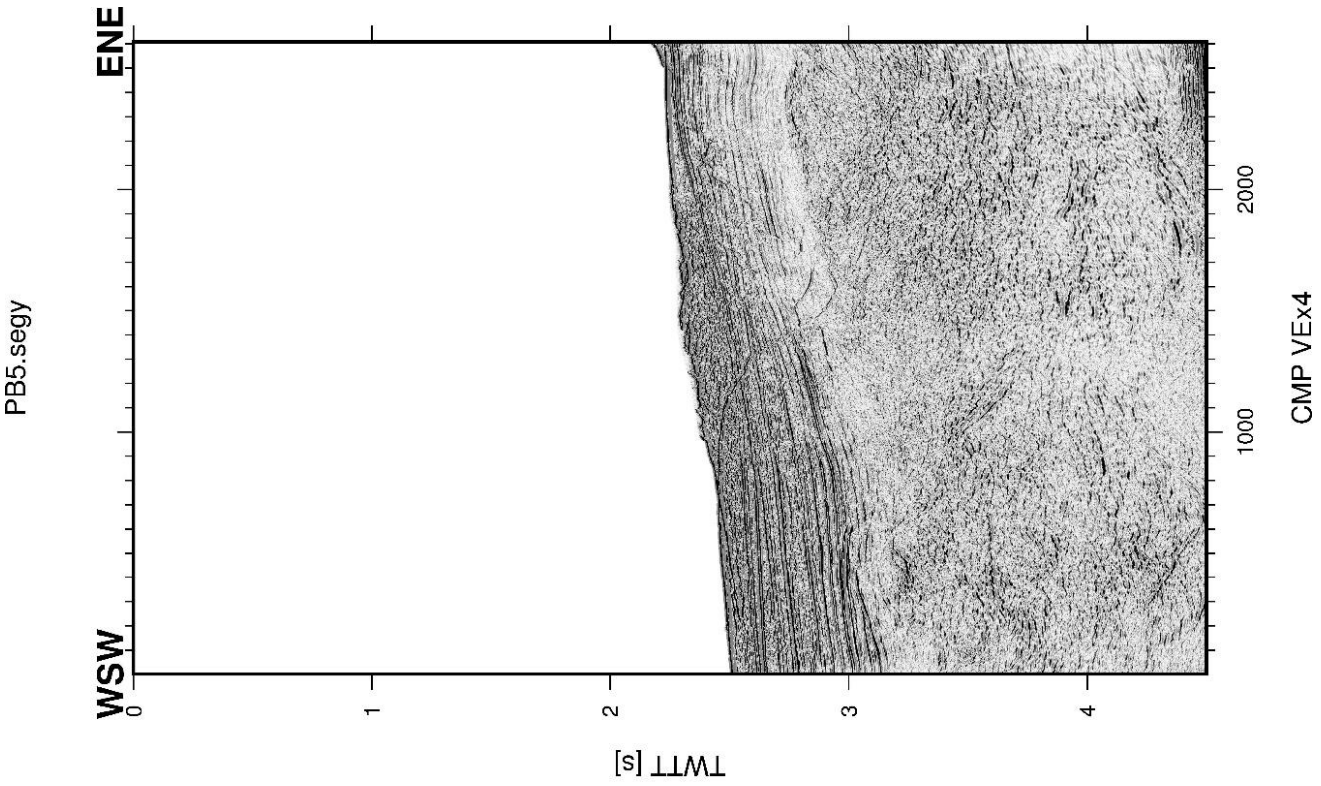
ENE
WSW
PB5.segy
CMP VEx4
2000
1000
0
1
2
3
4
TWTT [s]

11. Sediment sampling

11.1. Introduction

During the INSIGHT Cruise, a total of 16 Gravity Cores (GC) have been carried out in order to recover sediment samples from a number of active fault systems, submarine slides and mud/salt diapirs of the Gulf of Cadiz. Sediment was recovered at all stations, resulting in a total of x successful deployments and sediment sampling during the cruise (Figure 11.1 and Table 11.1).

11.2. The Marques de Pombal Fault sediment cores

Three sediment cores have ben aquired in the Marques de Pombal área. Core #01 has been acquired near the highest part of the Marques de Pombal área. Core #02 has been acquired in a slide area, while core #03 has been acquired in a stable area.

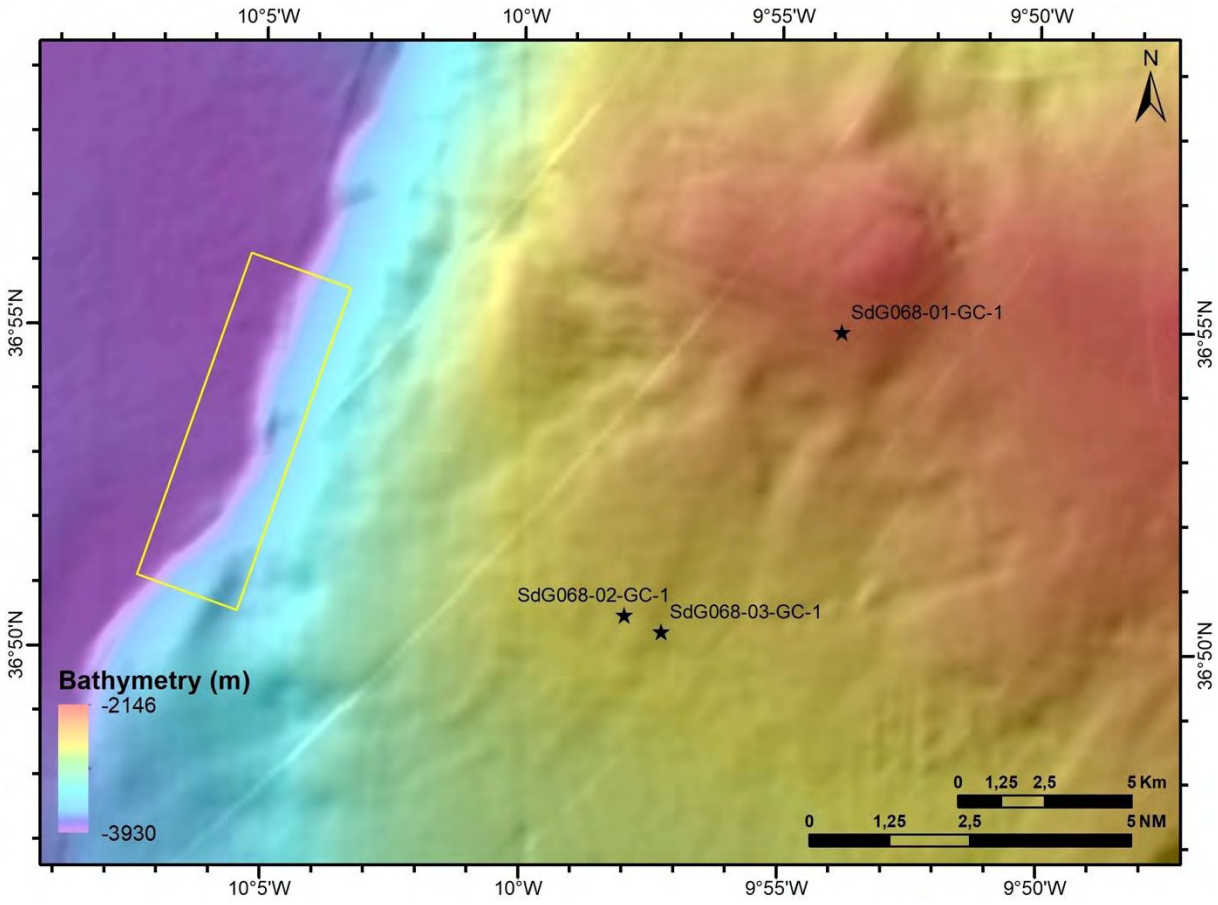

Figure 11.1. *Map showing the location of the gravity cores in the Marques de Pombal area.*

11.3. The Lineament South East & CWCoral mound sediment cores

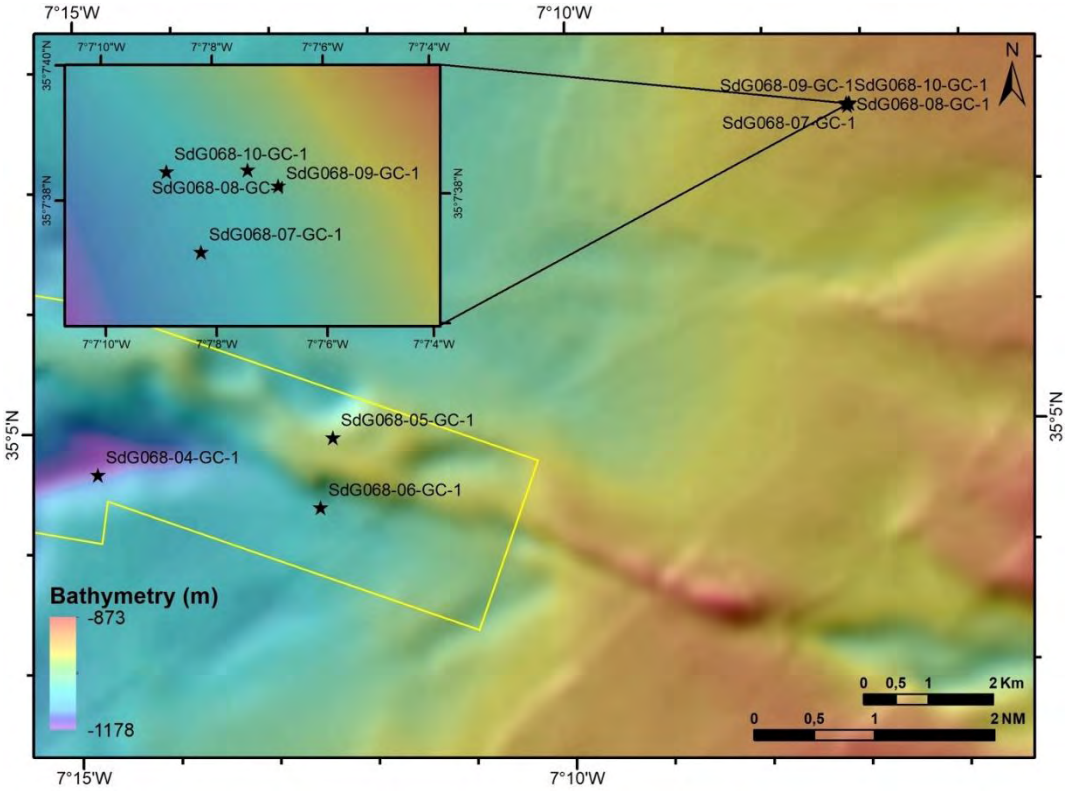

Figure 11.2. *Map showing the location of the gravity cores in the Lineament S-East area.*

11.4. The Ginsburg Mud Volcano

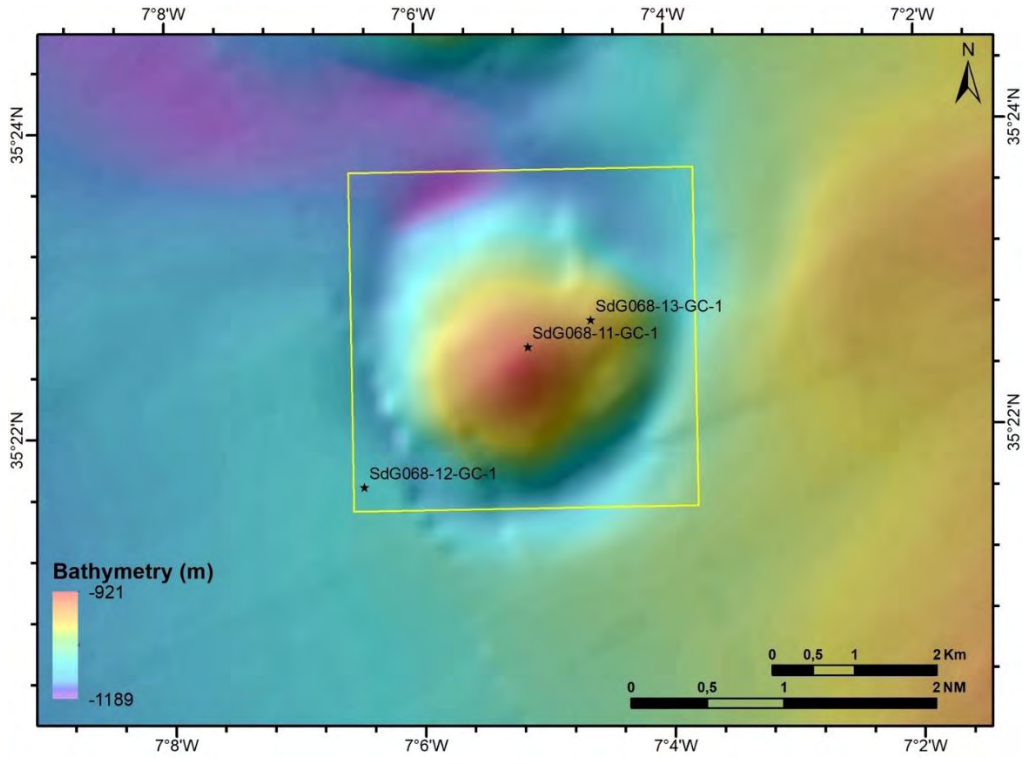

Figure 11.3. *Map showing the location of the gravity cores in the Ginsburg MV area.*

11.5. The Lolita Salt Diapir

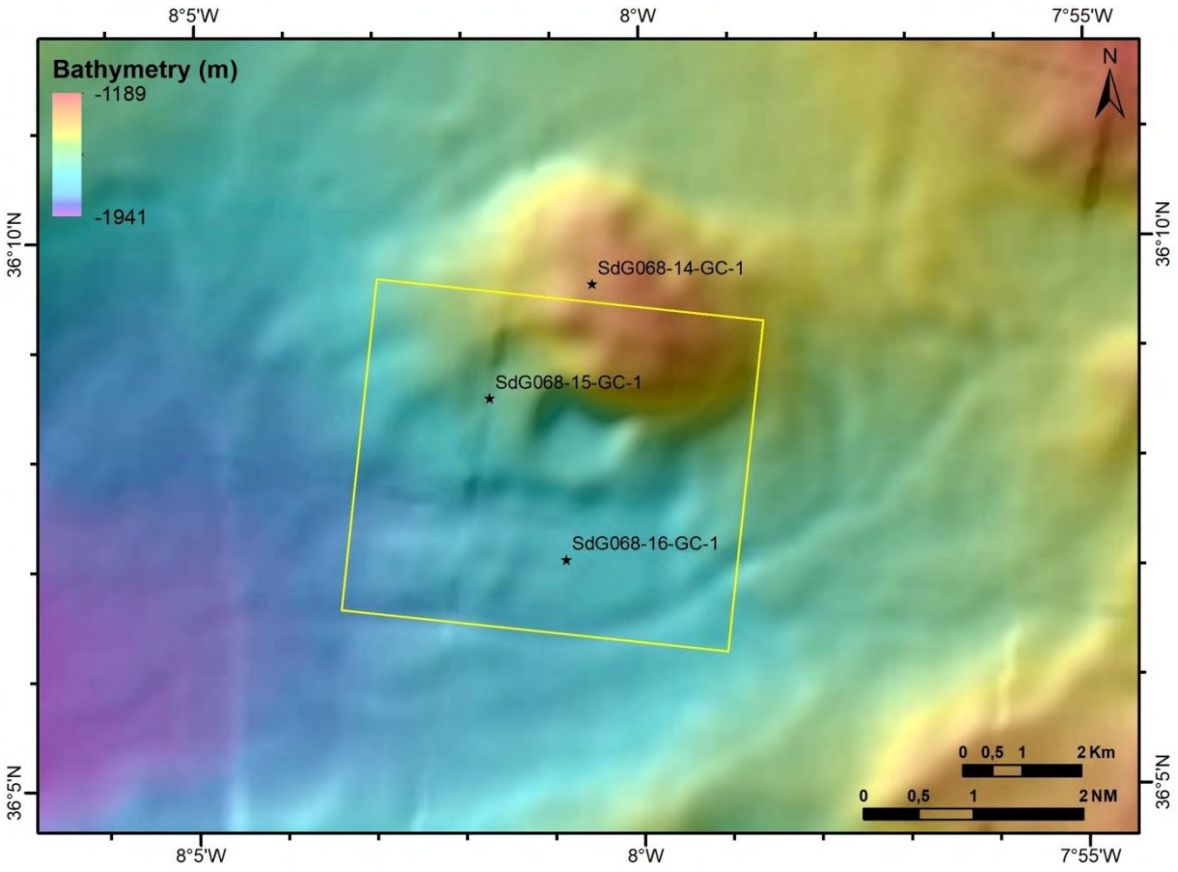

Figure 11.4. *Map showing the location of the gravity cores in the Lolita Salt diapir area.*

The aim of the sediment sampling is to study the changes in the sedimentation rate related to the activity of the main faults located in the Gulf of Cadiz (MPF, LSE), as well as mud volcanoes and the submarine slides asso ciated to te Lolita Salt diapir. With this purpose, the position of each sediment sampling station was designed on the basis of the available information on multibeam bathymetry, AUV micro-bathymetry and sediment sub-bottom profiles of the study area.

The Multi Corer (MUC) system of the UTM had not be used. Therefore, no MUC were recovered during the INSIGHT-Leg 1 cruise.

Table 11.1. *Location of the gravity cores acquired during INSIGHT-Leg1 cruise.*

Sampling Station	Depth (m)	Recovery (m)	Area	Observations	Lat Deg./Dec.Min.	Long Deg./Dec.Min.
SdG068-01	1703	2,43	Pombal	Hanging Wall	36º54.9406'	-9º53.8149'
SdG068-02	2667,54	2,12	Pombal	Hanging Wall	36º50.5130'	-9º57.9727'
SdG068-03	2664	2,48	Pombal	Hanging Wall	36º50.5130'	-9º57.9727'
SdG068-04	1175	2,03	LSE	Pull Apart	35º04.6557'	-7º14.8136'
SdG068-05	990	2,16	LSE	North of Fault	35º04.9310'	-7º12.4220'
SdG068-06	1058	1,54	LSE	South of Fault	35º04.25'	-7º12.56'
SdG068-07	921,4	2,85	LSE	CWCM	35º07.62'	-7º07.14'
SdG068-08	913	4,02	LSE	CWCM	35º07.64'	-7º07.1255'
SdG068-09	913,5	2,26	LSE	CWCM	35º07.636'	-7º07.11165'
SdG068-10	923	3,4	LSE	CWCM	35º07.64'	-7º07.15'
SdG068-11	930	1,62	GMV	Top	35º22.55'	-7º05.13'
SdG068-12	1102	2,63	GMV	Off	35º21.65'	-7º06.46'
SdG068-13	990	2,68	GMV	Terrace	35º22.72'	-7º04.62'
SdG068-14	1254,68	2,02	LoSD	Top	36º09.5938'	-8º00.5432'
SdG068-15	1565	1,82	LoSD	Slide	36º08.56'	-8º01.71'
SdG068-16	1703	0,66	LoSD	Deposit	36º07.0810'	-8º00.8643'

11.6. Methodology

11.6.1. Gravity coring

A gravity corer system from the UTM was used during the SHAKE Cruise (Figure 11.2). It is a galvanized steel pipe of 9 cm of diameter, containing a PVC tube of 7 cm of internal diameter, which through the operation is filled with sediment. The head of the GC weights ~700 Kg.

a)

b)

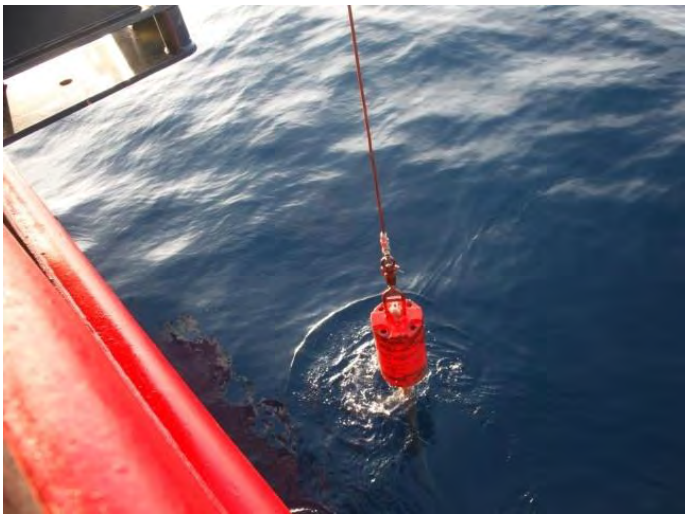

Figure 11.2. *a) Gravity corer system onboard the RV Sarmiento de Gamboa. b). Gravity corer deployment.*

The gravity corer was deployed through the specific system attached at the gunwale of the R/V Sarmiento de Gamboa. The coring operation consists of:

1. Sinking of the instrument at 80 m/min.
2. At an altitude of around 100 meters over the seafloor, the winch stops and the instrument is sank at 100 m/min, to ensure the probability of maximum sediment penetration.
3. The corer penetrates and samples the seafloor.
4. Corer is recovered at velocities of 10-20 m/min, gradually increasing towards 80-90 m/min.

Lances of 3 and 5 meters were specifically chosen for each deployment in order to ensure the maximum possible recovery without reaching the total length of the lance, which would cause the loose of the youngest sediment-record.

Right after recovery, gravity cores were measured, labeled and cut in 1.5-meter-long sections in the humid lab (Figures 11.3 and 11.4). Lowermost sediments contained in the core-catcher were introduced in labeled plastic bags. Finally, all the recovered sections and samples were stored in a refrigerated room at 4ºC in order to preserve the sediment moisture and other physicochemical properties.

a) b)

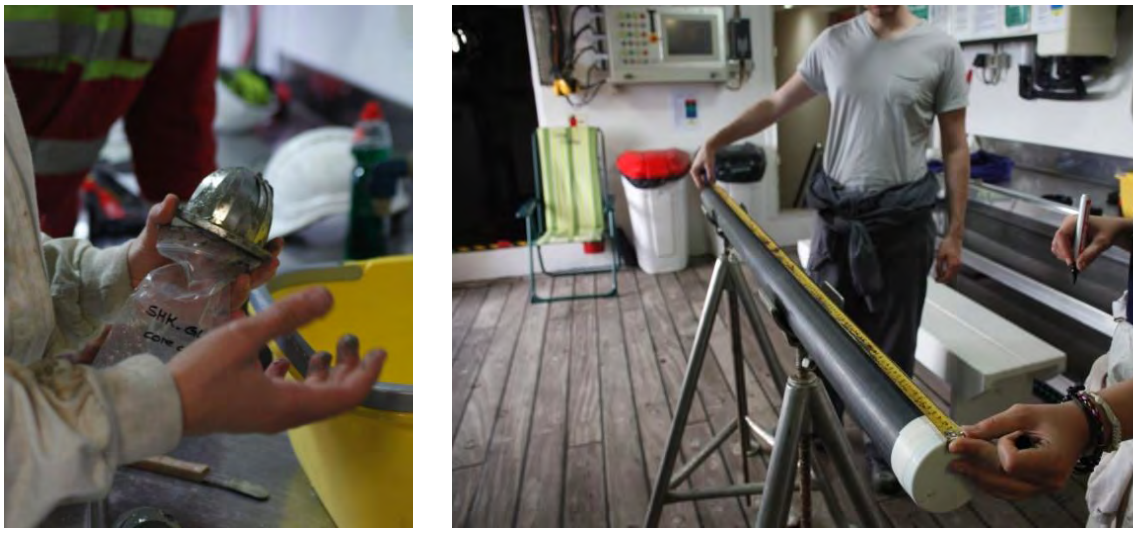

Figure 11.3. *a) Sampling the sediment in the core catcher. b) Core length measurement.*

a) b)

Figure 11.4. *a) Gravity corer cut in sections. b) Labeling the sections of the gravity core.*

12. References

Baptista, M., S. Heitor, J. Miranda, P. Miranda, and L. M. Victor (1998a). The 1755 lisbon tsunami: evaluation of the tsunami parameters. *Journal of Geodynamics*, 25 (2), 143-157.

Baptista, M.A. and Miranda, J.M., 2009. Revision of the Portuguese catalog of tsunamis. *NHESS*, 9, 25-42.

Bartolome, R., E. Gràcia, D. Stich, S. Martinez-Loriente, D. Klaeschen, F. L. Mancilla, C. LoIacono, J.J. Dañobeitia, and N. Zitellini (2012). Evidence for active strike-slip faulting along theEurasia-Africa convergence zone: Implicationsfor seismic hazard in the SW Iberian Margin. *Geology*, 40 (6), 495-498.

Buforn, B., C.S. de Galdeano, and A. Udias (1995). Seismotectonics of iberomaghrebian region. *Tectonophysics*, 248, 247-261.

Buforn, E., Bezzeghoud, M., Udías, A. & Pro, C. (2004). Seismic sources on the Iberia-African Plate boundary and their Tectonic Implications. *Pure Appl. Geophys*., 161, 623-646.

Crutchley, G.J., Berdnt, C., Klaeschen, D., Masson, D.G., 2011. Insights into active deformation in the Gulf of Cadiz from new 3-D seismic and high-resolution bathymetry data. G3, 12(7), Q07016.

Cunha, T., Watts, A.B., Pinheiro, L.M.-, Myklebust, R., 2010. Seismic and brevity anmaly evidence of large-scale compressional deformation off SW Portugal. *EPSL*, 293, 171-179.

Fukao, Y. (1973). Thrust faulting at a lithospheric plate boundary: The Portugal earthquake of 1969. *Earth and Planetary Science Letters*, 18, 205-216.

Geissler, W.H., Matias, L., Stich, D., Carrilho, F., Jokat, W., Monna, S., IbenBrahim, A., Mancilla, F., Gutscher, M.A., Sallarès, Zitellini, N., *GRL*, 37, 1-6.

Gràcia, E., J. Dañobeitia, J. Vergés, R. Bartolomé, D. Córdoba (2003a), Crustal architecture and tectonic evolution of the gulf of cadiz (SW Iberian Margin) at the convergence of the eurasian and african plates. *Tectonics*, 22 (4), 1033-1058

Gràcia, E., J. Dañobeitia, J. Vergés, and P. team (2003b). Mapping active faults offshore Portugal (36ºN-38ºN): Implications for seismic hazard assessment along the southwest iberian margin, *Geology*, 31, 83-86.

Grimison, N.L., W.P. Chen, (1986). The Azores-Gibraltar plate boundary: Focal mechanisms, depths of earthquakes and their tectonic implications, *J. Geophys. Res.* 91, 2029-2047.

Gutscher, M., J. Malod, J. Rehault, I. Contrucci, F. Kingelhoefer, L. Mendes-Victor, and W. Spakman (2002). Evidence for active subduction beneath gibraltar, Geology, 30 (12), 1071-1704.

Hayward, N., A. Watts, G. Westbrook, and J. Collier (1999). A seismic reflection and gloria study of compressional deformation in the gorringe bank, eastern north atlantic, Geophysical Journal International, 138, 831-850.

Hensen, C., Scholz, F., Nuzzo, M., Valadares, V., Gràcia, E., Terrinha, P., Liebetrau, V., Kaul., N., Silva, S., Martínez-Loriente, S., Bartolomé, R., Piñero. E., et al. (2015). Strike-slip faults mediate the rise of crustal derived fluids and mud volcanism in the deep sea. *Geology*, 43, 339-342.

Leon. R., et al., 2012.New discoveries of mud volcanoes on the Moroccan Atlantic continental margin (Gulf of Cádiz): morpho-structuralcharacterization. *Geo-Mar. Lett.,* doi 10.1007/s00367-012-0275-1.

Martínez-Loriente, S., E. Gràcia, R. Bartolome, V. Sallarès, C. Connors, H. Perea, C. Lo Iacono, D. Klaeschen, P. Terrinha, J. J. Dañobeitia, and N. Zitellini (2013). Active deformation in old oceanic lithosphere and significance for earthquake hazard: Seismic imaging of the Coral Patch Ridge area and neighboring abyssal plains (SW Iberian Margin), *Geochem.Geophys.Geosyst.,* 14, 2206–2231, 2014.

Martínez-Loriente, S., V. Sallarès, E. Gràcia, R. Bartolome, J. J. Dañobeitia, and N. Zitellini (2014). Seismic and gravity constraints on the nature of the basement in the Africa-Eurasia plate boundary: New insights for the geodynamic evolution of the SW Iberian Margin. *JGR*, 119, 127-149.

Mascle, J., Mary, F., Praeg, D., Brosolo, Laetitia, Camrea, L., Ceramicola, S., Dupré, S., Distribution and geological control of mud volcanoes and other fluid/free gas seepage features in the Mediterranean Sea and nearby Gulf fo Cadiz. *Geo-Mar Lett.*, DOI 10.1007/s00367-014-0356-4.

Medialdea T., Somoza, L., Pinheiro, L.M., Fernández-Puga, M.C., Vázquez, J.T., León R., Ivanov, M.K., Magalhães V., Díaz del Río, V., Vegas R (2009) Tectonics and mud volcano development in the Gulf of Cádiz. *Mar Geol* 261, 48–63.

Minning, M., Hebblen, D., Hensen, C., Kopf, A., 2006. Geotechnical and geochemical investigatyions of the marques de pombal landsldies at the Portuguese continental margin. *NWG*, 187-198.

Nocquet, J.M. & Calais, E. Geodetic Measurements of Crustal Deformation in theWestern Mediterranean and Europe. Pure Appl. Geophys., 161, 661-681.

Silva, S. Terrinha, P., Matias, L., Duarte, J., Roque, C., Ranero, C.R., Geissler, W.H., Zitellini, N (2017). Micro-seismicity in the Gulf of Cadiz: Is there a link between micro-seismicity, high magnitude earthquakes and active faults? *Tectonophysics*, 717, 226-241.

Somoza L, Díaz-del-Río V, León R, Ivanov M, Fernández-Puga MC, Gardner JM, Hernández-Molina FJ, Pinheiro LM, Rodero J, Lobato A, Maestro A, Vázquez JT, Medialdea T, Fernández-Salas LM (2003) Seabed morphology and hydrocarbon seepage in the Gulf of Cadiz mud volcano area: acoustic imagery, multibeam and ultrahigh resolution seismic data. Mar Geol 195:153–176.

Stich, D., Ammon, C.J. & Morales, J. (2003). Moment tensor solutions for small and moderate earthquakes in the Ibero-Maghreb region. J. Geophys. Res., 108. B3, 2148-2168.

Stich, D., Serpelloni, E., Mancilla, F., Morales, J., 2006. Kinematics of the Iberia–Maghreb plate contact from seismic moment tensors and GPS observations. *Tectonophysics*, 426, 295-317.

Stich, D., F. Mancilla, de L., S. Pondrelli, and J. Morales (2007). Source analysis of the february 12th 2007, Mw 6.0 Horseshoe earthquake: Implications for the 1755 lisbon earthquake. *Geophysical Research Letters*, 34, L12, 308.

Stich, D., Martín, R., Jose Morales, J., 2010. Moment tensor inversion for Iberia–Maghreb earthquakes 2005–2008, *Tectonophysics* 483, 390–398.

Terrinha, P., L. Pinheiro, J. Henriet, L. Matias, M. Ivanov, J. Monteiro, A. Akhmetzhanov, A. Volkonskaya, T. Cunha, P. Shaskin, and M. Rovere (2003). Tsunamigenic-seismogenic structures, neotectonics, sedimentary processes and slope instability on the southwest Portuguese margin. *Marine Geology*, 195 (1-4), 55-73.

Terrinha, P., Matias, L., Vicente, J., Duarte, J., Luís, J., Pinheiro, L., Lourenço, N., Diez, S.,Rosas, F., Magalhães, V., Valadares, V., Zitellini, N., Roque, C., Víctor, L.M., 2009. Morphotectonics and strain partitioning at the Iberia–Africa plate boundary from multibeam and seismic reflection data. *Mar. Geol.,* 267, 156–174.

Toyos, M.H., Medialdea, T., Leom, R., Somoza, L., González, F.J., Melémdez, N. (2016). Evidence of epoisodica long-lived eruptions in teh Yuma, Ginsburg, Jesus Baraza and Tasyo mud volcanoes, Gulf of Cadiz. *Geo-Mar.Lett.,* 36, 197-214.

Van Rensbergen P, Depreiter D, Pannemans B., Moerkerke G, Van Rooij D, Marsset B, Akhmanov G, Blinova V, Ivanov M, Rachidi M, Magalhaes V, Pinheiro L, Henriet J-P (2005) The El Arraiche mud volcano field at the Moroccan Atlantic slope, Gulf of Cadiz. *Mar Geol* 219:1–17

Vizcaino, A., E. Gràcia, R. Pallàs, J. Garcia-Orellana, C. Escutia, D. Casas, V. Willmott, S. Diez, A. Asioli, and J. Dañobeitia (2006). Sedimentology, physical propertiesand ages of mass-transport deposits associated to the marquês de pombal fault, southwest portuguese margin. *Norwegian Journal of Geology,* 86 (3), 177-186.

Zitellini, et al., 2001. Source of 1755 Lisbon Earthquake and tsunami investigated. *EOS Trans. Am. Geophys. Union* 82, 282–285.

Zitellini, N., M. Rovere, P. Terrinha, F. Chierici, L. Matias, and BIGSETS Team (2004). Neogene through quaternary tectonic reactivation of SW Iberian passive margin, *Pure Appl. Geophys.,* 161, 565-587.

Zitellini, N., E. Gràcia, L. Matias, P. Terrinha, M. de Abreu, G. DeAlteriis, J. Henriet, J. Dañobeitia, D. Masson, T. Mulder, R. Ramella, L. Somoza, and S. Diez (2009). The quest for the africa-eurasian plate boundary west of the straits of Gibraltar. *Earth Planetary Science Letters*, 280 (1-4), 13-50.

Annex 1. INSIGHT-Leg 1 meteo and state of the sea

30 April – 12h		
Wind	350º	12 kn
Sea	320º	2 m wave
Barometer	1019 MPa	
Tº air	25º	
Tº water	20º	

1 May – 12h		
Wind	350º	12 kn
Sea	330º	1.5 m wave
Barometer	1022 MPa	
Tº air	22º	
Tº water	16º	

2 May – 12h		
Wind	260º	12 kn
Sea	270º	1 m wave
Barometer	1021 MPa	
Tº air	18º	
Tº water	13º	

3 May – 12h		
Wind	020º	22 kn
Sea	320º	1,5 m wave
Barometer	1021 MPa	
Tº air	19º	
Tº water	14º	

4 May – 12h		
Wind	010º	18 kn
Sea	350º	3 m wave
Barometer	1017 MPa	

Tº air	18º
Tº water	15º

5 May – 12h		
Wind	340º	5 kn
Sea	350º	1-1.5 m wave
Barometer	1017 MPa	
Tº air	23º	
Tº water	17º	

6 May – 12h		
Wind	070º	16 kn
Sea	020º	1-1.5 m wave
Barometer	1016 MPa	
Tº air	20º	
Tº water	17º	

7 May – 12h		
Wind	030º	21 kn
Sea	330º	1-1.5 m wave
Barometer	1018 MPa	
Tº air	22º	
Tº water	18º	

8 May – 12h		
Wind	360º	12 kn
Sea	330º	1-1.5 m wave
Barometer	1019 MPa	
Tº air	18º	
Tº water	13º	

9 May – 12h

Wind	030º	14 kn
Sea	032º	1.5 m wave
Barometer	1019 MPa	
Tº air	18º	
Tº water	16º	

10 May – 12h		
Wind	031º	8 kn
Sea	030º	1 m wave
Barometer	1019 MPa	
Tº air	19º	
Tº water	17º	

11 May – 12h		
Wind	029º	9 kn
Sea	032º	1 m wave
Barometer	1021 MPa	
Tº air	21º	
Tº water	17º	

12 May – 12h		
Wind	033º	8 kn
Sea	032º	1 m wave
Barometer	1023 MPa	
Tº air	20º	
Tº water	17º	

13 May – 12h		
Wind	002º	19 kn
Sea	033º	2.5 m wave
Barometer	1024 MPa	
Tº air	18º	
Tº water	14º	

14 May – 12h		
Wind	001º	25 kn
Sea	034º	2.5 m wave
Barometer	1022 MPa	
Tº air	17º	
Tº water	14º	

15 May – 12h		
Wind	005º	18 kn
Sea	035º	2.5 m wave
Barometer	1019 MPa	
Tº air	22º	
Tº water	18º	

16 May – 12h		
Wind	100º	21 kn
Sea	100º	2 m wave
Barometer	1016 MPa	
Tº air	20º	
Tº water	16º	

Annex 2. INSIGHT-Leg 1 cruise operations

All times are given in local time (UTC + 2h).

CAMPAÑA: INSIGHT - Leg1

30/04/2018 al 17/05/2018

Operation	Speed	Distance (NM)	Time (hrs)	Date
Departure Vigo / Start SHAKE Cruise Leg1				30/04/2018 00:00
Transit Vigo-MP	**10**			**01/05/2018 08:00**
Gravity core SdG068-01				01/05/2018 08:24
AUV Dive 1			12	01/05/2018 17:31
Line MCS MP03	3.5			02/05/2018 03:44
Line MCS MP04	3.5			02/05/2018 06:18
XBT MP				02/05/2018 07:38
Gravity core SdG068-02				02/05/2018 13:19
Gravity core SdG068-03				02/05/2018 15:35
AUV Dive 2			18	02/05/2018 18:51
Line MCS MP05	3.5			02/05/2018 22:15
Line MCS MP06	3.5			03/05/2018 00:46
Line MCS MP07	3.5			03/05/2018 03:36
Line MCS MP08	3.5			03/05/2018 06:37
Line MCS MP09	3.5			03/05/2018 09:10
Line MCS MP11a	3.5			03/05/2018 12:50
Line MCS MP11b	3.5			03/05/2018 13:22
Transit MP-LSW	**8**			**03/05/2018 22:05**
XBT LSW				04/05/2018 08:52
Echosounders calibration profile				04/05/2018 09:04
AUV Dive 3			12	04/05/2018 15:53
Line MCS LSW12	3.5			04/05/2018 19:16
Line MCS LSW13	3.5			04/05/2018 22:07
Line MCS LSW14	3.5			05/05/2018 00:42
Line MCS LSW15	3.5			05/05/2018 03:44
Line MCS LSW16	3.5			05/05/2018 06:34
AUV Dive 4			18	05/05/2018 15:45
Line MCS LSW01	3.5			05/05/2018 19:20
Line MCS LSW02	3.5			05/05/2018 23:53
Line MCS LSW23	3.5			06/05/2018 04:08
Line MCS LSW23 CRASH				06/05/2018 04:14
Line MCS LSW23	3.5			06/05/2018 05:53
AUV Dive 5			12	06/05/2018 18:47
Line MCS LSW11	3.5			07/05/2018 01:03
Line MCS LSW10	3.5			07/05/2018 04:03
Line MCS LSW09	3.5			07/05/2018 07:01
Line MCS LSW08	3.5			07/05/2018 09:57

AUV Dive 6			18	07/05/2018 18:01
Line MCS LSW17	3.5			07/05/2018 21:44
Line MCS LSW18	3.5			08/05/2018 00:44
Line MCS LSW19	3.5			08/05/2018 04:51
Line MCS LSW20	3.5			08/05/2018 08:33
Transit LSW-LSE	**8**			**08/05/2018 17:46**
Gravity core SdG068-04				09/05/2018 08:43
AUV Dive 7			18	09/05/2018 11:30
Line MCS LSE06	3.5			09/05/2018 15:48
Line MCS LSE05	3.5			09/05/2018 19:59
Line MCS LSE03	3.5			10/05/2018 00:02
XBT LSE				10/05/2018 09:08
AUV Dive 8			12	10/05/2018 10:54
Line MCS LSE13	3.5			10/05/2018 13:47
Line MCS LSE15	3.5			10/05/2018 17:25
AUV Dive 9			18	11/05/2018 03:12
Line MCS LSE07	3.5			11/05/2018 05:43
Line MCS LSE08	3.5			11/05/2018 09:42
Line MCS LSE09	3.5			11/05/2018 13:25
Gravity core SdG068-05				11/05/2018 18:44
Gravity core SdG068-06				11/05/2018 23:53
Gravity core SdG068-07				12/05/2018 04:15
Gravity core SdG068-08				12/05/2018 05:09
Gravity core SdG068-09				12/05/2018 05:56
Gravity core SdG068-10				12/05/2018 06:43
Transit LSE-GMV	**8**			**12/05/2018 07:25**
Gravity core SdG068-11				12/05/2018 10:31
AUV Dive 10			18	12/05/2018 14:28
Line MCS GMV01	3.5			12/05/2018 17:25
Line MCS GMV02	3.5			12/05/2018 21:28
Line MCS GMV03	3.5			13/05/2018 01:03
Gravity core SdG068-12				13/05/2018 11:45
Gravity core SdG068-13				13/05/2018 13:06
Transit GMV-LoSD	**8**			**13/05/2018 14:20**
AUV Dive 11			18	14/05/2018 01:36
Removal of non-working streamer sections*				14/05/2018 03:30
XBT LoSD				14/05/2018 15:48
Gravity core SdG068-14				14/05/2018 19:04
Gravity core SdG068-15				14/05/2018 23:23
AUV Dive 12			12	15/05/2018 02:15
Line MCS LoSD01	3.5			15/05/2018 04:53
Line MCS LoSD02	3.5			15/05/2018 08:56
Line MCS LoSD05	3.5			15/05/2018 12:13
Gravity core SdG068-16				15/05/2018 17:16

Line MCS LoSD06	3.5			15/05/2018 21:07
Line MCS LoSD03	3.5			16/05/2018 02:53
Line MCS LoSD07	3.5			16/05/2018 08:46
Transit LoSD-Cádiz				**16/05/2018 13:30**
END of Leg1				

*From now on, a 250 m streamer was used.